University of Alberta

NEURAL CIRCUITRY AND NEUROTRANSMITTERS UNDERLYING VERTEBRATE WALKING

by

Ksenija Jovanović

A thesis submitted to the Faculty of Graduate studies and Research in partial fulfillment of the requirements for the degree of Doctor of Philosophy

Division of Neuroscience

Edmonton, Alberta

Fall 1999

National Library of Canada
Acquisitions and Bibliographic Services
395 Wellington Street
Ottawa ON K1A 0N4
Canada

Bibliothèque nationale du Canada
Acquisitions et services bibliographiques
395, rue Wellington
Ottawa ON K1A 0N4
Canada

Your file Votre référence

Our file Notre référence

The author has granted a non-exclusive licence allowing the National Library of Canada to reproduce, loan, distribute or sell copies of this thesis in microform, paper or electronic formats.

The author retains ownership of the copyright in this thesis. Neither the thesis nor substantial extracts from it may be printed or otherwise reproduced without the author's permission.

L'auteur a accordé une licence non exclusive permettant à la Bibliothèque nationale du Canada de reproduire, prêter, distribuer ou vendre des copies de cette thèse sous la forme de microfiche/film, de reproduction sur papier ou sur format électronique.

L'auteur conserve la propriété du droit d'auteur qui protège cette thèse. Ni la thèse ni des extraits substantiels de celle-ci ne doivent être imprimés ou autrement reproduits sans son autorisation.

0-612-46859-3

Canada

University of Alberta

Library Release form

Name of Author:	Ksenija Jovanović
Title of Thesis:	"Neural Circuitry and Neurotransmitters Underlying Vertebrate Walking"
Degree:	Doctor of Philosophy
Year this Degree Granted:	1999

Permission is hereby granted to the University of Alberta Library to reproduce single copies of this thesis and to lend or sell such copies for private, scholarly, or scientific research purposes only.

The author reserves all other publication and other rights in association with the copyright in the thesis, and except as hereinbefore provided, neither the thesis nor any substantial portion thereof may be printed or otherwise reproduced in any material form whatever without the author's prior written permission.

Ksenija Jovanović

4632 – 151 Street
Edmonton, AB
T6G 5N8

SEPTEMBER 20 1999
Date

University of Alberta

Faculty of Graduate Studies and Research

The undersigned certify that they have read, and recommend to the Faculty of Graduate Studies and Research for acceptance, a thesis entitled *"Neural Circuitry and Neurotransmitters Underlying Vertebrate Walking"* submitted by Ksenija Jovanović in partial fulfillment of the requirements for the degree of *Doctor of Philosophy*

R. B. Stein
Dr. Richard B. Stein

K. G. Pearson
Dr. Keir Pearson

D. J. Bennett
Dr. David Bennett

P. A. Smith
Dr. Peter Smith

Teresa Krukoff
Dr. Teresa Krukoff

Alan Roberts
Dr. Alan Roberts

Sept. 20, 1999
Date

I wish to dedicate this thesis to my parents without whom this entire adventure would never have been possible...

ABSTRACT

Locomotion can be generated in the vertebrate spinal cord by neuronal networks known as central pattern generators (CPGs). However, their action is constantly modified by extrinsic modulatory inputs and sensory feedback to compensate for an ever changing environment. To address questions of locomotor rhythm generation and its modulation in a walking vertebrate, we used an *in vitro* preparation isolated from a mature aquatic amphibian, the mudpuppy (*Necturus maculatus*). The preparation consisted of the first five segments of the spinal cord and the forelimb(s) attached by the brachial nerves. During chemically induced locomotion, electromyographic activity was recorded unilaterally or bilaterally from elbow flexor and extensor muscles. Combined use of pharmacological and immunostaining techniques revealed that some of the conventional neurotransmitters (i.e., serotonin, glycine, GABA) prominent in higher and lower vertebrates also affect locomotion in the mudpuppy. While not essential for rhythmogenesis, activation of serotonergic, glycinergic and GABAergic systems play a role in the control of locomotor frequency. In addition, glycine and GABA are important in mediating the reciprocal antagonism that coordinates the locomotor rhythm. The modulatory action of serotonin may be exerted by a well developed spinal serotonergic system.

A subsequent study, combining chemical and microstimulating techniques with sectioning of the spinal cord revealed that the CPG for forelimb locomotion comprises at least two distinct centers responsible for producing rhythmic elbow flexion and extension. The two centers can operate independently in the absence of reciprocal inhibitory interconnections between them. Sensory input was shown to interact with the

flexion/extension networks to reset the ongoing walking rhythm in a phase-dependent manner. Intracellular recording revealed that the majority of interneurons within flexor and extensor centers were active during walking and were classified into four phasic types in the step cycle. Differential longitudinal distribution along the spinal cord of the four types of interneurons was in agreement with the existence of separate flexor and extensor centers.

Preliminary experiments conducted on a novel two-limb preparation showed that roughly one segment of the spinal cord contains neural circuitry capable of generating walking-like activity that involves both forelimbs. Midsagittal sectioning of this segment did not abolish activity in both disconnected sides indicating that each spinal hemisegment contains neuronal elements capable of producing rhythmic bursting. However, the resulting bursts were mutually uncorrelated indicating importance of crossed spinal connections for coordination of the two limbs. The results contribute to the growing body of evidence for a common role of neuromodulatory substances in the control of locomotion among vertebrates. The distinctly localized rhythmogenic centers suggest that more complex neuronal networks probably contain small modular pattern generators which can be assembled to meet changing behavioral needs.

ACKNOWLEDGEMENTS

First, I would like to thank to my supervisor Dick Stein for giving me the opportunity to pursue my PhD in his laboratory and for his guidance, support and friendship during this period.

I would also like to thank the members of my supervisory and examining committees - Drs. Keir Pearson, Peter Smith, Theresa Krukoff and David Bennett - for useful and constructive interactions throughout the program. Many thanks go to Keir Pearson for showing me what real enthusiasm for science is all about and for numerous helpful suggestions over the past six years. I wish to thank my external examiner Dr. Alan Roberts for the time and effort that he contributed on my behalf.

A special thank you goes out to John Greer for making my first lab rotation a pleasant experience and for having such a calming effect during the frustrating days. I also thank him for beautiful conversations, music, humour and for always helping me whenever I need it.

I would like to thank my parents and brother for their tender care, love and support and for always being there for me despite the physical distance separating us. Many heartfelt thanks go to my "Canadian family" Milica, Sasha, Ljilja and Dragan Krstić for their love and support and for making Edmonton my second home. I also thank Marguerite Wieler for being my friend, confidant, English teacher and sister, for sharing with me the good times and the bad times, the laughters and tears. Many thanks go to Vivian Mushahwar for her help during the final stages of my thesis, her humour, friendship and for showing me what dedicated work is all about. I also thank her for being a patient and gracious flatmate. Thanks are also due to my coworker and friend Ken Yoshida whose patience and excellent knowledge of computer programming and electronics made my scientific life much easier.

I also thank Arthur Prochazka for his genuine concern, humour and insightful discussions we had. I thank Dave Bennett for fun and dynamic scientific exchanges and for letting me use his lab, especially, his printer when all other printers were out of order. Thanks go, of course, to the many of good friends I have made during my stay in

Edmonton. To all the Neuroscience, Physiology and Pharmacology graduate students and staff, I had a great pleasure of knowing you, thanks for being so much fun!

I would also like to extend my gratitude to the secretarial staff Toni Stringam, Carol Ann Johnson and Brenda Topliss for always being so patient, friendly and efficient. I thank Zoltan Kenwell and Rob Rolf for their help with computers, printers, never ending noise and old equipment problems.

Finally, I would like to thank the Alberta Heritage Foundation for Medical Research and NCE Canada for providing the financial support to make this work possible.

TABLE OF CONTENTS

CHAPTER 1

GENERAL INTRODUCTION 1
INTRODUCTION 1
CENTRAL GENERATION OF LOCOMOTION 2
MODULATION OF LOCOMOTOR CPGs 5
SENSORY MODULATION OF LOCOMOTOR CPGs 6
ACTIVITY OF NEURONS DURING LOCOMOTION 8
INTERLIMB COORDINATION DURING LOCOMOTION 10
CONCLUSIONS 12
THESIS OBJECTIVES 12
REFERENCES 15

CHAPTER 2

SEROTONERGIC MODULATION OF THE MUDPUPPY (*Necturus maculatus*) LOCOMOTOR PATTERN *IN VITRO* 26
INTRODUCTION 26
MATERIALS AND METHODS 28
In vitro preparation 28
Immunocytochemistry 29
RESULTS 30
Pharmacology 30
Immunocytochemistry 38
DISCUSSION 46
Pharmacology of 5-HT action 47
Immunocytochemistry 48
REFERENCES 52

CHAPTER 3

EFFECTS OF INHIBITORY NEUROTRANSMITTERS ON THE MUDPUPPY (*Necturus maculatus*) LOCOMOTOR PATTERN *IN VITRO* 57
INTRODUCTION 57
MATERIALS AND METHODS 59
In vitro preparation 59
I. Exogenous application of the drugs 60
II. Immunocytochemistry 64
RESULTS 64
Role of Glycinergic system in Necturus locomotion 64

GABAergic system activation and its role in mudpuppy locomotion
Role of GABA in Necturus locomotion 70
Role of $GABA_A$ receptors in Necturus locomotion 71
Role of $GABA_B$ receptors in Necturus locomotion 76
Immunocytochemistry 76
DISCUSSION 81
Glycine 84
GABA 87
REFERENCES 91

CHAPTER 4

IDENTIFICATION, LOCALIZATION AND MODULATION OF NEURAL NETWORKS FOR WALKING IN THE MUDPUPPY (*Necturus maculatus*) SPINAL CORD 96
INTRODUCTION 96
MATERIALS AND METHODS 98
Retrograde labeling of motoneuron pools 98
In vitro walking preparation 98
Micro-stimulation 99
Surgical isolation of regions of the spinal cord 102
Resetting walking rhythm by stimulation of regions of the cord, dorsal roots, and ventral roots 102
Correlation analysis 102
RESULTS 105
Motoneuron pools innervating the elbow flexor and extensor muscles 105
Identification of the elbow flexor and extensor centers 106
Surgical isolation of the flexor and extensor centers 109
Resetting of the walking rhythm 114
DISCUSSION 124
Flexor and extensor centers 129
Inhibitory coupling 131
Sensory modulation 131
REFERENCES 133

CHAPTER 5

INTERNEURONS IN THE NEURAL NETWORKS FOR WALKING IN THE MUDPUPPY *(Necturus maculatus)* SPINAL CORD 138
INTRODUCTION 138
MATERIALS AND METHODS 140

Recording and filling cells 140
Stimulation of the ventral roots 142
Correlation Analyses 145
RESULTS 150
Identification of interneurons 150
Phasic classification of the cells 153
Longitudinal distribution of the recorded cells in the spinal cord 156
Cells with membrane potentials oscillating at walking frequency 160
Connectivity of the rhythmic cells 160
DISCUSSION 165
Four types of interneurons related to walking 165
Differential longitudinal distribution of the four types of cells 166
Voltage oscillation of interneurons in relation to walking 168
Connectivity of the circuitry 168
REFERENCES 170

CHAPTER 6

LOCALIZATION OF RHYTHMOGENIC NETWORK CONTROLLING BIPEDAL LOCOMOTION IN THE MUDPUPPY (*Necturus maculatus*) 178
INTRODUCTION 178
MATERIALS AND METHODS 179
In vitro preparation 179
Analysis 181
RESULTS 188
Effects of bilateral dorsal rhizotomy 188
Effects of rostro-caudal sectioning of the spinal cord 193
Motor pattern produced in isolated C3 spinal segment 194
Midsagittal section 197
DISCUSSION 197
Characteristics of control locomotor pattern 200
Effects of bilateral deafferentation 200
Effects of rostro-caudal sectioning of the spinal cord (C3 isolated) 201
Rhythmicity in C3 spinal hemisegments 203
Statistical significance 203
Concluding remarks 204
REFERENCES 206

CHAPTER 7

GENERAL DISCUSSION 210
REFERENCES 216

APPENDIX

APPLICATION OF INTRAFASCICULAR ELECTRODES TO THE *IN VITRO* MUDPUPPY PREPARATION 217
INTRODUCTION 217
MATERIAL AND METHODS 218
Electrode construction 218
Animal preparation 222
Ventral root stimulation 223
Compound action potential recording 224
RESULTS 225
Ventral root stimulation 225
Compound action potential recording 230
DISCUSSION 235
REFERENCES 239

LIST OF FIGURES

Figure 2-1. Effects of 5-HT on NMDA-induced locomotion in vitro 32

Figure 2-2. Effects of 5-HT uptake inhibition on NMDA induced locomotion. 34

Figure 2-3. Effects of non-specific 5-HT_1/ 5-HT_2 receptor antagonist methiothepin on NMDA-induced locomotion. 36

Figure 2-4. Coronal sections through the spinal cord showing radially oriented processes of a group of 5-HT immunoreactive neurons in the fourth segment 39

Figure 2-5. Horizontal sections through the spinal cord depicting the relationships of 5-HT positive neuronal profiles with the wall of the central canal (cc) or the midline (m). 41

Figure 2-6. Horizontal sections depicting relationships between the types of 5-HT immunoreactive fibers. 44

Figure 3-1. Effects of glycine on NMDA-induced locomotion in vitro 62

Figure 3-2. Additional glycine effects 66

Figure 3-3. Effects of strychnine on NMDA-induced locomotion in vitro 68

Figure 3-4. Effects of GABA on NMDA-induced locomotion in vitro. 72

Figure 3-5. Effects of $GABA_A$ receptor antagonist bicuculline on NMDA-induced locomotion. 74

Figure 3-6. Effects of $GABA_B$ receptor substances on NMDA-induced locomotion. . . 77

Figure 3-7. Horizontal sections through the spinal cord depicting the localization of GABA positive neuronal profiles and processes. 79

Figure 3-8. Horizontal sections depicting relationships of glycine immunoreactive neuronal profiles and processes with the ependymal lining of the central canal. 82

Figure 3-9. Schematic diagram of the actions of the inhibitory neurotransmitters on the locomotor circuitry. 85

Figure 4-1. Microphotographs of the spinal cord. 100

Figure 4-2 Chemically-induced independent activation of the elbow flexor and extensor centers. 103

Figure 4-3. Electrically induced independent activation of the elbow flexor and extensor centers. 107

Figure 4-4 Isolation of the flexor center. 110

Figure 4-5 Isolation of the extensor center. 112

Figure 4-6. Rhythmic flexor and extensor EMG bursts were generated by a region spanning C3 ventral root. 115

Figure 4-7. Decoupling of the two centers by surgical separation of the cord. 117

Figure 4-8. Resetting of the walking-like rhythm by dorsal root stimulation. 120

Figure 4-9. Resetting of the walking-like rhythm by reafferent input consequent to limb movement. 122

Figure 4-10. Resetting the walking-like rhythm induced by stimulation of the flexor center 125

Figure 4-11. Schematic localization of elbow flexor and extensor centers and modeling of the neural networks required for walking. 127

Figure 5-1. Microphotographs of cross sections (40μm thick) of the spinal cord. 143

Figure 5-2. Four types of rhythmic cells. 146

Figure 5-3. Example of a transition interneuron. 148

Figure 5-4. Spike-triggered short latency excitation of the extensor muscle. 151

Figure 5-5. Longitudinal distribution of cells recorded in the C2 and C3 segments. . . 154

Figure 5-6. Example of flexor interneurons recorded intra- and extra-cellularly in the presence of NMDA (40 μM). 157

Figure 5-7. Longitudinal distribution of the cells recorded along the spinal cord at a resolution of 1 mm. 161

Figure 5- 8. Rhythmic discharges on top of membrane voltage undulations. 163

Figure 6-1. Mudpuppy in vitro preparation 182

Figure 6-2. Phase plots of pooled data obtained from seven animals 185

Figure 6-3. Control locomotor pattern recorded from the forelimbs in vitro 189

Figure 6-4. Locomotor pattern following bilateral dorsal rhizotomy 191

Figure 6-5. Locomotor pattern generated in isolated C3 spinal segment 195

Figure 6-6. Rhythm in midsagittally hemisected C3 spinal cord segment 198

Figure 7-1. Schematic illustrating localization of the elbow flexor and extensor centers and rostro-caudal distribution of serotonergic (5-HT), GABAergic and glycinergic cells in the brachial spinal cord of the mudpuppy. 211

Figure A1 - is a drawing of the intrafascicular electrode and it's implant scheme. 220

Figure A2 - Stimulating through a LIFE implanted in the C3 ventral root results in activation of elbow flexor and extensor muscles. 226

Figure A3 Peak to peak EMG were compared for supra maximal stimulation with intrafascicular electrodes in the C3 ventral root and with hook electrodes around the C3 spinal nerve. 228

Figure A4 - Supra-maximal stimuli were delivered through the elbow extensor intra-muscular electrode. 231

Figure A5 - shows the three traces recording through intrafascicular electrodes at three levels of stimuli. 233

CHAPTER 1

GENERAL INTRODUCTION

INTRODUCTION

All animals, vertebrates and invertebrates alike, depend on locomotion. The ability to locomote largely determines their survival skills as it allows them to gather food, seek new habitats as well as to avoid obstacles and predators. As a result of the constantly changing environment and their dynamic interactions with it, animals have developed many different forms of locomotion such as swimming, crawling, hopping, walking, running, etc. Despite an obvious diversity, one of most apparent features of locomotion is its rhythmic stereotyped repetitiveness. In fact, this feature is also shared by many other rhythmic movements like scratching, chewing, breathing and cardiac pacing, only to mention some of them.

It is universally accepted that locomotion, as many other rhythmic movements, can be generated within the vertebrate spinal cord even in the absence of sensory feedback or descending inputs from higher brain centers. Neuronal networks responsible for producing coordinated spatio-temporal patterns typical of different rhythmic behaviors are called central pattern generators (CPGs; Székely 1969; Delcomyn 1980; Grillner et al. 1991; Kahn and Roberts 1982; Pearson 1993; Smith et al. 1988; Stein et al. 1984). A CPG is viewed as an assembly of neurons which, by virtue of their intrinsic properties and/or synaptic interactions, is capable of generating and controlling rhythmic motor output. In order to understand how a neural network can produce a rhythmic patterned-output, all of the neurons active during the rhythmic activity must be considered, the synaptic relationships between neurons should be determined and the intrinsic properties of the neurons and synapses should be characterized. Although there are only a few circuits for which most of these criteria have been met, it is becoming clear that pattern generating networks may share a common pool of "building block" mechanisms (Getting

1988; 1989; Kiehn et al. 1997; Marder and Calabrese 1996) linked together in different combinations. Each combination could generate a different pattern, thereby explaining the diversity of rhythmic behaviors.

This introductory chapter reviews our current knowledge regarding central pattern generators for locomotion. Even though, the wealth of literature on detailed CPG organization emanates from studies in invertebrates, the material covered will be limited to the literature pertaining to vertebrate locomotion while data from invertebrates and CPGs for other rhythmic behaviors will be discussed as required. Roles of descending supraspinal structures (Armstrong 1986; Jordan 1991; Rossignol 1996; Shik 1997) in activating and/or modulation of spinal CPGs will not be reviewed and attempts will be made to avoid unnecessary repetition of details represented in the introductions of the individual chapters.

CENTRAL GENERATION OF LOCOMOTION

The first demonstration that spinal networks can generate the details of rhythmic locomotor output resulted from Graham Brown's experiments (1911; 1914) using acute spinal and deafferented cats. He proposed the half-center model to explain alternating activation of flexor and extensor muscles during cats' hindlimb stepping. Each half-center was thought to activate either flexor or extensor muscles while the connection between the two half-centers was thought to be mutually inhibitory to ensure that when one center is active the other is silent. Modern support for this scheme has come from studies on spinal reflexes following administration of drugs (DOPA and clonidine) known to release the walking rhythm (Lundberg 1979; Rossignol et al. 1998; Viala and Buser 1969). More comprehensive evidence for central origin of locomotion was obtained from the newt (Székely et al. 1969) and cat (Grillner and Zangger 1979) where the isolated parts of brachial or caudal spinal cord, respectively, can also generate rhythmic motor output even in the absence of the afferent input. The latter work not only confirmed but also refined and expanded Brown's initial observations providing a framework for a new concept of

multiple unit burst generators (Grillner 1981; Grillner and Wallén 1985). Unlike half-centers, each unit burst generator can generate rhythmic output on its own and be combined with other unit burst generators thereby participating in the production of different behaviors.

***In vitro* studies**

Although these early studies contributed a great deal to revealing and defining spinal locomotor networks, they were not able to provide a detailed insight into the electrophysiological, pharmacological and anatomical properties of CPG networks. Alternatively, model systems, allowing for the use of *in vitro* nervous system preparations, have contributed significantly to our understanding of the organization of the spinal locomotor systems. For example, in lower vertebrates like the lamprey and *Xenopus*, the relative simplicity of the locomotor behavior and the underlying neural network allowed for a detailed analysis of these systems. In both systems it has been possible to identify many of the neurons that are part of the neural networks generating locomotor activity, to characterize the cellular properties of these neurons and to establish some of the synaptic connections within the networks (Buchanan 1996; Buchanan and Cohen 1982; Dale 1991; Grillner et al. 1998; Grillner and Matsushima 1991; Roberts and Clarke 1982; Roberts et al. 1997; Roberts et al. 1998; Wallén 1997). Furthermore, the wealth of biological data on locomotor networks in these animals has given rise to several types of computer models (Roberts and Tunstall 1990; Hagevic and McClellan 1994; Wallén et al. 1992) that proved to be useful for interpreting biological results, supporting conclusions or suggesting additional experiments.

Contrary to the initial expectations in this field of research, it has become apparent in recent years that CPGs are not single, independent and discrete entities. Instead, evidence has accumulated that many of the neurons involved in the pattern generation may contribute to more than one behavior. These behaviours generally involve either the same muscle groups or functionally related muscle groups (Dickinson 1995; Pearson 1993). The concept of multi-functional networks that can be re-configured to provide different behavioural outputs was first elaborated by Getting and Dekin (1985) to explain the

control of swimming and defensive withdrawal in the mollusc *Tritonia*. A number of recent studies have shown that the spinal networks controlling locomotor rhythms may also share neurons with one another. For instance, similarity of the movements involved in hatching, walking and swimming in the chick suggests that they may be produced by a single motor pattern generator which is reconfigured to give behaviourally different outputs (Bekoff 1992). Similarly, it has been suggested that neurons are shared between struggling and swimming behaviour in *Xenopus* embryo (Soffe 1993), swimming, burrowing and crawling in the lamprey (Ayers et al. 1983; Paggett et al. 1998) and between different forms of scratching in the turtle (Berkowitz and Stein 1994a, b). Reconfiguration of spinal networks may be accomplished by the action of afferent signals from the periphery, signals from supraspinal structures or the neuromodulatory substances (Harris-Warrick 1988 Pearson 1993; Stein and Smith 1997).

In recent years, valuable data have been obtained from immature animals such as chick embryos (Landmesser and O'Donovan 1984; O'Donovan et al. 1992) the neonatal rat (Bracci et al. 1996; Cazalets et al. 1992; Kudo and Yamada 1987; Kiehn and Kjaerulff 1998) neonatal mouse (Hernandez et al. 1991; Tao and Droge 1992; Bonnot and Didier 1998), and wallaby (Ho 1997). Although they provide important information on locomotor CPGs in vertebrates, there are some disadvantages inherent to each of these preparations. Lamprey and *Xenopus* embryos do not walk but rather swim. Immature animals, on the other hand, undergo developmental changes affecting different aspects of their motor systems such as electrophysiological characteristics of the motoneurones (Fulton and Walton 1981; 1986; Walton and Fulton 1986), neural connectivity and myelination (Miyata et al. 1987; Saruhashi et al. 1994) and pharmacology of the spinal cord (Antal et al. 1994; Cherubini et al. 1991; Sakatani et al. 1991). Thus, one may ask to what extent these models are relevant for understanding the spinal CPG of walking vertebrates and whether there are common mechanisms underlying the performance of similar behaviors.

MODULATION OF LOCOMOTOR CPGs

One of major advances in analysis of motor pattern generation is the recognition that the functional properties of CPGs can be modified by the action of neuromodulators. By changing the strengths of particular synapses and/or altering the membrane properties of neurons in the network, neuromodulators can enable neuronal circuits to adapt to changing environmental demands and also to establish correct configuration of a neuronal circuit for a specific behavior. For instance, a quadruped can locomote with alternation or synchrony of opposing limbs. This can involve various muscles acting in different synergies and different phases, depending on whether the animal is walking uphill or downhill (Stein and Smith 1997). Therefore, the circuitry that is generating such a flexible output must be able to produce changes in the phasing of rhythmic motoneuron activity depending on the circumstances. While the cellular basis for such flexibility in vertebrate locomotor CPG still lacks full understanding, work in the stomatogastric system of decapod crustaceans demonstrates that pattern generating circuits are capable of extreme reorganization (Harris-Warrick and Marder 1991; Katz and Harris Warrick 1990; Harris Warrick 1988). The differences in the motor patterns produced by different neuromodulators in this system can range from variations in the phasing of motor neurons to the complete reorganization of separate pattern-generating circuits into one combined, functionally new circuit (Dickinson et al. 1990; Meyrand et al. 1991). The extent to which similar actions of neuromodulators occur in vertebrate locomotion is difficult to assess, mainly because only a few motor circuits were sufficiently well defined. Nevertheless, recent recordings from neonatal rat spinal cord *in vitro* show that different motor outputs can be produced under the influence of different modulatory substances (Bracci et al. 1996; Cowley and Schmidt 1994; Kiehn and Kjaerulff, 1996). In addition, animal behavior can be affected not only by modulation of CPG network itself but also by the modulation at all possible sites in the nervous system, including muscles and neuromuscular junction, sense organs such as stretch receptors, motoneurones and neurons of pattern generating network as well as activating and coordinating inputs (Harris-Warrick and Marder 1991; Harris-Warrick 1993).

In intact animals neural networks receive simultaneous input from many modulatory neurons. Numerous, naturally occurring substances including amino acids, biogenic amines and peptides have been shown to affect one or more parameters of an ongoing locomotor pattern such as the duration and intensity of motor bursts and/or frequency of locomotion (Barthe and Grillner 1995; Cazalets et al. 1998; Sillar et al. 1997; Grillner et al. 1991 Krieger et al. 1994). Since it is likely that many of these substances are active at the same time, networks are modulated by a continuously varying mixture of transmitters. The relative contribution of one substance may be significant under some conditions but only produce subtle effects at other times. This issue is further complicated by the fact that modulatory substances are often colocalized in a single neuron. Indeed in several preparations, conventional transmitters and peptides are packed into different vesicles and released as a function of stimulation frequency (Harris-Warrick and Marder 1991; Marder and Calabrese 1996). Because of this, the major problem in this field of research has been defining the CPG components so that the targets of modulation and its effects can be unambiguously studied. Although, this has only been accomplished in a few invertebrate systems some important generalizations emerged regarding modulation of rhythmic patterns, including locomotion. Specifically, neuromodulators can modulate ongoing motor activity (Grillner and Matsushima 1991; Harris-Warrick 1988; Sillar et al. 1997), they can initiate locomotion or "prime" the CPG to respond more effectively to inputs from other sources (Barbeau and Rossignol 1990, 1991; Grillner 1986; Sigvardt 1989; Harris-Warrick 1988) and reconfigure the CPG circuit to produce different behaviours or variations of behaviours (Bracci et al. 1996; Cowley and Schmidt 1994; Kiehn and Kjaerulff 1996).

SENSORY MODULATION OF LOCOMOTOR CPGs

While it is well established that locomotor output may occur in its absence, the role of sensory input in pattern-generating circuits is still under investigation. The prevailing notion is that it plays a corrective role, adjusting centrally generated motor output to

perturbations in the environment such as those occurring in every day locomotion. In doing so, sensory signals can influence different aspects of the step cycle such as the temporal order of motor activity, transition from one phase of the movement to another and the magnitude of the ongoing movement (Pearson 1993; Pearson 1995; Rossignol et al. 1988; Rossignol 1996). For example, two events thought to be involved in regulating stance to swing transition during locomotion are extension at the hip (Grillner and Rossignol 1978) and unloading of leg extensor muscles (Duysens and Pearson 1980; Conway et al. 1987). Although the afferents that signal hip extension still have not been identified, it is likely that muscle spindle afferents arising from the hip flexor muscles are involved (Hiebert et al. 1996). The ability of muscle spindle afferents to modulate fictive locomotor rhythm is also indicated by the findings that rhythmic imposed movements at the hip can entrain and reset locomotor rhythm in spinal and decerebrate cat (Andersson and Grillner 1983; Kriellaars et al. 1994). Alternatively, the signals that indicate unloading of leg extensors largely arise from activation of Ib afferents originating from force sensitive Golgi tendon organs (Whelan et al. 1995). Thus, swing is initiated when the leg is extended (stretching flexor muscles) and unloaded (reduced force in extensor muscles). The functional significance of regulating phase transition by afferent feedback has not been fully established. One contribution may be to ensure that a certain phase of a movement is not initiated until a defined biomechanical state of the system has been achieved (Pearson 1993).

Afferent feedback has also been shown to play an important role in reinforcing centrally generated motor activity. Studies in walking systems of cats and humans have shown that afferent feedback from leg proprioceptors contributes significantly in reinforcing stance phase. The reinforcing action arises from both the force sensitive receptors (Golgi tendon organs) and from primary muscle spindle afferents in extensor muscles (Guertin et al. 1995; McCrea et al. 1995; Pearson and Collins 1993). The functional significance of reinforcing reflexes appears to be load compensation since any increase in load results in reflex reinforcement of activity in the load bearing muscle. This in turn, counteracts the increased load (Prochazka et al. 1997a,b).

Sensory inputs are not only passively relayed to the central circuits but they are also influenced by the pattern-generating networks and/or the command signals which activate these networks (Prochazka 1996; Rossignol et al. 1988; Sillar 1989, 1991). Therefore, the action of a sensory signal depends on the state of the pattern generator and/or motor task (Akazawa et al. 1982; Capaday and Stein 1986; Forssberg 1979; Pearson 1993; Pearson and Ramirez 1997).

The effect of sensory input is not always merely corrective in nature. Work in the locust flight system shows that the corrective phasing for the activity of the wing elevator motor neurons, even in the absence of perturbations, cannot be produced without proprioceptive feedback (Pearson and Ramirez 1997). Similarly, in the lamprey, proprioceptive neurons that sense the bending of the spinal cord (edge cells) have essentially the same properties as any other component of the locomotion generating network, including the ability to entrain and reset the rhythm (Grillner et al. 1998; Wallén 1997).

ACTIVITY OF NEURONS DURING LOCOMOTION

As the concept of CPG for locomotion is almost universally accepted, an important contemporary problem is to determine the cellular mechanisms responsible for generating the temporal sequence of activity in different groups of motoneurons. Despite considerable progress over the last decade, our understanding of their operation is still superficial mainly due to the complexity of the vertebrate spinal cord. To achieve a functional understanding of locomotor pattern generation, knowledge of membrane and synaptic properties of individual interneurons as well as their patterns of interconnections is required, in addition to elucidating the modulation of synaptic transmission and cellular conductances. Since the vertebrate adult nervous system contains many classes of neurons interlinked in complex circuitry, relating the activity and properties of individual classes of neurons to neural function is very difficult. Although rhythmically active during locomotion, motoneurons are traditionally considered not to be a part of locomotor CPGs.

However, recent studies (Roberts et al. 1997; O'Donovan and Ritter 1995; Roberts and Perrins 1995; Staras et al. 1998) suggest that motoneurons may have a dynamic role in the maintenance of the patterned output during locomotion.

Due to numerous problems in classifying interneurons, possible candidates for members of a CPG are those whose activity is modulated in phase with the motor rhythm. Attempts to classify them as such have gained conflicting results. In 1972 Orlovsky and Feldman recorded for the first time (extracellularly) from rhythmically active interneurons in the cat spinal cord demonstrating that 37% of these interneurons could be classified as mixed bursters with their activity spanning consecutive phases of the step cycle. Subsequent studies (Edgerton et al. 1976; Grillner 1981), confirmed these findings suggesting that interneurons can be active during all phases of the locomotor cycle, with only a crude segregation into different populations. In contrast, studies by Baev et al. (1979) revealed that the majority of recorded interneurons could be classified as flexion or extension related while only 10% could be classified as mixed bursters. This obvious discrepancy was explained by the lack of sensory input and the possibility that cyclic afferent inflow was required to convert flexor and extensor interneurons into mixed interneurons (Baev et al. 1979). The hypothesis that afferent input is capable of changing the phase of activity of a muscle during locomotion is supported by the work done by Perret and collaborators (Perret and Cabelguen 1976; Perret 1986). Likewise, studies in curarized rabbits have led to the classification of rhythmically active interneurons as related either to flexion or extension (Viala et al.1991). More recently it has been demonstrated that rhythmically active interneurons with mixed or transitional bursting properties are common in the cervical spinal cord inervating the forelimb of the fictive cat (Hishinuma and Yamaguchi 1990, Terakado and Yamaguchi 1990). However, when these interneurons were further subdivided so that only last order interneurons were taken into account, they again were classified as either flexor-like or extensor-like (Terakado and Yamaguchi 1990; Ichikawa et al. 1991). Although many of these inteneurons may not be part of the CPG, these data indicate a much greater complexity for the rhythm generator then suggested by the half-centre scheme. Presently, models of vertebrate central pattern

generation have been proposed for several species: lamprey (Grillner et al. 1991), *Xenopus* embryo (Roberts et al. 1986; Roberts et al. 1997), urodeles (Székely 1965; Kling and Székely 1968) and cat (Jankowska et al. 1967).

Use of lower vertebrates with simpler nervous systems has lessened the problem of complexity and allowed for new insights into the mechanisms for pattern generation (Roberts et al. 1986; 1997; Grillner et al. 1991; 1998). As a result of the variety of new approaches such as transverse spinal cord slices (Hochman et al. 1994; Hounsgaard and Kjaerulff 1991) dissociated spinal cord neurons (Dale 1991), and paired intracellular recordings (Roberts et al. 1986) some of the circuit properties involved in the generation of locomotion are beginning to be understood. Moreover, results of studies that utilised neuronal activity markers, such as the expression of the immediate early gene *c-fos* (Bajaron et al. 1992; Dai et al. 1990), 2-deoxyglucose (Viala et al. 1988) or sulphorhodamine accumulation (Kjaerulff et al. 1994) indicate that most of the neurons that are simultaneously active with motoneurons are localised around the central canal and are confined mainly to the ipsilateral laminae V-VII, and to the contralateral lamina VIII (Puskar and Antal 1997). Although they provided useful information regarding the basis of locomotor mechanisms a full understanding of locomotion in higher vertebrates still appears to be an elusive goal.

INTERLIMB COORDINATION DURING LOCOMOTION

Limbed vertebrates move their limbs in a coordinated fashion during locomotion. During out of phase movements, such as walking and trotting, limbs alternate whereas during in phase movements, such as quadrupedal galloping, movements of a pair of limbs occur nearly at the same time (Grillner 1981; Rossignol 1996; Wetzel and Stuart 1976). A great deal of knowledge on this subject comes from work on cats in which hindlimbs are traditionally studied at the expense of forelimbs. In some of these studies the variance in interlimb stepping patterns has been emphasised and the facultative capabilities of neural control programs have been stressed while the association of interlimb coordination during

stepping with any known neuronal pathway has been viewed as highly speculative (English 1978; Forssberg et al. 1980). Contrasting this stance, Miller and colleagues (1975) have postulated that interlimb coordination in stepping occurs according to a few basic patterns with little emphasis on variance. According to this concept, each pattern is associated with a program and all of the characteristic patterns of locomotion are said to be a result of different interactions of these programs. That these concepts may not be mutually exclusive was proposed by English (1978).

The understanding of neural mechanisms responsible for interlimb coordination has been facilitated by the development of experimental replicas of locomotion. Models put forward to explain the central origin of vertebrate locomotion such as the half-center model (Brown 1911; 1914), the unit burst generator model (Grillner 1981) and the modular concept (Jordan 1991) all assume that neurons responsible for generating the rhythm of an individual limb are located ipsilaterally in the spinal cord while coordination between the left and the right hindlimbs is hypothesized to occur as the result of interactions between the sets of contralateral half-centers, modules or unit burst generators. Numerous studies (for review see McClellan 1996) have implicated reciprocal glycinergic inhibition in mediating these interactions. In contrast, the "bilateral shared core concept" (Stein et al. 1995) suggests that the contralateral spinal circuitry generates a part of the ipsilateral scratch rhythm, leading to the proposal that a bilateral neuronal core is shared by the left and right limb pattern generators, with elements coordinating interlimb phase embedded in the pattern generator. While this hypothesis explains well some aspects of turtle scratching the location of the bilateral neuronal core is not clear at present. Furthermore, its applicability in explaining the neuronal control of multi-limb locomotion in other vertebrates has not been established. Recent studies in which the spinal cord was split midsagittally (Kjaerulff and Kiehn 1996; Tao and Droge 1992) or chemically decoupled (Cowley and Schmidt 1995; Kremer and Lev-Tov 1997; Ho 1997; Bracci et al. 1996) demonstrate that locomotor rhythms for one limb persist in isolated hemicords. However, correct phase coupling characteristic of normal locomotion in these cases is clearly missing. Whether this is a result of removal of interactions between the

hemicords or bilateral neuronal core it is not presently clear.

CONCLUSIONS

At the beginning of the century Graham Brown (1911) proposed that the generation of the rhythmic stepping in the cat depends on mutual inhibition between the two half-centers exciting flexor and extensor motoneurons. While numerous studies confirmed the central origin of locomotion, they also emphasized the importance of modulatory and sensory inputs in adjusting the pattern to changing behavioral and environmental demands. These studies also revealed that spinal rhythmogenesis could result from cellular mechanisms that do not require synaptic inhibition, although inhibition is certainly necessary to ensure temporal phasing of motor patterns. However, details of the cellular mechanisms responsible for the switching of the activity between the two half-centers remain largely unknown. Despite the variety of preparations and methods used to address this question, interneurons associated with the half-centers are far from being fully identified. A major impediment being the difficulty in determining the patterns of interconnections between interneurons. Although studies in lower vertebrates (i.e., lamprey and *Xenopus*) have succeeded in approaching this goal, understanding the pattern generation in walking vertebrates remains in its infancy.

THESIS OBJECTIVES

The objective of this thesis was to investigate two major issues regarding the neural control of vertebrate locomotion: generation of central patterns for locomotion and the role of neuroactive substances in modulating centrally generated patterns. To reach this objective in a walking vertebrate, an *in vitro* preparation isolated from a mature aquatic amphibian mudpuppy (*Necturus maculatus*) was used, It consisted of the first five segments of the spinal cord and one or both forelimbs attached by their brachial nerves. This preparation proved to be well suited for this type of research as it displays the long

term viability typical of lower vertebrates while exhibiting the walking capabilities of higher vertebrates. Furthermore, it allows for simultaneous observation of the actual behaviour (i.e., rhythmic movements of the forelimbs) and recording of the motor output (EMG). Seminal work on swimming (lamprey and *Xenopus)* and immature preparations (neonatal rat, mouse, wallaby) has greatly advanced our understanding of the multileveled mosaic of locomotor mechanisms. However, the great number of cells and the immaturity of neonatal preparations, on one hand, and swimming, rather then walking behaviour , on the other hand, make it difficult to determine the functional significance of the data obtained from these preparations for the mature walking pattern. It is hoped that, by building on what is already known, this work may contribute to the formulation of new and more general ideas regarding control of locomotion in walking vertebrates.

The specific objectives for each project are outlined below, presented in the order in which the work commenced.

Chapters 2. and 3. Numerous studies have implicated neuroactive substances (serotonin, glycine, GABA) in initiating and/or shaping locomotion in different species. Therefore, specific goals of the first two studies were to validate the mudpuppy preparation pharmacologically and establish whether the same neuroactive substances, featuring prominently in lower and higher vertebrates, affect mudpuppy locomotor CPG in a similar fashion. An ensuing issue was to determine whether the effects of the modulatory substances were mediated solely via descending projections from supraspinal centres or endogenous modulatory networks residing in the spinal cord. In order to reach these goals combined pharmacological, electrophysiological and immunostaining techniques were used.

Chapter 4. CPG underlying forelimb locomotion in the mudpuppy is known to reside in the spinal cord segment spanning the third dorsal root. The objectives of this study were to investigate whether this network can be further divided into distinct CPG subunits governing rhythmic flexion and extension. As it has previously been shown that sensory input during locomotion represents an important source of corrective cues during locomotion, another objective of this study was to investigate how sensory input from the

moving limb affects the ongoing central program for locomotion.

Chapter 5. The objective of this study was to identify interneurons within previously described flexor and extensor centres and to classify them according to the phase of the step cycle when they were active. In addition, the link between the oscillatory properties of interneurons and the walking behaviour, and the connectivity between the interneurons and motoneurons were also explored.

Chapter 6. One of the important tasks of the spinal CPG is to maintain the proper left-right or interlimb coordination during locomotor activity. Therefore, the objective in this study was to examine the location of the rhythmogenic network underlying bipedal locomotion in the mudpuppy. For this purpose a novel preparation, containing the spinal cord and both forelimbs attached, was developed. By documenting the effects of acute transverse and midsagittal sectioning of the spinal cord on the overall locomotor pattern, an attempt was also made to discern a possible role of descending and segmental mechanisms in interlimb coordination.

Appendix Studies of locomotion and identification of underlying neurons rely heavily on tests such as ventral and dorsal root stimulation. Multiple hook or suction electrodes often present a poor choice due to the introduction of mechanical instability and overcrowding of the preparation. Here, a new method was tested that would reduce this complexity by removing rigidly held hook electrodes and replacing them with implantable intrafascicular electrodes.

REFERENCES

Akazawa K, Aldridge JW, Steeves JD, Stein RB (1982) Modulation of stretch reflexes during locomotion in the mesencephalic cat. J Physiol 329:553-567

Andersson O, Grillner, (1983) Peripheral control of cat's step cycle II. Entrainment of the central pattern generators for locomotion by sinusoidal hip movements during fictive locomotion. Acta Physiol Scand 118:229-239

Antal M, Berki ACs, Horvath L, O'Donovan M (1994) Developmental changes in distribution of GABA-immunoreactive neurons in the embryonic chick lumbosacral spinal cord. J Comp Neurol 341:1-9

Armstrong DM (1986) Supraspinal contributions to the initiation and control of locomotion in the cat. Prog Neurobiol 26:273-361

Ayers JL, Carpenter GA, Currie S, Kinch J (1983) Which behavior does the lamprey central motor program mediate? Science 221:1312-1314

Baev, KV, Degtyarenko AM, Zavadskaya TV, Kostyuk PG (1979) Activity of lumbar interneurons during fictitious locomotion in thalamic cat. Neurophysiology 11:244-250

Bajaron I, Gossard JP, Hultborn H (1992) Induction of *fos* expression by activity in the spinal rhythm generator for scratching. Brain Res 588:168-172

Barbeau H, Rossignol S (1990) The effects of serotonergic drugs on the locomotor pattern and on cutaneous reflexes of the adult chronic spinal cat. Brain Res 514:55-67

Barbeau H, Rossignol S (1991) Initiation and modulation of the locomotor pattern in the adult chronic spinal cat by noradrenergic, serotonergic and dopaminergic drugs. Brain Res 546:250-260

Barthe J-Y, Grillner S (1995) neurotensin induced modulation of spinal neurons and fictive swimming in the lamprey. J Neurophysiol 73:1308-1312

Bekoff A (1992) Neuroethological approaches to the study of motor development in chicks: achievements and challenges. J Neurobiol 23:1486-1505

Berkowitz A, Stein PSG (1994a) Activity of descending propriospinal axons in the turtle hindlimb enlargement during two forms of fictive scratching: broad tuning to regions of the body surface. J Neurosci 14:5089-5104

Berkowitz A, Stein PSG (1994b) Activity of descending propriospinal axons in the turtle

hindlimb enlargement during two forms of fictive scratching: phase analysis. J Neurosci 14:5105-5119

Bonnot A, Didier M (1998) Hemisegmental localization of rhythmic networks in the lumbosacral spinal cord of neonate mouse. Brain Res 793:135-148

Bracci E, Ballerini L, Nistri A (1996) Localization of rhythmogenic networks responsible for spontaneous bursts induced by strychnine and bicuculline in the rat isolated spinal cord. J Neurosci 16:7063-7076

Brown TG (1911) The intrinsic factors in the act of progression in the mammal. Proc R Soc Lond B Biol Sci 84:308-319

Brown TG (1914) On the nature of the fundamental activity of the nervous centers: together with the analysis of the conditioning of the rhythmic activity in the progression, and a theory of the evolution of function in the nervous system. J Physiol (Lond) 48:18-46

Buchanan JT (1996) Lamprey spinal interneurons and their role in swimming activity. Brain Behav Evol 48:287-296

Buchanan JT, Cohen AH (1982) Activities of identified interneurons, motoneurons, and muscle fibers during fictive swimming in the lamprey and effects of reticulospinal and dorsal cell stimulation. J Neurophysiol 47:948-960

Capaday C, Stein RB (1986) Amplitude modulation of the soleus H-reflex in the human during walking and standing. J Neurosci 6:1308-1313

Cazalets JR, Sqalli-Houssaini Y, Clarac F (1992) Activation of central pattern generators for locomotion by serotonin and excitatory amino acids in neonatal rat. J Physiol 455:187-204

Cazalets JR, Bertrand S, Sqalli-Houssaini Y, Clarac F (1998) GABAergic control of spinal locomotor networks in the neonatal rat. In: Kiehn O, Harris-Warrick R, Jordan L, Hultborn H, Kudo N (eds) Neural mechanisms for generating locomotor activity. Annals of the New York Academy of Sciences, New York, pp 168-180

Cherubini E, Gaiarsa JL, Ben-Ari Y (1991) GABA: an excitatory transmitter in early postnatal life. Trends Nuerosci 14:515-519

Conway BA, Hultborn H, Kiehn O (1987) Proprioceptive input resets central locomotor rhythm in the spinal cat. Exp Brain Res 68:643-656

Cowley KC, Schmidt BJ (1994) A comparison of motor patterns produced by N-methyl-

D-aspartate, acetylcholine and serotonin in the in vitro neonatal rat spinal cord. Neurosci Letts 171:147-150

Cowley KC, Schmidt BJ (1995) Effects of inhibitory amino acids antagonists on reciprocal inhibitory interactions during rhythmic motor activity in the in vitro neonatal rat spinal cord. J Neurophysiol 74:1109-1117

Dai X, Douglas JR, Nagy JI, Noga BR, Jordan LM (1990) Localization of spinal neurons activated during treadmill locomotion using *c-fos* immunohistochemical method. Soc Neurosci Abstr 16:889

Dale N (1991) The isolation and identification of spinal neurons that control movement in the *Xenopus* embryo. Eur J Neurosci 3:1025-1035

Delcomyn F (1980) Neural basis of rhythmic behavior in animals. Science 210:492-498

Dickinson PS (1995) Interactions among neural networks for behavior. Curr Opin Neurobiol 5:792-7981

Dickinson PS, Meccas C, Marder E (1990) Neuropeptide fusion of two motor pattern generator circuits. Nature 344:155-158

Duysens JD, Pearson KG (1980) Inhibition of flexor burst generation by loading ankle extensor muscles in walking cats. Brain Res 187:321-332

English AW (1978) Interlimb coordination during stepping in the cat: an electromyographic analysis. J Neurophysiol 42:229-243

Edgerton VR, Grillner S, Sjostrom A, Zangger P (1976) Central generation of locomotion in vertebrates. In: Herman R, Grillner S, Sjostrom A, Zangger P (eds) Neural control of locomotion. Plenum Press, New York, pp 439-464

Forssberg H (1979) Stumbling corrective reaction: a phase dependent compensatory reaction during locomotion. J Neurophysiol 42:936-953

Forssberg H, Grillner S, Halbertsma J, Rossignol S (1980) The locomotion of the low spinal cat. II. Interlimb coordination. Acta Physiol Scand 108:283-295

Fulton B, Walton KD (1981) Calcium dependent spikes in neonatal rat spinal cord *in vitro*. J Physiol 317:25-26P

Fulton B, Walton KD (1986) Electrophysiological properties of neonatal rat motoneurones studied *in vitro*. J Physiol 370:651-678

Getting PA (1988) Comparative analysis of invertebrate central pattern generators. In: Cohen AH, Rossignol S, Grillner S (eds) Neural control of rhythmic movements in vertebrates. Wiley and Sons, New York, pp 101-127

Getting PA (1989) Emerging principles governing the operation of neural networks. Ann Rev Neurosci 12:185-204

Getting PA, Dekin MS (1985) Mechanisms of pattern generation underlying swimming in *Tritonia*. IV. Gating of central pattern generator. J Neurophysiol 53:466-480
Grillner S (1981) Control of locomotion in bipeds, tetrapods, and fish. In: Brooks VB (ed) Handbook of physiology. American Physiological Society, Bethesda, MD, pp 1179-1236

Grillner S (1986) The effects of L-DOPA on the spinal cord-relation to locomotion and the half-center hypothesis. In: Grillner S, Stein PSG, Stuart DG, Forssberg H, Herman RM (eds) Neurobiology of vertebrate locomotion, Macmillan, London, pp 269-277

Grillner S, Rossignol S (1978) On the initiation of the swing phase of locomotion in chronic spinal cats. Brain Res 146:269-277

Grillner S, Zangger P (1979) On the central generation of locomotion in the low spinal cat Exp Brain Res 34:241-261

Grillner S, Wallen P (1985) The ionic mechanisms underlying N-methyl-D-aspartate receptor-induced, tetrodotoxin-resistant membrane potential oscillations in lamprey neurons active during locomotion. Neurosci Letts 60:289-294

Grillner S, Matsushima T (1991) The neural network underlying locomotion in lamprey-synaptic and cellular mechanisms. Neuron 7:1-15

Grillner S, Wallen P, Brodin L (1991) Neural network generating locomotor behavior in lamprey: circuitry, transmitters, membrane properties and simulation. Ann Rev Neurosci 14: 169-199

Grillner S, Wallen P, Brodin L, Lansner A (1991) Neuronal network generating locomotor behavior in lamprey. Ann Rev Neurosci 14:169-199

Grillner S, Parker D, El Manira A (1998) Vertebrate locomotion-A lamprey perspective. In: Kiehn O, Harris-Warrick R, Jordan L, Hultborn H, Kudo N (eds) Neural mechanisms for generating locomotor activity. Annals of the New York Academy of Sciences, New York, pp 1-18

Guertin P, Angel MJ, Perreault MC, McCrea DA (1995) Ankle extensor group I afferents excite extensors throughout the hindlimb during fictive locomotion in the cat J Physiol

(Lond) 487:197-209.

Hagevik A, McClellan A (1994) Coupling of spinal locomotor networks in larval lamprey revealed by receptor blockers for inhibitory amino acids: neurophysiology and computer modeling. J Neurophysiol 4:1810-1829

Harris-Warrick RM (1988) Chemical modulation of central pattern generators. In: Cohen AH, Rossignol S, Grillner S (eds) Neural control of rhythmic movements in vertebrates. Wiley and Sons, New York, pp 285-331

Harris-Warrick RM (1993) Pattern generation. Curr Opin Neurobiol 3:982-988

Harris-Warrick RM Marder E (1991) Modulation of neural networks for behavior. Ann Rev Neurosci 14:39-57

Hernandez P, Elbert K, Droge MH (1991) Spontaneous and NMDA evoked motor rhythms in neonatal mouse spinal cord: An in vitro study with comparison to in situ activity. Exp Brain Res 85:66-74

Hiebert GW, Whelan PJ, Prochazka A, Pearson KG (1995) Suppression of the corrective response to loss of ground support by stimulation of extensor group I afferents. J Neurophysiol 73:416-420

Hishinuma M, Yamaguchi T (1990) Cervical interneurons oligosynaptically excited from primary afferents and rhythmically active during forelimb fictive locomotion in the cat. Neurosci Letts 111:287-291

Ho S (1997) Rhythmic motor activity and interlimb co-ordination in the developing pouch young of a wallaby (*Macropus eugenii*). J Physiol 501:623-636

Hochman S, Jordan LM, MacDonald JF (1994) N-methyl-D-aspartate receptor-mediated voltage oscillations in neurons surrounding the central canal in slices of rat spinal cord. J Neurophysiol 72:565-577

Hounsgaard J, Kjaerulff O (1991) Ca^{+2} -mediated plateau potentials in a subpopulation of interneurons in the ventral horn of the turtle spinal cord. Eur J Neurosci 4: 183-188

Ichikawa Y, Terakado Y, Yamaguchi T (1991) Last order interneurons controlling activity of elbow extensor motoneurones during forelimb fictive locomotion in the cat. Neurosci Letts 121:37-39

Jankowska E, Jukes MGM, Lund S, Lundberg A (1967) The effects of DOPA on the spinal cord. 6. Half-centre organization of interneurons transmitting effect from the flexor

reflex afferents. Acta Physiol Scand 70:389-402

Jordan LM (1991) Brainstem and spinal cord mechanisms for the initiation of locomotion. In: Shimamura M, Grillner S, Edgerton VR (eds) Neurobiological basis of human locomotion. Tokyo, Japan Scientific Societies, pp 3-20

Kahn JA, Roberts A (1982) Experiments on the central pattern generator for swimming in amphibian embryos. Phyl Trans R Soc Lond B 296:229-243

Katz PS, Harris-Warrick RM (1990) Actions of neuromodulatory neurons in a simple motor system. Trends Neurosci 13:367-373

Kiehn O, Hounsgaard J, Sillar K (1997) Basic building blocks of vertebrate spinal central pattern generators. In: Stein PSG, Grillner S, Selverston AI, Stuart DG (eds) Neurons networks and motor behavior. The MIT Press, Cambridge, MA, pp 47-59

Kiehn O, Kjaerulff O (1998) Distribution of central generators for rhythmic motor outputs in the spinal cord of limbed vertebrates. In: Kiehn O, Harris-Warrick R, Jordan L, Hultborn H, Kudo N (eds) Neural mechanisms for generating locomotor activity. Annals of the New York Academy of Sciences, New York, pp 110-129

Kiehn O, Kjaerulff O (1996) Spatiotemporal characteristics of 5-HT and dopamine-induced hindlimb locomotor activity in the in vitro neonatal rat. J Neurophysiol 75:1472-1482

Kjaerulff O, Barajon I, Kiehn O (1994) Sulphrhodamine-labelled cells in the neonatal rat spinal cord following chemically induced locomotor activity in vitro. J Physiol 478:265-273

Kjaerulff O, Kiehn O (1996) Distribution of networks generating and coordinating locomotor activity in the neonatal rat spinal cord in vitro: a lesion study. J Neurosci 16:5777-5794

Kling U, Székely (1968) Simulation of rhythmic nervous activities. I. Function of networks with cyclic inhibitions. Kybernetik 5:89-103

Kremer E, Lev-Tov A (1997) Localization of the spinal network associated with generation of hindlimb locomotion in the neonatal rat and organization of its transverse coupling system. J Neurophysiol. 77:1155-1170

Krieger P, Tegner J, El Manira A, Grillner S (1994) Effects of metabotropic glutamate receptors activation on the cellular and network level in the lamprey spinal cord. Neuroreport 5:1760-1762

Kriellaars DJ, Brownstone RM, Noga BR, Jordan LM (1994) Mechanical entrainment of fictive locomotion in decerebrate cat. J Neurophysiol 71:2074-2086

Kudo N. Yamada T (1987) N-methyl-D,L-aspartate-induced locomotor activity in a spinal cord-hindlimb muscle preparation of the newborn rat studied in vitro. Neurosci Letts 75:43-48

Landmesser L, O'Donovan MJ (1984) Activation patterns of embryonic chick hindlimb muscles recorded *in ovo* and in an isolated spinal cord preparation. J Physiol 347:189-204

Lundberg A (1979) Multisensory control of spinal reflex pathways. Prog Brain Res 30:11-28

McClellan AD (1996) Organization of spinal locomotor networks: contributions from model systems. Comments Theor Biol 4:63-91

Marder E, Calabrese RL (1996) Principles of rhythmic motor pattern generation. Physiol Rev 76:687-717

McCrea DA, Shefchyk SJ, Stephens MJ, Pearson KG (1995) Disynaptic group I excitation of synergist ankle extensor motoneurones during fictive locomotion. J Physiol (Lond) 487:527-539

Miller S, van der Burg J, van der Meche FGA (1975) Locomotion in the cat: basic programmes of movement. Brain Res 91: 239-253

Meyrand PJ, Simmers J, Moulins (1991) Construction of a pattern generating circuit with neurons of different networks. Nature Lond 351:60-63

Miyata Y, Nakano S, Yashuda H (1987) Postnatal transient expression of long lasting descending inhibitory effects on spinal reflexes in the rat. Neurosci Res 4:268-278

O'Donovan MJ, Sernagor E, Sholomenko G, Ho S, Antal M, Yee W (1992) Development of spinal motor networks in the chick embryo. J Neurosci 14:6354-6369

O'Donovan MJ, Ritter A (1995) Optical recording and lesioning of spinal neurons during rhythmic activity in the chick embryo spinal cord. In: Taylor A, Gladden MH, Durbaba R (eds) Alpha and gamma motor systems. Plenum press, New York and London, pp 557-563

Orlovsky GN, Feldman AG (1972) Classification of lumbosacral neurons by their discharge pattern during evoked locomotion. Neurophysiology 4:311-317

Paggett KC, Gupta V, McClellan AD (1998) Adaptive variations of undulatory behaviors in larval lamprey: comparison of swimming and burrowing. Exp Brain Res 119:213-223

Pearson KG (1993) Common principles of motor control in vertebrates and invertebrates. Ann Rev Neurosci 16:265 297

Pearson KG (1993) Proprioceptive regulation of locomotion. Curr Opin Neurobiol 5:786-791

Pearson KG, Collins DF(1993) Reversal of the influence of group Ib afferents from plantaris on activity in medial gastrocnemius muscle during locomotor activity. J Neurophysiol 70:1009-1017

Pearson KG, Ramirez JM (1997) Sensory modulation of pattern-generating circuits. In: Stein PSG, Grillner S, Selverston AI, Stuart DG (eds) Neurons networks and motor behavior. The MIT Press, Cambridge, MA, pp 225-235

Perret C, Cabelguen JM (1976) Central and reflex participation in the timing of locomotor activations of a bifunctional muscle, the semi-tendinosus, in the cat. Brain Res 106:390-395

Perret C (1986)Synaptic influences contributing to the pattern of limb motoneuron activity during fictive locomotion in the cat. In: Grillner S, Stein PSG, Stuart DG, Forssberg H, Herman RM (eds) Neurobiology of vertebrate locomotion. Macmillan Press, pp 173-184

Prochazka A (1996) Proprioceptive feedback and movement regulation. In: Rowell L and Sheperd JT (eds) Handbook of physiology. American Physiological Society, Bethesda, MD, pp 89-127

Prochazka A, Gillard D, Bennett DJ (1997) Positive force feedback control of muscles. J Neurophysiol 77:3226-3236

Prochazka A, Gillard D, Bennett DJ (1997) Implications of positive feedback in the control of movement. J Neurophysiol 77:3237-3251

Puskar Z, Antal M (1997) Localization of last order interneurons in the lumbar spinal cord of rats. J Comp Neurol 389:377-389

Roberts A, Clarke JDW (1982) The neuroanatomy of an amphibian embryo spinal cord Phyl Trans Roy Soc B 296:195-212

Roberts A, Perrins R (1995) Positive feedback as a general mechanism for sustaining rhythmic and non-rhythmic activity. J Physiol (Paris) 89:241-248

Roberts A, Tunstall MJ (1990) Mutual re-excitation with post inhibitory rebound: A simulation study on the mechanisms for locomotor generation in the spinal cord of *Xenopus* embryos. Eur J Neurosci 2:11-23

Roberts A, Soffe SR, Perrins R (1997) Spinal networks controlling swimming in hatchling *Xenopus* tadpoles. In: Stein PSG, Grillner S, Selverston AI, Stuart DG (eds) Neurons networks and motor behavior. The MIT Press, Cambridge, MA, pp 83-89

Roberts A, Soffe SR, Wolf ES, Yoshida M, Zhao FY (1998) Central circuits controlling locomotion in young frog tadpoles. In: Kiehn O, Harris-Warrick R, Jordan L, Hultborn H, Kudo N (eds) Neural mechanisms for generating locomotor activity. Annals of the New York Academy of Sciences, New York, pp 19-34

Roberts A, Soffe SR, Dale N (1986) Spinal interneurons and swimming in frog embryos. In: Grillner S. et al., Neurobiology of vertebrate locomotion. Macmillan, London and New York, pp 279-306

Rossignol S (1996) Neural control of stereotypic limb movements. In: Rowell L and Sheperd JT (eds) Handbook of physiology. American Physiological Society, Bethesda, MD, pp 174-216

Rossignol S, Chau C, Brustein E, Giroux N, Bouyer H, Barbeau H, Reader TA (1998) Pharmacological activation and modulation of the central pattern generator for locomotion in the cat. In: Kiehn O, Harris-Warrick R, Jordan L, Hultborn H, Kudo N (eds) Neural mechanisms for generating locomotor activity. Annals of the New York Academy of Sciences, New York, pp 346-359

Rossignol S, Lund JP, Drew T (1988) the role of sensory inputs in regulating pattern of rhythmical movements in higher vertebrates. In: Cohen AH, Rossignol S, Grillner S (eds) Neural control of rhythmic movements in vertebrates. Wiley and Sons, New York, pp 201-283

Sakatani K, Hassan AZ, Chesler M (1991) $GABA_A$ sensitivity of dorsal column axons and in vitro comparison between adult and neonatal rat spinal cords. Dev Brain Res 61:139-142

Saruhashi Y, Young W, Hassan AZ, Park R (1994) Excitatory and inhibitory effects of serotonin on spinal axons. Neuroscience 61:645-653

Shik ML (1997) Locomotor patterns elicited by electrical stimulation of the brain stem in the mudpuppy. Motor Control 1:354-368

Sigvardt KA (1989) Modulation of properties of neurons underlying rhythmic movements in vertebrates. Semin Neurosci 1:55-65

Sillar KT (1991) Spinal pattern generation and sensory gating mechanisms. Curr Opin Neurobiol 1:583-589

Sillar KT (1989) Synaptic modulation of cutaneous pathways in the vertebrate spinal cord. Semin Neurosci 1:45-54

Sillar KT, Kiehn O, Kudo N (1997) Chemical modulation of vertebrate motor circuits. In: Stein PSG, Grillner S, Selverston AI, Stuart DG (eds) Neurons networks and motor behavior. The MIT Press, Cambridge, MA, pp 183-193

Soffe SR (1993) Two distinct rhythmic motor patterns are driven by common premotor and motor neurons in a simple vertebrate spinal cord. J Neurosci 13:4456-4469

Smith JC, Feldman JL, Schmidt BJ (1988) Neural mechanisms generating locomotion studied in mammalian brain stem-spinal cord in vitro. FASEB J 2:2283-2288

Staras K, Kemenes G, Benjamin PR (1998) Pattern-generating role for motoneurons in a rhythmically active neuronal network. J Neurosci 18:3669-3688

Stein PSG (1984) Central pattern generators in the spinal cord. In: Davidoff RA (ed) Handbook of the spinal cord: anatomy and physiology. Dekker, New York, Vol. 2-3:647-672

Stein PSG, Smith JL (1997) Neural an biomechanical strategies for different forms of vertebrate hindlimb motor tasks. In: Stein PSG, Grillner S, Selverston AI, Stuart DG (eds) Neurons networks and motor behavior. The MIT Press, Cambridge, MA, pp 62-73

Stein PSG, Victor JC, Field EC, Currie SN (1995) Bilateral control of hindlimb scratching in the spinal turtle: contralateral spinal circuitry contributes to the normal ipsilateral motor pattern of fictive rostral scratching. J Neurosci 15:4343-4355

Székely G (1965) Logical network for controlling limb movements in urodela. Acta Physiol Acad Sci Hung 27:285-289

Székely G Czéh G, Voros G (1969) The activity pattern of limb muscles in freely moving normal and deafferented newts. Exp Brain Res 9:53-62

Tao Y, Droge MH (1992) Comparison of spontaneous motor pattern generation in non-hemisected and hemisected mouse spinal cord. Neurosci Letts 144:116-120

Terakado Y, Yamaguchi T (1990) Last order interneurons controlling activity of elbow flexor motoneurons during forelimb fictive locomotion in the cat. Neurosci Letts 111:292-296

Viala D, Buisseret-Delmas C, Portal JJ (1988) An attempt to localize the lumbar locomotor generator in the rabbit using 2-deoxy-^{14}C glucose autoradiography. Neurosci Letts 86:139-143

Viala D, Viala G, Jordan L (1991) Interneurons of the lumbar cord related to spontaneous locomotor activity in the rabbit. Rhythmically active inetrneurones. Exp Brain Res 84:177-186

Wallén P (1997) Spinal networks and sensory feedback in the control of undulatory swimming in lamprey. In: Stein PSG, Grillner S, Selverston AI, Stuart DG (eds) Neurons networks and motor behavior. The MIT Press, Cambridge, MA, pp 76-81

Wallén P, Ekeberg O, Lansner A, Brodin L, Traven H, Grillner S (1992) A computer model for realistic simulation of neural networks. II. The segmental network generating locomotor rhythmicity in the lamprey. J Neurophysiol 68:1939-1950

Walton KD, Fulton B (1986) The ionic mechanisms underlying the firing properties of rat neonatal motoneurons studied *in vitro*. Neuroscience 19:669-683

Wetzel MC, Stuart DG (1976) Ensemble characteristics of cat locomotion and its neural control. Prog Neurobiol 7:1-98

Whelan PJ, Hiebert GW, Pearson KG (1995) Stimulation of the group I extensor afferents prolongs the stance phase in walking cats. Exp Brain Res 103:20-30

CHAPTER 2

SEROTONERGIC MODULATION OF THE MUDPUPPY (*Necturus maculatus*) LOCOMOTOR PATTERN *IN VITRO*

INTRODUCTION

Rhythmic stereotyped movements such as locomotion can be generated within the central nervous system (CNS) by neuronal networks called central pattern generators (CPGs; Delcomyn 1980; Grillner 1985). However, the functional CPG needs to be continuously shaped by the activity of extrinsic modulatory inputs and sensory feedback to assure that it is generating the most appropriate behavior for each situation. Numerous comparative studies (Getting and Dekin 1985; Grillner et al. 1991; Harris-Warrick 1988; Marder 1987; Ramirez and Pearson 1991) have shown that the activity of these networks can be triggered and/or modulated by several neuroactive substances, including 5-HT. *In vitro* preparations as well as reduced chronic preparations of vertebrate spinal cord, displaying rhythmic motor output, in combination with the selective pharmacological agents have been used to increase our understanding of 5-HT's role in the control of locomotion. In neonatal rats, 5-HT has been shown to initiate an alternating pattern of left and right ventral root bursts as well as to modulate the frequency of the fictive locomotion (Cazalets et al. 1992). 5-HT also alters neural activity underlying swimming in newly hatched *Xenopus laevis* tadpoles by increasing the duration and intensity of ventral root motor bursts in each cycle (Sillar et al. 1992). In the adult lamprey, 5-HT markedly increases the duration of ventral root discharge during each cycle and reduces locomotor frequency (Harris-Warrick and Cohen 1985; Christenson et al. 1989).

A version of this chapter has been published. Jovanović K, Petrov T, Greer JJ, Stein RB (1996) Exp Brain Res 111:57-67

In addition, 5-HT depresses transmission from reticulospinal neurons that are involved in the control of locomotion (Buchanan and Grillner 1991). In adult mammals, 5-HT-mediated transmission appears not to be essential for initiation of locomotion (Barbeau and Rossignol 1991; Steeves et al. 1980). Nevertheless, 5-HT has been shown to modulate the locomotor pattern of chronic spinal cat walking on a treadmill in chronic experiments (Barbeau and Rossignol 1990) with the most prominent action being an increase in step length and an augmentation of contraction in hindlimb extensor and flexor muscles. In paralyzed rabbits, 5-HT released by a treatment with its precursor 5-hydroxytryptofan (5-HTP) enhances the amplitude of EMG bursts predominantly in the flexors, and induces locomotion in acute spinal rabbits (Viala and Buser 1969). Thus, 5-HT can be involved either in initiation or modulation of certain motor behaviors and it acts to enhance or regulate the motor pattern.

We have begun to study systems modulating the CPG for locomotion in the mudpuppy *(Necturus maculatus)*. Although an aquatic amphibian, the mudpuppy walks with an alternating quadrupedal gait (Wheatley et al. 1992) allowing one to study walking in a well developed adult organism. In addition, it displays the long term viability and simplicity typical of lower vertebrate preparations, as well as the morphological characteristics and walking capability of higher vertebrate preparations. In this report we demonstrate modulatory actions of 5-HT on the locomotor rhythmogenesis in the isolated spinal cord of the mudpuppy. When bath applied, after NMDA-induced locomotion, 5-HT causes a dose-dependent increase in the step cycle duration and enhances the duration of the EMG bursts. While these experiments show that 5-HT can affect the CPG for locomotion, they do not provide conclusive evidence that the endogenous serotonergic system exerts the same effects. To investigate whether an endogenous serotonergic system is present in the mudpuppy spinal cord we have used a combination of 5-HT receptor antagonists and an uptake inhibitor in conjunction with immunocytochemical labeling of 5-HT. Our combined pharmacological and anatomical results suggest that 5-HT may play an important role in adjusting the CPG rhythm to produce adaptive movements appropriate for continually changing environmental demands.

MATERIALS AND METHODS

In vitro preparation

Twenty seven adult mudpuppies (20-30 cm long) were used for the pharmacological part of the study. The *in vitro* preparation was isolated as described by Wheatley et al. (1992). Following anaesthesia by immersion in a solution of 3-aminobenzoic-acid ethyl ester (1 g/l, Sigma), a dorsal laminectomy was performed from the first to the fifth vertebrae. The first five segments of the spinal cord with the attached forelimb were than removed from the rest of the body and placed in a Sylgard-lined petri dish superfused with cooled (15° C) and oxygenated Ringer's solution of the following composition (mM): 115 NaCl; 2 $CaCl_2$; 2 KCl; 1 $MgCl_2$; 5 Hepes; glucose 1 g/l, pH 7.3. While in the petri dish, the brachial plexus was exposed, the paraspinal muscles removed and bipolar teflon coated silver wires (75 μm) inserted into the elbow flexor *(Brachialis)* and extensor *(Extensor ulnae)* muscles for electromyographic (EMG) recording during locomotion. After a recovery period of approximately one hour, the preparation was transferred to a recording chamber and placed dorsal side up. The spinal cord and the forelimb were then stabilized by pinning the vertebral column and the procoracoid cartilage to the Sylgard Resin (Dow Corning) coating the base of the chamber. Throughout the course of experiments, the preparation was superfused with a cooled (15-18° C) and oxygenated spinal cord Ringers at a flow rate 5-10 ml/min.

Locomotion was induced chemically by adding 60 μM NMDA together with 10 μM D-Serine (D-Ser) to the superfusate (Wheatley et al. 1992). After a well defined walking pattern was established (approximately 15 min. following NMDA), 5-HT and related substances were applied directly into the bath. Each cycle of drug application was followed by washout with Ringer's solution. The cycle was repeated several times with locomotion being induced each time by superfusing the preparation with NMDA and D-Ser. Both NMDA and D-Ser were obtained from Sigma. 5-HT, 5-HT uptake inhibitor zimelidine, 5-HT_{1A} agonist (+)-8-hydroydipropyl-aminotetralin hydrobromide (8-OH-DPAT), non-selective 5-HT_2 /5-HT_1 antagonist methysergide maleate, nonselective 5-HT_1/5-HT_2 antagonist methiothepin mesylate, 5-HT_{2C} antagonist cyproheptadine HCl, 5-

HT_3 antagonists granisetron and tropisetron were obtained from Research Biochemicals Incorporated (Natick, USA). All drugs were freshly prepared (4 mM) in Ringer's solution and diluted to the appropriate concentration prior to use. To test their effects, 5-HT receptor antagonists were first applied to the bath alone. In separate trials the same antagonists were administered following the agonist application.

The effects induced by applying different concentrations of drugs were monitored and simultaneously recorded. EMG recordings were preamplified, high-pass filtered (10 Hz), rectified and low-pass filtered (300 Hz) and stored on a computer's hard disk using a commercially available disk storage program (Axotape, Axon Instruments). All channels of data were digitally sampled at 50 Hz and later analyzed using a customized software package written by Drs. Sophie De Serres and Marc Bélanger. All results presented, were analyzed using paired Student's t-tests and were significant at $P<0.05$. The results were expressed as mean±SD. EC_{50} and IC_{50} represent concentrations at which 50% of the maximum excitatory and inhibitory effects were observed, respectively. These values were derived using a non-linear least squares fit to Menton-Michaelis kinetics.

Immunocytochemistry

A total of eight adult mudpuppies were used. After anaesthesia in 3-aminobenzoic acid ethyl ester a laminectomy of the entire spinal column was performed. The animals were spinalized by sectioning the spinal cord at the caudal border of the medulla. The spinal cords were then removed from the rest of the body and fixed by immersion in ice cold 4% paraformaldehyde in 0.1 M phosphate buffer (pH 7.4). Tissues were kept in the solution overnight and then, for cryoprotection, transferred to 30% sucrose solution at 4°C for 3-4 hours. Spinal cords were partitioned into segments before sectioning. After being frozen and cut either coronally or horizontally, the cryostat sections were then processed for 5-HT immunocytochemistry. Two series of coronal sections (45 μm in thickness) of the spinal cords from four animals were collected in PBS. One series was processed immunocytochemically; the second one was kept for the control of the immunocytochemical reaction. The spinal cords of another four animals were cut horizontally (45 μm) and all sections were stored in separate wells to keep them in order.

For the immunocytochemical visualization of 5-HT, free floating sections were incubated for 12-14 hours with anti-rabbit 5-HT antibody (Cambridge Research Biochemicals, Cambridge, U.K.),diluted 1:1500 in 0.1 M PBS, containing O. 3% Triton X-100 and 2% normal goat serum. Tissues were then processed according to the ABC method of Hsu et al. (1981) as previously described (Petrov et al. 1992). Briefly, following 3 x 10 min rinses in PBS they were sequentially reacted with biotinylated goat anti-rabbit antibody (1:200) for 2 hours and ABC reagent (1:100) for 1 hour (Vector Labs Inc., Burlingame, CA). After 3 x 10 min rinses in PBS, sections were treated with 0.05% diaminobenzidine and 0.035% hydrogen peroxide in 0.1 M PBS for 4-5 min. All incubations were carried out at room temperature. No immunocytochemical staining was observed in control sections, processed after omission of the primary antibody.

RESULTS

Pharmacology

The central pattern generator for locomotion in the isolated mudpuppy spinal cord was activated by adding 60 μM NMDA and 10 μM D-Ser to the superfusing Ringer's solution. The induced locomotor pattern was similar to that recorded in intact animals walking on an underwater treadmill (Wheatley et al. 1992). The locomotor activity developed over the first 15 minutes after the beginning of the superfusion, reaching a steady state within the next 5-10 minutes. Then, the preparation would continue with well-coordinated locomotion for 2-4 hours. At the end of this period, the locomotor pattern would become unstable. To recover a regular alternating pattern, the preparation was washed with Ringer's solution for 30-60 min. Following the onset of the wash, locomotor activity would stop completely within 15-60 minutes. Locomotion could be induced repeatedly over a 2- to 4-day period.

When applied to the bath alone, 5-HT (0.1-100 μM) was not capable of initiating locomotion. However, when an application of 5-HT followed NMDA-induced locomotion, the walking pattern was altered. The most pronounced effect was an increase

in the step cycle duration. Thus, following an application of 5-HT the frequency of the locomotor rhythm was reduced. This effect was dose-dependent (EC_{50}~10 μM) and it reached its maximum (72% increase in the cycle duration) with 75 μM 5-HT in the bath (n=9; Fig. 2-1).

Two experimental paradigms were used to determine the presence of the endogenous release of 5-HT. First, the 5-HT uptake blocker zimelidine (0.1-100 μM) was applied to the bath. Like 5-HT, zimelidine caused an increase in EMG burst durations and reduced the frequency of the locomotor rhythm (Fig. 2-2) in a dose-dependent (EC_{50}~0.5 μM; n=4) and reversible manner. At saturation, the resulting increase in the cycle duration was 47%. Second, the actions of selected agonists and antagonists against subtypes of 5-HT receptors were tested. In all cases they were tested in at least three different experiments.

Among the antagonists only methiothepin, a nonselective 5-HT_1/5-HT_2 antagonist, altered the cycle duration in a way opposite to 5-HT's action. This effect was readily observable when methiothepin was applied (0.1-100 μM) prior to 5-HT. Following the application of methiothepin, the cycle duration decreased in a dose-dependent (IC_{50}~10 μM; n=5), reversible manner and an apparent saturation of the effect was observed with between 60 and 100 μM methiothepin in the bath (Fig. 2-3). At saturation the resulting decrease in the cycle duration was 50%. In contrast, when preceded with 5-HT, the application of methiothepin caused no significant change in the locomotor pattern. The effects of 5-HT were not reversed by applying the 5-HT_3 antagonist granisetron and tropisetron nor the 5-HT_{2C},, antagonist cyproheptadine and non-selective 5-HT_2 /5-HT_1 receptor antagonist methysergide. The latter, not only failed to antagonize 5-HT effects but also displayed an agonist-like action on the locomotor frequency. This effect was reversible.

Among the agonists, only 5-HT_{1A} agonist 8-OH-DPAT was tested. The drug not only failed to mimick the effect of 5-HT but also in 1 case (out of three) acted as an antagonist, causing a decrease of the cycle duration.

Figure 2-1. Effects of 5-HT on NMDA-induced locomotion *in vitro*
(A) The perturbations of the locomotor rhythm caused by exogenously applying 5-HT were observed by means of EMG recordings. Traces on the left side represent rectified and smoothed EMG activity recorded from flexor and extensor ulnae muscles. When 5-HT was added to the bathing solution at the concentrations indicated, there was a dose-dependent increase in the cycle duration and a prolongation of the EMG burst. At the same time, no change in the alternating pattern between antagonistic muscles was observed. **(B)** 5-HT dose-response curve summarizing the changes in the cycle duration produced by increasing concentrations of 5-HT. The cycle duration (expressed as a fraction of a control cycle duration before application of 5-HT) is plotted *versus* the concentration of 5-HT in the bathing solution. The curve was generated from data compiled from nine animals. Each point shows the mean±SD.

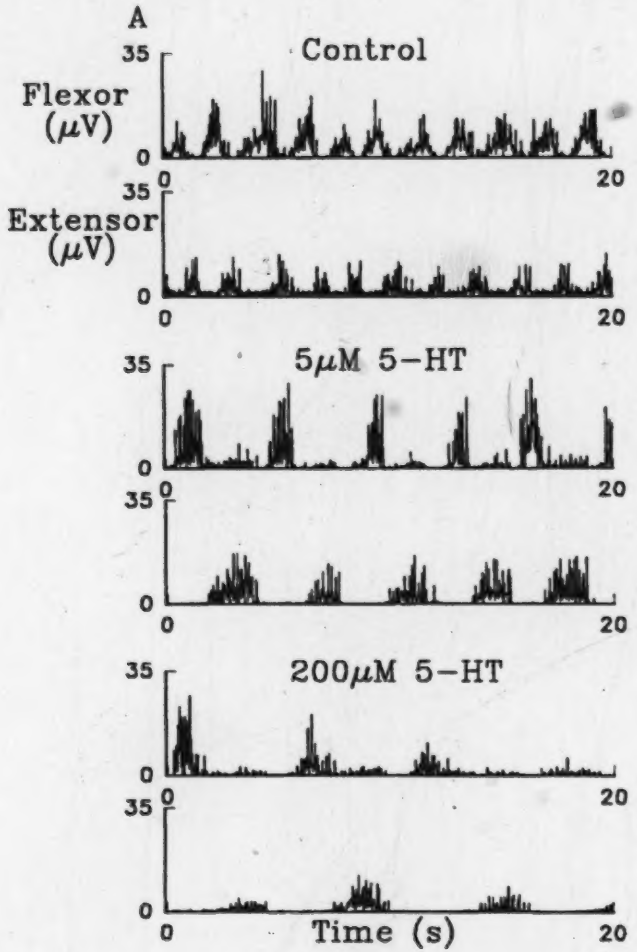
A
Control
Flexor
(μV)
Extensor
(μV)
5μM 5-HT
200μM 5-HT
35
0
20
Time (s)

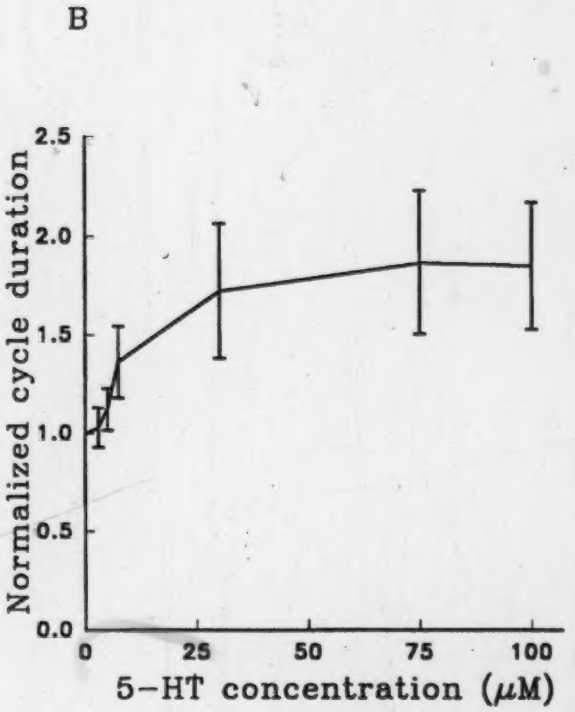
B
Normalized cycle duration
2.5
2.0
1.5
1.0
0.5
0.0
0
25
50
75
100
5-HT concentration (μM)

Figure 2-2. Effects of 5-HT uptake inhibition on NMDA induced locomotion. **(A)** An inhibition of 5-HT uptake mechanisms mimicked the effects previously observed with 5-HT. When applied to the spinal cord bathing solution, zimelidine caused a dose-dependent increase in the step cycle duration as well as a prolongation of EMG bursts. **(B)** Summary of the effect of increasing concentration of zimelidine on the cycle duration. The data from four animals illustrate a dose-dependent increase in the cycle duration, with the most pronounced effects observed at small concentrations of the drug.

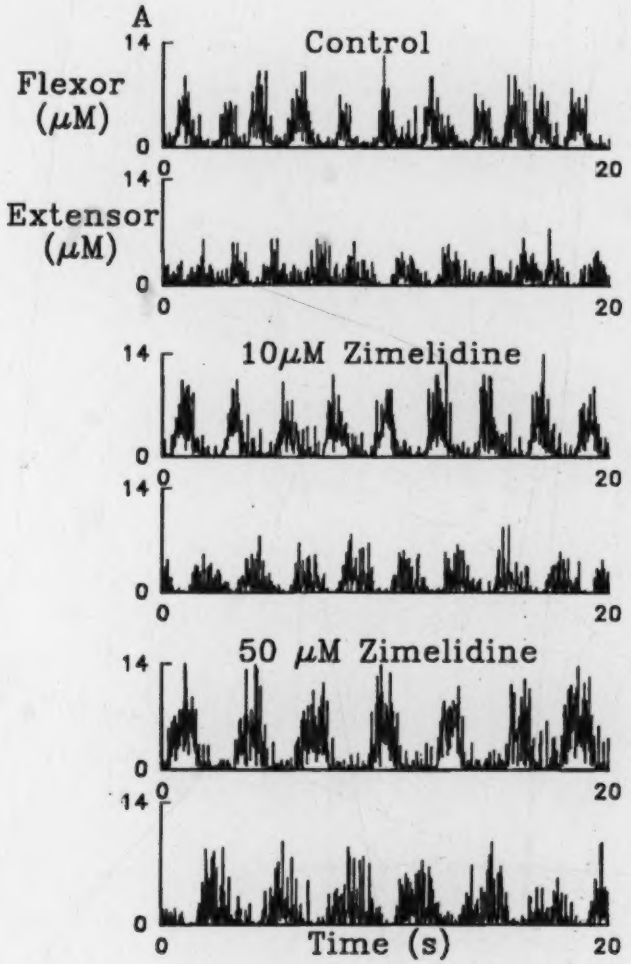
A
Control
Flexor
(μM)
Extensor
(μM)
10μM Zimelidine
50 μM Zimelidine
14
0
20
Time (s)

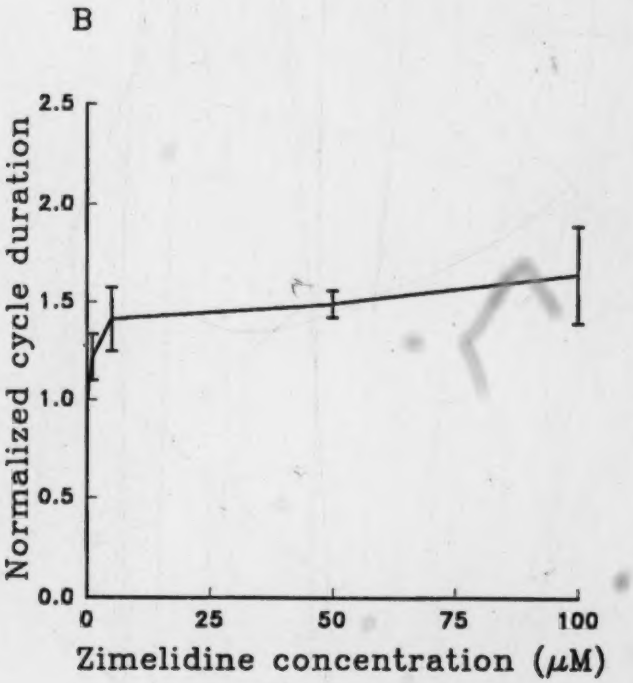
B
Normalized cycle duration
2.5
2.0
1.5
1.0
0.5
0.0
0
25
50
75
100
Zimelidine concentration (μM)

Figure 2-3. Effects of non-specific 5-HT_1/ 5-HT_2 receptor antagonist methiothepin on NMDA-induced locomotion. **(A)** Methiothepin was capable of antagonizing endogenously released 5-HT. When applied to the bath alone, methiothepin caused a reduction of the cycle duration and a decrease in the EMG bursts without affecting the reciprocal EMG pattern. **(B)** Effects of increasing concentrations of methiothepin on the cycle duration are summarized from four animals and plotted against the antagonist concentration in the bathing solution.

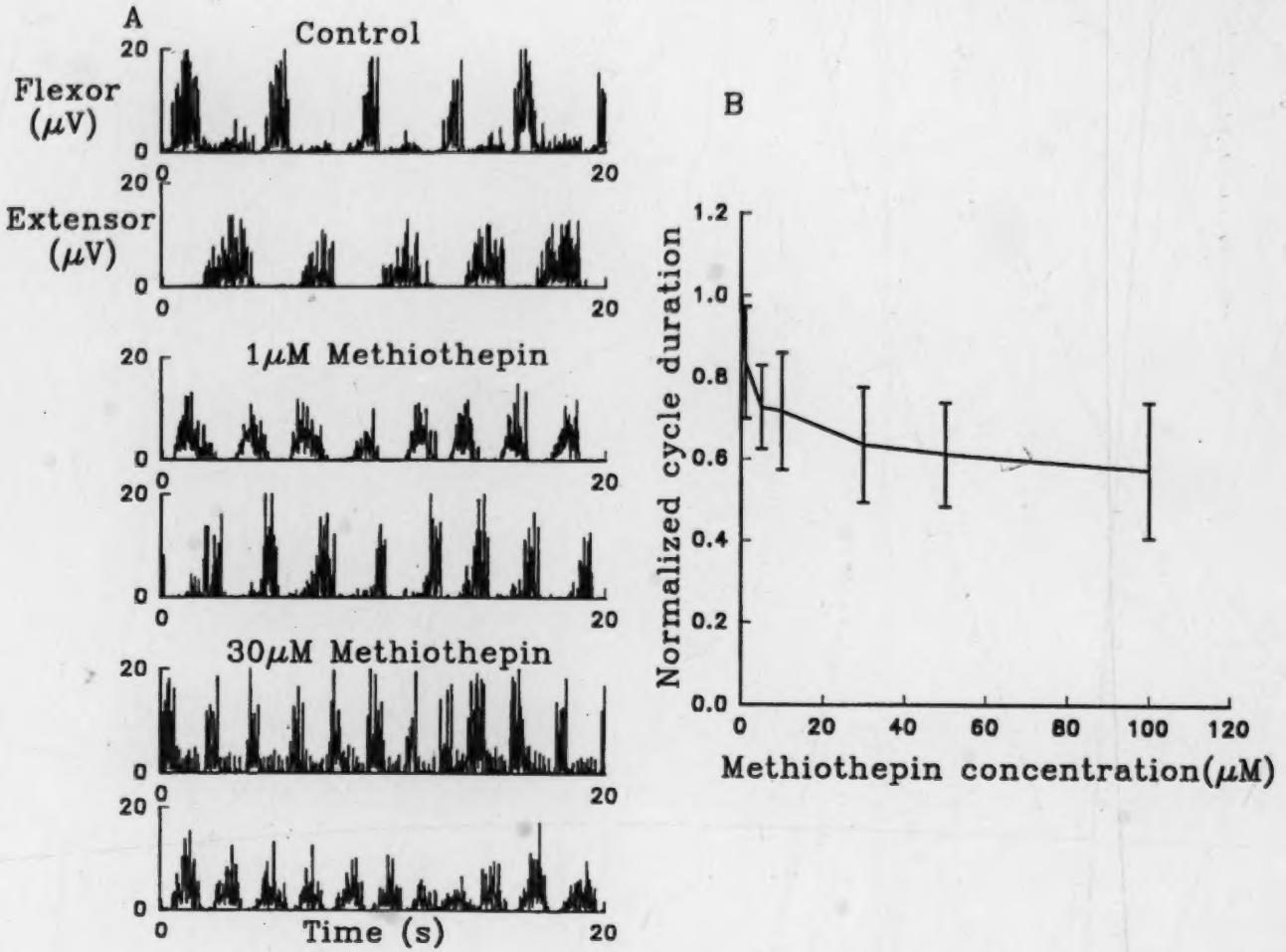
A
Control
Flexor
(μV)
Extensor
(μV)
1μM Methiothepin
30μM Methiothepin
Time (s)
B
Normalized cycle duration
Methiothepin concentration(μM)

Immunocytochemistry

Cell bodies

5-HT immunoreactive cell bodies were found at all levels of the spinal cord. They were observed grouped in clusters or as solitary neuronal profiles within the grey matter or at the border between the grey and white matter (Fig. 2-4). The vast majority of the 5-HT profiles was observed in the vicinity of the central canal and ventral to it (300-450 μm below the dorsal surface of the spinal cord).

Our observations concerning the rostro-caudal distribution of 5-HT neuronal somata are primarily derived from tissues that were sectioned horizontally. This method allowed us to study in greater detail the localization of the somata and the arborization pattern of the 5-HT immunoreactive processes, because the neurons rarely overlap as is the case when the staining is observed on coronal sections (compare Fig. 2-4 and Fig. 2-5). The greatest density of 5-HT immunoreactive profiles was observed between segments 2 and 6 where seven to ten cells could be detected per segment on each side of the midline. Between segments 7 and 10 the number of the immunoreactive neuronal profiles decreased to three or four per segment, and this number was even lower between segments 11-14, where we were not able to detect more than one or two cells per segment. Between segments 15 and 21 we observed an increase in the number of immunoreactive cells which was comparable to the numbers observed in the cervical segments (i.e., seven or eight cells per segment). Caudal to that level, we observed 1-3 neurons per segment, and in some cases there were segments that were devoid of 5-HT immunoreactive neuronal profiles.

In the spinal cord of the mudpuppy we were able to distinguish two morphologically distinct types of 5-HT-containing neurons intermixed in the grey matter and close to the central canal. Type I neurons were bipolar (Fig. 2-5 A. C) or multipolar (Fig. 2-5 B) cells with oval shape (15- 18 μm in diameter) with processes extending primarily in the lateral direction in the white matter. Very often the processes bifurcated forming a T shape with one collateral oriented rostrally and the other, in the opposite caudal direction (Figs. 2-5 C, 2-6 D).

Figure 2-4. Coronal sections through the spinal cord showing radially oriented processes of a group of 5-HT immunoreactive neurons in the fourth segment **(A)** and a single bipolar neuron in the seventh segment (*arrow* in **B**). Note that the grey matter, where the immunoreactive somata are located, has a gelatinous appearance, and can be clearly distinguished from the white matter (penetrated by immunopositive processes) which has a more compact appearance. The central canal is to the left. The dorsal (D) and lateral (L) directions are indicated by arrows in the upper right corner of each photomicrograph. *Scale bar* 30 μm.

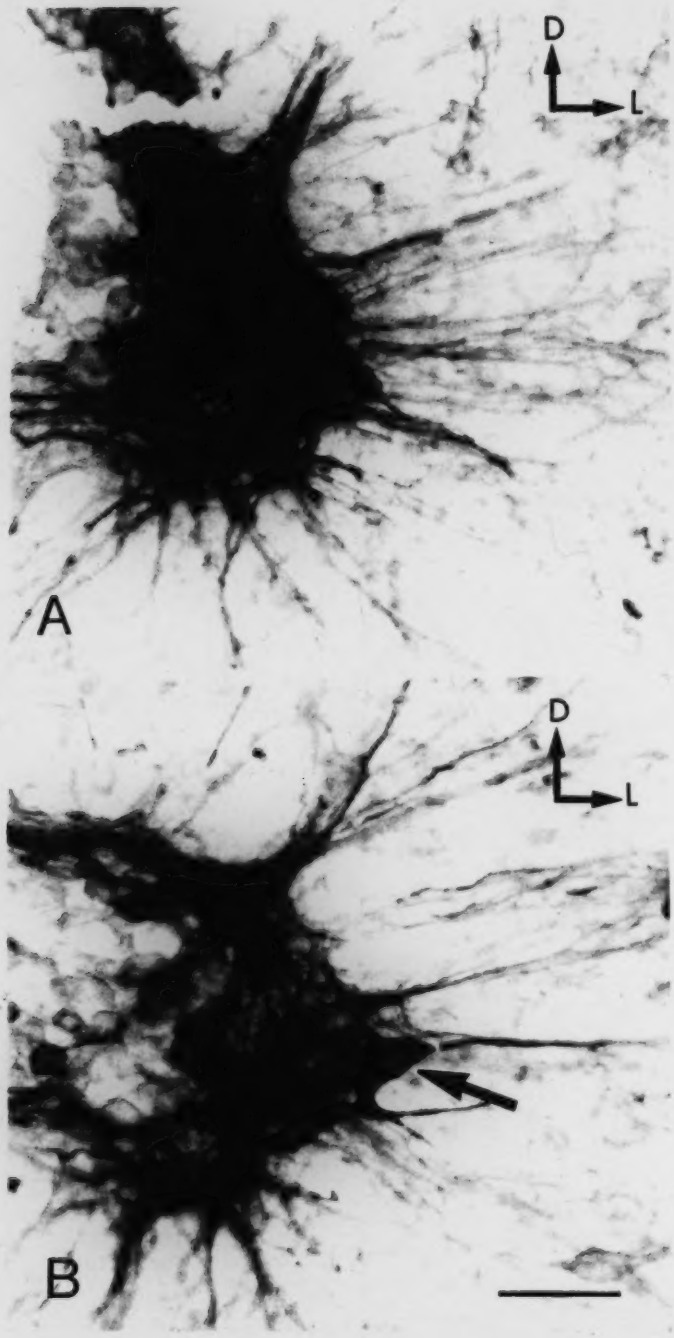
D
L
A
D
L
B

Figure 2-5. Horizontal sections through the spinal cord depicting the relationships of 5-HT positive neuronal profiles with the wall of the central canal (*cc*) or the midline (*m*). **(A)** Two type I neurons are located above the midline, and the thick process of one of them can be observed to course laterally. A fusiform (type II) neuron is located below the midline and its Two processes are oriented longitudinally. **(B)** A multipolar neuron (type I) with two processes, one oriented in the rostro-caudal direction and the other laterally. A second neuron of the same type is observed to the right. **(C)** A type I neuron with one process oriented laterally which bifurcates and gives rise to secondary branches that course in rostro-caudal direction. Note the close association (proximal to the bifurcation) with another 5-HT immunopositive fibre which runs longitudinally. The second primary process of the neuronal profile is oriented parallel to the midline. **(D)** Several neurons on both sides of the central canal with processes that penetrate the ependymal lining (*arrows*). Contacts between neighboring neurons are shown at higher magnification in **E** and **F** where processes **(E)** and somata **(F)** are closely apposed. The rostral (R) and lateral (L) directions are indicated by *arrows* in the upper right or left corner of each photomicrograph. Note the different orientation of F. *Scale bars* 30 μm.

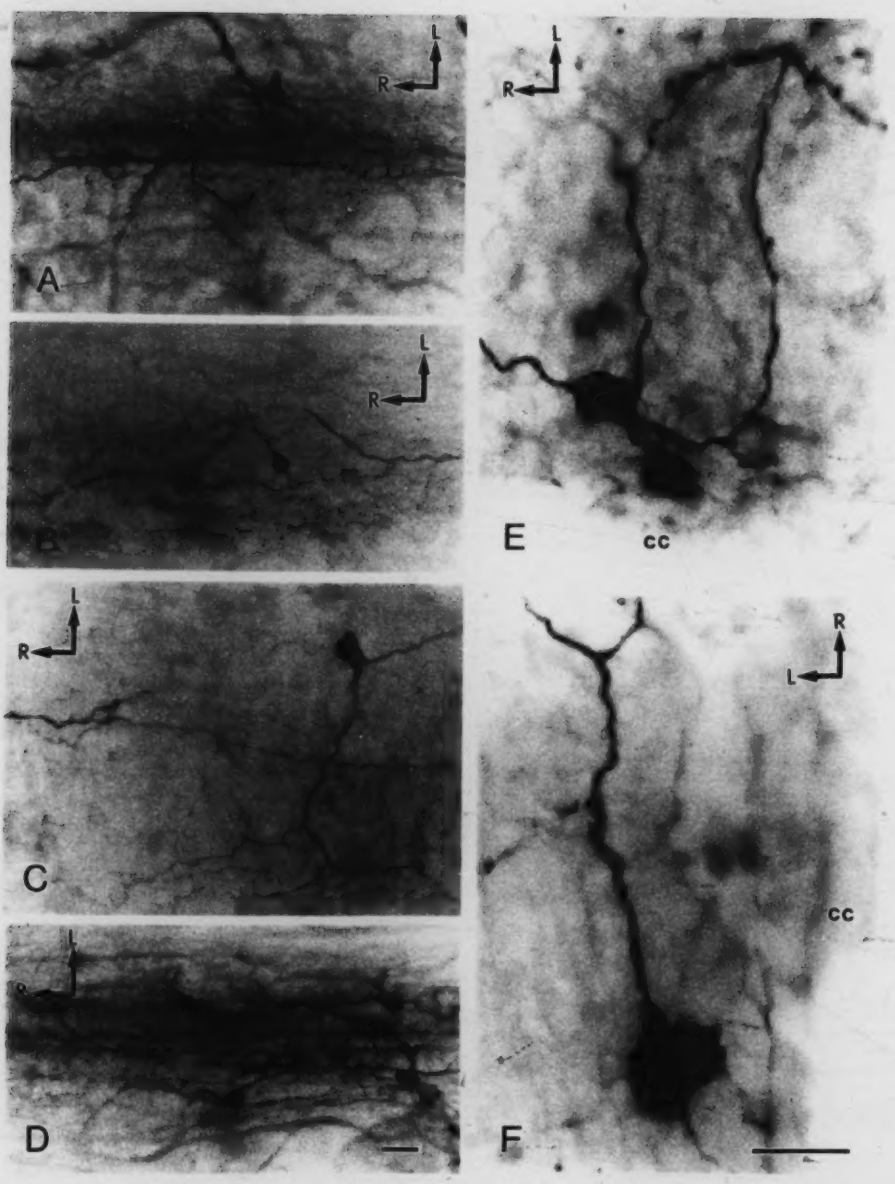
A
L
R
B
L
R
C
L
R
D
L
E
L
R
cc
F
R
L
cc

In some cases the processes of this type of neuron possessed numerous secondary, thinner branches that formed complex arborizations (Fig. 2-5 C, Fig. 2-6 E). Type I neuronal profiles were the predominant type of cells and were observed in all segments of the spinal cord.

Type II neurons were located primarily in segments 1-6 and their somata had a characteristic fusiform shape (the long axis being 20-25 μm and the short 5-7 μm), with two processes arising from each extremity of the soma (Fig. 2-5 A, the profile to the left). This type of neuron was usually located in close proximity to the central canal and its processes were oriented in rostrocaudal direction, parallel to the walls of the central canal. In some cases the processes of this neuronal type, and more rarely the processes of neuronal type I, appeared to penetrate the ependymal lining and were observed on the ventricular surface of the ependyma (Fig. 2-5 D). The details of the relationships between 5-HT immunopositive neuronal profiles also became clearer on horizontally sectioned tissues. Very often varicose neuronal processes were in contact (Fig. 2-5 E) or 5-HT labeled processes impinged on 5-HT positive somata. Another, less frequently observed, type of contact was close apposition of the somata of labeled profiles (Fig 2-5 F).

5-HT fibers

While observing the spinal cord from lateral to medial, we detected, at all levels, plexuses formed by intermixed thick (approximately 1.5 μm) and thin (less than 0.5 μm) fibers located in the submeningeal spinal cord (Fig. 2-6 A). These plexuses were more often observed in the sections cut through the ventral portions of the spinal cord. The thick fibers possessed large varicosities (4-6 μm in diameter), whereas the diameters of the varicosities associated with the thin fibers did not exceed 1 μm (Fig. 2-6 B). Between the lateral surface of the spinal cord and the central grey, many thin fibers were observed running primarily longitudinally within the axon columns (Fig. 2-6 C). They formed dense tracts and were primarily located laterodorsally and lateroventrally to the central grey region in all segments of the spinal cord (Fig. 2-6 C).

Figure 2-6. Horizontal sections depicting relationships between the types of 5-HT immunoreactive fibers. **(A)** A submeningeal plexus consisting of predominantly thick fibers which are oriented primarily in the lateral plane. The lateral surface of the spinal cord is towards the top of the photomicrograph. *Curved arrows* indicate contacts between longitudinally and laterally oriented fibers. **(B)** Higher power reveals association of large varicosities (*big arrows*) with thick fibers, and small varicosities (*small arrows*) with thin fibers. **(C)** A dense plexus of thin 5-HT immunoreactive fibers within the white matter which are oriented primarily in the rostrocaudal plane. **(D)** The course of two thick varicose fibers can be followed in the grey and white matter for a distance of 300-400 μm. **(E)** The process of a neuron located in proximity to the midline makes contact with a submeningeal 5-HT fibre (*arrowheads*). Note that the branch to the right also appears to be in contact with the external surface of the spinal cord. The rostral (R) and lateral (L) directions are indicated by *arrows* in the upper right or left corner of each photomicrograph. *Scale bars* 30 μm (*m*, midline).

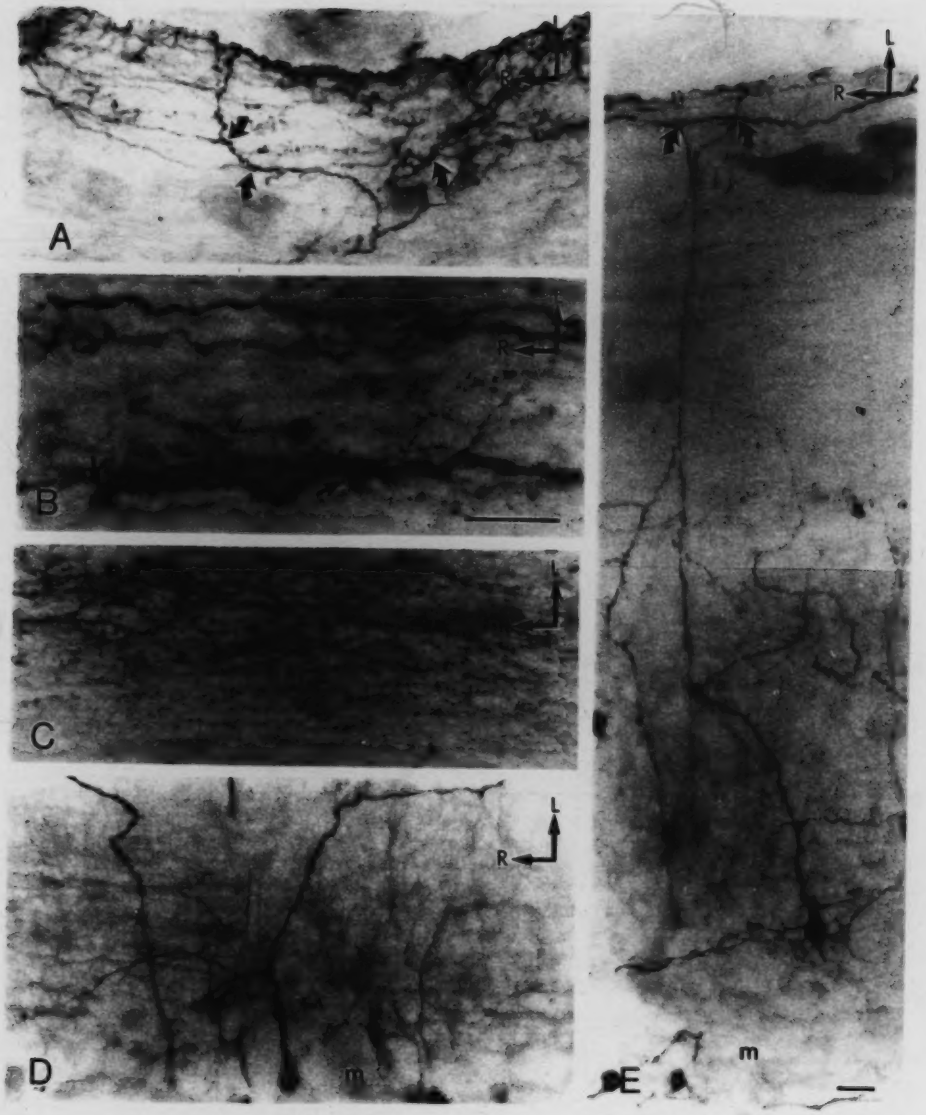
A
B
C
D
E
L
R
m

Occasionally, laterally oriented thick fibers arising from 5-HT somata were observed within these tracts or in the white matter closer to the midline, which is virtually devoid of longitudinal thin fibers (Fig. 2-6 D). Occasionally such processes traversed the whole width of the spinal cord laterally and were associated with thick fibers running in the rostro-caudal direction (Fig 2-6 D).

DISCUSSION

In the present study, by utilizing combined pharmacological and immunocytochemical techniques, we provided evidence for a role of 5-HT in modulating the CPG underlying locomotion in the mudpuppy, as well as evidence for the presence of an intrinsic spinal serotonergic system. The effects of 5-HT on the mudpuppy locomotor pattern were demonstrated by both an increase in the overall step cycle duration and an increase in the duration of EMG bursts. 5-HT was shown to exert its action in a reversible and dose-dependent manner, without affecting the alternating pattern between antagonistic muscles.

In contrast to the well pronounced effects on the NMDA-induced locomotor pattern, 5-HT failed to induce locomotion when applied to the bath alone. This is consistent with previous studies in the lamprey (Harris-Warrick and Cohen 1985), chronic spinal cats (Barbeau and Rossignol 1990, 1991) and the low spinal decerebrate cats (Grillner and Shik 1975). However, this differs from results obtained from neonatal rats (Cazalets et al. 1992) and curarized and decerebrate rabbits (Viala and Buser 1969) where 5-HT induced locomotion. Although these discrepancies may be attributed to methodological and interspecies differences, they may also reflect the developmental stage or the specific age of the systems under investigation.

The failure of 5-HT to elicit locomotion when applied alone suggests that, in the mudpuppy spinal cord, the transmitter is involved in modulating ongoing activity rather than activating the CPG for locomotion. The slowing of the locomotor rhythm, caused by 5-HT, suggests that its action occurred at the level of the CPG itself. However, this does not exclude the possibility that 5-HT may be also acting on motor neurons as reported in

other studies (Hounsgaard and Kiehn 1989; Hounsgaard et al. 1988; Takahashi and Berger 1990; Wang and Dun 1990). Whether the observed effects on locomotion result from an action of the drug solely on interneurons or on motoneurones as well remains to be determined.

By adding zimelidine, a selective 5-HT uptake inhibitor, to the bath solution we confirmed that endogenous release of 5-HT takes place during NMDA-induced locomotion and, furthermore, that the transmitter modulates the CPG underlying locomotion in the mudpuppy. The effect of zimelidine, and thus presumably an endogenous release of 5-HT, was similar to that observed with the application of 5-HT.

Pharmacology of 5-HT action

Previous pharmacological studies (Kaczmareck and Levitan 1987; Nicoll et al. 1990) have reported that 5-HT can act at presynaptic and/or postsynaptic sites at different levels of the CNS. This action can be exerted by either directly hyperpolarizing (Wang and Dun 1990) and depolarizing motoneurones (Takahashi and Berger 1990; Wang and Dun 1990), or setting the gain of neurons by facilitating the action of excitatory neurotransmitters (Barbeau and Rossignol 1990; Wallén et al. 1989). These studies also suggest that presynaptic action of 5-HT is mostly mediated via the 5-HT_1 receptor subtype, whereas the 5-HT_2 receptor subtype mediates the postsynaptic action.

Although an attempt was made, we were not able pharmacologically to characterize the receptor type involved in mediating 5-HT effects. The reasons for this may be multiple. Despite a range of new pharmacological agents with increased selectivity for different 5-HT receptor types, a clear differentiation is not always possible. This probably reflects their similar amino acid sequence and the likelihood that they share the same second messenger system (Hartig 1989). In addition, 5-HT and related agonists and antagonists have been reported to modify not only the function of their own receptors but also the function of nicotinic acetylcholine receptors (Garcia-Colunga and Miledi 1995). The negative results regarding the 5HT_3 receptor antagonists, granisetron and tropisetron, suggested that the observed effects were not mediated by this receptor type. However,

the possibility that a different receptor subtype is present on the membrane of mudpuppy neurons, as compared to mammalian species, cannot be entirely excluded. Methysergide, a nonselective 5-HT_1/5-HT_2 antagonist, not only failed to antagonize the effect of 5-HT but displayed an agonist-like action by increasing the cycle duration. Similar action of methysergide has been reported in a number of tissues (Dunlop and Fischbah 1978; Grillner et al. 1981; Holtz et al. 1986; Saito et al. 1982) which probably explains why its mode of action has been recently revised (Hoyer et al. 1994). On the other hand a nonselective 5-HT_1/5-HT_2antagonist, methiothepin antagonized 5-HT effects only when applied prior to the 5-HT. This suggests that exogenously applied concentrations of 5-HT are probably greater then those released under physiological conditions or that the receptor sites at which the two substances act are different.

The 5-HT_1 agonist 8-OH-DPAT was incapable of mimicking the effects of 5-HT, probably for two reasons. Firstly, 5-HT may not interact with this receptor type in the mudpuppy spinal cord. Secondly, 8-OH-DPAT has been shown (Wang and Dun 1990) to mimic the hyperpolarizing action of 5-HT in the neonatal rat motoneurones in vitro, mediated via a 5-HT_{1A} receptor type. However, this is opposite to an inhibiting action of 5-HT on K^+ conductances, a mechanism implicated in 5-HT control of locomotion (Wallén et al. 1989). Although we have not done any intracellular recording to prove that the same mechanisms are involved in our preparation, the agreement with other studies suggests a similar action.

Immunocytochemistry

Our findings on serotonergic modulation of the CPG for locomotion in the mudpuppy are well supported by the data obtained with immunocytochemistry. These data demonstrate that the serotonergic neurons, fibers and varicosities are distributed widely, but not uniformly, throughout the mudpuppy spinal cord. Although 5-HT immunoreactive cell bodies were found at all levels of the spinal cord, the majority of them were localized within the brachial (between segments 2 and 6) and lumbar (between segments 15 and 21) spinal cord. Anatomically, these segments largely correspond to the regions of the cord

from which the brachial and sciatic plexuses originate, providing innervation of the mudpuppy forelimb and hindlimb muscles respectively (Gilbert 1977). Previous anatomical studies (Stephens and Holder 1985; Székely and Czéh 1967) have shown that motoneuronal pools supplying forelimb muscles are distributed from the rostral half of C3 to the caudal half of C5 segment. These findings were further elaborated by Wheatley at al. (1994), demonstrating that the pattern generator to the forelimb of the mudpuppy resides in an area covering parts of two brachial segments (C2, C3) of the cord. Taken together these findings demonstrate not only that 5-HT neurons are present but also appropriately localized in the cord to interact with the central pattern generator. Whether they exert their action on the CPG directly or indirectly is currently not clear.

The 5-HT cell bodies are mainly localized ventrolateral to the central canal at a depth of 300-450 μm below the dorsal surface of the cord. Previous work (Jovanović and Bélanger, unpublished observation) found two types of neurons localized within the ventrolateral grey matter at the depth of 300-450 μm below the dorsal surface of the cord. Smaller cells (up to 40 μm) and larger cells (up to 100 μm) were thought to correspond to interneurons and motoneurons respectively. Thus, the 5-HT neurons seem to be well placed within the cord to influence the activity of both interneurons and motoneurons.

Two types of 5-HT neurons were differentiated according to their shape, diameter and arborization patterns. Frequently, neighboring 5-HT neurons were found in close proximity, suggesting that they may be capable of influencing each other's activity. As has been suggested in other animal models, this may be a mechanism for increasing the reliability and local synchrony of neuronal firing during certain motor acts (Arshavsky et al. 1993; Perrins and Roberts 1 995a, b).

Thin and thick processes extending from these cells were found in both the grey and the white matter. They mainly contributed to dense longitudinal tracts. Some were observed to project laterally, making contacts with the thick fibers descending from more rostral segments. The fact that thin fibers mainly contributed to dense ventrolateral and dorsolateral longitudinal tracts may suggest involvement of 5-HT not only in the control of locomotor activity but also in the control of sensory information coming from the

periphery.

Serotonergic processes showed a varicose appearance along their length indicating the presence of release sites along these processes. Since varicosities are considered to be a light microscopic equivalent of synapses being observed with electron microscopy (Zahm et al. 1985), our observations suggest that release of 5HT takes place in both the white and grey matter. This is in contrast to what has been observed in higher vertebrates, where the white matter is specialized for longitudinal fiber tracts and synaptic interactions occur mainly in the grey matter (Bowker et al. 1982; Dalhstrom and Fuxe 1965: Oliveras et al. 1977; Mizukawa et al. 1980). In the lamprey (Van Dongen et al. 1985) and other lower vertebrates (Ritchie and Leonard 1982; Ritchie et al. 1983) configurations similar to what we observed in the mudpuppy have been reported. Similar to the lamprey and teleost fishes, the mudpuppy can also swim with undulatory movements. Therefore, the differences mentioned above may reflect the specializations occurring during the transition from swimming to fully limbed locomotion typical of terrestrial organisms. These differences may also reflect differences in the basic synaptic organization of the spinal cord between the mudpuppy and higher vertebrates, as well as serotonin's involvement in a globally acting system of modulation in the mudpuppy spinal cord (Beaudet and Decarries 1978; Maxwell et al. 1983). The fact that processes of serotonergic cells, particularly Type II, appeared to contact cerebrospinal fluid by penetrating the ependymal lining, may strengthen this assumption. The morphological differences we observed between 5-HT neurons may also reflect their functional differences, suggesting their involvement in different aspects of motor control.

In summary, our present results suggest that an endogenous release of serotonin can affect the CPG for locomotion in the mudpuppy by reducing the frequency of the burst discharge and increasing the duration of bursts without affecting the alternating activity between antagonistic muscles. However, serotonin is not capable of inducing locomotion on its own. Accordingly, serotonin appears not to affect mechanisms underlying the pattern generation but rather to modulate ongoing locomotion. Similar motor effects observed in the mudpuppy and the other in vitro models provides further evidence for the

notion (Jacobs 1976) that serotonin plays a common role throughout the vertebrate phylum. However the presence of a more elaborate spinal 5-HT system in the mudpuppy, typical of more primitive species such as elasmobranch and teleost fishes, may indicate that at least part of spinal 5-HT function was taken over by higher (supraspinal) structures during phylogenesis.

REFERENCES

Arshavsky YI, Orlovsky GN, Panchin V, Roberts A, Soffe SR (1993) Neuronal control of swimming locomotion: analysis of the pteropod mollusc *Clione* and embryos of the amphibian *Xenopus*. Trends Neurosci 16: 227-233

Barbeau H, Rossignol S (1990) The effects of serotonergic drugs on the locomotor pattern and on cutaneous reflexes of the adult chronic spinal cat. Brain Res. 514:55-67

Barbeau H, Rossignol S (1991) Initiation and modulation of the locomotor pattern in the adult chronic spinal cat by noradrenergic, serotonergic and dopaminergic drugs. Brain Res. 546: 250-260

Beaudet A, Decarries L (1978) The monoamine innervation of rat cerebral cortex: synaptic and nonsynaptic nerve terminals. Neuroscience 3: 851-860

Bowker RM, Westlund KN, Sullivan MC, Coulter JD (1982) Organization of the descending serotonergic projections to the spinal cord. In: Kuypers H, Martin GF (eds) Descending Pathways to the Spinal Cord. Prog Brain Res. 57: 239-265

Buchanan JT, Grillner S (1991) 5-Hydroxytriptamine depresses reticulospinal excitatory postsynaptic potentials in motoneurons of the lamprey. Neurosci Lett 112:71-74

Cazaletz JR, Squalli-Houssaini Y, Clarac F (1992) Activation of the central pattern generators for locomotion by serotonin and excitatory amino acids in neonatal rat. J Physiol (Lond) 455:187-204

Christenson J, Franck J, Grillner S (1989) Increase in endogenous level of 5–hydroxytriptamine levels modulates the central network underlying locomotion in the lamprey spinal cord. Neurosci Lett 100: 188-192

Dahlstrom A, Fuxe K (1965) Evidence for existence of monoamine neurons in the central nervous system. II. Experimentally induced changes in the intraneuronal amine levels of bulbospinal neuron systems. Acta Physiol Scand [Suppl]) 247:5-36

Delcomyn F (1980) Neural basis of rhythmic behavior in animals. Science 210: 492-498

Dunlap K, Fischbah GD (1978) Neurotransmitters decrease the calcium component of sensory neurone action potential. Nature 276:837-839

Garcia-Colunga J, Miledi R (1995) Effects of serotonergic agents on neuronal nicotinic acetylcholine receptors. Neurobiology 92:2919-2923

Getting PA, Dekin MS (1985) *Tritonia* swimming: a model system for integration within the rhythmic motor systems. In: Selverston AI (ed) Model Neural Networks and Behavior. Plenum Press, pp 3-20

Gilbert SG (1 986) Pictorial Anatomy of the *Necturus.* University of Washington Press

Grillner S (1985) Neurobiological bases of rhythmic motor acts in vertebrates. Science 228:143-149

Grillner S, Shik ML (1975) On the descending control of the lumbosacral spinal cord from the "mesencephalic locomotor region". Acta Physiol Scand 87:320-333

Grillner S, McClellan A, Sigvardt K, Wallen P, Wilen M (1981) Activation of NMDA receptors elicits "fictive locomotion" in lamprey spinal cord in vitro. Acta Physiol Scand 113:549-551

Grillner S, Wallen P, Brodin L (1991) Neural network generating locomotor behavior in lamprey: circuitry, transmitters, membrane properties and simulation. Ann Rev Neurosci 14:169-199

Harris-Warrick RM (1988) Chemical modulation of central pattern generators. In: Cohen AH, Rossignol S, Grillner S (eds) Neural Control of Movements in Vertebrates. Willey and Sons, New York, pp 285-331

Harris-Warrick RM, Cohen A (1985) Serotonin modulates the central pattern generator for locomotion in the isolated lamprey spinal cord. J Exp Biol 116:27-46

Hartig PR (1989) Molecular biology of 5-HT receptor. Trends Pharm Sci 10:64-69

Holtz GG, Shefner SA, Anderson EG (1986) Serotonin decreases the duration of action potentials recorded from tetraethylammonium-treated bullfrog dorsal root ganglion cells. J Neurosci 6:620-626

Hounsgaard J, Kiehn O (1989) Serotonin-induced bistability of turtle motoneurones caused by a nifedipine-sensitive calcium plateau potential. J Physiol (Lond) 414:265-282

Hounsgaard J, Hultborn H, Jesperson B, Kiehn O (1988) Bistability of α-motoneurones in the decerebrate cat and in the acute spinal cat after intravenous 5-hydroxytryptophan. J Physiol (Lond) 405:345-367

Hoyer D, Clarke DE, Fozard JR, Hartig PR, Martin GR, Milecharane EJ, Saxena PR, Humphrey PPA (1994) VII International union of pharmacology classification of receptors for 5-hydroxytriptamine (serotonin). Pharmacol Rev 46:157-203

Hsu SM, Raine L, Fanger H (1981) Use of avidin-biotin peroxidase complex (ABC) in immunoperoxidase techniques. J Histochem Cytochem 29:577-588

Jacobs BL (1976) An animal behavior model for studying central serotonergic synapses. Life Sciences 19:777-785

Kaczmarek LK, Levitan IB (1987) Neuromodulation. Oxford University Press, New York, pp 247-273

Marder I (1987) Neurotransmitters and neuromodulators. In: Selverston AI, Moulins M (eds) The Crustacean Stomatogastric system. Springer-Verlag, Berlin, Heidelberg, New York pp 263-300

Maxwell DJ, Leranth C, Verhofstad AAJ (1983) Fine structure of serotonin-containing axons in the marginal zone of the rat spinal cord. Brain Res 266:253-259

Mizukawa K (1980) The segmental detailed topographical distribution of monoaminergic terminals and their pathways in the spinal cord of the cat. Anat Anzeiger 147:125-144

Nicoll RA, Malenka RC, Kauer J (1990) Functional comparison of neurotransmitter receptor subtypes in mammalian central nervous system. Physiological Rev 70:513-565

Oliveras JL, Bourgin S, Herry F, Besson JM, Hamon M (1977) The topographical distribution of serotonergic terminals in the spinal cord of the cat: Biochemical mapping by the combined use of microdissection and microassay procedures. Brain Res 138:393-406

Perrins R, Roberts A (1995a) Cholinergic contribution to excitation in a spinal locomotor central pattern generator in *Xenopus* embryos. J Neurophysiol 73:1013-1019

Perrins R, Roberts A (1995b) Cholinergic and electrical motoneuron-to motoneuron synapses contribute to on cycle excitation during swimming in *Xenopus* embryos. J Neurophysiol 73:1005-1012

Petrov T, Krukoff TL, Jhamandas JH (1992) The hypothalamic paraventricular and lateral parabrachial nuclei receive collaterals from raphe nucleus neurons: A combined double retrograde and immunocytochemical study. J Comp Neurol 318:18-26

Ramirez JM, Pearson KG (1991) Octopamine induces bursting and plateau potentials in insect neurones. Brain Res 549:332-337

Ritchie TC, Leonard RB (1982) Immunocytochemical demonstration of serotonergic cells, terminals and axons in the spinal cord of the stingray, *Dasyatis sabina.* Brain Res 240:334-337

Ritchie TC, Livingston CA, Hughes MG, McAdoo DJ, Leonard RB (1983) The distribution of serotonin in the CNS of an elasmobranch fish: immunocytochemical and biochemical studies in the Atlantic stingray, *Dasyatis sabina.* J Comp Neurol 221:429-433

Saito K, Ito S, Kitazawa T, Ohga A (1 982) Selective inhibition by methysergide of the monosynaptic reflex discharge in the isolated spinal cord of the newborn rat. Brain Res 251:117-125

Sillar KT, Wedderburn JF, Simmers AJ (1992) Modulation of swimming rhythmicity by 5-hydroxytriptamine during post-embryonic development in *Xenopus laevis.* Proc R Soc Lond B 50:107-114

Steeves JD, Schmidt BJ, Skovgard BJ, Jordan LM (1980) The effect of noradrenaline and 5-hydroxytriptamine depletion on locomotion in the cat. Brain Res 185:349-362

Stephens N, Holder N (1985) A horseradish peroxidase study of moto neuron pools of the forelimb and hindlimb musculature of the axolotl. Proc R Soc Lond B 224:325-339

Székely G, Czéh G (1967) Localization of motoneurons in the limb moving spinal cord segments of ambystoma. Acta Physiol Acad Sci Hung 32:3-18

Takahashi T, Berger AJ (1990) Direct excitation of rat spinal motoneurones by serotonin. J Physiol (Lond) 423:63-76

Van Dongen PAM, Hokfelt T, Grillner S, Verhofstad AAJ, Steinbusch HWM (1985) Possible target neurons of 5-Hydroxytryptamine fibers in the lamprey spinal cord: immunocytochemistry combined with intracellular staining with Lucifer yellow. J Comp Neurol 234:523-535

Viala D, Buser P (1969) The effects of DOPA and 5-HTP on rhythmic efferent discharges in hindlimb nerves in the rabbit. Brain Res 12:437-443

Wallén P, Buchanan JT, Grillner S, Hill RH, Christenson J, Hokfelt T (1989) Effects of 5-Hydroxytryptamine on the afterhyperpolarization, spike frequency regulation, and oscillatory membrane properties in lamprey spinal cord neurons. J Neurophysiol 61:759-768

Wang MY, Dun NJ (1990) 5-Hydroxytryptamine responses in neonate rat motoneurones *in vitro.* J Physiol (Lond) 430: 7-103

Wheatley M, Edamura M, Stein RB (1992) A comparison of intact and in-vitro locomotion in an adult amphibian. Exp Brain Res 88:609-614

Wheatley M, Jovanović K, Stein RB, Lawson V (1994) The activity of interneurons during locomotion in the *in vitro Necturus* spinal cord. J Neurphysiol 71:2025-2032

Zahm DS, Heimer L (1985) Synaptic contacts of ventral striatal cells in the olfactory tubercule of the rat: correlated light and electron microscopy of anterogradely transported *Phaseolus vulgaris*-leucoagglutinin . Neurosci Lett 60:169-175

CHAPTER 3

EFFECTS OF INHIBITORY NEUROTRANSMITTERS ON THE MUDPUPPY (*Necturus maculatus*) LOCOMOTOR PATTERN *IN VITRO*

INTRODUCTION

Inhibition plays an important role in generating and/or coordinating rhythmic motor patterns throughout the animal kingdom. Reciprocal inhibition plays a crucial role in the control of the leech heart beat (Calabrese and Peterson 1983; Marder and Calabrese 1996), the generation of a rhythmic motor pattern in the lobster stomatogastric ganglion (Selverston et al. 1983; Marder and Calabrese 1996), and the coordination of bilateral (Dale et al. 1990; Grillner and Matsushima 1991; Roberts et al. 1983) and tetrapod locomotion (Grillner 1981; McClellan 1996 Noga et al. 1993). Two principal neurotransmitters involved in mediating inhibitory processes are glycine and γ-amino butyric acid (GABA). *In vitro* studies of the lamprey (Alford and Williams 1989; Cohen and Harris-Warrick 1984; Hagevik and McClellan 1994) and the *Xenopus* embryo (Roberts et al. 1984; Dale 1985; Soffe 1989) have shown that after blocking glycine receptors, rhythmic motor output can still occur in each half of their central nervous systems. Thus, glycinergic transmission is not necessary for generating the swimming rhythm. However, glycinergic crossed inhibition serves to couple the phase of independent rhythm generators in each half of the respective spinal cords, allowing the production of a coordinated alternating motor pattern typical of swimming. Similar findings have been reported in the cat (Noga et al. 1993; Pratt and Jordan 1987), neonatal mouse (Droge and Tao 1993), neonatal rat (Cowley and Schmidt 1995) and the neonatal wallaby (Ho 1997).

A version of this chapter has been accepted for publishing. Jovanović K, Petrov T, Stein RB (1999) Exp Brain Res (in press)

This suggests that glycine receptor activation is not required for motor rhythm generation but may mediate reciprocal antagonism underlying inter- and intralimb locomotor patterns.

Contrary to the role proposed for glycine, GABA appears to be more involved in providing for gain control and gating of the sensory input during ongoing locomotion. There is general consensus in both invertebrate (Clarac and Cattaert 1996; El Manira and Clarac 1991) and vertebrate (Dubuc et al. 1988; Stuart and Redman 1991) studies that a presynaptic GABAergic modulation of the sensory afferent transmission occurs during locomotion. In the lamprey, the efficiency of both the inhibitory and excitatory transmission is modulated phasically and can be gated at different levels by a combined action of $GABA_A$ and $GABA_B$ receptors. Acting in concert, pre- and postsynaptic GABA mechanisms have been shown to reduce the burst frequency and modify the intersegmental coordination (Tegnér et al. 1993). In neonatal rats, GABA affects both the duration and amplitude of the rhythmic motor output by activating $GABA_A$ and $GABA_B$ receptors (Cazalets et al. 1994). Furthermore, there is evidence that GABA affects network inter- and intralimb coordination (Cowley and Schmidt 1995; Kremer and Lev-Tov 1997). Together with glycine, GABA may also be involved in mediating recurrent inhibition (Schneider and Fyffe 1992).

In the present study we used an *in vitro* preparation of the mudpuppy to further clarify the role of inhibitory neurotransmitters in vertebrate locomotion. The mudpuppy, an aquatic amphibian, has a number of features that make it well suited for examining the neural mechanisms for generation and modulation of locomotor activity. This *in vitro* preparation stays alive for several days when superfused with cooled and oxygenated Ringer solution. Despite being an aquatic amphibian, the mudpuppy walks with an alternating quadrupedal gait characterized by robust and long lasting EMG activity. Furthermore, it is the first adult *in vitro* preparation that allows simultaneous observation of the actual behavior (i.e., rhythmic movement of the forelimb) and recording of a motor output (EMG).

We demonstrate here that GABAergic and glycinergic systems are active during NMDA-induced locomotion in the mudpuppy. Their activity does not appear to be

essential for the rhythm generation, but rather coordinates the alternation between flexors and extensors in a limb. Activation of glycine and $GABA_A$ receptors seems to be more important for the rate control and the regularity of the EMG pattern. $GABA_B$ receptor activity, on the other hand, alters the amplitude and frequency of EMG bursts leaving the alternating pattern largely unaffected.

A preliminary report of this work has been published in abstract form (Jovanović et al.1996b).

MATERIALS AND METHODS

In vitro preparation

Experiments (n=52) were conducted on an *in vitro* spinal cord preparation isolated from adult mudpuppies as approved by the Animal Welfare Committee at the University of Alberta. Prior to dissection, the animals were anesthetized by immersion in a solution of 3-aminobenzoic acid ethyl ester (Sigma, 1 g/l). The skin and underlying muscles were removed and a dorsal laminectomy was performed from the first to the fifth vertebrae. The first five segments of the spinal cord (C1-C5) with the attached forelimb were than removed from the rest of the body and placed in a Sylgard-lined petri dish superfused with cooled (15^{0}C) and oxygenated Ringer solution of the following composition (mM): 115 NaCl; 2 $CaCl_2$; 2 KCl; 1.8 $MgCl_2$; 5 Hepes; pH 7.3; glucose, 1g/l. While in the petri dish, the brachial plexus was exposed, the paraspinal muscles removed and bipolar teflon-coated silver wires (75μM) inserted into the elbow flexor (*Brachialis*) and extensor (*Extensor ulnae*) muscles for electromyographic (EMG) recording during locomotion. After a recovery period of approximately one hour, the preparation was transferred to a Sylgard-lined recording chamber and placed dorsal side up. The spinal cord and the forelimb were then stabilized by pinning the vertebral column and the procoracoid cartilage to the base of the chamber. Throughout the course of experiments the preparation was superfused with a cooled (15-18^0 C) and oxygenated Ringers at a flow rate of 5-10 ml/min.

Locomotion was induced chemically by adding 30-90 μM N-methyl-D-aspartic acid (NMDA) together with 10 μM D-serine to the superfusing solution. After a well defined locomotor pattern was established, two types of experiment were performed.

I. Exogenous application of the drugs

To study the role of inhibitory neurotransmitters in the locomotor rhythm and pattern generation glycine, GABA and some of their respective agonists and antagonists were applied directly into the bath. In different experiments, the following drugs were used: GABA (0.75-900 μM), bicuculline methbromide (0.8-20 μM), muscimol (0.5-8 μM), baclofen (0.5-100 μM), CGP-35348 (5-100 μM), nipecotic acid (0.05-4 mM), glycine (0.1-4 mM) and strychnine (1-100 μM). Each cycle of drug application was followed by a washout with Ringer solution. Following the washout, locomotion could be induced repeatedly by superfusing the preparation with NMDA and D-serine. The NMDA, D-serine, glycine and strychnine were obtained from Sigma Chemical (St. Louis, MO, USA). The GABA-uptake inhibitor nipecotic acid, $GABA_A$ antagonist bicuculline methbromide, $GABA_A$ agonist muscimol and $GABA_B$ agonist baclofen hydrochloride were obtained from Research Biochemical Inc. (Natick, MA, USA). The $GABA_B$ antagonist CGP-35348 was generously provided by Novartis Pharmaceutics Canada Inc. All drugs were freshly prepared in distilled water and diluted to the appropriate concentration prior to use.

The effects elicited by applying different concentrations of drugs were observed as changes in the control cycle duration, normalized to 1, and in the flexor and extensor EMGs which were simultaneously recorded. EMG recordings were preamplified, rectified and filtered (10-300 Hz) and stored on a computer's hard disk using commercially available data acquisition software (Axotape, Axon Instruments). All channels of data were digitally sampled at 50 Hz and later analyzed using a customized software package written by Drs. Ken Yoshida and Marc Bélanger. The EMG amplitude was determined as an average peak voltage of flexor and extensor bursts by using an analysis routine, custom written for Matlab v4.2 (the Math Works, Natick, MA, USA). "n" refers to the number of experiments. The results regarding changes in the cycle duration were pooled and plotted

in the figures as the mean±S.E.M. These values were derived for each drug using a nonlinear least squares fit to a modified Michaelis-Menton equation:

1) $T=1+ CM/(C+ C_{50})$

where T is the normalized cycle time and C_{50} represents a drug concentration C at which 50% of the maximum effect (M) was observed. All fitted curves had a reduction in variance (ρ^2) greater then 90% indicating highly significant results. In addition to the cycle duration, we quantified the relative phase of flexor to extensor activity using a cross-correlation analysis routine, custom written for Matlab v4.2 (the MathWorks, Natick, MA, USA). The flexor to extensor angle was determined as the delay to the peak of cross-correlation (hatched box) divided by cycle period and multiplied by 360^0. The cycle period was defined either as the time between two consecutive minima of the cross-correlation (marked by arrows; Fig. 3-1 C) or as the time between onsets of two consecutive flexor bursts. These values typically agreed to within 10%. Dose-response curves, depicting changes in the cycle duration as a function of increasing drug concentrations, were constructed by using cycle duration values obtained from burst onset analysis while the relative phase of flexor to extensor activity was calculated using cycle duration values obtained by means of cross-correlation analysis.

Figure 3-1. Effects of glycine on NMDA-induced locomotion *in vitro*

The perturbations of the locomotor rhythm caused by exogenously applied glycine were observed by means of EMG recordings. **(A)** Control episode of locomotor activity elicited by applying NMDA and D-serine to the bath. EMG activity recorded unilaterally from elbow flexor and extensor muscles was rectified and smoothed. **(B)** 1mM glycine caused an increase of the cycle duration and switch from a regular alternating pattern to a less regular and more synchronous EMG pattern. **(C)** The phase relationship between flexor and extensor EMGs was quantified by cross-correlation analysis. The flexor to extensor angle was determined as the delay to the peak of cross-correlation (hatched box) divided by cycle period. The cycle period was determined as the time between two consecutive minima of the cross-correlation (marked by arrows). A negative value for the peak near zero in the control cross-correlation **(C)** indicates that the flexor and extensor EMGs are relatively out of phase while a positive value **(D;** 1 mM) indicates that they are relatively in phase.

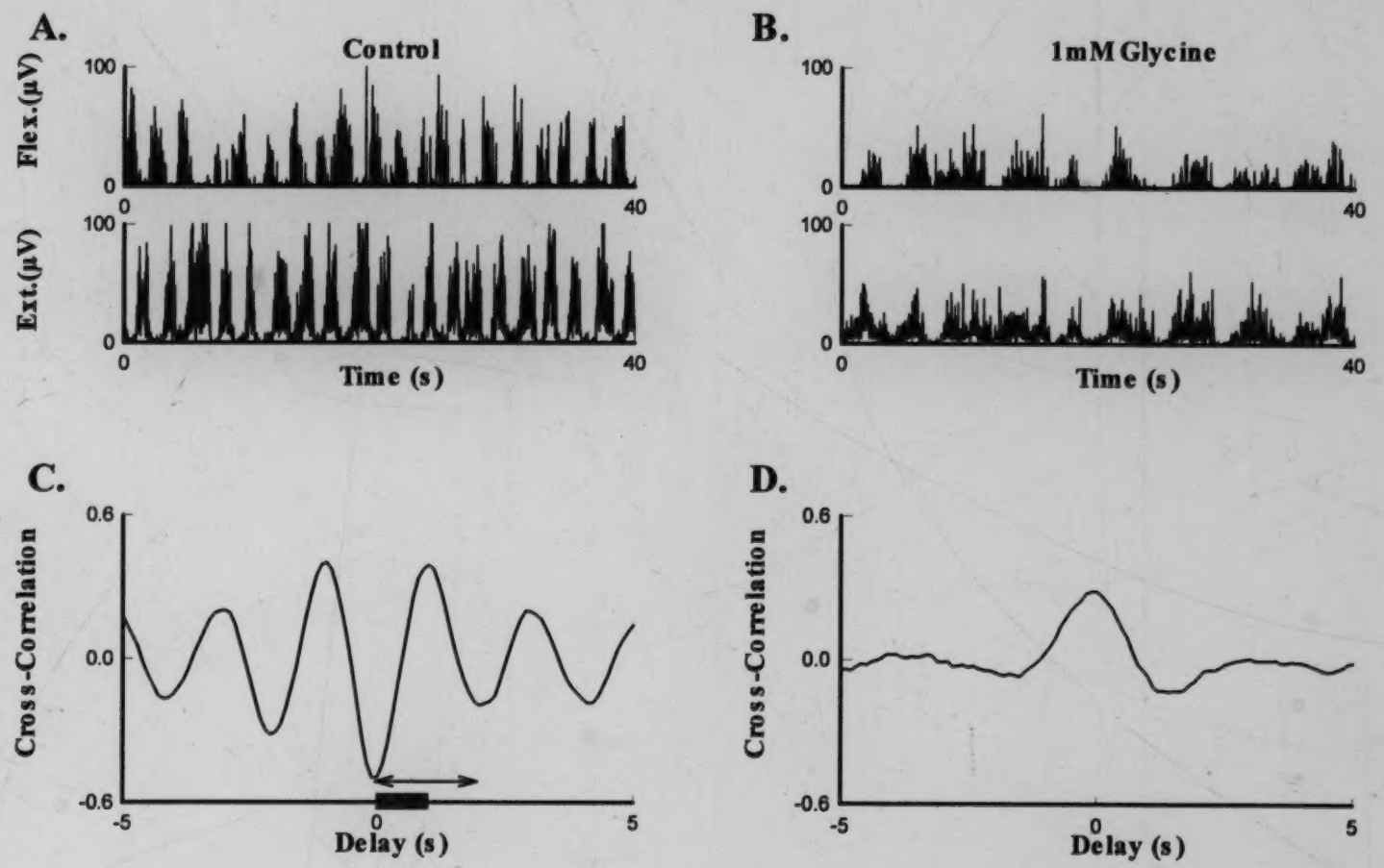
A.
Control
Flex.(μV)
Ext.(μV)
100
0
0
40
Time (s)
B.
1mM Glycine
C.
Cross-Correlation
0.6
0.0
-0.6
-5
0
5
Delay (s)
D.

II. Immunocytochemistry

In a separate set of experiments eight adult mudpuppies were used to detect GABA (n=4) and glycine (n=4) immunocytochemically. A laminectomy of the entire spinal column was performed under anesthesia with 3-aminobenzoic acid ethyl ester. The animals were spinalized by sectioning the spinal cord at the caudal border of the medulla. The spinal cords (segments 1-6) were than removed and fixed by immersion in an iced solution of 4% paraformaldehyde and 0.5% glutaraldehyde in 0.1 phosphate buffer (pH 7.4, 16-18 h). Tissues were cryoprotected in 30% sucrose solution at 4°C. Before sectioning, spinal cords were partitioned into segments and sectioned serially with a cryostat in the horizontal plane (50 μm in thickness). Sections were stored in separate wells to keep them in order.

For the immunocytochemical visualization of GABA and glycine, free-floating sections were incubated for 12-14 hours with antibodies raised in guinea pig (anti-GABA) or in rabbit (anti-glycine; Chemicon Int. Inc., Temecula, CA), diluted 1:1000 or 1:250 respectively in 0.1M PBS, containing 0.3% Triton X-100 and 2% normal goat serum. Tissues were then processed according to the ABC method of Hsu et al. (1981) as previously described (Petrov et al. 1991; Petrov et al. 1992; Jovanović et al. 1996a). Briefly, following 3 x 10 min rinses in PBS they were sequentially reacted with biotinylated goat anti-guinea pig or anti-rabbit antibody (1:200) for 2 hours and ABC reagent (1:100) for 1 hour (Vector Labs Inc., Burlingame, CA). After 3 x 10 min rinses in PBS, sections were treated with 0.05% diaminobenzidine and 0.035% hydrogen peroxide in 0.1M PBS for 10-20 min. All incubations were carried out at room temperature. No immunocytochemical staining was observed in control sections, processed after omission of the primary antibodies.

RESULTS

Role of Glycinergic system in Necturus locomotion

Rhythmic motor patterns, including locomotion, are generally characterized by

alternating activity between functionally antagonistic muscles. This pattern is largely based on reciprocal inhibition mediated by glycine (for review see McClellan 1996). To examine whether the mudpuppy's locomotion is based on a similar mechanism glycine was first applied directly to the bath during NMDA-induced locomotion (n=6). Fig. 3-1 A and B show sample data from one experiment. Several effects of glycine can be seen: 1) the pattern goes from an alternation between the flexor and extensor EMGs to a synchronous activation. This is confirmed by calculating cross-correlation functions (Fig. 3-1 C, D). The peak at zero delay is strongly negative in the control trial, but becomes positive in the presence of glycine. In fact, the phase angle between the flexor and extensor EMGs changed smoothly from being out of phase (180^0-106^0) to being in-phase (near 0^0), as the glycine concentration increased (Fig. 3-2 C). 2) The rhythmicity of the pattern is also less pronounced, as can be seen from the shape of the cross-correlation functions at increasing values of delay (3-1 D). 3) The amplitude of the flexor and extensor bursts steadily declined with increasing concentrations (Fig. 3-2 A, B). 4) The cycle duration increased systematically (Fig. 3-2 D), as the glycine concentration increased. They can be well fitted by equation 1 (the correlation coefficient of the fit is ρ^2= 0.99). The maximum value (M=2.31) gives the asymptotic value that the cycle duration approaches as the glycine concentration is increased. The concentration at which the effect is half maximal is C_{50}=1.47 mM. The effects of exogenous glycine were reversible upon washout in Ringer solution.

Application of strychnine, a glycine receptor antagonist, to the bath alone did not induce locomotion. Only sporadic, tonic discharges were observed in one or both muscles. However, during NMDA-induced locomotion, different concentrations of strychnine caused the normal alternating EMG pattern to become synchronous (Fig. 3-3). As confirmed by cross-correlation analysis (Fig. 3-3 C, D), strychnine caused a synchronization of the EMGs; i.e., the flexor to extensor phase was reduced to 0^0 in four out of six preparations tested. In these animals the control phase between the flexor and extensor activity, which ranged between 180^0 and 90^0 , was reduced to 0^0 in the presence of increasing concentrations of strychnine.

Figure 3-2. Additional glycine effects

Increasing concentrations of glycine also caused a depression of EMG amplitude **(A, B)** in both flexor and extensor muscles and reduced flexor to extensor phase angle **(C;** same animal as in **Fig. 3-1)**. Dose-response curve **(D)** summarizing the changes in the cycle duration produced by increasing concentrations of glycine. The cycle duration was calculated as the interval between the onsets of two consecutive flexor bursts. An average cycle duration, for each drug concentration, was obtained by taking at least twenty step cycles. The cycle duration (expressed as a fraction of a control cycle duration, before application of glycine) is plotted versus the concentration of glycine in the bath. The curve was generated from data compiled from six animals. Each point shows the mean±S.E.M.

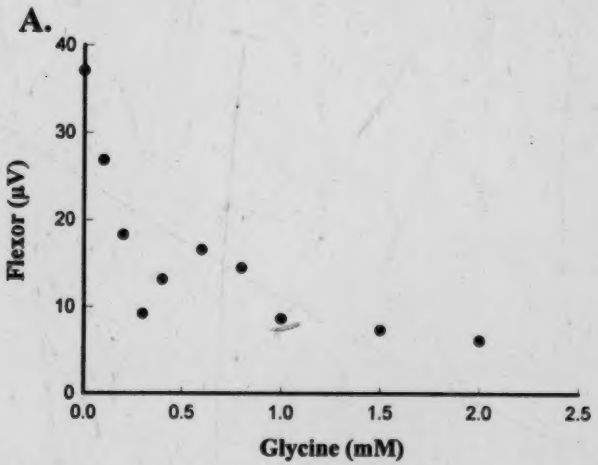
A.
Flexor (μV)
40
30
20
10
0
0.0
0.5
1.0
1.5
2.0
2.5
Glycine (mM)

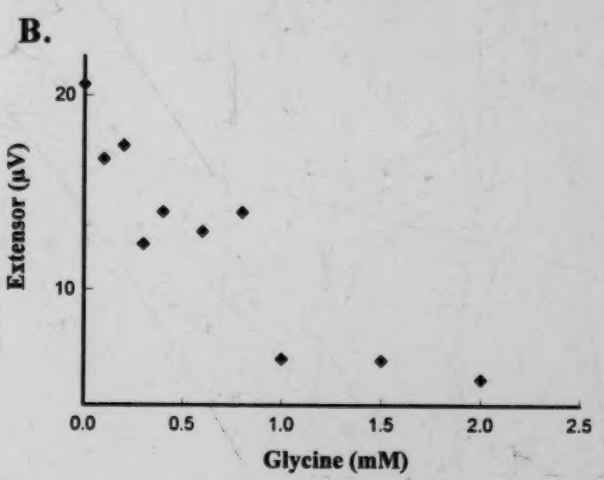
B.
Extensor (μV)
20
10
0.0
0.5
1.0
1.5
2.0
2.5
Glycine (mM)

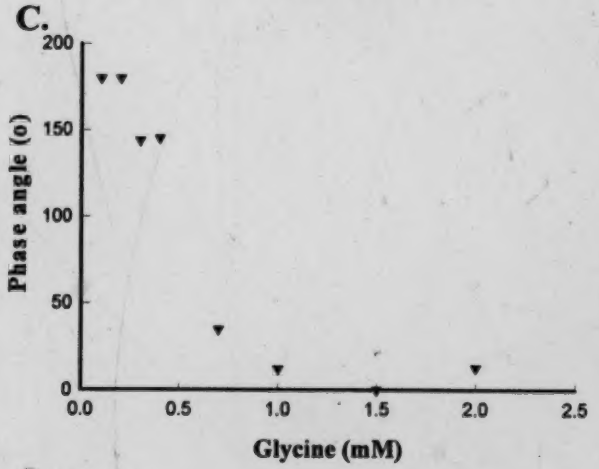
C.
Phase angle (o)
200
150
100
50
0
0.0
0.5
1.0
1.5
2.0
2.5
Glycine (mM)

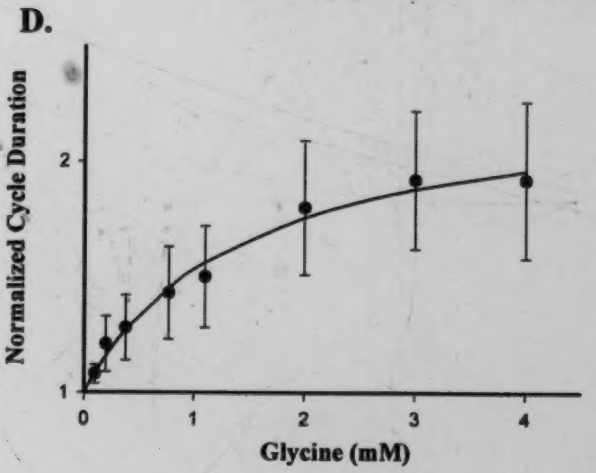
D.
Normalized Cycle Duration
2
1
0
1
2
3
4
Glycine (mM)

Figure 3-3. Effects of strychnine on NMDA-induced locomotion *in vitro*
(A) Control episode of locomotor activity elicited by adding NMDA and D-serine to the bath. EMG activity recorded unilaterally from elbow flexor and extensor muscles was rectified and smoothed. **(B)** 100 μM strychnine induced an increase of the cycle duration and switch from a regular alternating pattern to a synchronous EMG pattern. **(C)** Cross-correlogram of a control EMG recording illustrating normal out-of-phase relationship between antagonistic motor pools. **(D)** 100 μM strychnine caused synchronization of EMG bursts. **(E)** At lower concentrations strychnine tended to decrease cycle duration (an increase in the cycle frequency), whereas at higher concentrations lengthened the cycle duration. The curve was generated by using data from four animals.

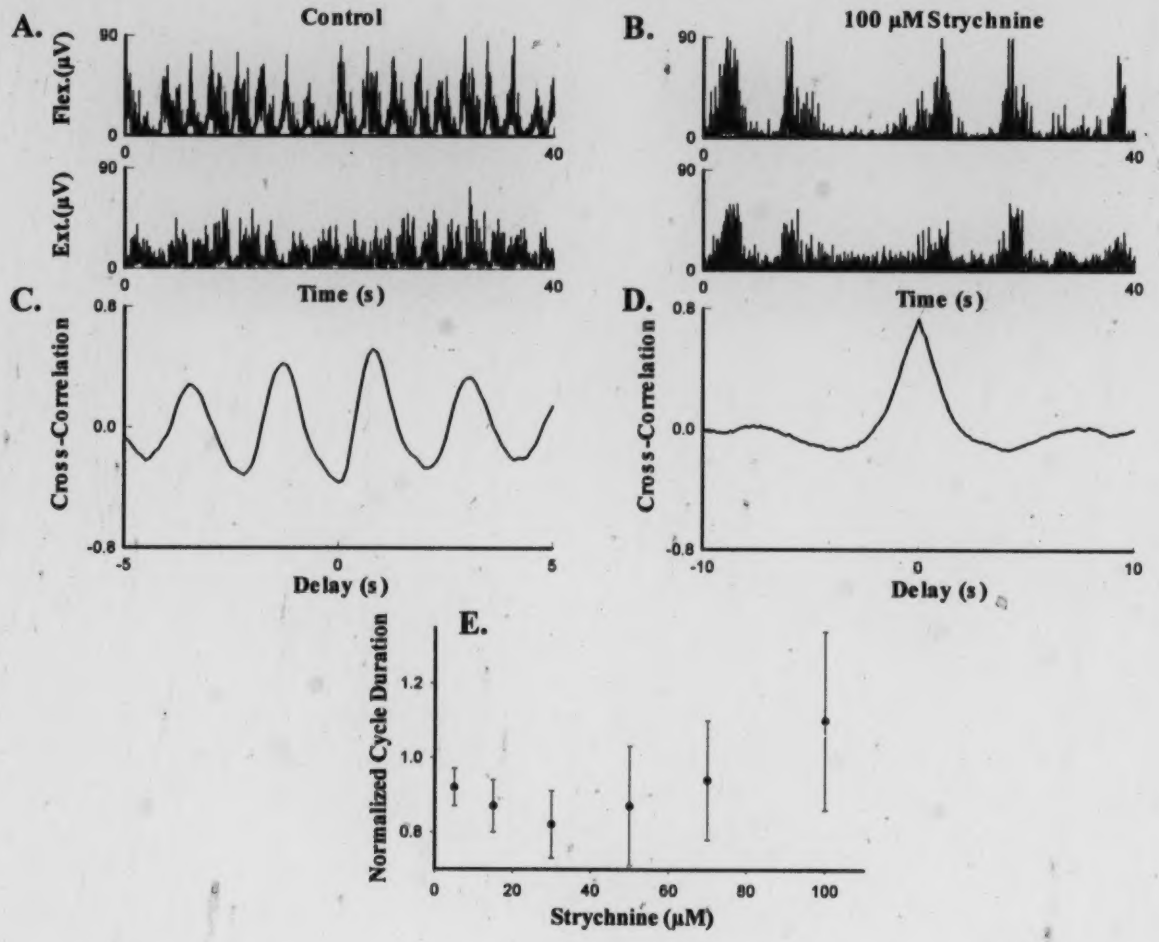
A.
Control
Flex.(μV)
Ext.(μV)
90
0
40
B.
100 μM Strychnine
C.
Time (s)
Cross-Correlation
0.8
0.0
-0.8
-5
5
Delay (s)
D.
-10
10
E.
Normalized Cycle Duration
1.2
1.0
0.8
20
60
80
100
Strychnine (μM)

At lower concentrations (0.5-30 μM) strychnine often produced a transient increase in the frequency (i.e. decrease in the cycle duration, Fig. 3-3 E) and amplitude of the rhythmic EMG alternation before establishing a synchronous pattern. Once established, this synchronous rhythmic activity was characterized by longer cycle durations although the difference was not statistically significant due to the variability between experiments (Fig. 3-3 E). In the remaining two of six preparations the effects of strychnine were not analyzed because the rhythmic EMG activity was replaced by random firing with little or no detectable rhythmic bursting. Following washout, the rhythmic EMG activity could be induced again. However, the rhythm was slower (cycle duration approximately doubled compared to the control) and the EMG activity remained synchronous. While the effects of exogenous glycine were completely reversible upon washout in Ringers solution strychnine's effects were not.

GABAergic system activation and its role in mudpuppy locomotion

Role of GABA in Necturus locomotion

When applied to the bath solution alone, GABA did not initiate locomotion. After locomotion was induced by NMDA, adding GABA (0.8-900 μM; n=11) lengthened the cycle period and/or suppressed the rhythmic EMG bursting (Fig. 3-4A, B, C). In addition, the pattern became much more variable. In two animals, increasing concentrations of GABA led to a full EMG synchronization as the flexor to extensor phase was reduced from around 160^0 to 0^0 (not shown). In the remaining nine animals the control phase, ranging between 180^0-105^0, was reduced to a range between 72^0-34^0 with GABA concentrations reaching 0.7-0.9 mM. The effects of GABA were reversible and dose-dependent (C_{50}=108 μM; ρ^2=0.99), generally reaching a maximum (M=2.75) with bath concentrations exceeding 700 μM GABA (Fig. 3-4 C). At concentrations exceeding 1 mM, a slow random discharge with no regular rhythmicity persisted.

To investigate whether an endogenous GABA release occurs during NMDA-induced locomotion and, if so, to establish its functional role, nipecotic acid, a GABA uptake blocker, was added to the bath. Like exogenous GABA, nipecotic acid (0.1-4

mM; n=8) induced an increase in the step cycle duration, although it was smaller in magnitude (compare Fig. 3-4 C and 3-4D). Increased concentrations of nipecotic acid, and presumably endogenous GABA, also induced a decrease in the EMG amplitude and a switch from an alternating to an irregular and eventually overlapping EMG pattern. In all animals the control phase, ranging between 180^0-105^0 was reduced to 97^0-12^0 in the presence of 4 mM nipecotic acid. Unlike with GABA, complete EMG synchronization was never observed with nipecotic acid in the bath. The observed effects were dose-dependent (Fig. 3-4D) and reversible upon washout with Ringer solution. To test whether the effects evoked by nipecotic acid were specific and to determine what type of GABA receptor was mediating them, the $GABA_A$ and $GABA_B$ receptor antagonists bicuculline and CGP-35348, respectively were added to the bath following the application of nipecotic acid (n=3). The increase in the cycle period induced by nipecotic acid was counteracted by both antagonists (not shown). While CGP-35348 appeared to preferentially affect the cycle duration, episodes of weak and/or irregular EMG activity occurred in the presence of bicuculline. The effects of bicuculline suggest that endogenous activation of $GABA_A$ receptors, during NMDA-induced locomotion, affects both the EMG burst frequency and its regularity.

Role of $GABA_A$ receptors in Necturus locomotion

When applied to the bath alone, or in combination with strychnine, a $GABA_A$ receptor antagonist bicuculline was not capable of eliciting locomotion, but its addition (0.8-20 μM; n=6) during ongoing locomotion affected both the locomotor rhythm and pattern (Fig. 3-5A, B, C, D). Cycle period decreased (Fig. 3-5 E) while the normal alternating pattern was disrupted and was replaced with EMG co-activation. In two animals, increasing concentrations of bicuculline resulted in full EMG synchronization as the flexor to extensor phase was reduced from around 130^0 to 0^0 (not shown). In the remaining four animals the control phase, ranging between 180^0-120^0, was reduced to 113^0-5^0 in the presence of 40 μM bicuculline. Bicuculline generally had a potent action on the cycle duration, producing its maximum effect at 10 μM ($M=0.71$; $C_{50}=0.18$ μM;

Figure 3-4. Effects of GABA on NMDA-induced locomotion *in vitro*.
(A, B) Bath application of GABA suppressed locomotor activity and disrupted the phase relationship between antagonistic motor pools. **(C)** GABA dose-response relationship reflecting the changes in the cycle duration produced by increasing concentrations of GABA. The curve was generated by using data from eleven animals. **(D)** Summary of the effect of increasing concentration of nipecotic acid on the cycle duration. An inhibition of GABA uptake mechanisms mimicked the effects previously observed with GABA. The data obtained from eight animals illustrate a dose-dependent increase in the cycle duration the magnitude of which was smaller then one induced by exogenous GABA (compare to Fig. 3-4C).

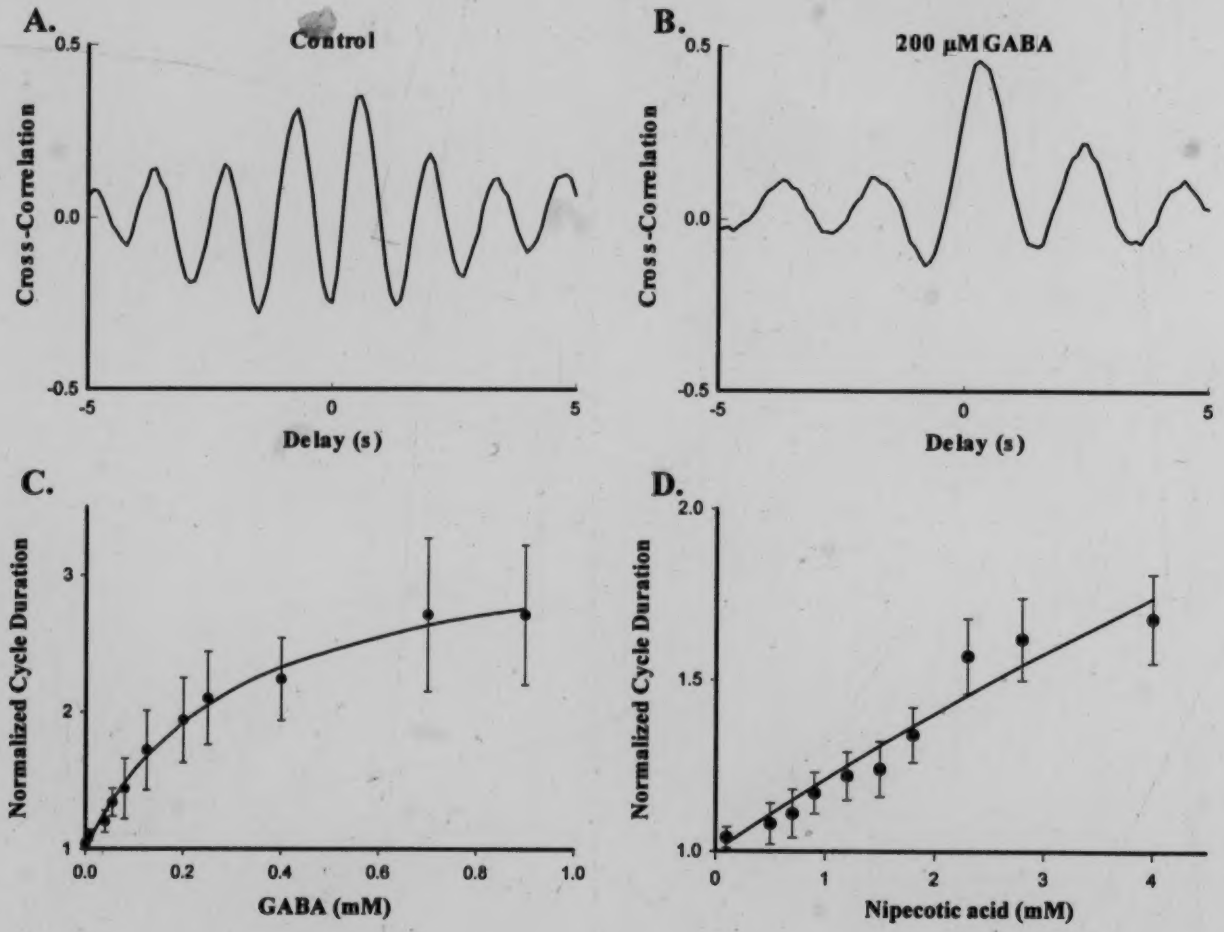
A.
Control
Cross-Correlation
0.5
0.0
-0.5
-5
0
5
Delay (s)
B.
200 µM GABA
Cross-Correlation
0.5
0.0
-0.5
-5
0
5
Delay (s)
C.
Normalized Cycle Duration
3
2
1
0.0
0.2
0.4
0.6
0.8
1.0
GABA (mM)
D.
Normalized Cycle Duration
2.0
1.5
1.0
0
1
2
3
4
Nipecotic acid (mM)

Figure 3-5. Effects of $GABA_A$ receptor antagonist bicuculline on NMDA-induced locomotion. **(A)** Control episode of locomotor activity elicited by applying NMDA and D-serine to the bath. **(B)** 10 μM bicuculline caused a decrease of the cycle duration and switch from a regular alternating pattern to a less regular and more synchronous EMG pattern. **(C)** A negative value for the peak near zero in the control cross-correlation indicates that the flexor and extensor EMGs are relatively out of phase. **(D)** Bath application of bicuculline caused the step cycle to speed up followed by a gradual reduction of the flexor to extensor phase. Please notice that cross-correlation function is shifted so that its positive peak is now closer to zero indicating that EMGs are becoming relatively in phase. **(E)** The data from six animals illustrates a dose-dependant decrease in the cycle duration.

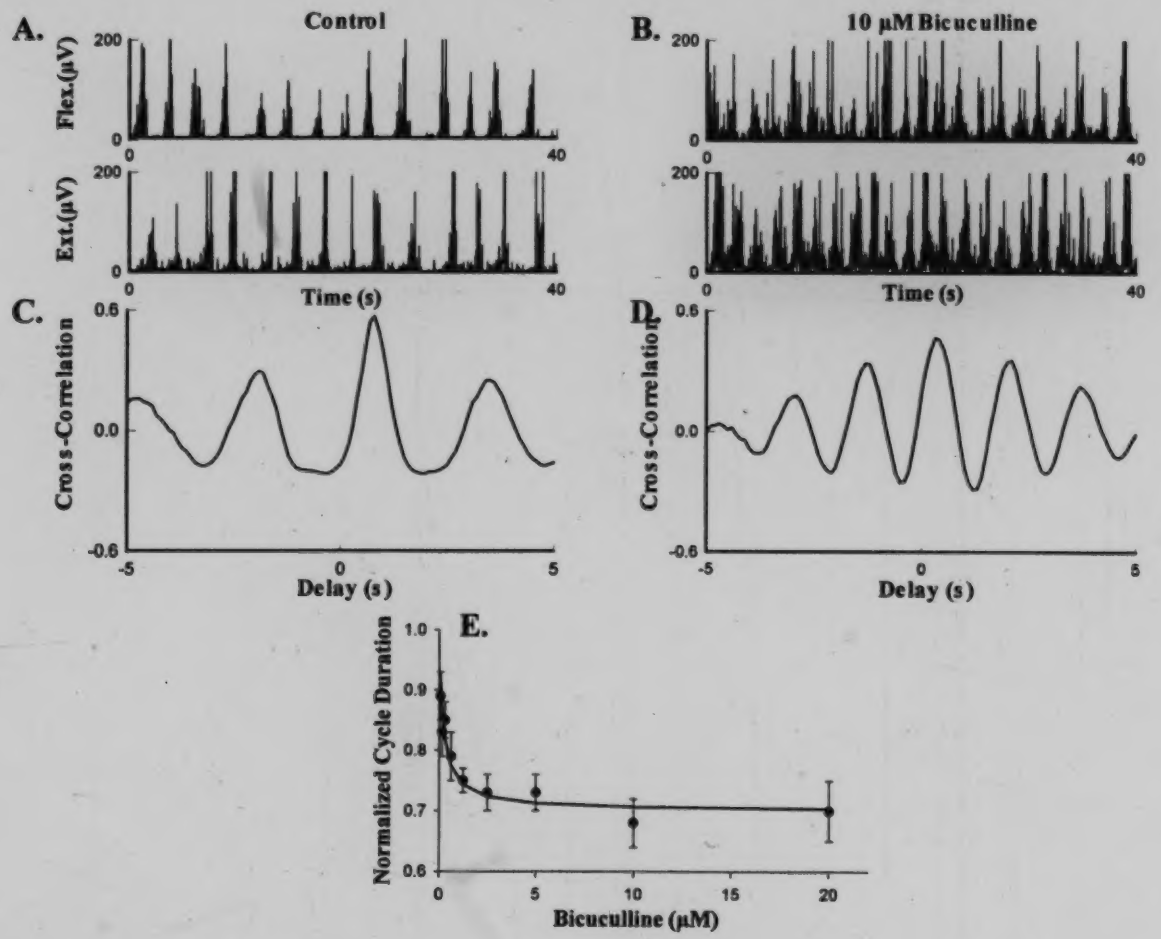
A.
Control
Flex.(μV)
Ext.(μV)
200
0
40
Time (s)
B.
10 μM Bicuculline
C.
Cross-Correlation
0.6
0.0
-0.6
-5
5
Delay (s)
D.
E.
Normalized Cycle Duration
1.0
0.9
0.8
0.7
0.6
10
15
20
Bicuculline (μM)

ρ^2=0.90). An increase in the EMG amplitude was observed in some preparations following application of bicuculline as well as episodes of weak and/or irregular EMG activity. These effects were suppressed by an application of the $GABA_A$ receptor agonist muscimol in all preparations tested (0.5-8μM; n=3). Muscimol appeared to be a very potent $GABA_A$ agonist, even in small concentrations, eventually causing a complete suppression of the locomotor activity. If applied alone, muscimol caused an immediate cessation of ongoing locomotor activity (not shown). The effects of bicuculline and muscimol were reversible after washout.

Role of $GABA_B$ receptors in Necturus locomotion

Bath application of baclofen, a $GABA_B$ receptor agonist, affected NMDA-induced locomotion by slowing the rhythm (Fig. 3-6C, D; 0.5-100 μM; n=6) and reducing the EMG amplitude. Its effect on the cycle duration was dose-dependent (Fig. 3-6 E; M=3.22; C_{50}=53 μM; ρ^2=0.996) and counteracted by the action of $GABA_B$ receptor antagonist CGP-35348 (Fig. 3-6F; M=0.71; C_{50}=20 μM; ρ^2=0.94; n=5). The EMG activity remained regular during the application of baclofen and the alternating pattern between the flexor and extensor muscles was hardly affected (compare Fig. 3-6 A and 3-6 B). In this example, baclofen reduced the flexor to extensor phase from about 180^0 to about 123^0. In the remaining animals the control phase (164^0-126^0) change, elicited by baclofen, ranged between 138^0-119^0.

Immunocytochemistry

GABA. GABA-immunoreactive cell bodies were found in all segments of the cervical spinal cord. They were observed grouped in clusters or as solitary neuronal profiles at the border between the grey and white matter (Fig. 3-7). We observed the clusters at a depth of 300-550 μm ventral to the dorsal surface of the spinal cord. Such clusters were present in the caudal part of the C2 segment, as well in segments C3 and C4. They were less prominent in the fifth and sixth segment. The GABA-immunopositive neuronal profiles were relatively simple, usually bipolar neurons that did not exceed 20 μm in diameter (Fig. 3-7, inset in A).

Figure 3-6. Effects of $GABA_B$ receptor substances on NMDA-induced locomotion. **(A, B)** EMG activity, recorded unilaterally from elbow flexor and extensor muscles, illustrating that $GABA_B$ antagonist baclofen mimicked the effects of GABA in that it caused the step cycle to slow down. Unlike with GABA, the EMG activity remained regular during the application of baclofen and the alternating pattern between the opposite muscles was largely unaffected (compare **C, D**). **(E)** The effect of increasing concentrations of baclofen on the cycle duration is summarized from six animals. **(F)** Baclofen's effect on the cycle duration was antagonized by the action of $GABA_B$ receptor antagonist CGP-35348. The data obtained from five animals illustrates antagonistic action of CGP-35348.

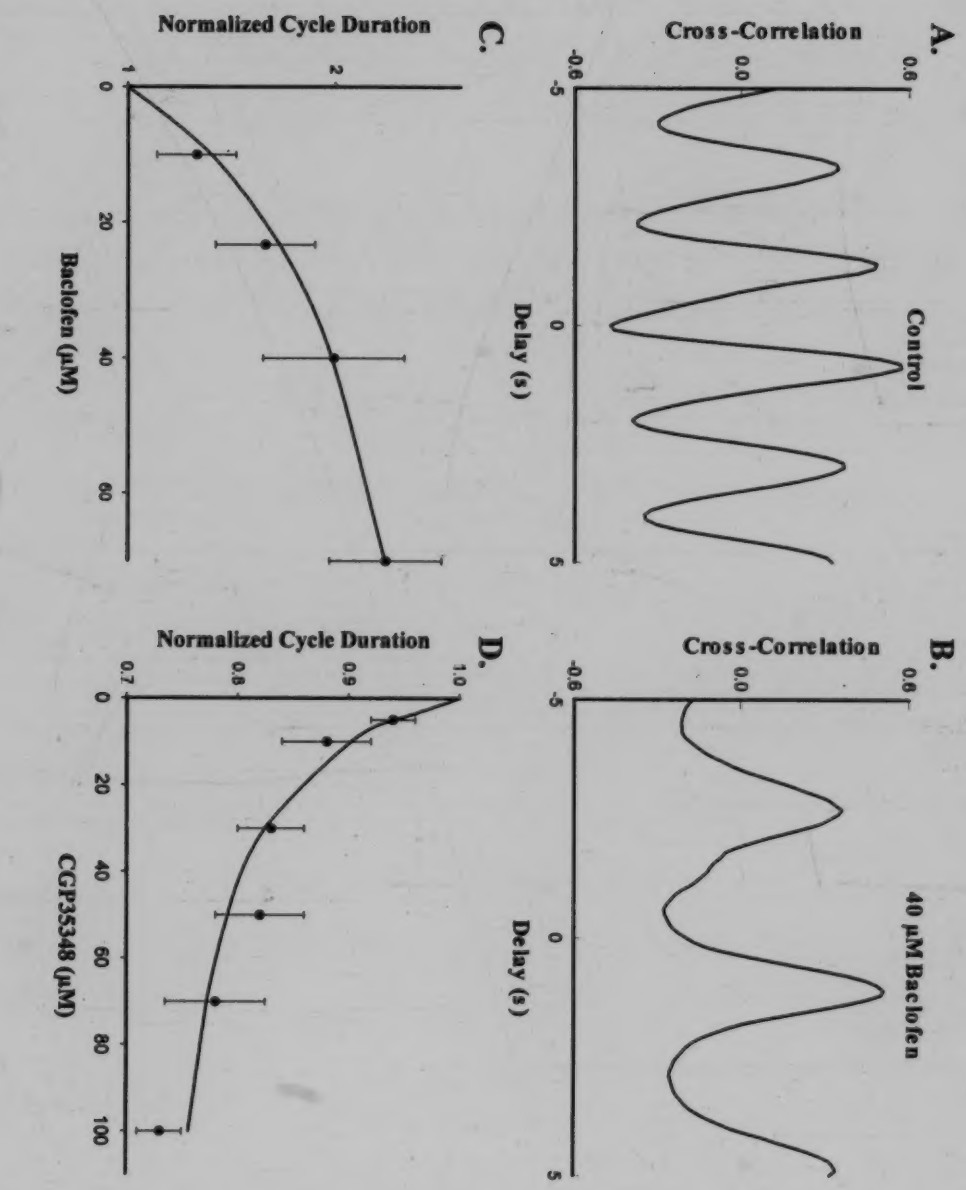
A.
Cross-Correlation
0.6
0.0
-0.6
-5
0
5
Delay (s)
Control
B.
Cross-Correlation
0.6
0.0
-0.6
-5
0
5
Delay (s)
40 µM Baclofen
C.
Normalized Cycle Duration
1
2
0
20
40
60
Baclofen (µM)
D.
Normalized Cycle Duration
0.7
0.8
0.9
1.0
0
20
40
60
80
100
CGP35348 (µM)

Figure 3-7. Horizontal sections through the spinal cord depicting the localization of GABA positive neuronal profiles **(A)** and processes **(B, C)**. **(A)** A group of GABA positive neurons at the border of the grey/white matter (between the open arrows) in the third segment, 300-350 μm below the dorsal surface. Their processes are directed towards the lateral surface of the spinal cord (open arrowhead), and to a lesser extent, in medial direction. Deeper in the spinal cord (500-550 μm) solitary GABAergic profiles could also be observed (inset). **(B)** Dorsal to the clusters of neurons shown in **A**, a dense network of fine immunopositive fibers is observed at equal distance from the midline (m, to the left) and the lateral surface of the spinal cord (open arrowhead, to the right) in the corresponding to **A** location (between the open arrows). **(C)** Higher power photomicrograph through the 5th segment (500-550 μm in depth) depicting GABA immunopositive fibers of different calibers, some of which possess varicosities (arrows). Note that the majority of the fibers are oriented in the lateral plane, whereas fewer course in rostro-caudal direction (curved arrows). The arrows in the upper right corner indicate rostral (R) and lateral (L) directions. Note the different orientation of **C**. Bars= 50 μm, except for inset in **A** (20 μm).

R
L
m
L
R
C

Their processes, were generally oriented in the medio-lateral plane.

In more dorsal sections, the border between the white and grey matter was occupied by immunopositive fibers (Fig. 3-7 B). The white matter at all rostrocaudal levels contained GABA- immunopositive fibers, but they were most noticeable in more ventral sections (400- 500 μm below the dorsal surface of the spinal cord). Occasionally, varicosities (2-3 μm in diameter) were observed on these fibers.

Glycine. The majority of the glycine-immunopositive neuronal profiles were observed at a depth of 350-600 μm below the dorsal surface of the spinal cord, primarily in the caudal part of segment 3, and throughout segments 4-6. The clusters contained fewer neurons which were less densely packed than the GABA-immunopositive profiles (compare Fig. 3-8 A to Fig. 3-7 A)

. These neurons were 18-20 μm in diameter with processes that projected laterally towards the white matter and medially towards the grey matter. Occasionally the medially oriented processes reached the ependymal lining of the wall of the central canal. The network of glycine-positive nerve fibers was more diffuse than the one formed by GABA-positive fibers; i.e., we did not detect the specific pattern in more dorsal sections as was shown in Fig. 3-7 B. Moreover, the white matter contained fewer glycinergic fibers (compare Fig. 3-8 B to Fig. 3-7 C). Glycine-immunopositive neuronal profiles were also observed in the immediate vicinity of the wall of the central canal. They were primarily located throughout segments 1-3 (Fig. 3-8C), 200-250 μm below the dorsal surface of the spinal cord. However, more caudal segments also contained such neurons, whose processes were intimately related to the ependymal lining or to each other (Fig. 3-8 D,C).

DISCUSSION

GABA and glycine are known to play an important role in controlling locomotor neuronal networks. They are implicated either in the generation or modulation of locomotion in a wide variety of species. The present study provides further evidence of their role in modulating the CPG underlying locomotion in a walking amphibian, the mudpuppy, as

Figure 3-8. Horizontal sections depicting relationships of glycine immunoreactive neuronal profiles and processes with the ependymal lining (ep) of the central canal (cc). **(A)** Glycine positive neurons at the grey/white matter border with short processes directed medially, as well as laterally. One neuron extends a long process which traverses the grey matter (arrows) and appears to penetrate the ependyma (double arrows). **(B)** The white matter contains glycine positive fibers that are oriented primarily in the medio-lateral plane. Note that there are fewer fibers than in **Fig. 3-7 C**. **(C)** A group of glycine positive neurons in the vicinity of the central canal. Some of their processes are oriented towards the central canal and appear to penetrate the ependymal lining. **(D)** Two neurons whose processes (arrows) run parallel to the wall of the central canal. **(E)** Contacts between neighboring neurons where a process of the caudal neuron is apposed on the soma of the rostral one (arrows). All photomicrographs are the same magnification except **A**. and are identically oriented. The arrows in the upper right corner in **B** indicate rostral (R) and lateral (L) directions. Abbreviations: bv, blood vessel. Bars= 50 μm.

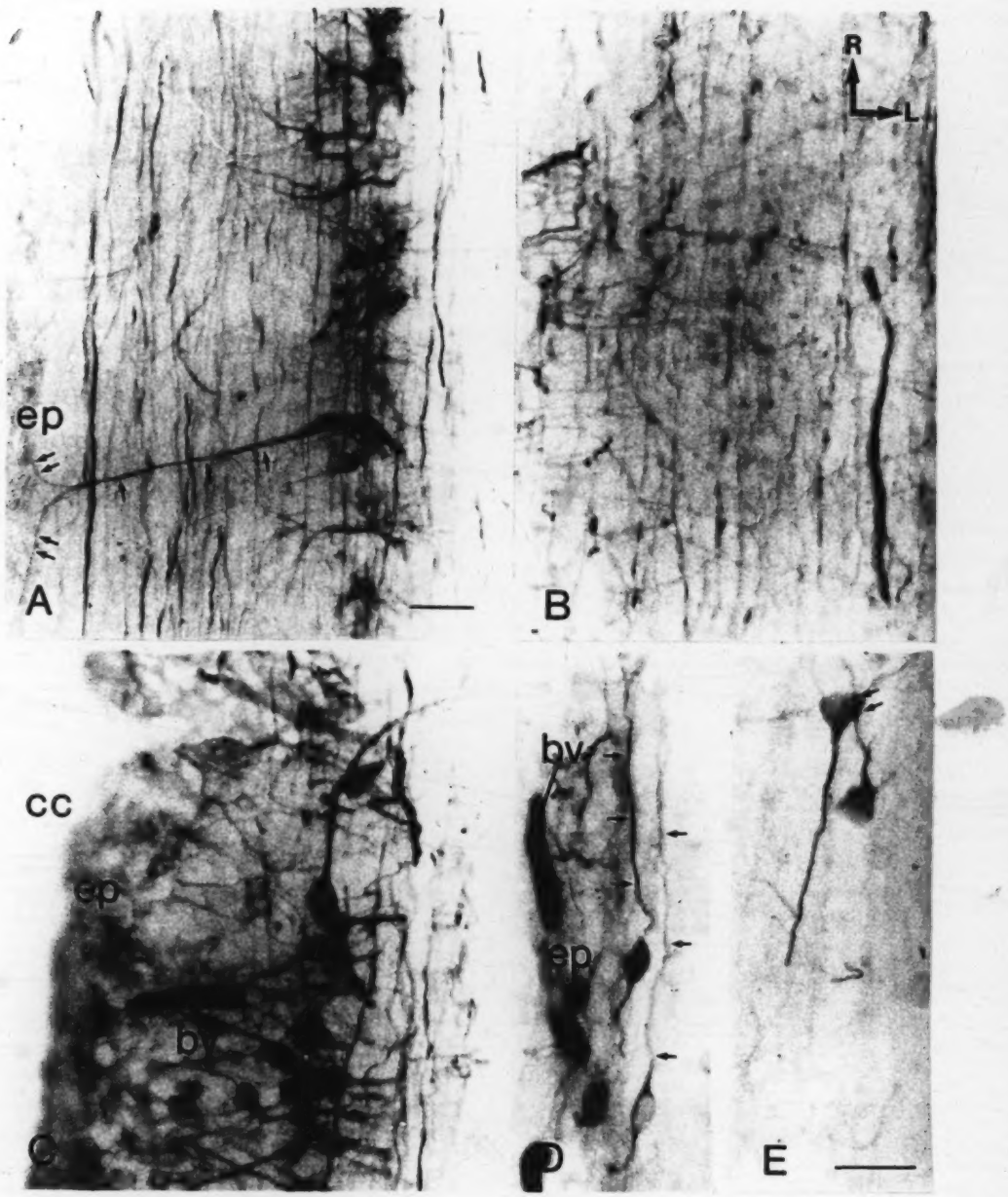
ep
A
R
L
B
cc
ep
b
C
bv
ep
D
E

well as evidence for the presence of spinal glycinergic and GABAergic systems. Our combined electrophysiological and anatomical data suggest that activation of these endogenous systems, during NMDA-induced locomotion, affects the phase relationship between antagonistic motoneuronal pools, causes change in the step cycle duration and/or in the regularity of the EMG pattern.

Glycine

The glycinergic inhibitory pathway was shown to play a key role in mediating alternation between contra lateral limbs (Kudo et al. 1991; Cowley and Schmidt 1995; Noga et al. 1993) and antiphase coupling between intralimb flexor and extensor muscles (Cowley and Schmidt 1995; Noga et al. 1993; Pratt and Jordan 1987) in walking vertebrates. The same pathway has also been implicated in providing alternation between contra lateral body sides in swimming vertebrates (Alford and Williams 1989; Cohen and Harris-Warrick 1984; Dale et al. 1990; Soffe 1987). As a way of assessing the role of glycinergic inhibition in mudpuppy locomotion strychnine, a glycine receptor antagonist, was applied to the bath. Ultimately, strychnine transformed flexor-extensor alternation into synchronous burst activity without blocking the rhythmicity. However, increasing concentrations of strychnine transiently increased the frequency of EMG alternation before switching to a synchronous pattern. A similar action of strychnine was reported in the lamprey (Hagevik and McClellan 1994; McPherson et al. 1994), neonatal rat (Cowley and Schmidt 1995) and neonatal mouse (Droge and Tao 1991). Recent modeling studies in the lamprey (Hagevik and McClellan 1994) shed more light onto this seemingly biphasic action of strychnine. They revealed that reciprocal inhibition between independent rhythm generators, present in each half of the CNS, can be gradually reduced and replaced by excitation, existing in parallel, due to increasing concentration of strychnine. Our previous study (Cheng et al. 1997) showed that, analogous to the other systems (see the Introduction), there are distinct flexor and extensor centres exhibiting an inherent rhythmicity. They are normally coupled by short latency inhibitory connections that use glycine and can be blocked by strychnine. Thus, as these connections are blocked, weaker excitatory connections are revealed (Fig. 3-9; dashed lines) so that synchronous activation

Figure 3-9. Schematic diagram of the actions of the inhibitory neurotransmitters on the locomotor circuitry. Separate flexor and extensor rhythm generating centres excite the corresponding groups of motoneurons and inhibit each other. Blocking this inhibition with glycine or $GABA_A$ antagonists produces synchronous activation, suggesting weak mutually excitatory connections (dashed lines). $GABA_B$ is thought to act presynaptically by blocking excitatory drive to the centres that may come from sensory input or descending connections. As a result the cycle duration is increased, but the alternating pattern is not affected. This figure is modified from Cheng et al. (1997)

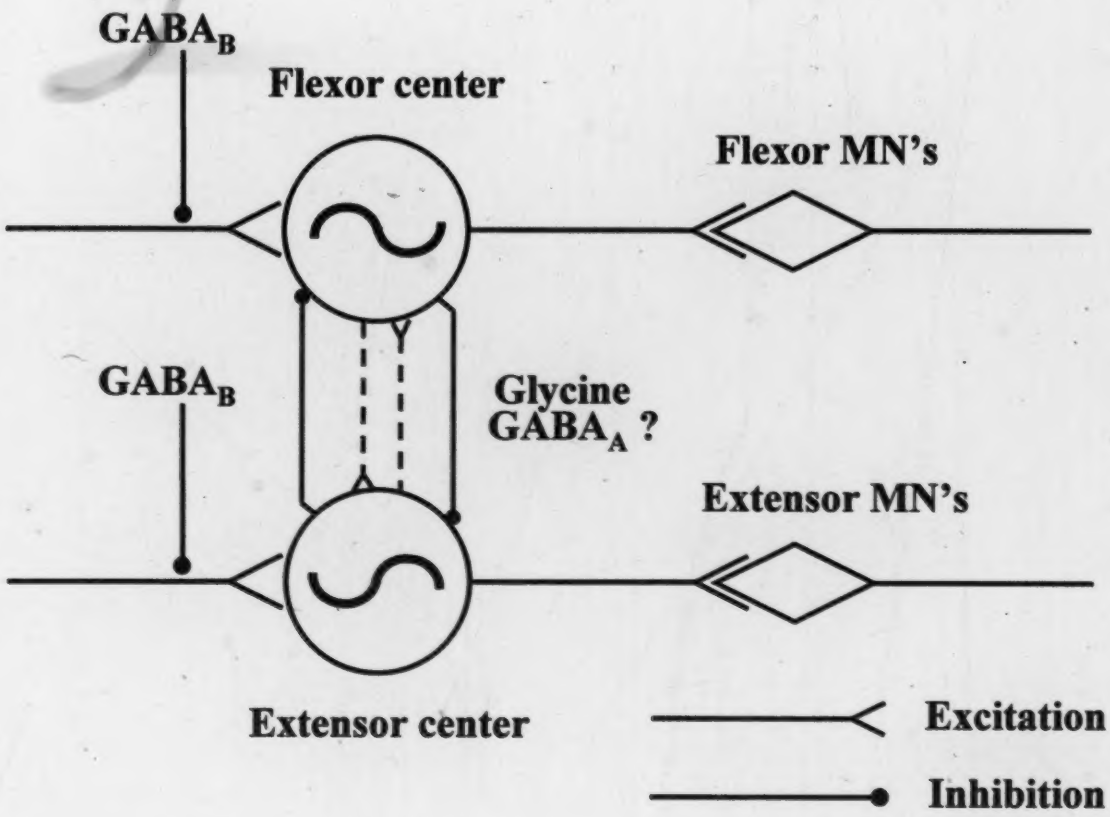
GABA$_B$
Flexor center
Flexor MN's
GABA$_B$
Glycine
GABA$_A$?
Extensor MN's
Extensor center
Excitation
Inhibition

of the two muscle groups results. Application of strychnine would initially block some inhibition, decreasing cycle time, but when all inhibition is removed longer-lasting synchronous bursts are produced.

Glycine is a major spinal inhibitory neurotransmitter (Curtis et al. 1968; Soffe 1987; Schneider and Fyffe 1992) and a cofactor in potentiating the role of NMDA in generating locomotion in the mudpuppy (Wheatley et al. 1992). However, in the present study D-serine was added to the bath. This compound can replace glycine in binding to the NMDA receptors, but not to the sites of its inhibitory action (Johnson and Ascher 1987; Benveniste et al. 1990). Under these circumstances, glycine increased the cycle duration (decreased the frequency of the locomotor rhythm) and also caused a switch from a normal alternating to a synchronous EMG activity. The reason for this change in pattern is not known.

Locomotor rhythm generation can occur in a variety of vertebrate preparations without glycinergic inhibition (for review see McClellan 1996). In mammals blockage of glycinergic inhibition does not prevent locomotor rhythmogenesis but promotes episodes of synchronous rhythmic discharge of flexors and extensors bilaterally (Cowley and Schmidt 1995; Noga et al. 1993). Similarly, in the mudpuppy, glycine receptors appear not to be required for rhythm generation, since the rhythmic EMG activity is not abolished by high concentrations of strychnine. However, these receptors are required to maintain stable, out-of-phase coupling between antagonistic motor pools, typical of forelimb walking. Whether this basic rhythmicity involves only excitatory synaptic mechanisms, specific cellular properties or some other inhibitory agents remains to be determined. Changes in the locomotor rhythm (cycle period) induced by glycine and strychnine suggest that their action occurs at the level of the CPG itself, although they may act on motoneurons as well (Schneider and Fyffe 1992; McPherson et al. 1994).

GABA

Similar to what was previously reported in neonatal rats (Cazalets et al. 1994; Cowley and Schmidt 1995) and the neonatal wallaby (Ho 1997) our results indicate the involvement of both glycinergic and GABAergic inhibitory pathways in control of forelimb

CPG in the mudpuppy. The slowing of the locomotor rhythm, caused by GABA, suggests that its action occurred at the level of the CPG itself. However, this does not exclude the possibility of GABA's direct action on motoneurons (Curtis et al. 1968; Schneider and Fyffe 1992). The action of endogenous GABA was mediated through both $GABA_A$ and $GABA_B$ receptors. An activation of $GABA_B$ receptors caused changes in the cycle duration and EMG amplitude without an apparent effect on locomotor pattern. $GABA_B$ receptors are generally presynaptic and are indicated in Fig. 3-9, acting on the excitatory drive to the rhythm generator. Such a locus of action would explain why the rhythm is slowed without affecting the pattern of alternation.

When endogenous GABA activity was potentiated by muscimol, a $GABA_A$ receptor agonist, the locomotor pattern was affected differently. In addition to an increase in the cycle duration, muscimol also caused a large decrease in the EMG amplitude and/or a total cessation of the rhythmic activity. This is not surprising as muscimol has been shown to be more potent than GABA itself in activating inhibitory receptor-ionophores in all tissues tested (Freeman 1973). Conversely, bicuculline, a $GABA_A$ receptor antagonist, reduced the cycle duration and caused an increase in variability of the EMG pattern. Bicuculline also caused normal alternating pattern to switch to a synchronous one. The observed effects were dose-dependent and reversible. A possible explanation of our results can be found in a variety of actions bicuculline exerts upon spinal neurons. In addition to its specific antagonism of GABA responses, bicuculline also causes reduction of K^+ conductances and prolongation of Ca^{++}-dependent action potentials. Although all the actions show dose-dependency, the relevant concentration range for each is different. The synaptic GABA antagonism is elicited at the lowest bicuculline concentrations (0.2-10 μM) while the direct, nonsynaptic actions on spinal neurons occurs at much higher concentrations (5-200 μM, Heyer et al. 1981). The effects we saw already reached a peak by 10 μM that in some experiments declined at higher concentrations.

Comparable results obtained in the trials with bicuculline and strychnine may also indicate a functional interplay between GABAergic and glycinergic systems during

locomotion in the mudpuppy. Similar findings obtained in recent studies on neonatal rats (Cowley and Schmidt 1995; Kremer and Lev-Tov 1997) may provide further support to this notion. Furthermore, frequent co-localization of the two receptor types (Todd et al. 1996; Bohlhalter et al. 1994) and co-localization of GABA and glycine within a single neuron (Todd and Sullivan 1990; Berki et al. 1995) strongly support the notion that GABA and glycine can act as cotransmitters in the spinal cord. Whether this is also true in the mudpuppy spinal cord remains to be determined so we have indicated $GABA_A$ in the diagram of Fig. 9, but with a question mark. When applied to the bath alone or in combination, strychnine and bicuculline were not able to induce the rhythmic activity. This differs from the results obtained from neonatal mammal in vitro preparations (Bracci et al. 1996; Cowley and Schmidt 1995; Droge and Tao1993). Although this discrepancy may be attributed to methodological and interspecies differences, it may also reflect developmental stage or the specific age of the system under investigation.

Immunocytochemistry

Our data demonstrate that GABAergic and glycinergic neurons, fibers and varicosities are present in the spinal cord of the mudpuppy with the majority of the immunoreactive cell bodies being localized between spinal segments C2-C6. Anatomically, these segments largely correspond to the spinal cord region from which the brachial nerves originate to innervate the mudpuppy's forelimb muscles (Gilbert 1986). They also contain motoneuronal pools supplying forelimb muscles (Székely and Czéh 1967; Stephens and Holder 1985) and the CPG to the mudpuppy's forelimb resides in this area, covering parts of segments C2 and C3 (Wheatley at al. 1994). Thus, it appears that glycinergic and GABAergic neurons are appropriately localized in the spinal cord to interact with the forelimb pattern generator.

The location and depth at which GABA and glycine immunoreactive cell bodies are found largely coincides with the depth and location of 5-HT neurons (Jovanović et al. 1996). This may indicate a possible involvement of 5-HT in the effects exerted by inhibitory neurotransmitters since 5-HT can induce glycine secretion (Minz et al. 1989). Moreover, 5-HT and GABA immunopositive terminals are also found in close apposition

(Petrov et al. 1991), suggesting that the two transmitters may affect each other's release. These findings may provide further support to the idea of complex interactions between different neurotransmitter systems in the mudpuppy spinal cord as well as their interactions with the spinal interneurons and motoneurones involved in generation and/or control of locomotion.

In addition to their similar distribution pattern GABAergic and glycinergic neurons show some distinct features. Both, GABAergic neurons and fibers seem to be more numerous then glycinergic ones. This may be due to GABA's role in control of sensory afferent messages reaching CNS during locomotion. However, a portion of these fibers may represent a projection of descending GABAergic system which also may play role in the endogenous control of the locomotor network. On the other hand, glycinergic neurons are found to penetrate ependymal lining probably contacting the cerebro-spinal fluid. Neurons contacting CSF were reported in various preparations (Brodin et al. 1990; Dale et al. 1987; Jovanović et al. 1996; Vigh et al. 1983). Morphological evidence suggests that they might be involved either in monitoring the composition of the CSF or acting as mechanoreceptors, but their significance remains to be elucidated.

Overall, our data suggest that inhibitory neurotransmission is not essential for locomotor rhythmogenesis within the mudpuppy spinal cord but may be required for establishing and maintaining the reciprocal antagonism underlying intralimb locomotor patterns. It also suggest that excitatory connections which synchronize the intralimb rhythm are masked by predominant inhibition. The similarity of these results to those obtained from the lamprey and tadpole on one hand and the neonatal rat on the other hand suggests that in changing from locomotion using the trunk (swimming) to locomotion using legs (walking), the control mechanisms in the spinal cord have been conserved.

REFERENCES

Alford S, Williams TL (1989) Endogenous activation of glycine and NMDA receptors in lamprey spinal cord during fictive locomotion. J Neurosci 9:2792-2800

Benveniste M, Clements J, Vyklický LJR, Mayer M (1990) A kinetic analysis of the modulation of N-methyl D-aspartic acid receptors by glycine in mouse cultured hippocampal neurons. J Physiol (Lond) 428:333-357

Berki ACs, O'Donovan MJ, Antal M (1995) Developmental expression of glycine immunoreactivity and its colocalization with GABA in the embryonic chick lumbosacral spinal cord. J Comp Neurol 362:583-596

Bohlhalter S, Mohler H, Fritschy JM (1994) Inhibitory neurotransmission in rat spinal cord: co-localization of glycine- and $GABA_A$-receptors at GABAergic synaptic contacts demonstrated by triple immunofluorescence staining. Brain Res 642:59-69

Bonanno G, Raiteri M (1993). Multiple $GABA_B$ receptors. TIPS 14: 259-261

Bracci E, Ballerini L, Nistri A (1996) Spontaneous rhythmic bursts induced by pharmacological block of inhibition in lumbar motoneurons of the neonatal rat spinal cord. J Neurophysiol.75:640-647

Brodin L, Dale N, Christenson J, Storm-Mathisen J, Hokfelt T, Grillner S (1990) Three types of GABA-immunoreactive cells in the lamprey spinal cord. Brain Res 508:172-175

Calabrese R, Peterson EL (1983) Neural control of heartbeat in the leech, *Hirudo medicinalis*. In: Roberts A, Roberts BL (eds) S.E.B. Symposium 37, Neural Origin of Rhythmic Movements. Cambridge University Press, London, pp 195-221

Cazalets JR, Sqalli-Houssaini Y, Clarac F (1994) GABAergic inactivation of the central pattern generators for locomotion in isolated neonatal spinal cord. J Physiol (Lond) 474:173-181

Cheng J, Stein RB, Jovanović K, Yoshida K (1997) Localization, activation and modulation of networks for walking in mudpuppy spinal cord. Society for Neuroscience Abstracts 23:207

Clarac F, Cattaert D (1996) Invertebrate presynaptic inhibition and motor control. Exp Brain Res 112:163-180

Cohen A, Harris-Warrick RM (1984) Strychnine eliminates alternating output during fictive locomotion in the lamprey. Brain Res 293: 164-167

Cowley KC, Schmidt BJ (1995) Effects of inhibitory amino acid antagonists on reciprocal inhibitory interactions during rhythmic motor activity in the *in vitro* neonatal rat spinal cord. J Neurophysiol 74:1809-1117

Curtis DR, Hösli L, Johnston GAR, Johnston IH (1968) The hyperpolarization of spinal motoneurones by glycine and related amino acids. Exp Brain Res 5:235-258

Dale N, Roberts A, Ottersen OP, Storm-Mathisen J (1987) The morphology of 'Kolmer-Agdhur cells', a class of cerebrospinal-fluid-contacting neurons in the frog embryo spinal cord by GABA immunocytochemistry. Proc R Soc Lond (Biol) 232:193-203

Dale N, Roberts A, Soffe, SR (1990) The anatomy, development and role of glycinergic neurons in the *Xenopus* embryo spinal cord. In: Ottersen OP, Storm-Mathisen J (eds) In: Glycine neurotransmission, John Wiley and Sons, pp. 329-353

Droge MH, Tao Y, (1993) Glycine effects on in vitro motor pattern generation in mouse spinal cord. Neurosci Lett 158:139-142

Dubuc R, Cabelguen JM, Rossignol S (1988) Rhythmic fluctuations of dorsal root potentials and antidromic discharges of primary afferents during fictive locomotion in the cat. J Neurophysiol 60: 2014-2036

El Manira A, Clarac F (1991) GABA-mediated presynaptic inhibition in crayfish primary afferents by non-A, and non-B GABA receptors. Eur J Neurosci 3: 1208-1218

Freeman AR (1973) Electrophysiological analysis of the actions of strychnine, bicuculline and picrotoxin on the axonal membrane. J Neurobiol 4:567-582

Gilbert SG (1986) Pictorial anatomy of the *Necturus.* University of Washington Press, Washington

Grillner S (1981) Control of locomotion in bipeds, tetrapods and fish. In: Handbook of Physiology, The Nervous System, Motor Control. Am Physiol Soc, Bethesda, MD, vol II:1179-1236

Grillner S, Matsushima T (1991) The neural network underlying locomotion in lamprey-synaptic and cellular mechanisms. Neuron 7:1-15

Grillner S, Wallén P (1980) Does the central pattern generator for locomotion in lamprey depend on glycine inhibition? Acta Physiol Scand 110:103-105

Hagevik A, McClellan A (1994) Coupling of spinal locomotor networks in larval lamprey revealed by receptor blockers for inhibitory amino acids: neurophysiology and computer

modeling. J Neurophysiol 4:1810-1829

Heyer EJ, Nowak LM, Macdonald R (1981) Bicuculline: A convulsant with synaptic and nonsynaptic actions. Neurobiology 31:1381-1390

Ho SM (1997) Rhythmic motor activity and interlimb co-ordination in the developing pouch young of a wallaby (Macropus eugenii). J. Physiol. 501:623-636

Hsu SM, Raine L, Fanger H (1981) Use of avidin-biotin peroxidase complex (ABC) in immunoperoxidase techniques. J Histochem Cytochem 29:577-588

Johnson P, Asher P (1987) Glycine potentiates the NMDA response in cultured mouse brain neurons. Nature 325:529-531

Jovanović K, Petrov T, Greer JJ, Stein RB (1996a) Serotonergic modulation of the mudpuppy (*Necturus maculatus*) locomotor pattern in vitro. Exp Brain Res 111:57-67

Jovanović K, Petrov T, Stein RB (1996b) Modulatory action of inhibitory neurotransmitters on the mudpuppy (*Necturus maculatus*) locomotor pattern. Society for Neuroscience Abstracts 22:1376

Kremer E, Lev-Tov A (1997) Localization of the spinal network associated with generation of hindlimb locomotion in the neonatal rat and organization of its transverse coupling system. J Neurophysiol. 77:1155-1170

Kudo N, Ozaki S, Yamada T (1991) Ontogeny of rhythmic activity in the spinal cord of the rat. In: Shimamura M, Grillner S, Edgerton VR (eds) Neurobiological basis of human locomotion. Japan Scientific Society Press, Tokyo, pp127-136

McClellan AD (1996) Organization of spinal locomotor networks: contributions from model systems. Comments Theor Biol 4:63-91

Marder E, Calabrese RL (1996) Principles of rhythmic motor pattern generation. Physiol Rev 76:687-717

McPherson DR, Buchanan JT, Kasicki S (1994) Effects of strychnine on fictive swimming in the lamprey: Evidence for glycinergic inhibition, discrepancies with model predictions, and novel modulatory rhythms. J Comp Physiol A 175:311-321

Mintz I, Gotow T, Korn H (1989) Effects of serotonergic afferents on quantal release at central inhibitory synapses. Science 245:190-192

Noga BR, Cowley KC, Huang A, Jordan LM, Schmidt BJ (1993) Effects of inhibitory amino acid antagonists on locomotor rhythm in the decerebrate cat. Society for Neuroscience Abstracts 19:541

Petrov T, Seitanidou T, Triller A, Korn H (1991) Differential distribution of GABA- and serotonin-containing afferents on an identified central neuron. Brain Res 559:75-81

Petrov T, Krukoff TL, Jhamandas JH (1992) The hypothalamic paraventricular and lateral parabrachial nuclei receive collaterals from raphe nucleus neurons: A combined double retrograde and immunocytochemical study. J Comp Neurol 318: 18-26

Pratt CA, Jordan LM (1987) Ia inhibitory interneurons and Renshaw cells as a contributors to the spinal mechanisms of fictive locomotion. J Neurophysiol 57:56-71

Roberts A, Dale N, Soffe SR (1984) Sustained responses to brief stimuli: swimming in *Xenopus* embryos. J Exp Biol 112:321-335

Schneider SP, Fyffe REW (1992) Involvement of GABA and glycine in recurrent inhibition of spinal motoneurones. J Neurophysiol 68:397-406

Selverston AI, Miller JP, Wadepuhl M (1983) Cooperative mechanisms for the production of rhythmic movements. In: Roberts A, Roberts BL (eds) S.E.B. Symposium 37, Neural Origin of Rhythmic Movements. Cambridge University Press, London, pp 55-87

Soffe SR (1989) Roles of glycinergic inhibition and N-methyl-D-aspartate receptor mediated excitation in the locomotor rhythmicity of one half of the *Xenopus* embryo CNS. Eur J Neurosci 1:561-571

Soffe SR (1987) Ionic and pharmacological properties of reciprocal inhibition in *Xenopus* embryo motoneurones. J Physiol (Lond) 382: 463-473

Stephens N, Holder N (1985) A horseradish peroxidase study of motoneuron pools of the forelimb and hindlimb musculature of the axolotl. Proc R Soc Lond (Biol) 224:325-339

Stuart GJ, Redman SJ (1991) The role of $GABA_A$ and $GABA_B$ receptors in presynaptic inhibition of Ia EPSPs in the cat spinal cord motoneurones. J Physiol (Lond) 447: 675-692

Székely G, Czéh G (1967) Localization of motoneurones in the limb moving spinal cord segments of Ambystoma. Acta Physiol Acad Sci Hung 32:3-18

Tegnér J, Matsushima T, El Manira A, Grillner S (1993) The spinal GABA system modulates burst frequency and intersegmental coordination in the lamprey: differential effects of $GABA_A$ and $GABA_B$ receptors. J Neurophysiol 69:647-657

Todd AJ, Sullivan AC (1990) Light microscope study of the coexistance of GABA-like and glycine-like immunoreactivities in the spinal cord of the rat. J Comp Neurol 296:496-505

Todd AJ, Watt C, Spike RC, Seighart W (1996) Colocalization of GABA, glycine, and their receptors at synapses in the rat spinal cord. J Neurosci 16:974-982

Vigh B, Vigh-Teichmann I, Manzano e Silva MJ, van den Pol AN (1983) Cerebrospinal fluid-contacting neurons of the central canal and terminal ventricle in various vertebrates. Cell Tissue Res 231:615-621

Wheatley M, Edamura M, Stein RB (1992) A comparison of intact and in-vitro locomotion in an adult amphibian. Exp Brain Res 88:609-614

Wheatley M, Jovanović K, Stein RB, Lawson V (1994) The activity of interneurons during locomotion in the in vitro Necturus spinal cord. J Neurophysiol 71:2025-2032

CHAPTER 4

IDENTIFICATION, LOCALIZATION AND MODULATION OF NEURAL NETWORKS FOR WALKING IN THE MUDPUPPY (*Necturus maculatus*) SPINAL CORD

INTRODUCTION

The spinal cord in vertebrates is capable of generating rhythmic motor behaviors, such as locomotion, with or without sensory input (Székely et al. 1969; Delcomyn 1980; Grillner 1981, 1985; Pearson 1993). The neural networks responsible for locomotion are composed of populations of interneurons and are often referred to as central pattern generators (CPGs). The organization of the CPGs for vertebrate locomotion is beginning to be understood at a cellular level. Grillner and his colleagues ((Grillner et al.1991, 1995; Grillner 1995, 1996) identified classes of excitatory and inhibitory interneurons and elucidated for the first time the circuitry responsible for generating and coordinating the bending motion of the trunk required for swimming in the lamprey. The circuitry that produces swimming has also been examined in a tadpole (Roberts et al. 1986, 1995; Perrins 1995). A pair of half centers that are mutually inhibitory is an essential feature of the characterized segmental circuits.

The circuitry for walking is much more difficult to determine experimentally, since it involves coordinated limb movement about multiple joints in different limbs. Progress is being made to localize the networks for walking (Bracci et al. 1996; Cazalets et al. 1995, 1996; Cowley and Schmidt 1996; Iwahara et al. 1991; Kjaerulff and Kiehn 1996; Kremer

A version of this chapter has been published. Cheng J, Stein RB, Jovanović K, Yoshida K, Bennett DJ, Han Y (1998) J Neurosci 18:4295-4304. Contribution to paper: Performed dissections and participated in majority of experiments, contributed to editing of manuscript.

and Lev-Tov 1997) and to identify interneurons in the mammalian spinal cord that could be involved in generating walking (Edgley et al. 1988; Hochman et al. 1994; Kiehn et al. 1996; Kjærulff et al. 1994; MacLean et al. 1995; Raastad et al. 1996; Shefchyk et al., 1990; Viala et al., 1991). However, the complexity of the mammalian spinal cord makes it extremely difficult to investigate the organization of the neuronal circuitry. The smallest functional unit was once assumed to be a center for each limb (Grillner 1981). Based on pieces of indirect evidence, Grillner attempted to subdivide the CPGs into several subunits, called "unit burst generators"(Grillner 1981). He assumed that there is one network for each group of close synergists. This attractive hypothesis is technically difficult to test with the available experimental preparations. To circumvent the complexity of the mammalian nervous system, we developed an *in vitro* walking preparation from an amphibian, the mudpuppy (*Necturus maculatus*) (Wheatley and Stein, 1992; Wheatley et al. 1992, 1994; Jovanović et al. 1996a). We show in this study that the CPG for each limb can be divided into generators that produce flexor or extensor rhythms independently.

A second issue concerns the interplay between sensory input from the moving limb and the operation of CPGs. In the cat, stimulation of low threshold extensor muscle afferents in the flexion phase initiates a new extensor burst but suppresses the flexor burst. Such stimulation in the extension phase prolongs the ongoing extensor burst and delays the onset of flexor burst (Duysens and Pearson 1980; Conway et al. 1987; Pearson 1993; Guertin et al. 1995; Rossignol 1996). Resetting effects of sensory input have also been shown in the neonatal rat (Kiehn et al. 1992; Iizuka et al 1997). Here we show a phase dependent resetting o f the ongoing walking-like rhythm by stimulation of the dorsal roots, ventral roots, and the elbow flexor or extensor generators. Part of this work has been reported in an abstract (Cheng et al. 1997).

MATERIALS AND METHODS

Twenty-six adult mudpuppies (22-30 cm in length) were used for the experiments. The animals were anaesthetized before surgery by application of 3-aminobenzoic acid ethyl ester (Sigma, St. Louis, MO.) to the water bath (1-2 g/l).

Retrograde labeling of motoneuron pools

We used two fluorescent tracers in complement to label the motoneuron pools of the elbow flexor (*Brachialis*) and extensor (*Extensor ulnae*) muscles. The contours of these muscles were visible through the skin in these animals. Fluorogold (7% in DMSO-saline; Fluorochrome, Englewood, NJ) was injected into the belly of the elbow extensor in the left limb and the belly of the flexor in the right limb in six animals (Richmond et al. 1994). Approximately 5 μl of the tracers was delivered using a 26 gauge needle over the course of 5 minutes in each muscle. A second tracer, fast blue (3% in DMSO-saline, 5 μl Sigma), was used in two animals to avoid overestimation of the number of the labeled motoneurons due to the diffusibility of fluorogold (Richmond et al. 1994). The animals were sacrificed under anaesthesia 3-22 days after injection. The target muscles were dissected and the tracks of the injection within these muscles were verified. To examine the labeled cells, the spinal cord was isolated, fixed overnight in 4% paraformaldehyde (PFA)/0.1 M sodium phosphate buffer pH 7.2-7.4, at 4 °C, transferred to 30% sucrose/PFA for 2 hours at 22 °C (or overnight at 4 °C) for cryoprotection, and sliced either coronally or horizontally in 40 μm cryostat sections (JUNG GM 3000, Lieca Canada Inc.). The sections were mounted sequentially onto slides (Fisherbrand, Fisher Scientific), coverslipped (Cytoseal™, Stephens Scientific), and inspected for the labelled motoneurons under a fluorescence microscope (Leitz, Wetzlar, Germany), equipped with type A filter (excitation band pass 340-380, suppression long pass 430 ηm) and with dark field-bright field illumination.

In vitro walking preparation

The preparation contained the first five segments of the spinal cord, the brachial nerves and the forelimb(s). A segment border is defined as midway between two adjacent spinal dorsal roots. The procedures for surgical dissection, electromyography (EMG), and

induction of walking are described in detail elsewhere (Wheatley et al. 1992). Briefly, following a dorsal laminectomy under anaesthesia, the first five segments of the spinal cord were isolated from the rest of the body with one or both forelimbs attached by the brachial nerves. The paraspinal muscles were removed. Pairs of fine teflon-coated silver wires (75 μm diameter) were inserted into the elbow flexor and extensor muscles for EMG recordings. The preparation was placed dorsal side up in a recording chamber superfused with continuously oxygenated Ringer's solution at a rate of 2-5 ml/min (NaCl 115 mM; KCl 2 mM; $CaCl_2$ 2 mM, $MgCl_2$ 1.8 mM, Hepes 5 mM, glucose g/l, pH 7.3). The cord and forelimb(s) were stabilized by pinning the vertebrate column and the procoracoid cartilage to the base of the chamber coated with Sylgard® resin (Dow Corning). Deafferentation was performed by cutting the dorsal roots within the spinal canal. Walking-like motions of the leg(s) were induced by bath application of 20-80 μM NMDA (Sigma) together with 5-20 μM D-serine, which potentiates effects of NMDA (Wheatley et al. 1992).

Micro-stimulation

Motor responses were elicited by stimulation of regions of the spinal cord with constant cathodic currents (Master 8, A.M.P.I., Jerusalem, Israel) through a stimulus isolator (Neuro Log NL800). The surface of the cord dorsum was first stimulated systematically with concentric tungsten electrodes (negative pole ~100 μ m in diameter) at a spatial resolution of 1.0 mm. At spots where extension or flexion was induced by trains of stimulation with the lowest threshold current, tungsten microelectrode (~10 μm diameter tips, 1~2 MΩ, Micro Probe Inc. Gaithersburg, MD) was then inserted into the predicted areas of the gray matter (200~500 μm deep), where interneurons were densely populated (see Fig. 4-1 B). Continuous trains of current pulses (40 Hz, 0.2 ms duration) were used to find regions where rhythmic flexion or extension of the limb could be induced by unpatterned stimulation. The peak current amplitudes ranged between 2 and 8 μA, which corresponded to an estimated stimulation volume of less than 100 μm radius (Ranck 1981; Yeomans 1990). The tracks of electrodes were examined in 40 μm frozen

Figure 4-1. Microphotographs of the spinal cord. **(A)** Motoneurons labelled retrogradely with fluorogold in a 40 μm thick horizontal section of the extensor motoneuron pool taken from C3 segment (midline top and rostral right). **(B)** Histology of the mudpuppy spinal cord stained with cresyl violet 40 μm thick coronal section from the C2 segment. There are ~80 cells in the grey matter on each side. One to three motoneurons are typically labeled retrogradely on each side, as shown in C and D. **(C)** Two extensor motoneurons are labeled retrogradely in a 40 μm thick coronal section from the C3 segment. **(D)** At the C3 ventral root entry level, both extensor motoneurons (left) and flexor motoneurons (right) are labeled. The C3 ventral root can be seen in this section. **(E)** A flexor motoneuron from the C2 segment.

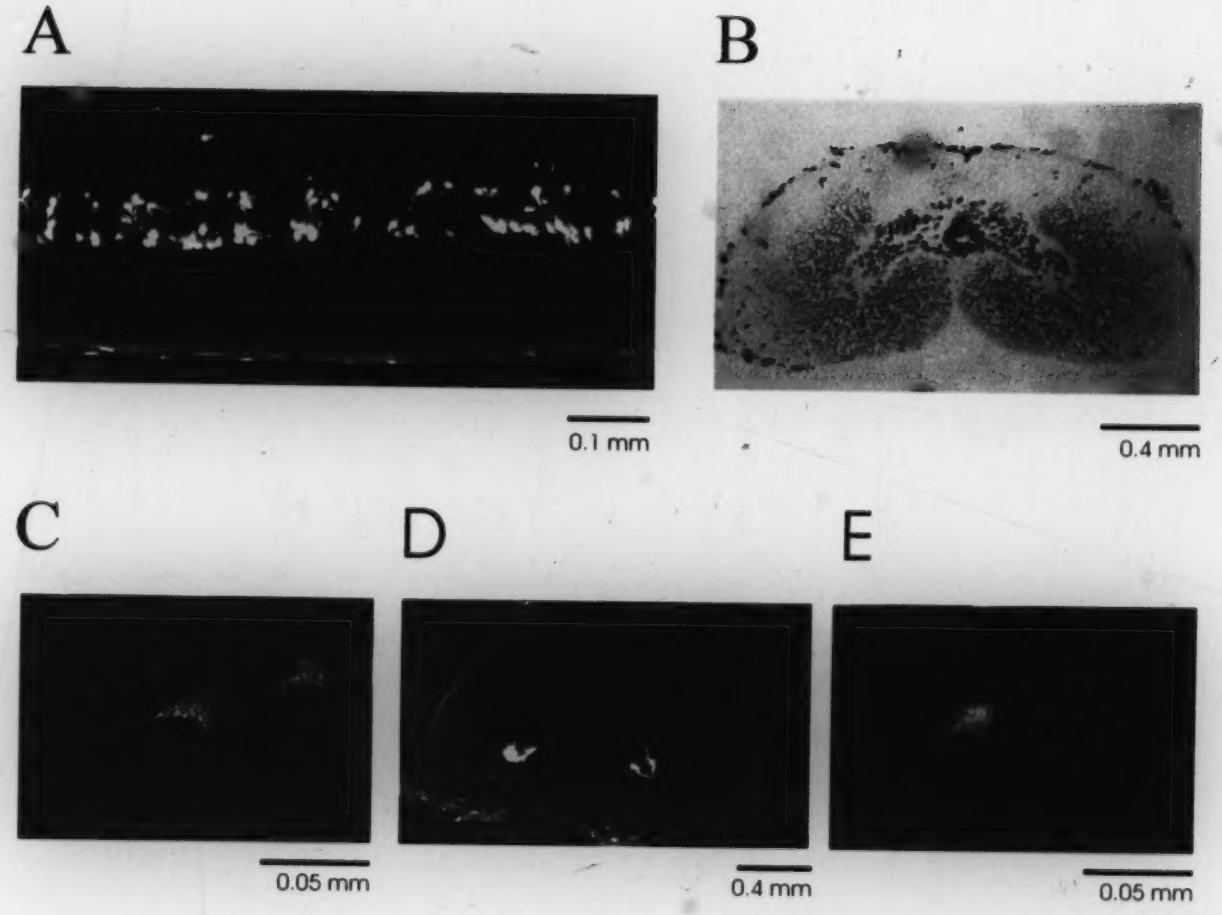
A
0.1 mm
B
0.4 mm
C
0.05 mm
D
0.4 mm
E
0.05 mm

sections stained with cresyl violet and were confirmed to be in the intermediate areas of the gray matter.

Surgical isolation of regions of the spinal cord

With the aid of a surgical dissection microscope (Leica), fine insect pins and iridectomy scissors were used to isolate regions of the cord. The unwanted regions were removed by vacuum suction to ensure the complete isolation. In cases in which two regions of the cord were necessary, a gap of at least 1 mm was produced between the separated regions attributable to the tension within the spinal cord.

Resetting walking rhythm by stimulation of regions of the cord, dorsal roots, and ventral roots

Trains of constant current pulses (40 Hz, 0.2 ms duration, 6 pulses) were delivered to specific regions of the cord dorsum (C2 or C3), dorsal roots, or ventral roots every other four to six step cycles. The stimulus intensity was 1.2 X motor thresholds (6 to 12 μA). The mean durations of the step cycles before and after each stimulation were measured and compared (Student's t-test). The phasic effects of the perturbation were examined by plotting the cycle duration of the stimulated steps against the timing of stimulation in each cycle. The slope of the best fitting straight line gave a measure of the degree of resetting (1represents complete resetting; Stein and Lee 1981).

Correlation analysis

The phase relationship between the flexor and extensor EMG bursts was quantified by cross-correlation analysis, and the rhythmicity of the flexor and extensor bursts was tested by auto-correlation analysis whenever necessary. At least 50 step cycles were included for the analyses. A positive value for the peak near zero in the cross-correlation indicates that the two signals (flexor and extensor EMGs) are relatively in phase, while a negative value indicates that they are relatively out of phase. A value of 1 represents a perfect correlation. The exact phase relationship can be determined by measuring the time delay (see Fig. 4-2) as a fraction of the complete step cycle.

Figure 4-2 Chemically-induced independent activation of the elbow flexor and extensor centers. **(A)**Rhythmic flexor EMG bursts developed first after bath application of NMDA (60 μM) while the extensor was still tonically active (Induction). Alternation of flexor and extensor bursts then emerged with well coordinated rhythmic limb movement (Walking). The vertical dotted lines indicate the transition of activation from the flexor to extensor muscles. The flexor turned to tonic activation while rhythmic extensor bursts were still evident when the walking-like rhythm started to deteriorate after several hours of walking-like movement (Waning). The flexor and extensor bursts became synchronized for a short period during washout of NMDA (Washout). The EMG signals have been low-pass filtered at 20 Hz and rectified. **(B)** Cross-correlation analysis shows the antiphase relationship (negative peak value at 0) between the flexor and extensor bursts during walking. **(C)** During washout, the flexor and extensor bursts were synchronized, as shown by the in-phase relationship in cross-correlation (positive peak value at 0).

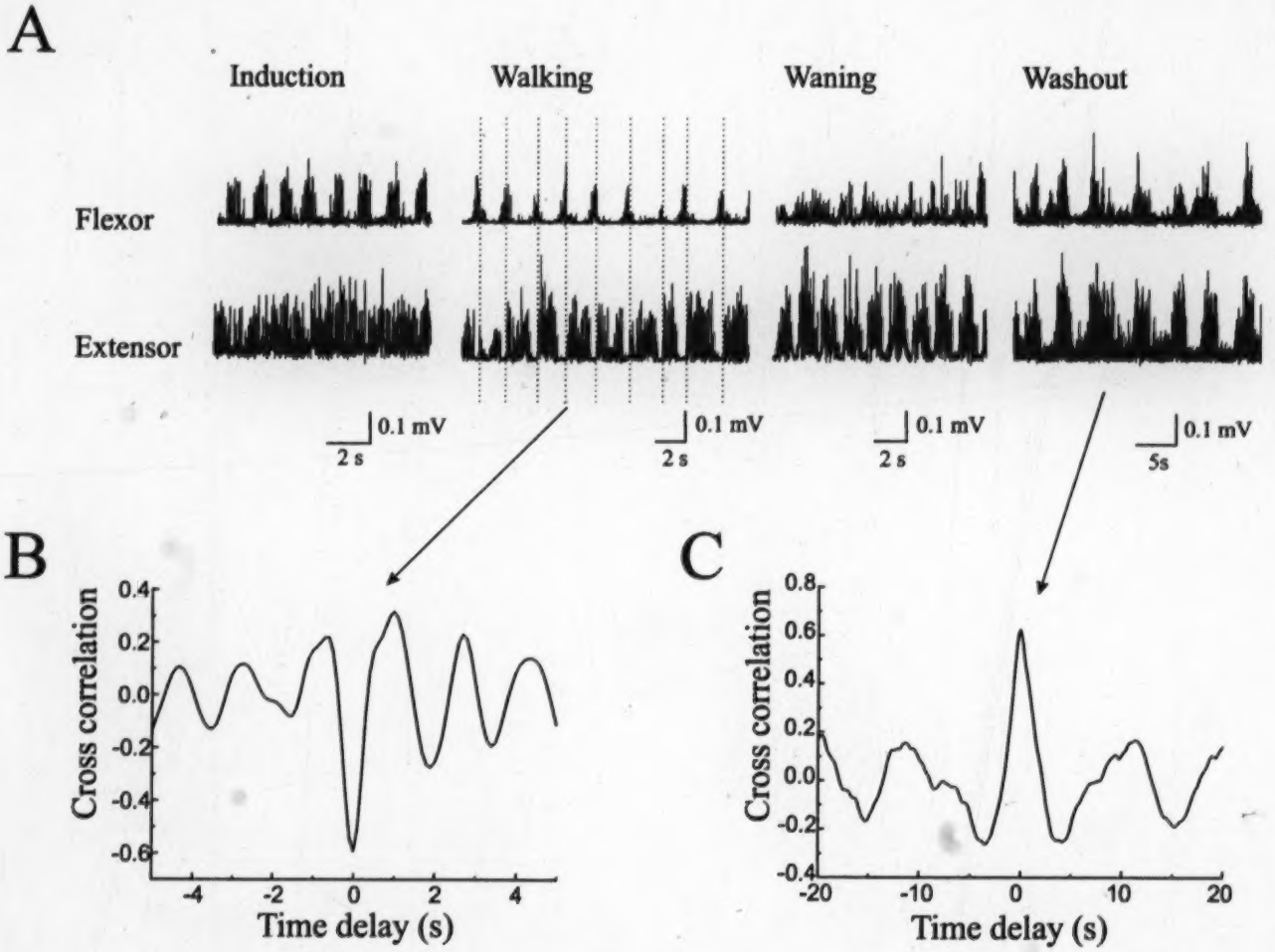
A
Induction
Walking
Waning
Washout
Flexor
Extensor
0.1 mV
2 s
0.1 mV
2 s
0.1 mV
2 s
0.1 mV
5s
B
Cross correlation
0.4
0.2
0.0
-0.2
-0.4
-0.6
-4
-2
0
2
4
Time delay (s)
C
Cross correlation
0.8
0.6
0.4
0.2
0.0
-0.2
-0.4
-20
-10
0
10
20
Time delay (s)

RESULTS

Motoneuron pools innervating the elbow flexor and extensor muscles

Retrograde labeling by flourescent tracers (fluorogold and fast blue) revealed the patterns of distribution of motoneurons innervating brachialis and extensor ulnae of the limb. The labeling was consistent between animals using both tracers. Figure 4-1 shows the distribution and morphology of the labeled cells. The flexor pool was localized mainly in the C2 segment (~ 3.0 mm long) and the extensor pool was localized in the caudal part of the C3 segments (~0.2~4.0 mm long). There was an overlap region at the rostral C3 segment (~ 0.4 mm), where motoneurons of both the flexor and extensor muscles were labeled. Part of the extensor motoneuron pool from the C3 is shown in Figure 4-1 A (horizontal section, midline top, rostral right). The motoneurons were organized approximately into two columns of cells. In the coronal plane, ~80 cells in the gray matter of each side were typically stained with cresyl violet within each 40 μm section (Fig. 4-1B). The cells around the central canal were excluded from the accounting since they were indicated to be ependymal cells (not labeled in silver staining). One to three motoneurons are typically labeled retrogradely in each 40 μm coronal section, the majority of the neurons in the gray matter appeared to be interneurons. The labeled motoneurons are exemplified in coronal sections (Fig. 4-1C, D),from the extensor pool and the overlapping region. Two extensor motoneurons were labeled retrogradely on the left side of a 40 μm thick coronal section from the caudal C3 segment (Fig. 4-1C). Both extensor (Fig. 4-1D, left) and flexor (Fig. 4-1D right) motoneurons were labeled at the entry level of the C3 ventral root which can be seen in this section. Partial reconstruction of a flexor motoneuron in the C2 segment shows the morphological details of its processes and orientation in the cord (Fig. 4-1E). The cell bodies of these motoneurons were 35-45 μm in diameter. The dendritic trees extended into the white matter of the ipsilateral side, toward the edge of the cord. The dotted line indicates the border of the grey matter. The axons were found to join the ventral roots either at the level of ventral root formation (Fig. 4-1D, E) or to ascend or descend up to ~3 mm within the ventral column of the white matter before entering the ventral roots (not shown). Note that the size of the cells

are not corrected for the shrinkage of the cord due to the dehydration process for fixation.

Identification of the elbow flexor and extensor centers

The flexor and extensor centers for the elbow joint were first identified by the use of microstimulation in six preparations. The cord dorsum was stimulated systematically with 1 mm resolution by continuous trains of constant current pulses, and the threshold for flexor and extensor responses was mapped (see Materials and Methods). Stimulation of the C2 segment induced flexor responses. The lowest threshold for the elbow flexor responses was localized in the middle of this region, ~0.5 mm lateral to the midline of the cord but medial to the flexor motoneuron column. At this spot, continuous trains of pulses induced rhythmic flexion of the forelimb about the elbow joint and rhythmic elbow flexor burst (Fig. 4-3). Note that these rhythmic responses occurred without activation of the elbow extensor. Their counterparts in the contralateral limb were also silent.
Stimulation of the C3-C5segments evoked extensor responses. The lowest threshold was localized in the caudal C3 segment, medial to the extensor motoneuron column. At this location, continuous trains of pulses induced rhythmic extension of the limb and elbow extensor bursts (Fig. 4-3). Again, the extensor was independent of its antagonist and its counterpart of the contralateral limb.

Stimulation of a region (~2 mm long) immediately rostral to the C3 dorsal root induced rhythmic extension of the wrist without noticeable EMG activities of the elbow flexor and extensor muscles. At higher intensity, stimulation of this region induced rhythmic alternation or co-contraction of the flexor and extensor bursts of the elbow (data not shown). Stimulation of the rostral part of C2 segment caused protraction of the limb about the shoulder joint. Retraction of the limb about the shoulder was induced by stimulation of caudal C4 and rostral C5.

Independent rhythmic activation of the of the elbow flexor and extensor muscles were also observed during bath application of glutamate receptor agonist NMDA in some preparations. Figure 4-2A shows an example of such chemically-induced independent activation. Figure 4-2A shows that rhythmic flexor bursts developed first during induction of walking-like motion, while excitation of the extensor was still tonic (Induction).

Figure 4-3. Electrically induced independent activation of the elbow flexor and extensor centers. Stimulation by continuous trains of constant current pulses at 40 Hz of the C2 segment medial to the flexor motoneuron pool induced rhythmic bursts of the elbow flexor muscle, while stimulation of the caudal part of the C3 segment produced rhythmic extensor bursts., all on the ipsilateral side of the stimulation (I-). The flexor and extensor muscles on the contralateral limb (C-) did not respond to the stimulation. The EMG has been rectified and low pass filtered at 30 Hz for clarity.

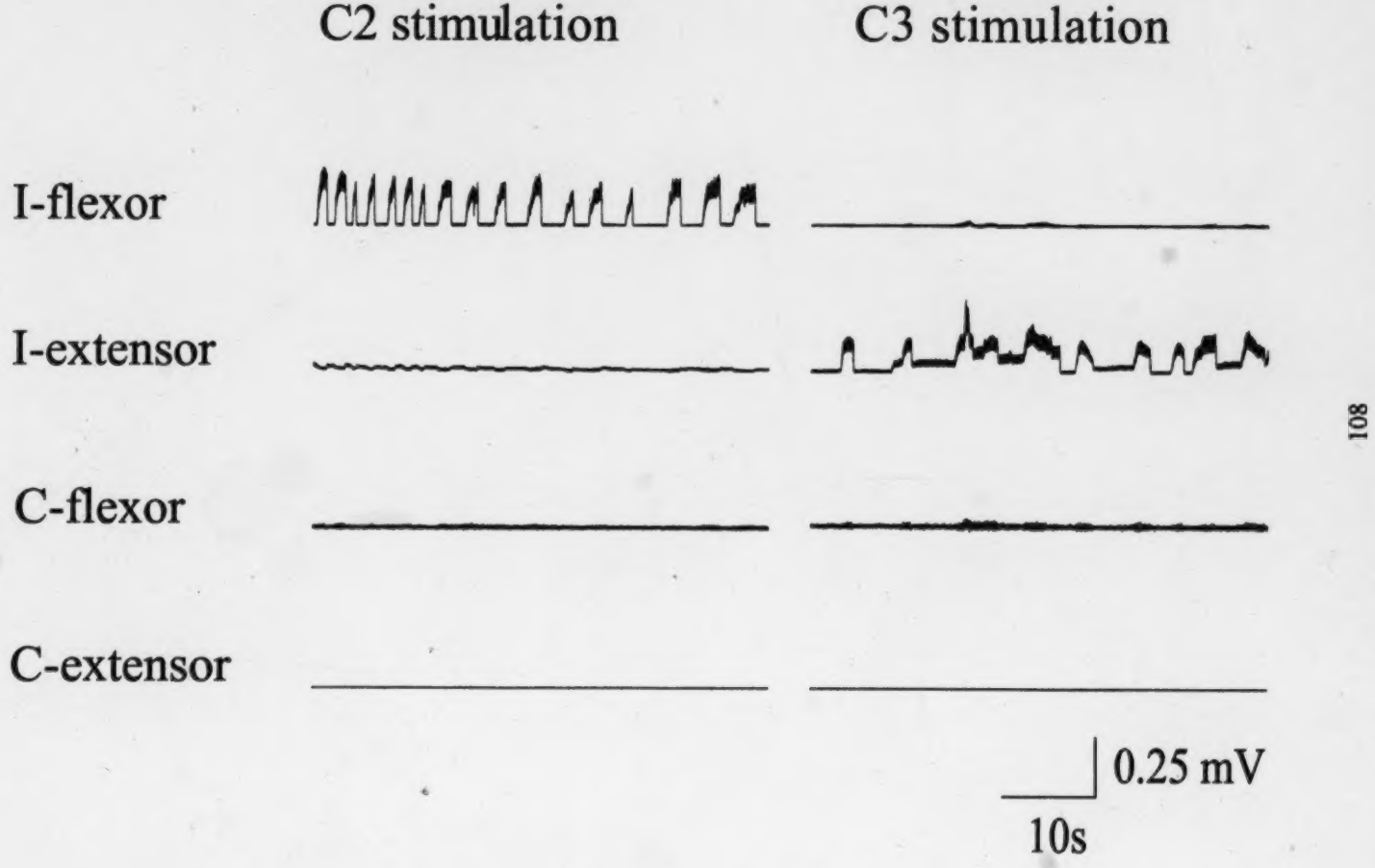
C2 stimulation
C3 stimulation
I-flexor
I-extensor
C-flexor
C-extensor
0.25 mV
10s

Then a regular walking-like rhythm became well established, and rhythmic alternation of flexor and extensor bursts emerged (Fig. 4-2 A, Walking). The flexor turned to more tonic activation, whereas rhythmic extensor bursts were still evident when the walking-like rhythm started to wane after several hours walking (Fig.4-2 A, Waning). The flexor and extensor bursts became synchronized for a short period during washout of NMDA (Fig. 4-2 A, Washout). It was noticed that the limb movement became jerky, and range of motion was reduced in conditions where one of the muscles became tonically active or the bursts of the antagonist muscles were synchronized. The cycle duration increased from 1.8 sec (Fig. 4-2 A, Walking) to 8.2 sec (Fig. 4-2 A, Washout). Cross-correlation analysis demonstrated an antiphase relationship (negative peak value near 0) between elbow flexor and extensor bursts during walking and an in-phase relationship (positive peak value near 0) during washout, as shown in Figure 4-2 B and C, respectively.

Surgical isolation of the flexor and extensor centers

This part of the study was performed in nine preparations. An isolated region spanning the C2 spinal roots (~4 mm long) generated rhythmic elbow flexor EMG bursts in the presence of NMDA (60 μM) and D-serine (15 μM). A schematic representation of the isolated region is shown in Figure 4-4 A. This region of the cord was connected to the forelimb by the C2 ventral root. The C2 dorsal root was cut, and the rest of the cord was removed. An example of rhythmic flexor bursts before and after the surgical isolation is shown in Figure 4-4 B. The extensor bursts were totally abolished while rhythmic flexor bursts remained, albeit at slower pace.

Similarly, an isolated part (~4 mm) of the C3 segment generated rhythmic extensor bursts in the presence of NMDA (80 μM) and D-serine (15 μM) through the C3 ventral root, which connected this part of cord with the forelimb. The C3 dorsal root was cut, and the rest of the cord was removed. Figure 4-5 shows the rhythmic elbow extensor bursts before and after the isolation, together with the schematic representation of the isolated region. The flexor bursts were completely abolished by the isolation while the extensor bursts were still evident, although the rhythmicity was less regular and the cycle duration was prolonged.

Figure 4-4 Isolation of the flexor center. **(A)** Schematic diagram of the surgery. The box highlights the isolated part of the C2 segment (~4 mm long). This region alone generated rhythmic elbow flexor EMG bursts through the C2 ventral root. The C2 dorsal root was cut, and the rest of the cord was removed. **(B)** Rhythmic alternating flexor and extensor bursts were evident in the presence of NMDA (60 μM) before the isolation. The vertical dotted lines indicate the transition from flexor burst to extensor bursts. The extensor bursts were totally abolished by the surgical isolation as indicated, whereas rhythmic flexor bursts remained.

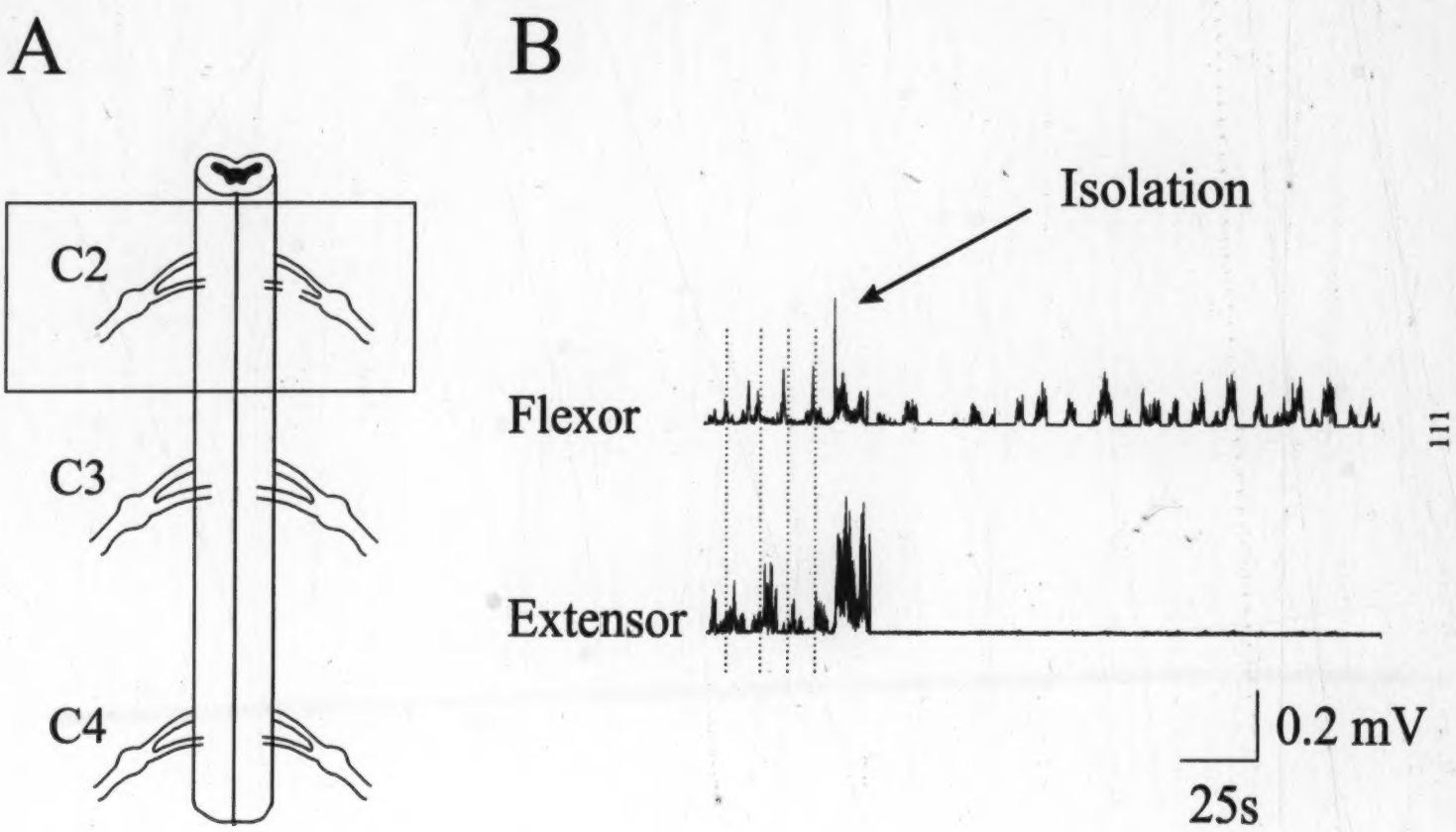
A
C2
C3
C4
B
Isolation
Flexor
Extensor
0.2 mV
25s

Figure 4-5 Isolation of the extensor center. **(A)** Schematic illustration of the surgery. The box highlights the isolated part of the C3 segment (~5 mm long) that generated rhythmic elbow extensor EMG bursts through the C3 ventral root. The C3 dorsal root was cut, and the rest of the cord was removed. **(B)** Rhythmic alternating flexor and extensor bursts were evident in the presence of NMDA (80 μM) before the isolation. The vertical dotted lines indicate the flexor and extensor transition of activation. The flexor bursts were totally abolished by the surgical isolation, while rhythmic extensor bursts remained.

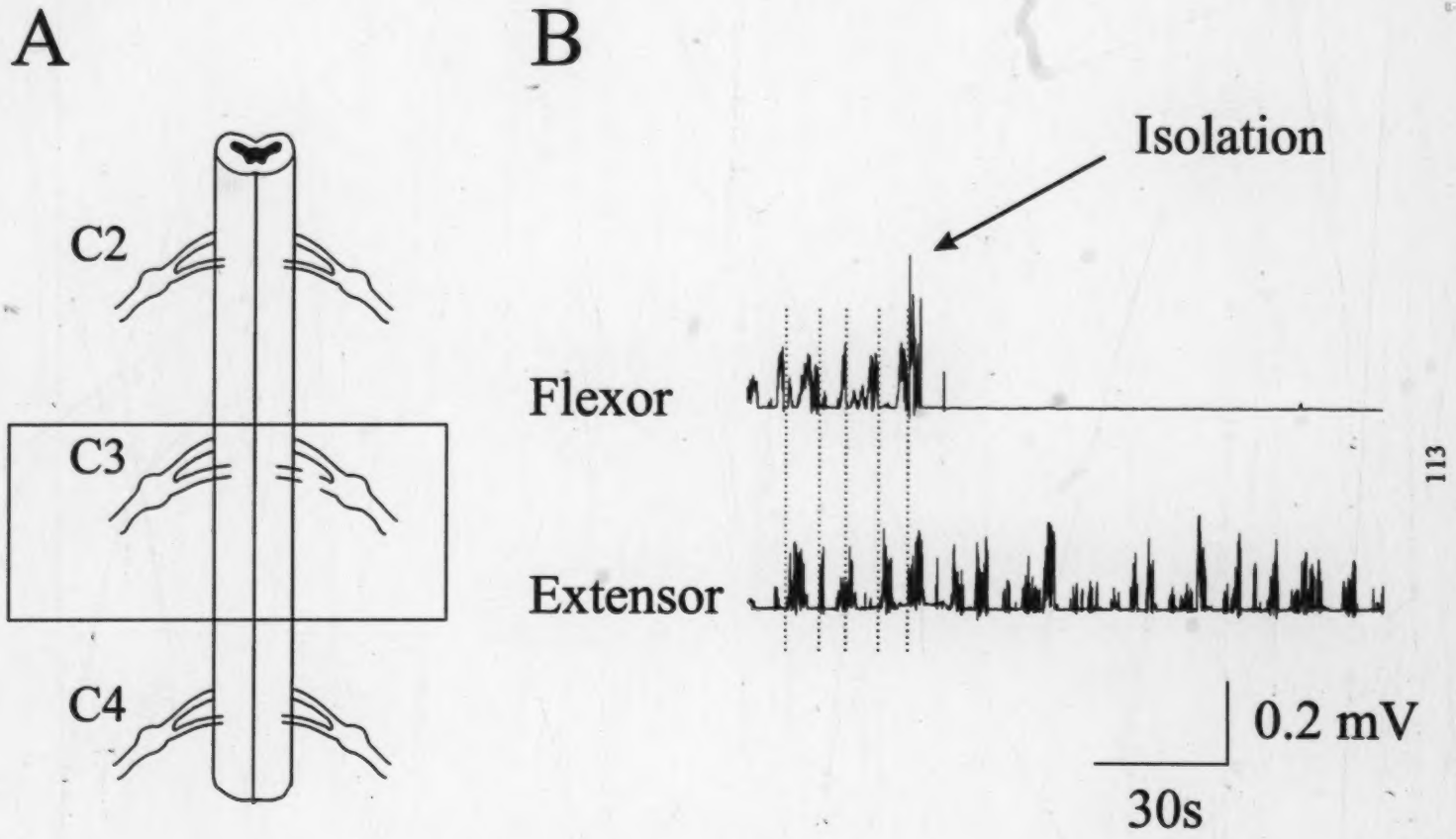
A
C2
C3
C4
B
Isolation
Flexor
Extensor
113
0.2 mV
30s

An isolated region spanning the C3 roots (~8 mm), generated rhythmic flexion and extension alternation of the limb and elbow flexor and extensor bursts through the C3 ventral root. This isolated part of the spinal cord is schematically shown in Figure 4-6 A. Note that the contralateral half of the cord was also removed through midsagittal line. The movement of the leg generated by this isolated segment was noted to be less smooth, and the range of motion was also reduced. The flexor and extensor EMG bursts, however, remained rhythmic, as exemplified in Figure 4-6B. Auto-correlation analysis confirmed the rhythmicity of the flexor and extensor activation with a cycle duration of ~5s (Fig.4-6 C, D). The phase relationship between the flexor and extensor bursts was quantified by cross-correlation analysis. Although the flexor and extensor bursts were less regular when compared with the less reduced preparation (Fig 4-2) they were clearly coupled with a time delay of 1.2 s. (Fig 4-6 E).

Separation of the two centers by a transverse section, just rostral to the C3 dorsal root revealed different rhythms of the flexor and extensor bursts. Figure 4-7 shows an example of such experiments. The histogram in Figure 4-7 depicts the onset delay between the flexor and extensor bursts before and after the separation, together with the schematic position of the section (inset). The flexor-extensor onset delay was relatively fixed at 0.8 s (Fig. 4-7, filled bars) before the separation. The rhythms generated by the two centers were decoupled by the separation (Fig. 4-7, open bars), leading to a randomized flexor-extensor onset relationship. The cycle durations were prolonged, particularly for the extensor bursts.

Resetting of the walking rhythm

Low intensity stimulation (a train of six pulses of 40 Hz at 1.2 X motor threshold) of each dorsal root (C2-C4) evoked motor responses in both the flexor and extensor muscles and reset the ongoing walking-like rhythm in a phase-dependent manner (n=6).

Figure 4-6. Rhythmic flexor and extensor EMG bursts were generated by a region spanning C3 ventral root (~8 mm long). The box in the schematic illustration of the surgery **(A)** highlights the isolated region. C3 dorsal root was cut. The rest of the cord, including the contralateral side, was removed. This isolated region produced rhythmic flexor and extensor bursts through the C3 ventral root in the presence of NMDA (80 μM). **(B)** Auto-correlation analysis confirmed the rhythmicity of the flexor **(C)** and extensor **(D)** bursts. Cross-correlation analysis revealed the coupling of the flexor and extensor activation with a time delay of ~1.2 sec **(E)**.

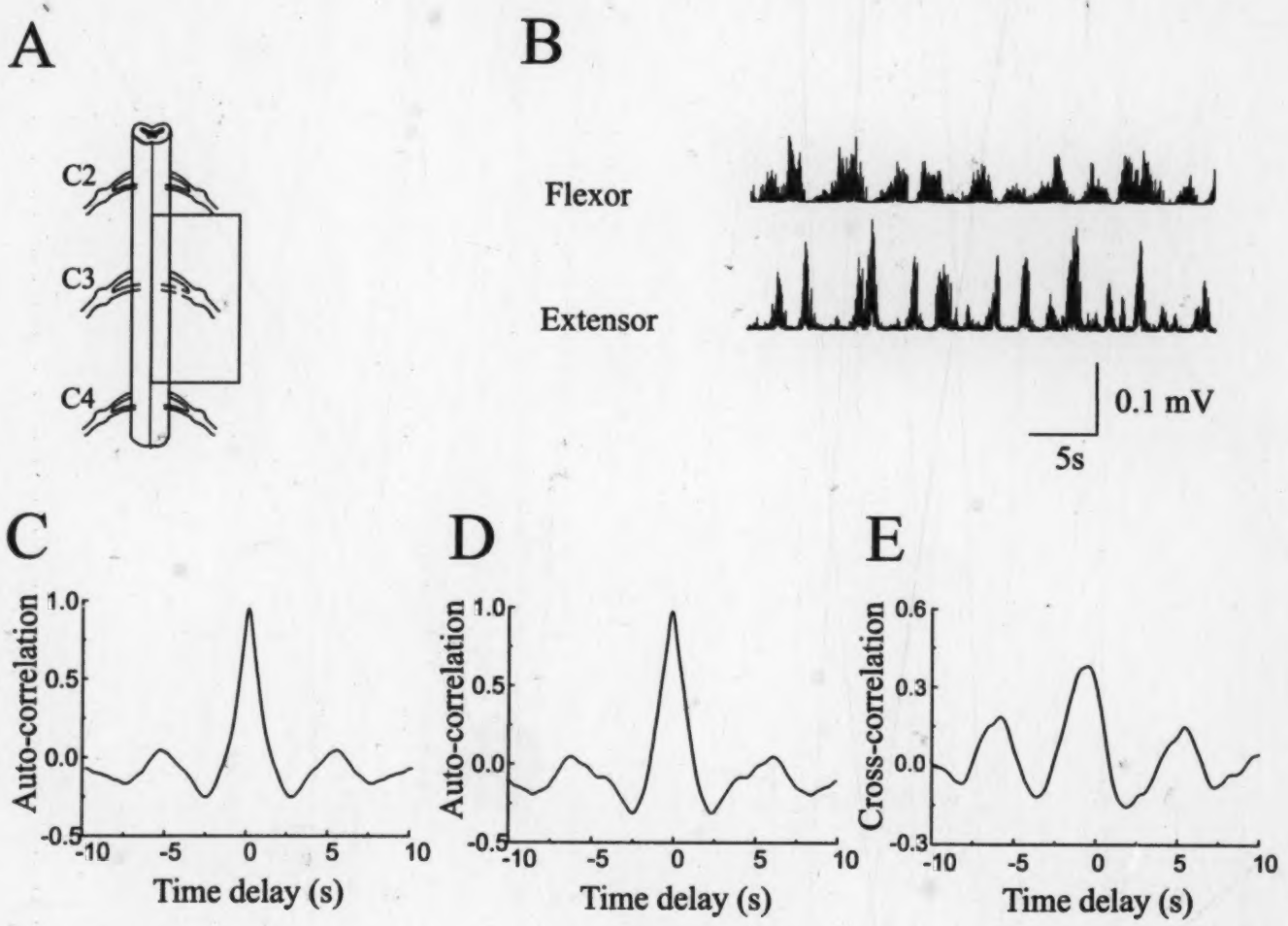
A
C2
C3
C4
B
Flexor
Extensor
0.1 mV
5s
C
Auto-correlation
1.0
0.5
0.0
-0.5
-10
-5
0
5
10
Time delay (s)
D
Auto-correlation
1.0
0.5
0.0
-0.5
-10
-5
0
5
10
Time delay (s)
E
Cross-correlation
0.6
0.3
0.0
-0.3
-10
-5
0
5
10
Time delay (s)

Figure 4-7. Decoupling of the two centers by surgical separation of the cord. The onset delay between the flexor and extensor EMG bursts was relatively fixed (filled bars) before the separation at the position shown in the inset. After the separation, the rhythms generated by the two centers were decoupled as indicated by the wide spread of the onset delay between the flexor and extensor bursts (open bars).

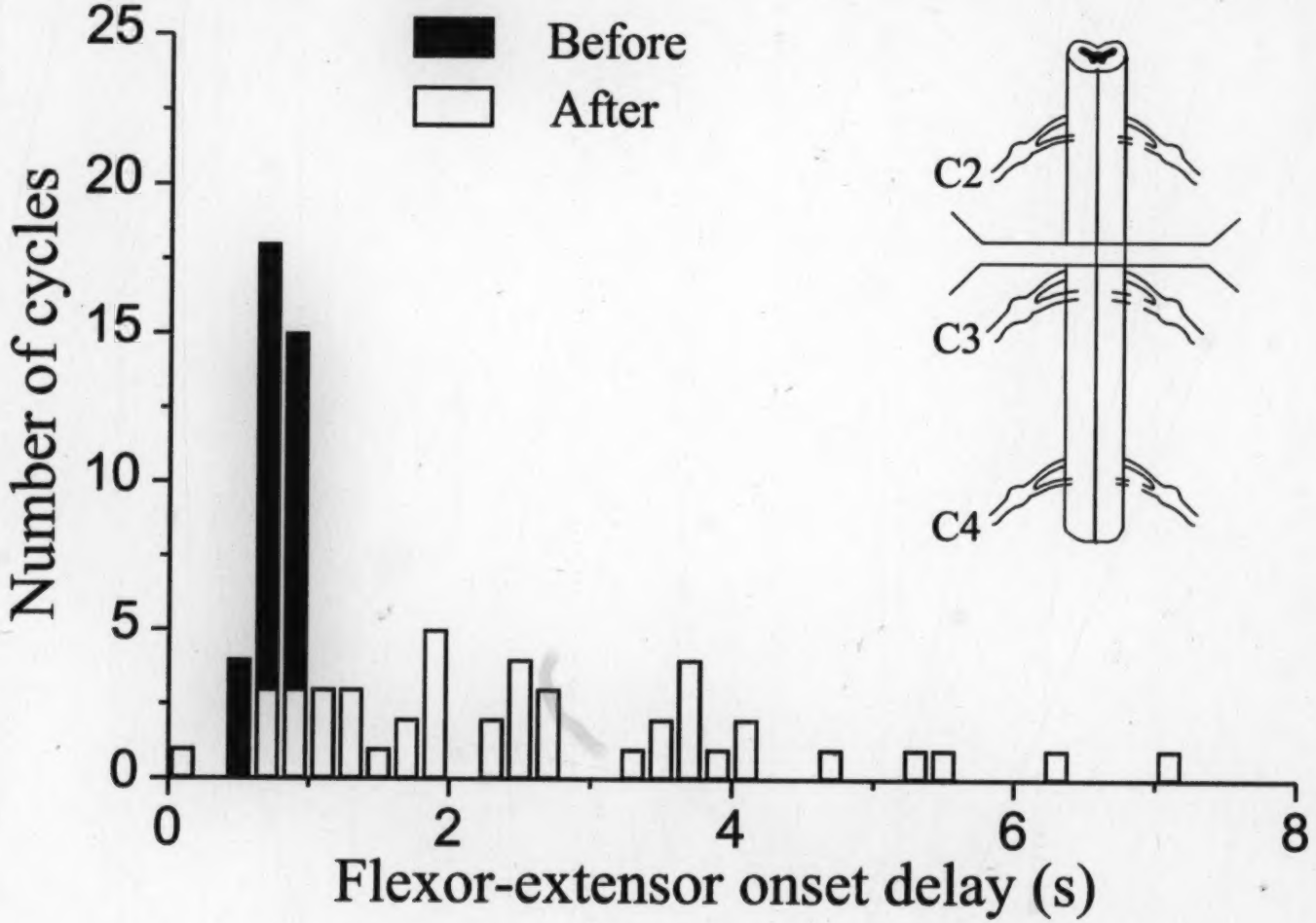
Before
After
Number of cycles
25
20
15
10
5
0
0
2
4
6
8
Flexor-extensor onset delay (s)
C2
C3
C4

Figure 4-8 illustrates the resetting effects of C3 dorsal root stimulation. The cycle duration was measured as offset-to offset of adjacent flexor bursts, as shown in Figure 4-8 A. The stimulated step (Fig. 4-8A, During) was either shortened (top trace) or prolonged (bottom trace) depending on the timing of stimulation. Plotting the cycle duration against the timing of the stimulation (0 represents offset of flexion) revealed that the cycle duration varied as a function of the timing of the stimulation. The slope of the best straight line fit, 0.912, indicates the effectiveness of stimulation in resetting the rhythm (a slope of 1 represents perfect resetting). Stimulation of the C3 dorsal root showed the strongest effects among the three dorsal roots. Also shown in Figure 4-8 are the mean cycle durations immediately after the stimulated step, which were not significantly different from each other in this case. A small but statistically significant slope also occurred in the step cycle immediately after the stimulated step in two of six preparations. The resetting effects of stimulating different roots (C2-C4) were compared. Preferential effects on flexor or extensor rhythms from a particular dorsal root were not found.

Resetting of the walking-like rhythm was also induced by stimulation of ventral roots (C2-C4) in a phase-dependent manner (n=4). Deafferentation by dorsal rhizotomy abolished the resetting effects of ventral root stimulation. Figure 4-9 shows an example of such observation. Stimulating the C3 ventral root partially reset the cycle duration (Fig. 4-9A). This effect was removed by dorsal rhizotomy of all dorsal roots (Fig. 4-9 B). The mean cycle durations of the steps immediately before and after the stimulated steps were not significantly different. The average of these means is shown in Figure 4-9 A and B, horizontal line.

The effects of naturally occurring sensory input on the walking-like rhythm were investigated by comparing average cycle durations before and after cutting each of the C2-C4 dorsal roots. An observation consistent between the preparations (n=4) was that the cycle duration decreased after the C3 dorsal root was cut, regardless of the order of root cutting. Conversely, cutting the C2 dorsal root resulted in a longer cycle duration in all of the preparations. After all dorsal roots of the preparation were cut, the walking-like rhythm became faster in three of the four preparations. Figure 4-9 C illustrates the results

Figure 4-8. Resetting of the walking-like rhythm by dorsal root stimulation. **(A)** Examples of raw recordings of the flexor EMG showing the measurements of the cycle duration and the effects of stimulation on the cycle duration. A train of six pulses of 40 Hz at 1.2 X motor threshold intensity was delivered to the C3 dorsal root at times indicated by arrows. The cycle duration of the disturbed steps (During) was either shortened (top trace) or prolonged (bottom trace) depending on the timing of stimulation. The cycle duration of the steps immediately before or after the disturbed step were not substantially affected. **(B)** The cycle duration of the disturbed steps was plotted against the timing of the stimulation. The effect was phase-dependent. The slope (0.912) of the best straight line fit indicates the resetting effectiveness, with 1 indicating a perfect resetting. The mean cycle durations of steps before and after the stimulated step are also shown and are not significantly different

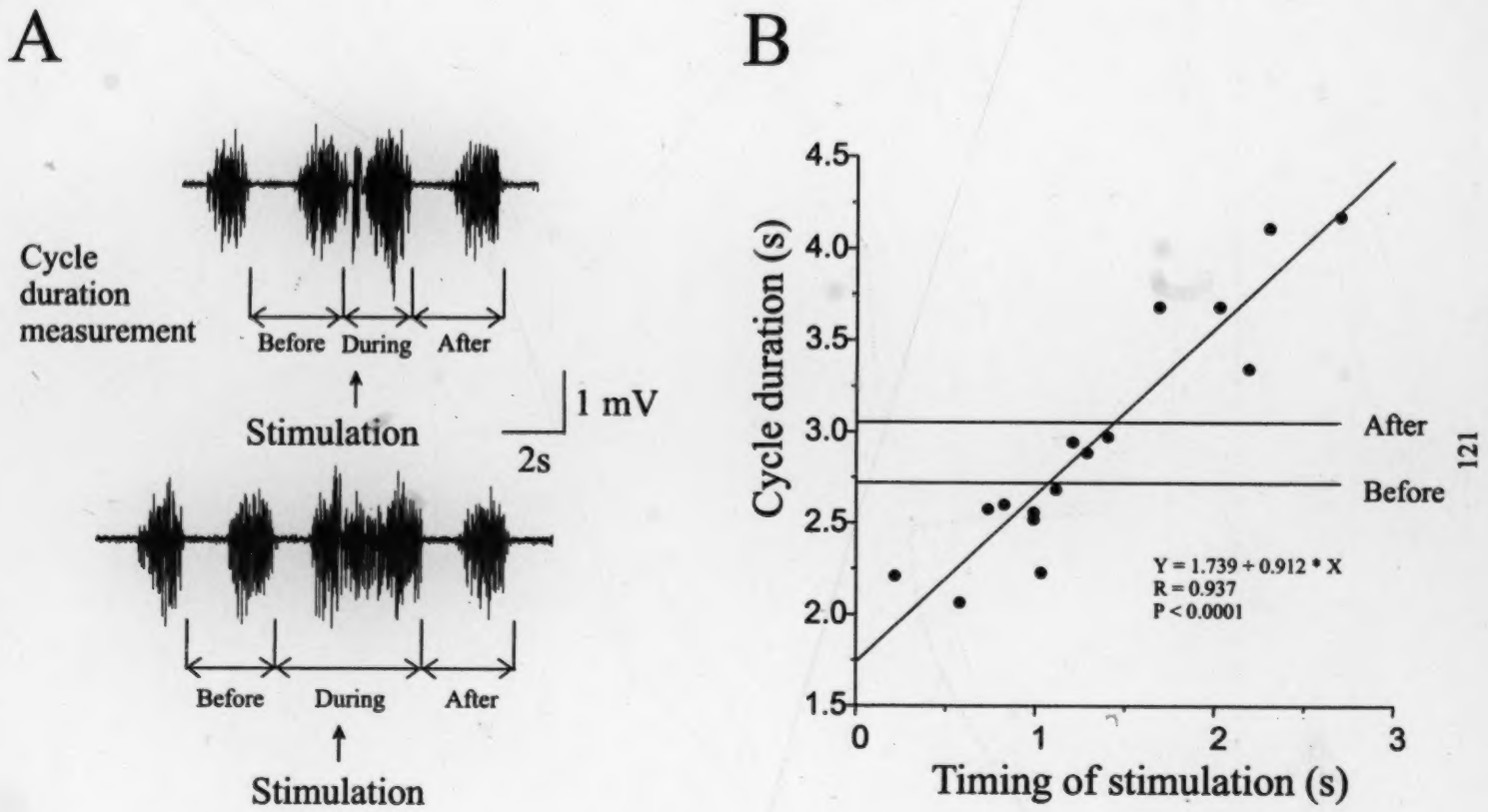
A
Cycle
duration
measurement
Before
During
After
Stimulation
1 mV
2s
Before
During
After
Stimulation
B
Cycle duration (s)
4.5
4.0
3.5
3.0
2.5
2.0
1.5
0
1
2
3
Timing of stimulation (s)
After
Before
Y = 1.739 + 0.912 * X
R = 0.937
P < 0.0001

Figure 4-9. Resetting of the walking-like rhythm by reafferent input consequent to limb movement. **(A)**Stimulation of the ventral root C3 by a train of 6 pulses of 40 Hz at 1.2 X the motor threshold intensity modulated the cycle duration in a phase-dependent manner and partially reset the walking-like rhythm. **(B)**Deafferentation by dorsal rhizotomy abolished the resetting effects of ventral root stimulation. The average of the mean cycle duration of the steps immediately before and after the stimulated cycle is shown as a horizontal line in **A** and **B**. (C) Dorsal root cutting, per se, significantly affected the walking cadence. Cutting the C3 dorsal root shortened the cycle duration compared with the precutting control (Ctl), whereas cutting the C2 dorsal root prolonged the cycle duration. Cutting the C4 and C5 dorsal roots also shortened the cycle duration.

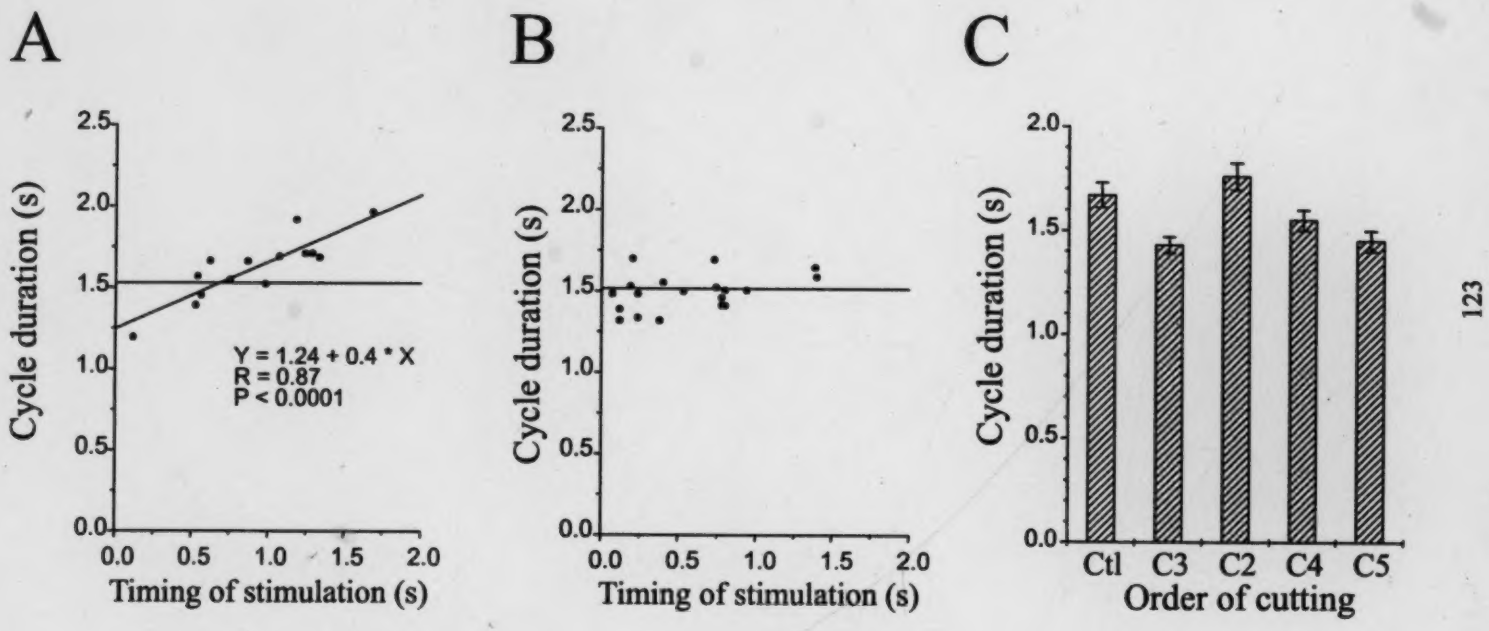
A
B
C
Cycle duration (s)
Timing of stimulation (s)
Y = 1.24 + 0.4 * X
R = 0.87
P < 0.0001
Ctl
C3
C2
C4
C5
Order of cutting

from a representative experiment. Note that cutting the C4 and C5 dorsal roots also shortened the cycle duration in this preparation.

Resetting of the walking rhythm was also induced by stimulation of regions of the cord (n=4). Figure 4-10 shows an example of such effect. The extensor bursts were terminated prematurely whenever stimulation was delivered to the flexor center in the C2 segment (Fig. 4-10A). The walking-like rhythm was completely reset in a phase-dependent manner, as indicated by the slope (1.007) of the best straight line fit (Fig. 4-10 B). The mean cycle durations of the steps immediately before and after the stimulated steps were not significantly different. The average of these mean durations is shown in Figure 4-10 B (horizontal line). Conversely, stimulating of the extensor center in the C3 segment initiated or prolonged the extensor bursts and terminated or delayed flexor bursts (data not shown). This reciprocal inhibition between the two centers was observed in all the preparations tested.

DISCUSSION

The results demonstrate that the neuronal networks for rhythmic flexor or extensor activation required for walking are distinctly localized in regions of the spinal cord. The elbow extensor center was localized in the C3 and C4 segments (Fig. 4-11 A). The motoneuron pool for flexor or extensor muscle was localized in close apposition to its pattern generator as revealed by the retrograde labeling experiments. The flexor and extensor centers can oscillate independently. These findings represent the first direct evidence that the so-called central pattern generators for walking can be divided in smaller subunits (Grillner, 1981). The results further show that the elbow flexor and extensor center are interconnected and that sensory input plays an important role in determining the rhythmicity of these centers. Together, these data constitute the basis for un updated model of the neural network for walking (Fig. 4-11 B). This model only incorporates data for elbow movements and may need to be extended, for example, to include protraction and retraction movements at the shoulder.

Figure 4-10. Resetting the walking-like rhythm induced by stimulation of the flexor center. **(A).** The extensor bursts were terminated prematurely whenever stimulation was delivered to the flexor center in the C2 segment as indicated by the stimulus artefact (four large brief peaks). **(B)** The cycle duration was modulated, and the walking-like rhythm was completely reset in a phase-dependent manner. The mean cycle duration of the steps immediately before and after the stimulated steps is indicated by the horizontal line.

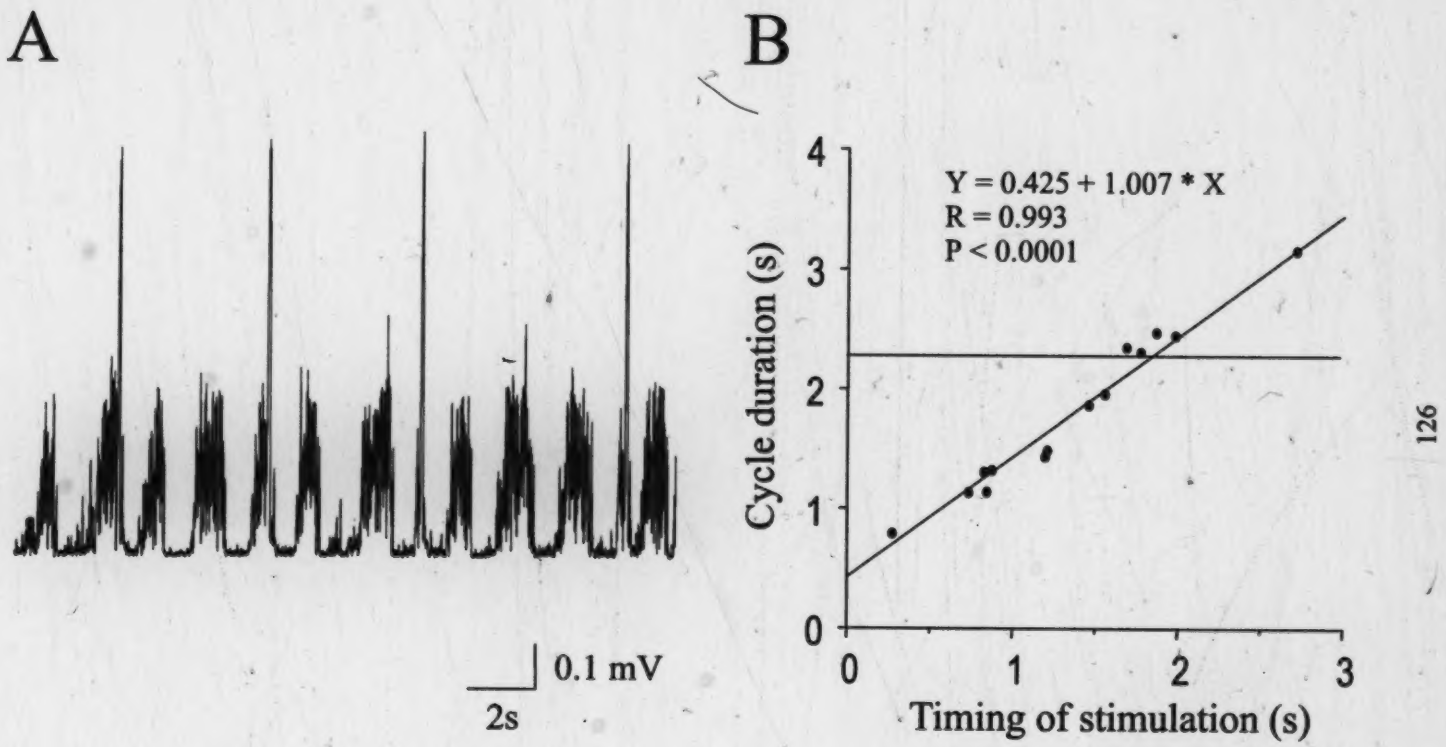
A
0.1 mV
2s
B
Y = 0.425 + 1.007 * X
R = 0.993
P < 0.0001
Cycle duration (s)
Timing of stimulation (s)
0
1
2
3
4

Figure 4-11. Schematic localization of elbow flexor and extensor centers and modeling of the neural networks required for walking. **(A)**Localization of the flexor center in the C2 and part of C3 segments (F) and the extensor center in the C3 and C4 segment (E) are based on the integration of data from electrical stimulation and surgical isolation experiments. A small overlap region at C3 spinal root level is also shown. **(B)** A model of neural networks required for walking is drawn based on the data presented in this work. This model contains independent flexor and extensor generators that drive flexor motoneuron pool and extensor motoneuron pool, respectively. There are inhibitory interconnections between the two centers. Somatosensory input makes both excitatory and inhibitory connections with each of the centers, modulates the activity of the neural network, and resets the ongoing walking-like rhythm in a phase-dependent manner.

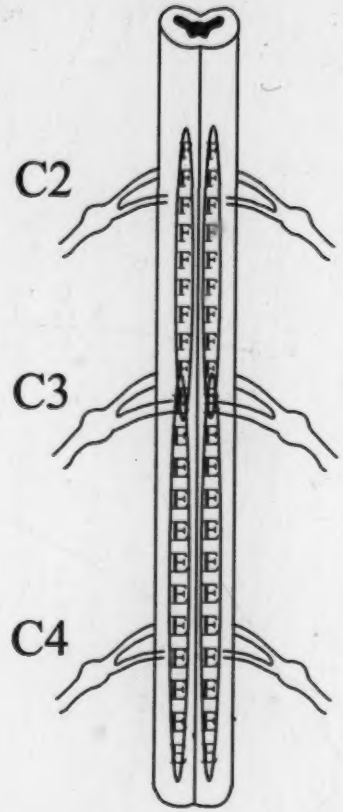
A
C2
C3
C4

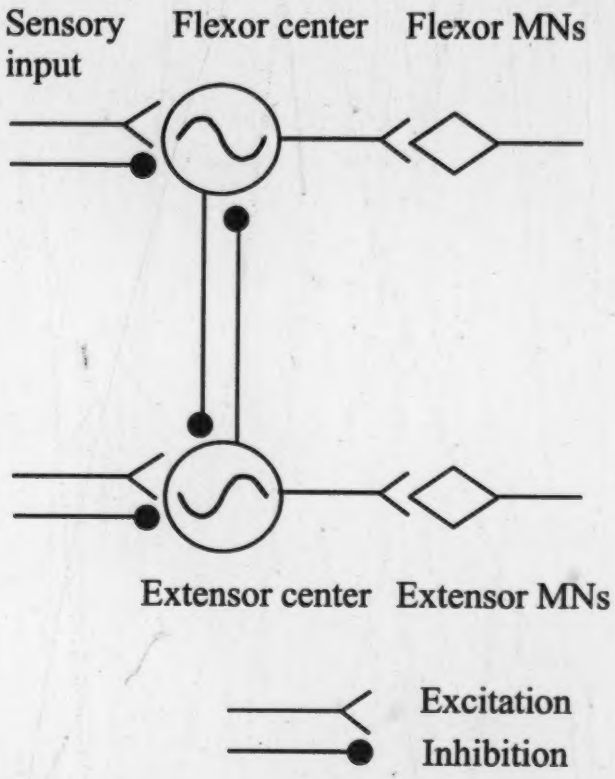
B
Sensory input
Flexor center
Flexor MNs
Extensor center
Extensor MNs
Excitation
Inhibition

Flexor and extensor centers

The conceptual framework for the organization of the central pattern generator for walking has been strongly influenced by the half-center model of Brown (1911), which was developed to account for the alternating activation of flexor and extensor muscles in the cat during walking. Brown envisaged that each pool of motoneurons for flexor or extensor muscles is driven by a corresponding half center of interneurons. Between the two half centers are inhibitory connections that ensure alternating activation of flexor and extensor muscles. This model assumes that rhythmicity in flexor and extensor half centers depends on the connectivity between the two half centers. Instead, our results showed that each of the two centers can generate rhythmic motor output for walking, independent of the other. This is indicated in Figure 4-11 B by the presence of separate rhythm generators for the flexor and extensor. Evidence for the separation came from several distinct experiments: 1) continuous trains of electrical stimulation to the flexor center (or the extensor center) induced rhythmic flexion (or extension) of the limb, independent of its antagonist and its counterpart in the contralateral limb (Fig. 4-2); 2) independent activation of one center was also sometimes induced by the glutamate receptor agonist NMDA (Fig. 4-3); 3) surgical isolation and separation of the regions of the cord provided unequivocal evidence for the existence of two distinct rhythmogenic centers. An isolated region of the C2 segment generated rhythmic flexion (Fig. 4-4). Similarly, part of the C3 segment in isolation generated rhythmic extensor bursts (Fig. 4-5). Separation of the two regions produced independent rhythms that had no phase relationship to one another (Fig. 4-7). Thus, electrical, chemical and anatomical evidence all argue strongly for the presence of two separate rhythm generators. A similar situation may apply to mammals as well, as suggested by recent work in the neonatal rat (Hochman and Schmidt 1998) and in the spinal cat (Stein RB, Pearson KG, Bennett DJ and De Serres S, unpublished observations). Generation of the rhythm may arise from interneurons with pacemaker properties or from neural networks within a center. Hochman et al. (1994) recorded NMDA-mediated membrane oscillations in interneurons in rat spinal cord slices in the absence of synaptic interaction. On the other hand, Wheatley et al. (1994) found that

the majority of the interneurons in the mudpuppy spinal cord had their peak firing at the transitions between flexion and extension phases and so may be responsible for switching the rhythm from one phase to another.

The neural network for walking may be divisible into even smaller units (reviewed by Rossignol, 1996). We have only recorded EMGs of the flexor and extensor muscles at the elbow. However, we did notice that stimulation of a region rostral to C3 dorsal root induced rhythmic extension of the wrist without noticeable EMG activities of the elbow flexor and extensor muscles. Further stimulation of the rostral part of the C2 segment activated the shoulder flexors and produced a protraction of the limb. Therefore, there appears to be a rostro-caudal gradient generating activity in shoulder, elbow and wrist muscles, which could be normally coupled with some phase shift like the segmental oscillators in the lamprey (reviewed by Grillner 1991). The surgical isolation experiments alone do not provide enough information to determine the precise boundary of the flexor and extensor centers (Fig. 4-11 A). Part of the flexor generator may extend to overlap the region of the extensor generator (or vise versa) and its activity may be masked after the removal of its motoneuron pool by the surgery. However, evidence from microstimulation experiments argues against the possibility of such overall overlap. Isolated rhythmic flexor activity was induced by stimulating the C2 segment and likewise isolated extensor activity was generated by stimulating the C3 segment (Figure 2), indicating distinct localization of the flexor and extensor centers. One could argue that the stimulation excited the motoneuron pool directly, as well as the pattern generator and thus activity may be seen only near the stimulation site. However, this possibility is unlikely, since the stimulation volume with the present parameters was estimated to be small (within 0.2 mm radius) relative to the length of the motoneuron column which could be as long as 4 mm, and thus the motor output was likely produced by the pattern generator.

The finding of distinctly localized rhythmogenic centers may reflect a principle of neural network organization that is common across species. Earlier studies have demonstrated that rhythmic output could be generated from isolated spinal cord segments. The minimal number of segments required was found to be eight in the dogfish (Grillner

1974), four in the lamprey (Cohen and Wallén 1980; Grillner et al. 1982), two in the cat (Deliagina et al. 1983) and one in the turtle (Mortin and Stein 1989; Stein et al. 1995). In the chick embryo, one segment was also able to generate rhythmic locomotor-like activities (Ho and O'Donovan 1993). Furthermore, a single hemisegment was observed to produce locomotor-like output in the neonatal rat (Cowley and Schmidt 1997). These observations, taken together, suggest that more complex neural networks with greater adaptability are probably built upon the small modular pattern generators.

Inhibitory coupling

Our observations do not contradict Brown's suggestion that reciprocal inhibition contributes to the normal rhythmic pattern (Brown, 1911, 1914). Stimulation of one center could terminate its antagonist and completely reset the walking-like rhythm (Fig. 4-10). Mutual inhibitory connections between the flexor and extensor centers are therefore included in Figure 4-11 B. They are presumably important for coordinating rhythmic limb movements by alternating activation of the flexors and extensors. The limb movements became jerky and the range of motion was reduced in conditions where one of the muscles became tonically active or the bursts of both muscles became synchronized (Fig. 4-3). Synchronized activation of the flexors and extensors has also been seen after blocking inhibitory transmission in the mudpuppy (Jovanović et al. 1996) and in the neonatal rat (Cowley and Schmidt 1994). This represents further evidence that the inhibitory connections are not essential for rhythm generation, but are important for coordinated gait. It also suggests that there are weaker excitatory connections between the flexor and extensor centers, but these have not been included in figure 4-11 B.

Sensory modulation

Afferent input resets and profoundly modulates the centrally generated rhythm. Our results show that the step cycle could be lengthened or shortened in a phase-dependent manner by low intensity stimulation of the dorsal roots (Fig. 4-8). This is indicated by the presence of both excitatory and inhibitory connections onto the flexor and extensor centers in Fig 4-11B. Ventral root stimulation produced a weaker degree of resetting (Fig. 4-9), but this is probably mediated by reafferent sensory input induced by muscle contraction and limb

movement, as dorsal rhizotomy completely abolished the effects. The sensory input appears to be representative of naturally occurring sensory information resulting from limb movement during locomotion. Indeed, dorsal rhizotomy alone induced consistent changes in step cycle duration, indicating that sensory input as a consequence of the walking motion interacts with the rhythmogenic networks and modulates the walking cadence. It appears that dorsal roots C2 and C3 carry the major portion of the information that affects the rhythm. The input through the C3 dorsal root on balance prolongs the step cycle duration and that through the C2 dorsal root on balance shortens the cycle duration. The overall effects of dorsal rhizotomy appear to be in favour of a faster rhythm, in agreement with findings in the rat (Iakhnitsa et al. 1987; Atsuta et al. 1991; Iwahara et al. 1991). The cellular basis for this interaction remains to be resolved, but the transitional interneurons described previously (Wheatley et al. 1994) may be involved. Functionally, sensory input in the extension phase may serve as a positive feedback to enhance the striding force and increase the range of the limb movement, thus increasing the step cycle durations (Pearson 1995, Whelan et al. 1995). Sensory input in the flexion phase, on the other hand, may be related to landing of the foot and used to trigger the onset of extensor activation, leading to shortened step cycles. As well as afferent effects on the CPG, the CPG affects afferent transmission. The same stimulus could lengthen or shorten the step cycle depending on its time in the cycle. The gain of many sensorimotor pathways is modulated in a phase-dependent manner during a variety of locomotor behaviors in humans and other mammals (Brooke et al.1997; Stein and Capaday 1988). Presynaptic inhibition appears to be involved in gating the sensory input (Stein 1995; Brooke et al.1997). How the activities of the networks for walking affect sensorimotor transmission in the mudpuppy requires further investigation. The length of the hemisected spinal cord necessary for generation of the elbow flexor and extensor rhythm is relatively small (8 mm; Fig. 4-6) and the cord contains a small number of relatively large interneurons (Fig. 4-1B). The organization of the flexor and extensor centers can be studied separately (Fig. 4-11B) and the connectivity between the two centers and between the CPGs and the sensory input is becoming clear.

REFERENCES

Atsuta Y, Garcia-Rill E, Skinner RD (1991) Control of Locomotion in vitro: I. Deafferentation. Somatosen Mot Res 8:45-53.

Bracci E, Ballerini L, Nistri A (1996) Localization of rhythmogenic networks responsible for spontaneous bursts induced by strychnine and bicuculline in the rat isolated spinal cord. J Neurosci 16:7063-7076.

Brooke JD, Cheng J, Collins DF, McIlroy WE, Misiaszek JE, Staines WR (1997) Sensori-sensory afferent conditioning with leg movement: gain control in spinal reflex and ascending paths. Prog Neurobiol 51:393-421.

Brown TG (1911) The intrinsic factors in the act of progression in the mammal. Proc. R. Soc. London Ser B 84:308-319.

Brown TG (1914) On the nature of the fundamental activity of the nervous centres: together with an analysis of the conditioning of rhythmic activity in progression, and a theory of the evolution of function in the nervous system. J Physiol (Lond) 48:18-46.

Cazalets JR, Borde M, Clarac F (1996) The synaptic drive from the spinal locomotor network to motoneurons in the newborn rat. J Neurosci 16:29S-306.

Cazalets JR, Borde M, Clarac F (1995) Localization and organization of the central pattern generator for hindlimb locomotion in newborn rat. J Neurosci 15:4943-4951.

Cheng J, Stein RB, Jovanović K, Yoshida K (1997) Localization, activation, and modulation of networks for walking in mudpuppy spinal cord. Soc Neurosci Abstr 23:207.

Cohen AH, Wallen P (1980) The neuronal correlate of locomotion in fish. "Fictive swimming" induced in an *in vitro* preparation of the lamprey spinal cord. Exp Brain Res 41:11-18.

Conway BA, Hultborn H, Kiehn 0 (1987) Proprioceptive input resets cental locomotor rhythm in the spinal cat. Exp Brain Res 68:643-656.

Cowley KC, Schmidt BJ (1997) Regional distribution of locomotor pattern-generating network in the neonatal rat spinal cord. J Neurophysiol 77:247-259.

Cowley KC, Schmidt BJ (1994) A comparison of motor patterns induced by N-methyl-D-aspartate, acetylcholine and serotonin in the *in vitro* neonatal rat spinal cord. Neurosci Lett 171:147-150.

Delcomyn F (1980) Neural basis of rhythmic behavior in animals. Science 210:492-498.

Deliagina TG, Orlovsky GN, Pavlova GA (1983) The capacity for generation of rhythmic oscillation is distributed in the lumbosacral spinal cord of the cat. Exp Brain Res 53:81-90.

Duysens J, Pearson KG (1980) Inhibition of flexor burst generation by loading ankle extensor muscles in walking cats. Brain Res 187:321-332.

Edgley SA, Jankowska E, Shefchyk S (1988) Evidence that mid-lumbar neurones in reflex pathways from group II afferents are involved in locomotion in the cat. J Physiol 403:57-71.

Giszter SF, Mussa-Ivaldi FA, Bizzi E (1993) Convergent force fields organized in the frog's spinal cord. J Neurosci 13:467-491.

Grillner S (1996) Neural networks for vertebrate locomotion. Sci Amer January 64-69.

Grillner S, Wallen P, Brodin L (1991) Neural network generating locomotor behavior in lamprey: circuitry, transmitters, membrane properties and simulation. Ann Rev Neurosci 14:169-199.

Grillner S (1985) Neurobiological bases of rhythmic motor acts in vertebrates. Science 228:143- 49.

Grillner S, McClellan A, Sigvardt K, Wallen P, William T (1982) On the neural generation of "fictive locomotion" in a lower vertebrate nervous system *in vitro.* In: Brain stem control of spinal mechanisms (Sjolund B, Bjorklund A, eds), pp 273-295. Amsterdam: Elsevier Biomedical Press.

Grillner S (1981) Control of locomotion in bipeds, tetrapods, and fish. In: Handbook of Physiology, Sec 2, The nervous system (Brookhardt JM, Mountcastle VB, eds), pp 1179-1236. Bethesda, MD: American Physiological Society.

Grillner S (1974) On the generation of locomotion in the spinal dogfish. Exp Brain Res 20:459- 470.

Guertin P, Angel MJ, Perreault MC, McCrea DA (1995) Ankle extensor group I afferents excite extensors throughout the hindlimb during fictive locomotion in the cat. J Physiol (Lond) 487: 197-209.

Ho S, O'Donovan MJ (1993) Regionalization and intersegmental coordination of rhythm-generating networks in the spinal cord of the chick embryo. J Neurosci 13: 1354-1371.

Hochman S, Jordan LM, MacDonald JF (1994) N-methyl-t)-aspartate receptor-mediated voltage oscillations in neurons surrounding the central canal in slices of rat spinal cord. J

Neurophysiol 72:565-577.

Hochman S, Schmidt B J (1998) Whole-cell recordings of lumbar motoneurons during locomotor like activity in the *in vitro* neonatal rat spinal cord. J Neurophysiol, in press.

Iakhnitsa IA, Bulgakova NV, Piliavskii AL (1987) Kinematic analysis of the different types of locomotor movement in rats after deafferentation. Neirofiziologiia 19:520-525.

Iizuka M, Kiehn O, Kudo N (1997) Development in neonatal rats of the sensory resetting of the locomotor rhythm induced by NMDA and 5-HT. Exp Brain Res 114:193-204.

Iwahara T, Atsuta Y, Garcia-Rill E, Skinner RD (1991) Locomotion induced by spinal cord stimulation in the neonate rat *in vitro.* Somatosen Mot Res 8:281-2S7.

Jovanović K, Petrov T, Greer JJ, Stein RB (1996) Serotonergic modulation of the mudpuppy *(Necturus maculatus)* locomotor pattern *in vitro.* Exp Brain Res 111:57-67.

Jovanović K, Petrov T, Stein RB (1996) Modulatory action of inhibitory neurotransmitters on the mudpuppy *(Necturus maculatus).* Soc Neurosci Abstr 22:1376.

Kiehn O, Johnson BR, Raastad M (1996) Plateau potentials in mammalian spinal interneurons during transmitter-induced locomotor activity. Neuroscience 75:263-273.

Kiehn O, Iizuka M. Kudo N (1992) Resetting from low threshold afferents of N-methyl-D- aspartate-induced locomotor rhythm in the isolated spinal cord-hindlimb preparation from newborn rats. Neurosci Lett 184:43-46.

Kjaerulff O, Kiehn O (1996) Distribution of networks generating and coordinating locomotor activity in the neonatal rat spinal cord *in vitro:* A lesion study. J Neurosci 16:5777-5794.

Kjaerulff O, Barajon I, Kiehn O (1994) Sulphorhodamine-labelled cells in the neonatal rat spinal cord following chemically induced locomotor activity *in vitro.* J Physiol (Lond) 47S:265-273

Kremer E, Lev-Tov A (1997) Localization of spinal network associated with generation of hindlimb locomotion in the neonatal rat and organization of its transverse coupling system. J Neurophysiol 77:1155-1170.

MacLean JN, Hochman S, Magnuson DSK (1995) Lamina VII neurons are rhythmically active during locomotor-like activity in the neonatal rat spinal cord. Neurosci Lett 197:9-12.

Mortin LI, Stein PSG (1989) Spinal cord segments containing key elements of the central

pattern generators for three forms of scratch reflex in the turtle. J Neurosci 9:2285-2296.

Pearson KG (1995) Proprioceptive regulation of locomotion. Curr Opin Neurobiol 5:786-91.

Pearson KG (1993) Common principles of motor control in vertebrates and invertebrates. Ann Rev Neurosci 16:265-297.

Perrins R (1995) The roles of central cholinergic and electrical synapses made by spinal motoneurones in Xenopus embryos. In: Alpha and Gamma Motor Systems (Taylor A, Gladden MH, Durbaba R eds), pp 48-50, New York: Academic.

Raastad M, Johnson BR, Kiehn O(1996) The number of postsynaptic currents necessary to produce locomotor-related cyclic information in neurons in the neonatal rat spinal cord. Neuron 17:729-738.

Ranck JB (1981) Extracellular stimulation. In: Electrical stimulation research techniques (Patterson MM, Keener RP, eds), pp 2-34, New York: Academic.

Richmond F JR, Gladdy R, Creasy JL, Kitamura S, Smits E, Thomson DB (1994) Efficacy of seven retrograde tracers, compared in multiple-labelling studies of feline motoneurones. J Neurosci Methods 53:35-46.

Roberts A, Soffe SR, Dale N (1986) Spinal interneurons and swimming in frog embryos. In: Neurobiology of Vertebrate Locomotion. (Grillner S, Stein PSG, Stuart D. Forssberg H, Herman RM eds), pp 279-306. London: Macmillan.

Roberts A, Tunstall MJ, Wolf E (1995) Properties of networks controlling locomotion and significance of voltage dependency of NMDA channels: simulation study of rhythmic generations sustained by positive feedback. J Neurophysiol. 73:485-495.

Rossignol S (1996) Neural control of stereotypic limb movements. In: Handbook of Physiology. Sec 12, Exercise: Regulation and Integration of Multiple Systems (Rowell LB, Shepherd JT, eds), pp 173-216. New York: Oxford.

Shefchyk S, McCrea D, Kriellaars D, Fortier P, Jordan L (1990) Activity of interneurons within the L4 spinal segment of the cat during brainstem-evoked fictive locomotion. Exp Brain Res 80:290-295.

Stein PSG, Victor JC, Field EC, Currie SN (1995) Bilateral control of hindlimb scratching in the spinal turtle: Contralateral spinal circuitry contributes to the normal ipsilateral motor pattern of fictive rostral scratching. J Neurosci 15: 4343-4355.

Stein RB (1995) Presynaptic inhibition in humans. Prog Neurobiol 47:533-544.

Stein RB, Capaday C (1988) The modulation of human reflexes during functional motor tasks. Trends Neurosci 11:328-332.

Stein RB, Lee RG (1981) Tremor and clonus. In: Handbook of Physiology, Sec 1, The nervous system, Vol II, Motor Control (Brooks VB ed), pp 235-243. Bethesda, MD: American Physiological Society.

Székely G, Czéh G, Voros G (1969) The activity pattern of limb muscles in freely moving normal and deafferented newts. Exp Brain Res 9:53-62.

Viala D, Viala G, Jordan L (1991) Interneurones of the lumbar cord related to spontaneous locomotor activity in the rabbit. I. Rhythmically active interneurones. Exp Brain Res 84:177-186.

Wheatley M, Jovanović K, Stein RB, Lawson V (1994) The activity of interneurons during locomotion in the *in vitro* Necturus spinal cord. J Neurophysiol 71:2025-2032.

Wheatley M, Stein RB (1992) An *in vitro* preparation of the mudpuppy for simultaneous intracellular and electromyographic recording during locomotion. J Neurosci Methods 42:129- 137.

Wheatley M, Edamura M, Stein RB (1992) A comparison of intact and *in vitro* locomotion in an adult amphibian. Exp Brain Res 88:609-614.

Whelan P J, Hiebert GW, Pearson KG. (1995) Stimulation of the group I extensor afferents prolongs the stance phase in walking cats. Exp Brain Res 103:20-30.

Yeomans JS (1990) Principles of brain stimulation. Oxford: Oxford UP.

CHAPTER 5

INTERNEURONS IN THE NEURAL NETWORKS FOR WALKING IN THE MUDPUPPY *(Necturus maculatus)* SPINAL CORD

INTRODUCTION

Rhythmic behaviors, such as locomotion, can be generated independently by neuronal networks in the spinal cord (Székely et al. 1969; Delcomyn 1980; Grillner 1981, 1985; Pearson 1993). Descending and sensory inputs play an important role in modulating the activities of the spinal neuronal networks so as to provide an adaptive capacity of locomotor patterns to a changing external environment (Jordan 1983, 1986, 1998; Armstrong 1986,1988; Pearson 1993, 1995; Rossignol 1996; Brooke et al. 1997). The work on the lamprey (Grillner 1985, 1996; Grillner et al.1991; Grillner and Matsushima 1991) and tadpole (Roberts et al. 1986, 1995; Perrins 1995) have opened the way to an understanding at the cellular level of the circuitry responsible for generating and coordinating the bending motion of the trunk required for swimming. An essential feature of the characterized segmental circuitry is a pair of half centers that are mutually inhibitory and contribute to burst generation.

Progress has also been made to localize the networks for walking, a more complex motor task that involves coordinated limb movement about multiple joints in different limbs (Deliagina et al. 1983; Iwahara et al. 1991; Yamaguchi 1992; Ho and O'Donovan 1993; Hochman et al. 1994; Kjaerulff et al., 1994; Cazalets et al. 1995, 1996; Noga et al. 1995; Maclean et al. 1995; Bracci et al. 1996; Kjaerulff and Kiehn 1996; Kiehn et al. 1996; Kremer and Lev-Tov 1997;

A version of this chapter is in preparation for submission for publication. Cheng J, Jovanović K, Bennett DJ, Han Y, Stein RB (1999). Contribution to paper: conducted 30% of experiments, filled cells with TMR-D, analyzed data and edited manuscript.

Cowley and Schmidt 1997; Magnuson and Trinder 1997). However, the complexity of mammalian spinal cord makes it experimentally difficult to investigate the neuronal organization of the circuitry for walking. By using a simpler, amphibian *in vitro* preparation (Wheatley and Stein 1992, Wheatley et al. 1992, 1994; Jovanović et al. 1996), we have been able to localize the neural networks for walking and demonstrate that the flexor and extensor centers for the elbow joint are distinctly localized in the spinal cord. This pair of centers can generate rhythmic motor output independent of each other, although inhibitory interconnections do exist between them (Cheng et al. 1998).

At least three models have been proposed over the course of this century for the neural circuitry of locomotion, namely the half-center model (Brown 1911, 1914), the ring model (Székely 1965), and the pacemaker model (DeLong 1978; Grillner and Matsushima 1991). Tests of these models rely heavily on recording identified interneurons in the cord during locomotor-like activities. Interneurons that could be involved in generating walking have been identified in the cat (Orlovsky and Feldman 1972; Feldman and Orlovsky 1975; McCrea et al. 1980; Jordan 1983; Arshavsky et al. 1984, 1986; Pratt and Jordan 1987; Edgley et al. 1988; Hishinuma and Yamaguchi 1990; Shefchyk et al. 1990; Terakado and Yamaguchi 1990), rabbit (Viala et al.; 1991), rat (Hochman et al., 1994; Maclean et al. 1995; Kiehn et al. 1996; Raastad et al. 1996), chick (O'Donovan et al. 1992), and mudpuppy (Wheatley et al. 1994). Oscillatory membrane properties of the cell membrane, independent of synaptic transmission, of interneurons as well as motoneurons have been reported in the rat (Hochman et al., 1994a, 1994b; Hochman and Schmidt 1998; Kiehn et al. 1996; MacLean et al. 1997, 1998) and in the turtle (Guertin and Hounsgaard 1998). However, their relation to the generation of walking remains speculative. Having found independent flexor and extensor centers, we have attempted in this study to identify interneurons within these centers, to classify them in phases of the step cycle, to investigate the link between the oscillatory properties of interneurons and the walking behavior, and to explore the connectivity between the interneurons and motoneurons. Part of this work has been reported in an abstract (Cheng and Stein 1998).

MATERIALS AND METHODS

Fifty-seven adult mudpuppies (22-28 cm in length) were used for the experiments. The *in vitro* mudpuppy walking preparation has been described previously (Wheatley and Stein 1992; Wheatley et al. 1992; Cheng et al. 1998). Briefly, following a dorsal laminectomy under anaesthesia [3-aminobenzoic acid ethyl ester (Sigma, St. Louis, MO. 1-2 g/l], the first five segments of the spinal cord were isolated from the rest of the body with the right forelimb attached by the brachial nerves. The paraspinal muscles were removed for stable recording from interneurons. A segment border is defined as midway between two adjacent spinal dorsal roots.

Rhythmic walking-like motion of the limb was induced by bath application of *N*-methyl-D-aspartate (NMDA, 20-120 μM, Sigma, St. Louis, MO) with 5-20 μM D-serine and monitored by electromyography (EMG) of the elbow flexor (*Brachialis*) and extensor (*Anconeus*) muscles. Pairs of fine teflon-insulated silver wires (75 μm in diameter; Medwire, Leico Industries Inc., New York, NY) were inserted into the muscles for EMG recording. The preparation was placed dorsal side up in a recording chamber superfused with continuously oxygenated Ringer's solution at a rate of 2-5 ml/min (NaCl 115 mM; KCl 2 mM; $CaCl_2$ 2 mM, $MgCl_2$ 1.8 mM, Hepes 5 mM, glucose 1 g/l, pH 7.35). The recording chamber consisted of two communicating subdivisions, one in the middle for the spinal cord and one for the limb. The cord was stabilized by pinning the vertebral column to the base of the recording chamber coated with Sylgard® resin (Dow Corning) while proximal ends of the forelimb were fixed to this base by the procoracoid cartilage. Recordings of interneurons were made during rhythmic walking-like movement of the limb of the preparation.

Recording and filling cells

Intracellular and extracellular recordings were made through the dorsal surface of the spinal cord starting approximately one hour after the dissection was accomplished. The recording microelectrodes (54~130 MΩ resistance when filled with 2M potassium acetate) were made from filament-containing glass capillaries (Borosilicate, o.d.= 1.5, mm i.d.=0.58 mm, AM Systems Inc. Everrett, WA, USA, or Clarke Electromedical, Redding, UK) with a puller (P-87, Sutter Instrument, CA, USA, or Narishige, Japan).

The recording chamber was placed on an air table. The *pia* of the dorsal surface of the C2 and C3 segments was removed, for better penetration of the recording microelectrode, with a pair of fine forceps under a dissection microscope (Leica, Switzerland). A fine micro-manipulator (Soma Scientific Instruments Inc., Irvine, CA, USA), which supported the headstage of the electrode, was secured to a 3-dimensional coarse manipulator (Soma Scientific Instruments Inc., Irvine, CA, USA). The tips of the electrodes were lowered by the use of the 3-D manipulator to the dorsal surface, in an area about 300 μm from the midline, at an angle of 70 degrees from the longitudinal plane of the cord. The electrodes were then driven by the fine manipulator through the dorsal white column (~ 200 μm) and into the gray matter (~200 to 500 μm deep). The depth of penetration of the electrode was not corrected for this angle, which remained approximately constant. Intracellular or extracellular potentials of the interneurons were amplified (Axoprobe 1A, Axon Instruments Inc., CA, USA), digitized (Digidata 1200A, Axon Instruments Inc.), and stored (Axoscope 7, Axon Instruments Inc., CA, USA) in a computer for later analysis. EMGs were simultaneously recorded from the elbow flexor and extensor muscles along with the interneuronal activity.

Some of the cells recorded intracellularly were filled with tetramethylrhodamine-dextran (2% solution of lysine fixable TMR-D; 3000 MW; Molecular Probes, Eugene, OR, USA) or Lucifer yellow (4%, Sigma) by including the dye in the tip of the recording electrode and passing current (1-3 ηA pulse, 2Hz; 80 % duty cycle, 2-30 min.; Carr et al. 1994) at the end of the recording. TMR-D could rapidly reveal fine morphological details (Fritzch 1993; Schmued et al. 1990) without interfering with the cell's function or the recording properties of the electrode (Carr et al. 1994).

To localize interneurons in relation to motoneurons innervating the elbow flexor and extensor muscles, we retrogradely labelled the motoneurons with intramuscular injection of fluorogold (Fluorochrome, Inc. Englewood, NJ, 7% in DMSO/saline) (Cheng et al. 1998). Fluorogold (~5 μl) was transcutaneously injected into the belly of the elbow extensor or flexor muscle. The animals (n=6) were then allowed to recover from the anaesthesia and survive for 3-4 days before being sacrificed for histological analysis of the spinal cords. Cresyl violet staining was used in four animals to visualize the overall

organization of the gray matter (Figure 5-1 A).

The spinal cords were isolated, fixed overnight in 4% paraformaldehyde (PFA)/0.1 M sodium phosphate buffer (pH 7.2-7.4) at 4 °C, transferred to 30% sucrose in 4% PFA for 2-4 hours at 22 °C (or overnight at 4 °C) for cryoprotection, and sliced coronally in 40-50 μm cryostat sections (JUNG GM 3000, Leica Canada Inc.). The sections were mounted sequentially onto subbed slides (Fisherbrand, Fisher Scientific), air dried, coverslipped (Cytoseal™, Stephens Scientific), and examined for the labelled cells under a fluorescence microscope (Leitz, Germany). Motoneurons filled with fluorogold were inspected with type A filter (excitation band pass 340-380 ηm, suppression long pass 430 ηm) and darkfield/brightfield illumination. Interneurons filled with the rhodamine compound were visualized with a N2.1 filter system with an excitation bandpass of 513-560 ηm and a barrier filter of 590 ηm.

Stimulation of the ventral roots

Stimulation of the ventral roots was conducted to test whether the recorded cell could be antidromically activated with constant cathodic currents (Master 8, A.M.P.I., Jerusalem, Israel) through a stimulus isolator (Neuro Log NL800). Single pulses (0.5 ms pulse duration) or trains of 6 pulses (40 Hz, 0.5 ms pulse duration, Cheng et al. 1998) were used to stimulate the ventral roots (C2-C4) innervating the forelimb. The stimulus intensity was up to 2 times motor threshold (10 to 20 μA). An intrafascicular electrode was employed in these experiments because of its advantages over traditional hook electrodes (Lefurge et al. 1991; Malagodi et al. 1989; Yoshida and Horch 1996). These electrodes produce smaller stimulus artifacts, do not require external support from micromanipulators, and allow for stimulation of multiple sites. Briefly, the electrodes were constructed from a 25 cm length of Teflon insulated 90% Pt 10% Ir wires (#7750, AM Systems, Carlsborg, WA). The diameter of the wire was 25 μm bare and 60-75 μm with insulation. A 250 to 500 μm segment of insulation was removed along the length of the wire, 3 cm from the end, by edgewise contact to a glowing Pt Ir filament foil. This bared segment becomes the stimulation site and is referred to as the active site of the electrode which is platinized by electrodeposition of finely divided platinum black. The impedance of the active site measured in normal (0.9%) saline at 1 kHz was between 50-400 KΩ.

Figure 5-1. Microphotographs of cross sections (40μm thick) of the spinal cord. There were approximately 80 cells in the gray matter on each side of the spinal cord (C2 segment) stained with cresyl violet **(A)**. One to three cells were motoneurons in the ventral lateral edge of the gray matter and were typically labelled retrogradely with fluorogold as exemplified (**B**, dorsal top and lateral right). Cells filled intracellularly with TMR-D **(C)** or Lucifer yellow **(D)** were localized in the intermediate area of the gray matter (dorsal top and lateral right; part of the tissue was torn during processing). They were spindle shaped **(D)** or round **(C)** and were small (15-20 μm) compared to the size of motoneurons (>25 μm).

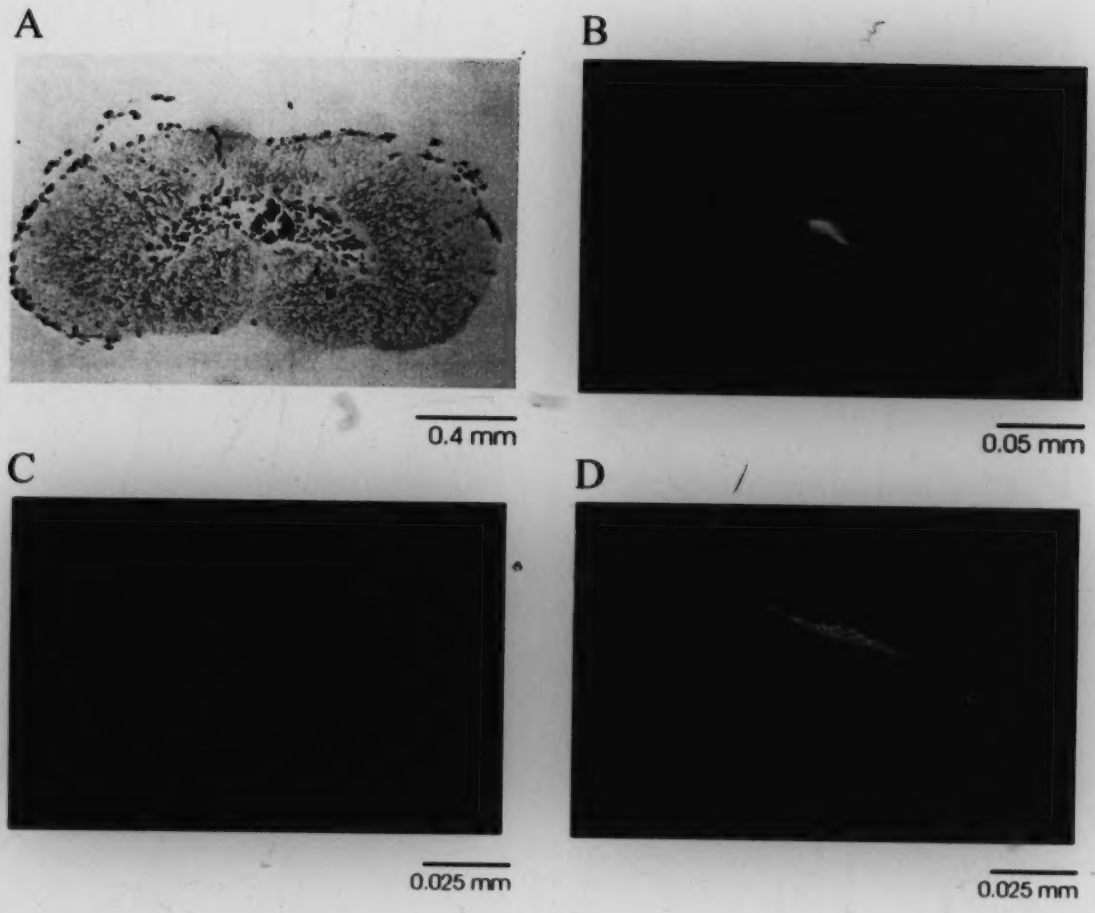
A
0.4 mm
B
0.05 mm
C
0.025 mm
D
0.025 mm

The electrodes were threaded through the spinal roots by means of an electrosharpened tungsten needle (15 mm long, 50 μm in diameter) attached to the end of the platinized electrode lead. The electrodes were implanted nearly perpendicular to the axis of the spinal roots and parallel to the longitudinal axis of the spinal cord. Thus, they were routed out without obstructing access of the recording microelectrode to the spinal cord. Care was taken to keep the active sites of the electrodes within the body of the spinal root to minimize the current shunting out of the root. A distantly placed intrafascicular electrode, with exposed area of up to 5 mm, was used as an indifferent electrode for stimulation.

Correlation Analyses

The phase relationship between the activity of the recorded cells and the activation of the elbow flexor and extensor muscles was quantified by spike-triggered averaging using a specially written program in Matlab. The rectified flexor and extensor EMGs were averaged with respect to the time of the spikes in each interneuron. A large EMG modulation in the spike triggered average means good phasic localization of the cell's bursting in a cycle. The timing of the peaks in the EMG, relative to the spikes, was then used to determine the phase of the spikes. Figure 5-2 A illustrates the division of the four phases, using the recording of an extensor interneuron as an example. Specifically, the extensor phase was defined as the period when the average extensor EMG was in the top 25% of the total change in a step cycle. The flexor phase was defined as the period when the extensor EMG was in the bottom 25% of the total change (or the flexor phase was in the top 25% of the total change). We typically selected whichever EMG had the stronger correlation with a given cell's spikes

The transition phases were the periods when the average EMG was in the middle 50% of the total change. There was often an overlap between the flexor phase defined by the average flexor EMG and the flexor-to-extensor phase defined by the average extensor EMG. For example, the cell in Figure 5-3 was classified as a F→E transition interneuron, based on the average extensor EMG, which had a stronger correlation to the firing of the cell. This is a modification from the method used by Wheatley et al. (1994), in which four

Figure 5-2. Four types of rhythmic cells. The rhythmic discharge of a cell located at 3 mm caudal to the C2 dorsal root was cross correlated to the activation of the extensor muscle of the elbow joint as revealed by spike-triggered average of EMGs triggered of the cell's action potential (**A**; see method section for details). A step cycle was divided into four phases relative to the spike-triggered average of the flexor and extensor EMGs (mV) (see text for details). The rhythmic cells were classified into four types according to their phasic discharge patterns in a step cycle. The number of each type of interneurons is shown in the bar graph (**B**). (F: flexor interneuron, E: extensor interneuron, F→E: flexor-to-extensor interneuron, E→F: extensor-to-flexor interneuron)

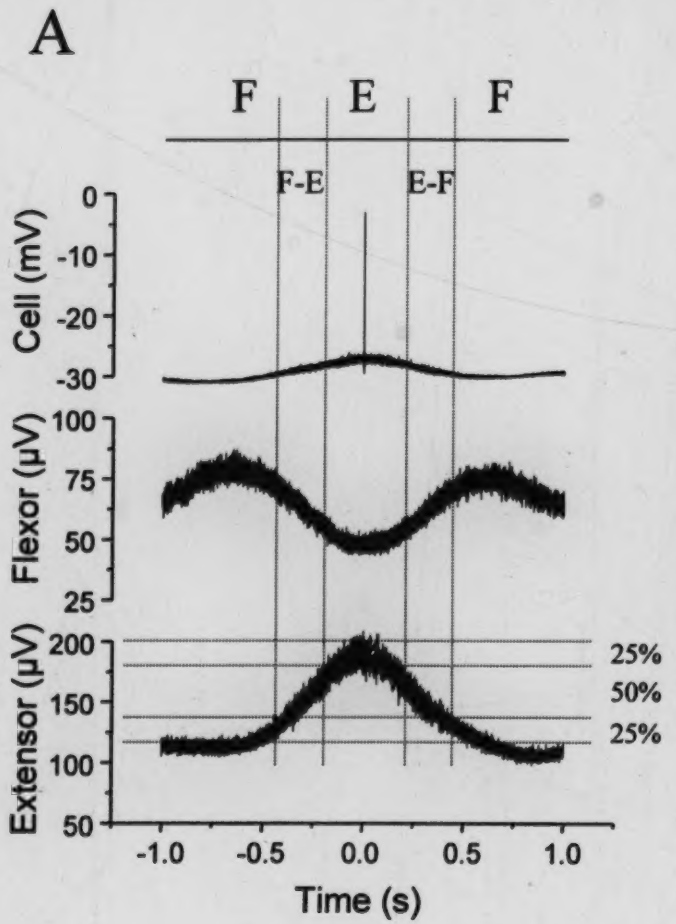
A
F
E
F
F-E
E-F
Cell (mV)
0
-10
-20
-30
Flexor (μV)
100
75
50
25
Extensor (μV)
200
150
100
50
25%
50%
25%
-1.0
-0.5
0.0
0.5
1.0
Time (s)

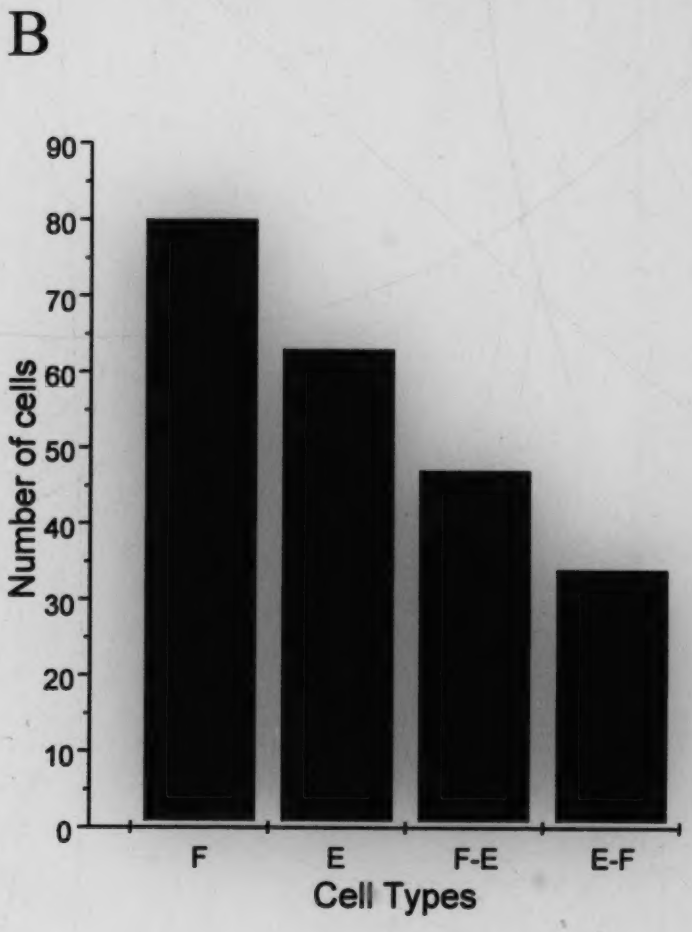
B
Number of cells
90
80
70
60
50
40
30
20
10
0
F
E
F-E
E-F
Cell Types

Figure 5-3. Example of a transition interneuron. **(A)** A cell fired rhythmically near the end of the flexor activation and the beginning of the extensor activation in the presence of NMDA (60 μM). **(B)** Rhythmic discharges of this cell were demonstrated by spike-triggered averaging to occur in the transition period between the peaks of flexor and extensor activation. See text for details of phase division.

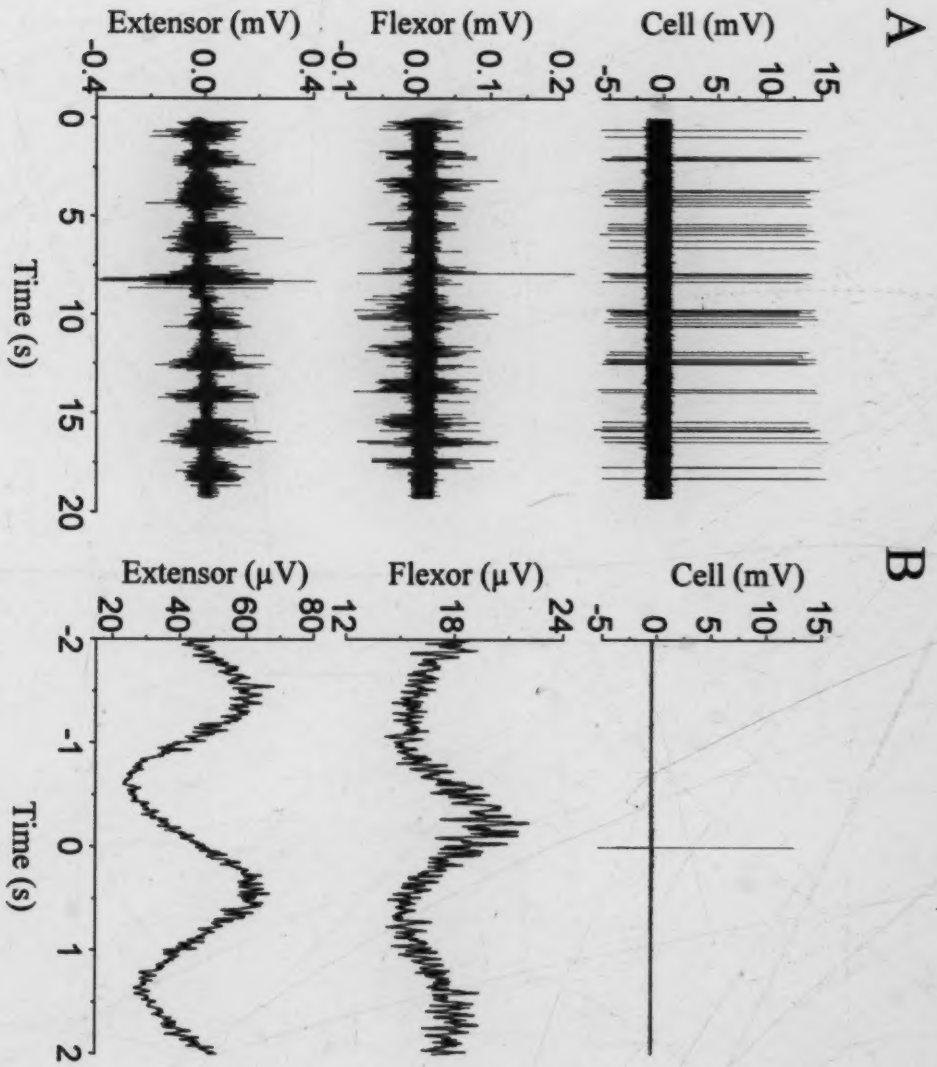
A
Extensor (mV)
Flexor (mV)
Cell (mV)
-0.4
0.0
0.4
-0.1
0.0
0.1
0.2
-5
0
5
10
15
0
5
10
15
20
Time (s)
B
Extensor (μV)
Flexor (μV)
Cell (mV)
20
40
60
80
12
18
24
-5
0
5
10
15
-2
-1
0
1
2
Time (s)

cell. This is a modification from the method used by Wheatley et al. (1994), in which four phases were defined by fixing the proportion in time for a step cycle, assuming an ideal sinusoidal pattern with a phase lag of 180° between the flexor and extensor activation. This modification takes into account variations in the patterns of the average EMGs and in the flexor-extensor phase lag which varied to some extent between animals and was often not exactly out of phase. Short latency, spike-triggered responses were examined to identify interneurons that make monosynaptic connections with the flexor or extensor motoneurons (e.g., Fig. 5-4 A).

RESULTS

A total of 328 cells were recorded during walking-like movement of the limb of the preparation induced by bath application of NMDA (20 to 120 μM), 240 of which were recorded intracellularly and 88 cells were recorded extracellularly. Of these cells, 224 (68.3%) were rhythmically active and correlated to the walking rhythm, as revealed by a spike-triggered average, 57 (17.4%) discharged tonically, and 47 (14.3%) fired sporadically. Figure 5-5 shows the distribution of the recorded cells along the longitudinal axis of the spinal cord at a resolution of 1 mm. All the cells recorded were located in the right side of the C2 and C3 segments. The number of cells recorded peaked in the rostral and caudal parts of the C2 segment

Identification of interneurons

The labeling experiments revealed an import feature in distribution of neurons in the gray matter of the spinal cord (Figure 5-1, see also Cheng et al. 1998). The motoneurons innervating the limb musculature are distinctively localized in the most ventrolateral part of the gray matter. Only one to three motoneurons can be found on each side of a 40 μm thick coronal section of the spinal cord (Fig. 5-1 B). They are localized more than 500 μm deep from the dorsal surface of the cord and 500 μm lateral to the midline. In contrast, there are approximately 80 interneurons in the same section on each side of the gray matter (Fig. 5-1 A). They are medial and dorsal to the motoneurons. Based on these findings, the electrophysiological recordings were made by penetrating the

Figure 5-4. Spike-triggered short latency excitation of the extensor muscle. **(A)** This cell, resided 2 mm rostral to the C3 dorsal root, 300 μm from the midline, and 230 μm from the dorsal surface, and triggered an excitation of the extensor muscle. The latency from the onset of the spike (s) to the onset of the muscle activation (m) was estimated to be 7-8 ms. The horizontal dotted lines denote 2 standard deviations around the mean of the average responses and the latency was chosen as the point where the values first exceeded this range. **(B)** Latency of motoneuron excitation to activation of the extensor. Stimulation (0.5 ms square wave, 1.2 times motor threshold) of the C3 dorsal root (s) induced responses (m) in the flexor and extensor muscles of the elbow joint with a latency of 6 ms. The latency from the firing of the cell to activation of the extensor motoneurons was estimated to be 1-2 ms (7-8 ms minus 6 ms), suggesting monosynaptic connections.

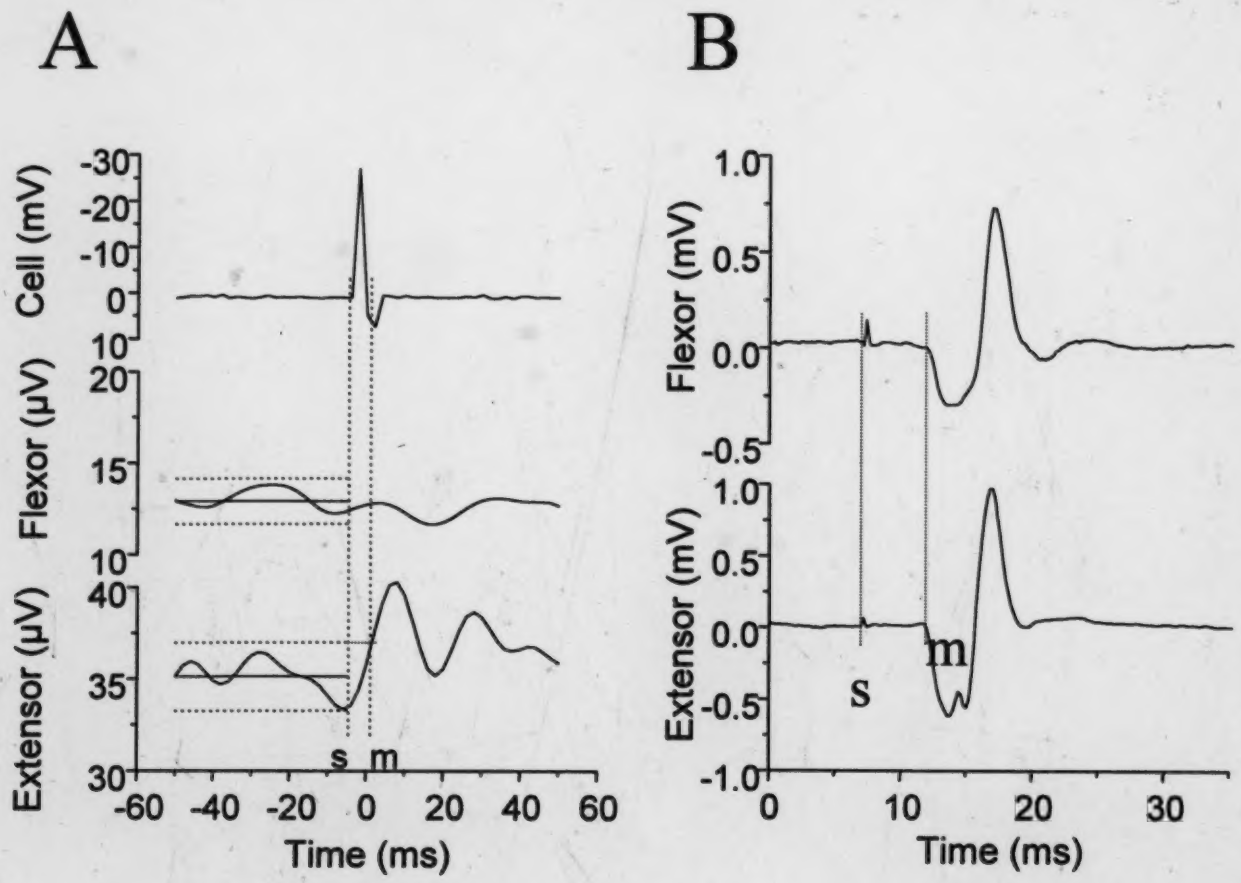
A
B
Cell (mV)
Flexor (μV)
Extensor (μV)
-30
-20
-10
0
10
20
15
10
40
35
30
s
m
-60
-40
-20
0
20
40
60
Time (ms)
Flexor (mV)
Extensor (mV)
1.0
0.5
0.0
-0.5
-1.0
s
m
0
10
20
30
Time (ms)

electrophysiological recordings were made by penetrating the cord from the dorsal surface, within 300 μm from the midline, and less than 500 μm deep from the dorsal surface to minimize the chances of recording from a motoneuron. Some of the cells recorded (n=13) were satisfactorily filled with TMR-D or Lucifer yellow. These cells were largely localized in the intermediate zone of the gray matter. They were either bipolar (Fig. 5-1 D), spindle shaped, or round with fine arborizations (Fig.5-1C) that extend to the white matter. The diameters of the cell bodies were about 15-20 μm. The location and morphology of these cells are distinctly different from those of the motoneurons, which are usually large in size (over 25 μm in diameter). In two cases, filling of a recorded cell resulted in labeling of two cells, the one being recorded and an adjacent cell. Motoneurons were occasionally recorded and filled but are not included in this report. 20 % of the recorded cells (n=58) were tested with stimulation of the ventral roots and none of them were activated antidromically.

The majority of rhythmically active cells recorded during locomotion, displayed depolarized resting membrane potentials. Therefore, records of cells with resting potentials of -40 mV or lower were considered to be intracellular while records with membrane potentials higher then -40 mV were considered to be extracellular. The membrane parameters of the cells quantified included average resting membrane potentials (-42 $\pm$ 18 mV), membrane resistance (51 $\pm$ 26 MΩ), and time constant (2.4 + 1.1 ms). The amplitude of the action potentials varied from 10 to 50 mV but was not quantified because the spikes were sometimes truncated due to the sampling rates (1-5 kHz) used for long-time recording. Since the same information on timing of the spikes could be obtained from either intracellular or extracellular recordings, poor penetrations, perhaps from processes with reduced membrane potentials, were accepted as long as they were stable enough to do the correlation analysis.

Phasic classification of the cells

The temporal relationship of discharge of the rhythmic cells to the activity of the flexor and extensor muscle about the elbow joint was revealed by cross-correlation analysis (spike-triggered average). Cells were classified as flexor (F) interneurons, flexor-to-extensor transition (F→E) interneurons, extensor (E) interneurons, and extensor-to-

Figure 5-5. Longitudinal distribution of cells recorded in the C2 and C3 segments. The number of cells is plotted against the longitudinal axis of the spinal cord at a resolution of 1 mm **(B)**. C2+4 denotes 4 mm rostral to the C2 dorsal root; C2-3 denotes 3 mm caudal to the C2 dorsal root, etc. C2-3 = C3+3. The distribution of the cells relative to the flexor (F) and extensor (E) motoneurons of the elbow joint is shown schematically **(A)**. The cells were classified into three groups according to their pattern of discharges **(C)**.

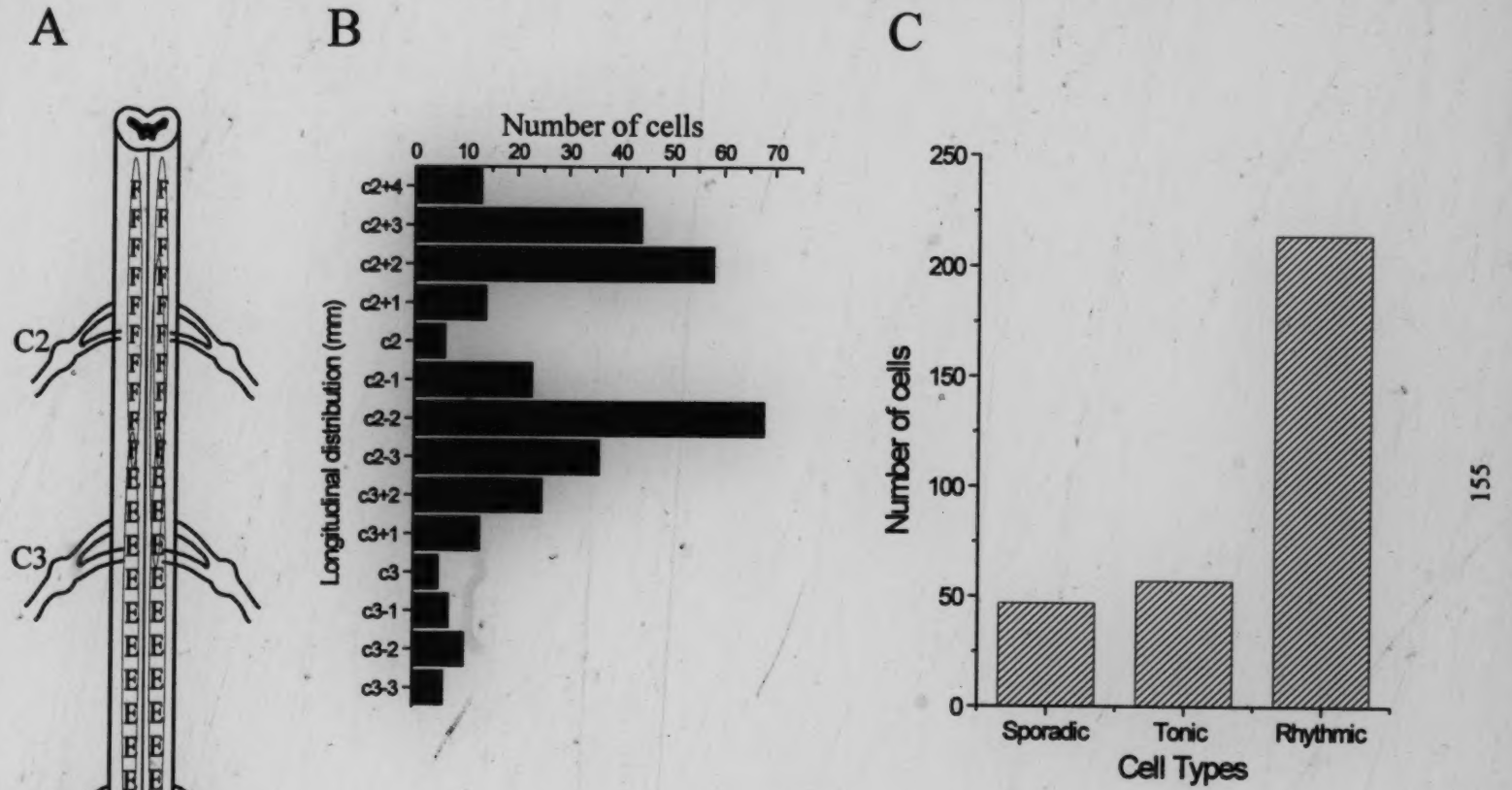
A
C2
C3
C4
B
Number of cells
0
10
20
30
40
50
60
70
Longitudinal distribution (mm)
c2+4
c2+3
c2+2
c2+1
c2
c2-1
c2-2
c2-3
c3+2
c3+1
c3
c3-1
c3-2
c3-3
C
Number of cells
250
200
150
100
50
0
Sporadic
Tonic
Rhythmic
Cell Types

flexor transition (E→F) interneurons, based on their phasic discharge patterns in a step cycle, (Figure 5-2 A; see Methods for details). Overall, 80 cells (36.7%) were classified as F interneurons, 63 (28.1%) as E interneurons, 47 (21.0%) as F→E transition interneurons, and 34 (15.2%) as E→F transition interneurons.

Figure 5-6 shows examples of flexor interneurons recorded in the presence of NMDA (40 μM). The cell shown in panel A was located in the dorsomedial part of the gray matter, 250 μm deep from the dorsal surface and 2 mm rostral to the C2 dorsal root. It did not respond to stimulation of ventral roots (C2 and C3) and did not show short latency responses in spike-triggered average of the flexor and extensor EMGs (Fig. 5-6C). Figure 5-6 also shows an example of extracellular recording of a cell that was located in the gray matter, 200 μm from the midline of the cord, 300 μm deep from the dorsal surface, and 2 mm rostral to the C2 dorsal root. It fired rhythmically in the flexor phase of a step cycle (Fig. 5-6 D) and was classified as a flexor interneuron (Fig. 5-6 E). Spike-triggered, short latency responses were not observed in this cell either.

An example of a transition interneuron is shown in Figure 5-3. This cell was located in the gray matter, 200 μm from the midline of the cord, 320 μm deep from the dorsal surface, and 1 mm rostral to the C2 dorsal root. It discharged rhythmically in the transition from the flexor bursts to the extensor bursts in the presence of NMDA (60 μM) and is classified as a flexor to extensor (F→E) interneuron. This is shown by raw recordings (Fig. 5-3 A) and spike-triggered EMG patterns (Fig. 5-3 B). Short latency responses in the spike-triggered average were not seen in this cell.

A proportion of cells (104/328) was not rhythmic. They discharged tonically (57 cells) or sporadically (47 cells) during NMDA induced walking motion of the limb. Spike-triggered averages revealed no cross correlation between the discharge of these cells and the flexor and extensor activities. The location of these cells was not distinctly different from that of the rhythmic cells (Figure 5-7).

Longitudinal distribution of the recorded cells in the spinal cord

All the cells were recorded from the C2 and C3 segments, where the flexor and extensor centers are localized. Figure 5-7 shows the longitudinal distribution of the cells

Figure 5-6. Example of flexor interneurons recorded intra- and extra-cellularly in the presence of NMDA (40 μM). Raw intracellular recording of a cell at 2 mm rostral to the C2 segment showed that this cell fired in the flexor phase of the step cycle **(A)**. This is confirmed by the average of the flexor and extensor EMGs (mV) **(B)**. There was no evidence of short latency responses in either the flexor or the extensor muscle triggered by the spikes of the cell **(C)**, suggesting the cell was a flexor interneuron. Similar amount of information could be provided by extracellular recording of interneurons as exemplified by the recording of a cell at 1 mm caudal to the C2 dorsal root **(D)**. The spike-triggered average suggests that this cell is also a flexor interneuron **(E)**.

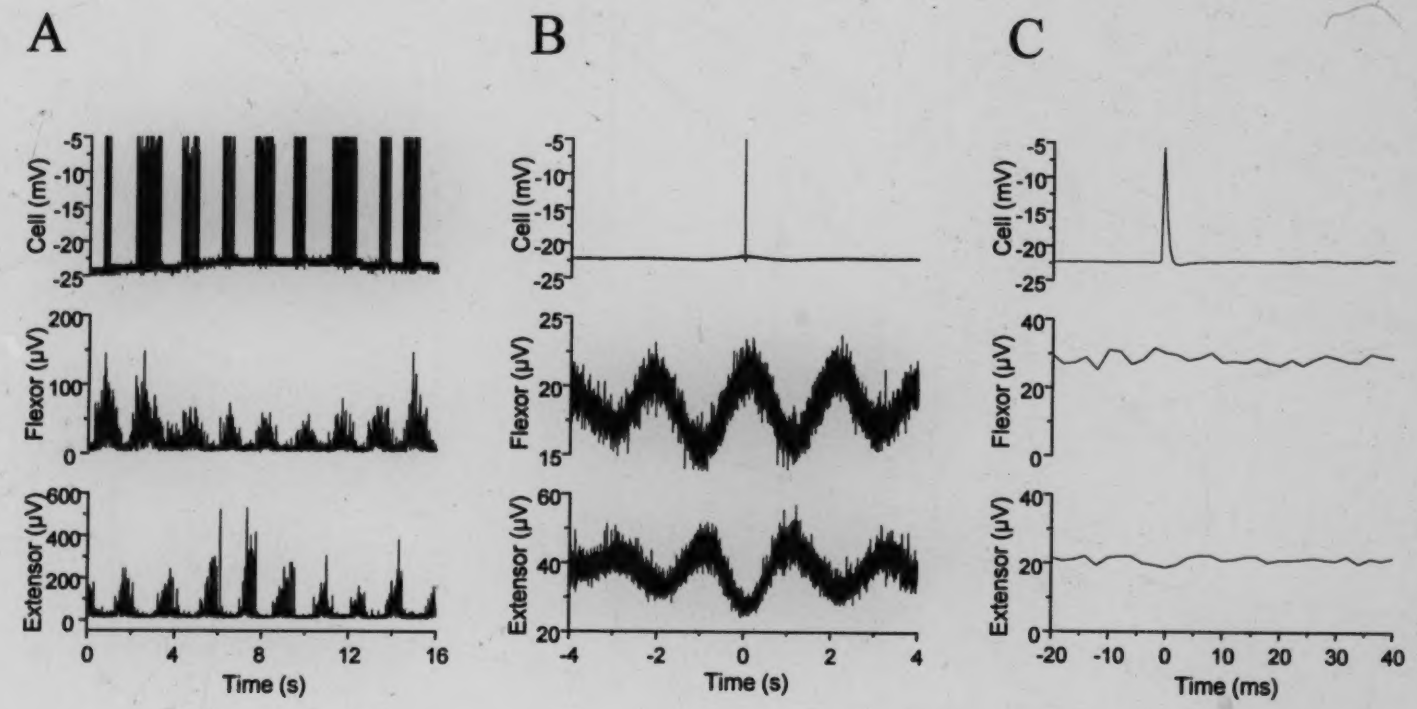
A
B
C
Cell (mV)
Flexor (μV)
Extensor (μV)
Time (s)
Time (ms)

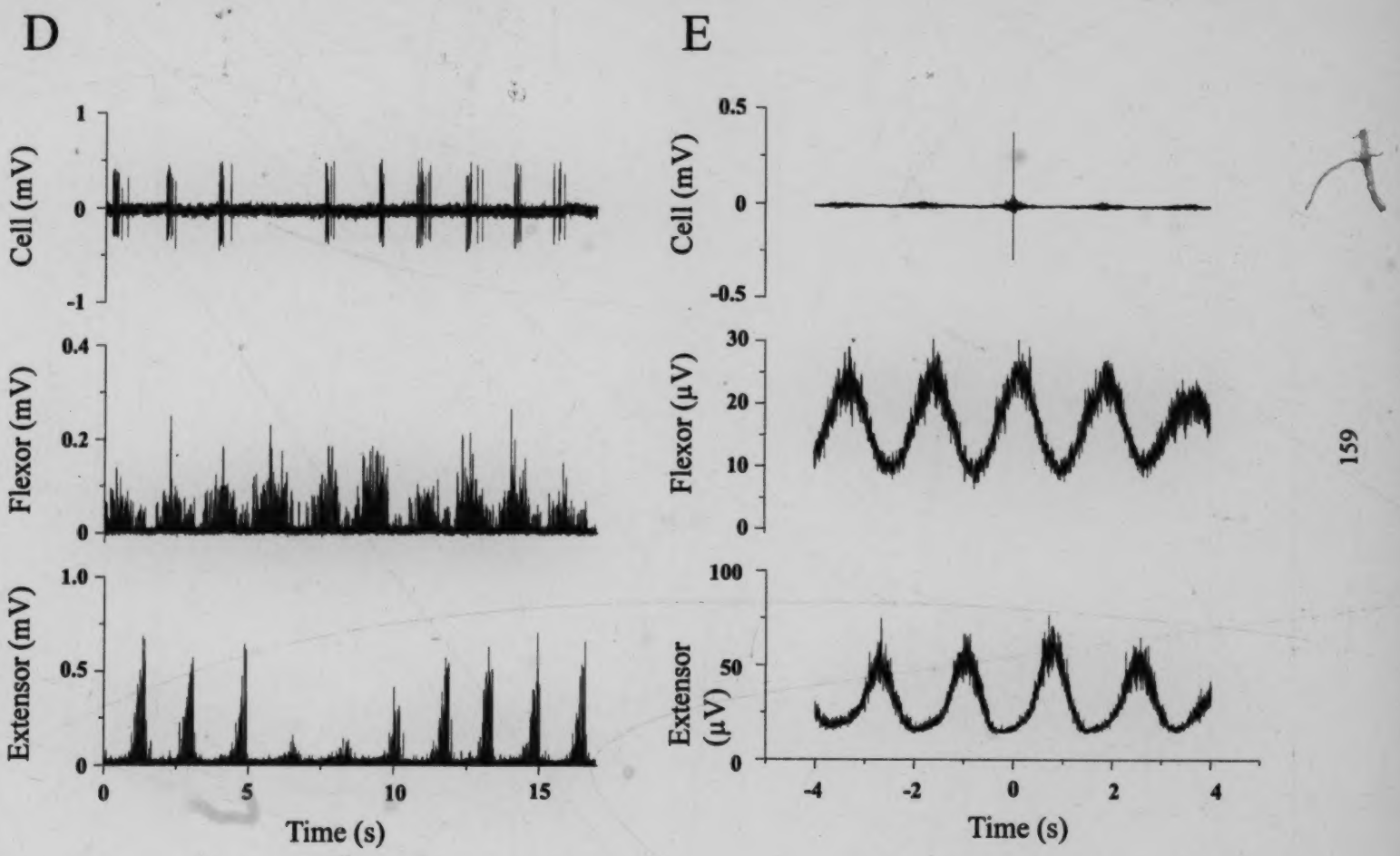
D
E
Cell (mV)
Flexor (mV)
Extensor (mV)
Flexor (μV)
Extensor (μV)
Time (s)
Time (s)
159

along the cord. The majority of the flexor interneurons were found in the region rostral and caudal to the C2 spinal roots (Figure 5-7 A). In contrast, the number of extensor interneurons peaked between the C2 and C3 roots (the border of the C2 and C3 segments, Figure 5-7 B), on average about 3 mm more caudally relative to the position of the flexor peak (Figure 5-7 C). The transition interneurons assumed a distribution pattern between these two groups. The tonically discharging interneurons were found rostrally, on average close to the flexor interneurons, while the sporadically firing interneurons were diffusely distributed.

Cells with membrane potentials oscillating at walking frequency

Some cells showed rhythmic membrane potential oscillations at the walking frequency in the presence of NMDA. Figure 5-8 A shows rhythmic depolarizing oscillations of a cell, which fired in the flexion phase of the walking pattern. This cell was located in the caudal part of the C2 segment, about 300 μm lateral to the midline of the cord, and at a depth of 460 μm from the dorsal surface. It did not respond to stimulation of the C2 and C3 ventral root at an intensity of 2 times motor threshold and was classified as a flexor interneuron. Application of depolarizing current (~0.1-0.2 nA) inactivated the action potentials, while leaving the membrane potential oscillating rhythmically at the walking frequency (Figure 5-8 B).

Connectivity of the rhythmic cells

Cross-correlation analysis was performed on all the cells recorded to explore the connectivity of these cells to the motoneurons of the flexor and extensor muscles. Spike-triggered short latency responses in these muscles could suggest direct connection of the recorded cell to the motoneurons (last order interneurons). Figure 5-4 shows an example of spike-triggered short latency excitation of the extensor muscle. This cell, localized in the rostral part of the C3 segment and classified as an extensor interneuron, triggered an excitation of the extensor muscle at an estimated latency of 7-8 ms (Fig. 5-4 A). The time for an action potential from the motoneurons to evoke muscle activation was measured to be about 6 ms at room temperature (20-22 °C). This was measured by stimulating the C3

Figure 5-7. Longitudinal distribution of the cells recorded along the spinal cord at a resolution of 1 mm. The X-axis (panels **A** and **B**) is the relative distance along the longitudinal axis of the spinal cord. C2+4 denotes 4 mm rostral to the C2 dorsal root; C2-3 denotes 3 mm caudal to the C2 dorsal root, etc. C2-3 is equal to C3+3. The median of each cell type (panels **A** and **B**) is shown by the horizontal line and the number. **(A)** The flexor interneurons were mainly localized in the rostral and caudal parts of the C2 segment. **(B)** The extensor interneurons were concentrated around the border of the C2 and C3 segments. **(C)** The mean location of the extensor interneurons was on average about 3 mm caudal to that of the flexor interneurons. In the intermediate locations were other types of cells, including flexor-to-extensor transition interneurons (F-to-E), extensor-to-flexor transition interneurons (E-to-F), tonic interneurons (Tonic), and sporadic interneurons (Sporadic). On the y-axis of this panel, 0 represents the C2 dorsal root; 1 denotes 1 mm rostral to the C2 dorsal root; -1 denotes 1 mm caudal to the C2 dorsal root, etc.

A. Flexor Interneurons

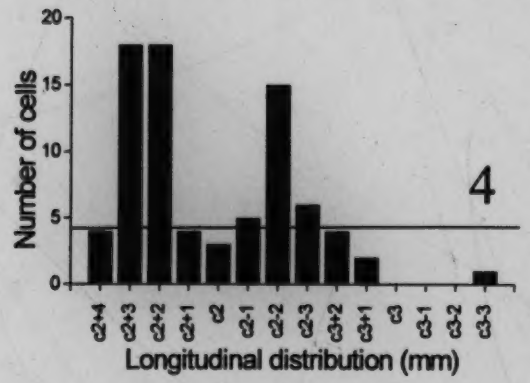

B. Extensor interneurons

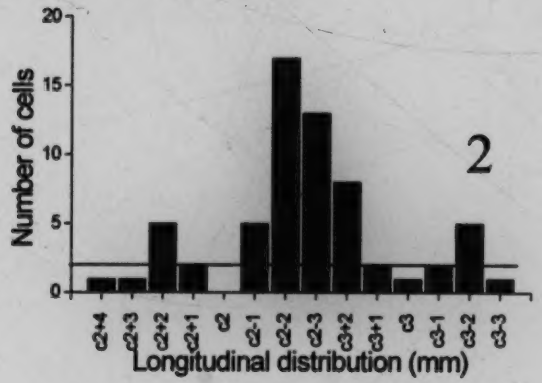

C. Location of cell types

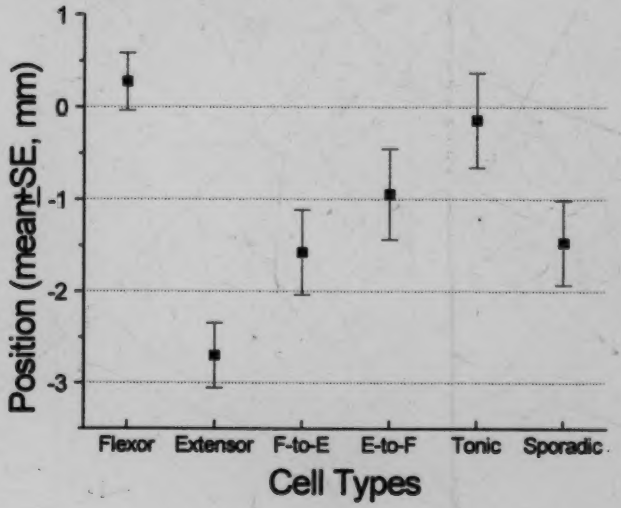

Figure5- 8. Rhythmic discharges on top of membrane voltage undulations. This cell was located 2 mm caudal to the C2 dorsal root, 300 μm from the midline, and 460 μm from the dorsal surface. **(A)** It fired rhythmically in phase with the flexor EMGs but did not trigger short latency responses in the flexor EMGs (not shown). Cell AC denotes AC coupled recording of the cell's activity. **(B)** Inactivation of the spikes by depolarizing current injection (~0.1-0.2 nA) eliminated the action potentials while the pattern of membrane potential oscillations did not change its temporal relationship to the flexor activation.

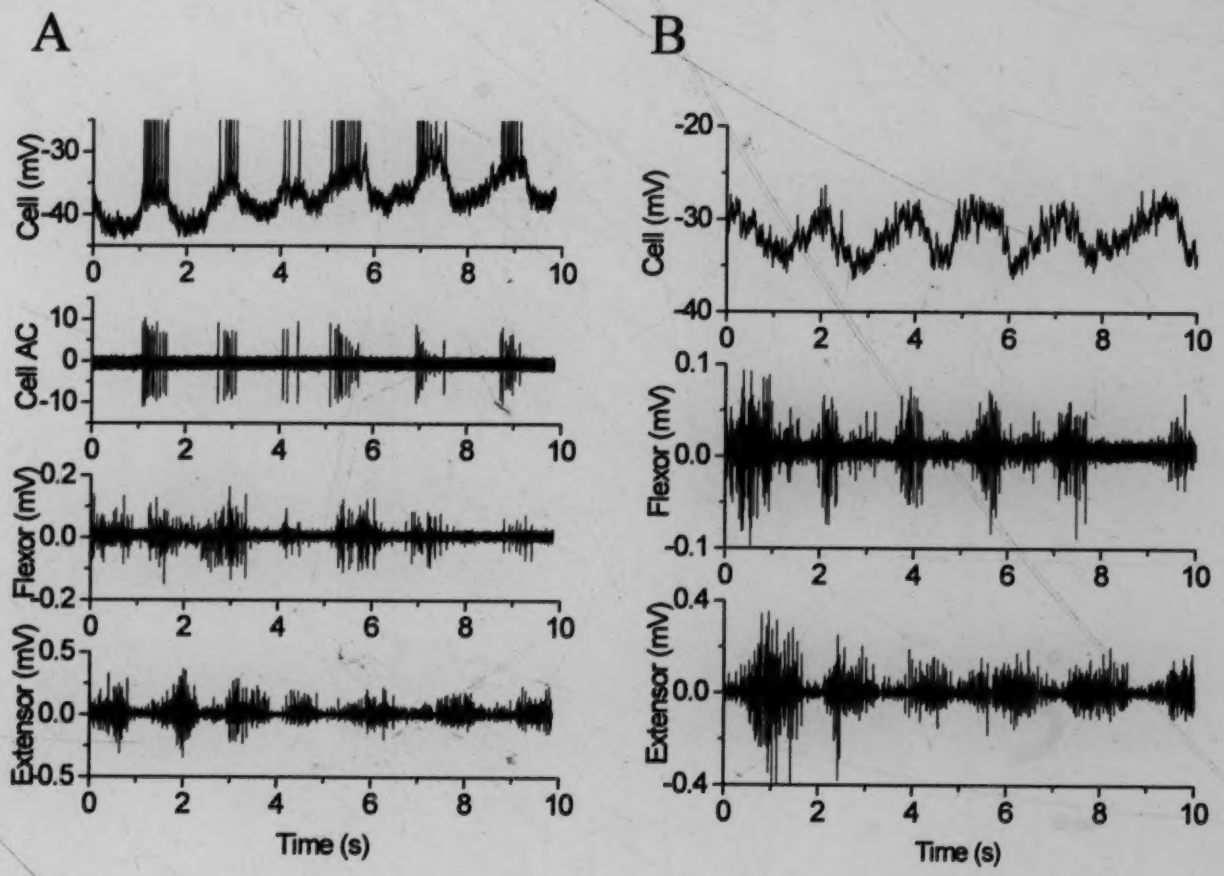
A
B
Cell (mV)
-30
-40
Cell AC
10
0
-10
Flexor (mV)
0.2
0.0
-0.2
Extensor (mV)
0.5
0.0
-0.5
-20
0.1
-0.1
0.4
-0.4
0
2
4
6
8
10
Time (s)

ventral root and measuring the onset latency of the extensor muscle activation (Fig. 5-4B). The latency from this cell to the motoneuron was likely 1-2 ms (7 to 8 minus 6 ms) and could be monosynaptic. This cell is therefore considered to be a last order extensor interneuron. Overall, 41 out of 224 cells showed spike-triggered short latency responses; 23 were classified as flexor interneurons and 17 as extensor interneurons. Three cells showed triggered responses with latencies shorter than 6 ms and were considered to be cells that were co-activated with or activated after motoneurons.

DISCUSSION

In this study we recorded interneurons in the neural networks for walking in the C2 and C3 segments, classified them into four groups in a step cycle, and mapped their longitudinal distribution along the spinal cord. A few interneurons showed oscillatory membrane properties that were independent of spike mediated synaptic transmission and were linked to the walking rhythm. Evidence was also presented that some cells were last order interneurons.

Four types of interneurons related to walking

The interneurons were identified by a combination of criteria. We targeted preferentially cells that were located in the intermediate gray where there are no motoneurons in this animal. The interneuronal nature of the recorded cells was confirmed by the lack of antidromic responses to ventral root stimulation, the lack of spike-triggered, short latency (less than 6 ms) responses in the flexor or extensor muscle about the elbow joint, and, in some case, intracellular labeling. These cells showed low average resting membrane potentials (-42 $\pm$ 18 mV) and small action potentials. These observations are consistent with those on neurons in the mudpuppy retina (Werblin and Dowling 1969; Miller and Dacheux 1976) where resting potentials were about -30 mV and action potentials were about 5 to 30 mV in the ganglion cells and amacrine cells. Therefore, the low negative membrane potentials and small action potentials may reflect the nature of this preparation. However, the possibility that the low resting membrane potentials may have

resulted from poor penetrations during electrode progression along dorso-ventral extent of the mudpuppy spinal cord cannot be excluded. To further clarify this issue more experiments are needed.

The majority of the cells recorded in the C2 and C3 segments (224/328) were related to walking. The firing patterns of these cells were time-locked to the walking-like motion and the activation of the flexor and extensor muscles of the forelimbs. They were classified as flexor interneurons (36.7%, 80/224), extensor interneurons (28.1%, 63/224), flexor to extensor interneurons (21.0%, 47/224), and extensor to flexor interneurons (15.2%, 34/224) based on the timing of their discharges in a step cycle. The percentage of transition interneurons (36.2%) we reported here is smaller than that reported earlier (Wheatley et al. 1994) where 68% (34/50) of the cells were considered to be transition interneurons. The factors that may have contributed to this discrepancy include the location, number of cells recorded and the way in which the flexion and extension phases were defined (see the Methods section).

Differential longitudinal distribution of the four types of cells

The results revealed the interneuronal substrate for the flexor and extensor centers we reported earlier (Cheng et al. 1998). There were two peaks in the longitudinal distribution of number of flexor interneurons, the first in the rostral part of the C 2 segment and the second in caudal part of the C2 segment (Fig. 5-7 A). One peak was observed for the extensor interneurons in the border between the C2 and C3 segments (Fig. 5-7 B). This is in agreement with the observation that a 4 mm long region of the cord rostral to the C2 ventral root (inclusive) in isolation generated rhythmic flexor bursts without extensor bursts. The flexor interneurons in the first peak may have generated the flexor rhythms. On other hand, a region of 5 mm long caudal to the C3 ventral root (inclusive) in isolation generated rhythmic extensor bursts without flexor bursts. This may be due to the removal of both peaks of the flexor interneurons in the C2 segment. An 8 mm long cord spanning the C3 ventral roots in isolation generated rhythmic alternating flexor-extensor bursts and walking-like motion of the forelimb about the elbow, reflecting the presence of a peak of flexor interneurons and a peak of extensor interneurons in this

region. There appear to be a substantial number of extensor interneurons caudal to the C3 ventral root, as a 5 mm long cord caudal to the C3 ventral root (inclusive) in isolation generated rhythmic extensor bursts without flexor bursts. The differential distribution of flexor and extensor interneurons may therefore constitute the basis for independent flexor and extensor centers (Cheng et al. 1998).

The concept of functional subunits, called unit burst generators by Grillner (1981) or modules by Jordan (1991), of neural networks for locomotion has gained support from observations in the lamprey (Cohen and Wallén 1980), turtle (Stein et al. 1995; 1998), mudpuppy (Cheng et al. 1997; 1998, Jovanović et al. 1998), frog (Saltiel et al. 1998; Bizzi et al. 1998) and neonatal rat (Hochman and Schmidt 1998). Evidence for independent flexor and extensor centres came from several distinct experiments, including electrical microstimulation, chemical stimulation, and surgical separation of specific regions of the spinal cord. The present work represents a further step toward the identification of the interneuronal composition of the locomotor networks.

The distribution of the transition interneurons is of interest. They had a mean position between the flexor and extensor interneurons. Perhaps, activation of the flexor interneurons sets into action the flexor-to-extensor cells, which in turn act on the extensor interneurons. Conversely, excitation of the extensor interneurons stimulates the extensor-to-flexor cells, which in turn activate the flexor interneurons. The switch between flexion and extension may be dependent upon the intrinsic membrane properties of these cells and the integration of input from the transition interneurons, the sensory pathways from the moving limbs, and the descending pathways of the supraspinal centers. This picture of information flow is supported by experimental observations where both excitatory and inhibitory input from the sensory pathways (Conway et al. 1987; Cheng et al. 1998; Hultborn et al. 1998), between the two centers (Cowley and Schmidt, 1994; Cheng et al. 1998), and from the supraspinal centers (Noga et al. 1995; Magnuson and Trinder 1997; Hultborn et al. 1998; Jordan 1998; Cheng and Magnuson 1999) have either been demonstrated or suggested.

Voltage oscillation of interneurons in relation to walking

Some interneurons showed rhythmic voltage oscillations in the presence of NMDA that were related to the walking patterns. Bursting of action potentials occurred in the depolarizing phase in some cells (Figure 5-8).

Pacemaker properties of interneurons activated by NMDA have been demonstrated for fictive swimming in the lamprey (Sigvardt et al 1985; Grillner and Wallén 1985; Wallén and Grillner 1985, 1987). Oscillations of membrane potentials independent of synaptic transmissions have also been observed in several interneurons in the neonatal rat spinal cord (Hochman et al. 1994; Schmidt et al. 1998). The present data, indicate that some interneurons within the rhythmogenic centers display rhythmic membrane oscillations, behavior implicated in generation of the locomotor rhythm. Some evidence from experiments in which oscillations remained after application of tetrodotoxin has been presented (Cheng and Stein, 1998) but more data are needed to establish whether these oscillations are due to endogenous properties of the interneurons.

Connectivity of the circuitry

The present data provide some information on the connectivity of the walking circuitry. The activity of a proportion of interneurons (41/224) was cross-correlated with short latency responses in the flexor or extensor muscles about the elbow joint (Figure 5-4). Based upon the estimated latency of the responses, some of these cells were considered to be last order interneurons to the flexor (n=23) or extensor (n=17) motoneurons. The latency of the responses was only estimated from a large number of spike-triggered responses in EMGs (100-500 sweeps) because of the lack of synchronization in onset of motor units. More precise measurement could have been done if recording had also been made from the ventral roots. Nevertheless, these data do support the notion that the flexor and extensor motoneurons receive locomotor drive from different sets of last order interneurons (Puskar and Antal 1997).

Overall, the present results are in agreement with the previous findings on distinct flexor and extensor rhythmogenic centers. In addition, there are indications that some of interneurons within these centers display subthreshold membrane oscillations, a behavior

implicated in the generation of locomotor rhythm in different species. However, the low resting membrane potentials encountered in these cells prevent us from drawing final conclusions on the role of these oscillations in generating of the locomotor rhythm in the mudpuppy. This subject is a current area of research.

REFERENCES

Armstrong DM (1986) Supraspinal contributions to the initiation and control of locomotion in the cat. Prog Neurobiol 26:273-361.

Armstrong DM (1988) The supraspinal control of mammalian locomotion. J Physiol 405:1-37.

Arshavsky YI, Gelfand IM, Orlovsky GN, Pavlova GA. Popova LB (1984) Origin of signals conveyed by the ventral spino-cerebellar tract and spino-reticulo-cerebellar pathway. Exp Brain Res 54:426-431.

Arshavsky YI, Orlovsky GN, Pavlova GA, Popova LB (1986) Activity of C3-C4 propriospinal neurons during fictitious forelimb locomotion in the cat. Brain Res 363:354-357.

Bizzi E, Saltiel P, Tresch M (1998) Modular organization of motor behavior. Zeitschrift fur Naturforschung. Section C. J Biosci 53:510-517.

Bracci E, Ballerini L, Nistri A (1996) Localization of rhythmogenic networks responsible for spontaneous bursts induced by strychnine and bicuculline in the rat isolated spinal cord. J Neurosci 16:7063-7076.

Brooke JD, Cheng J, Collins DF, McIlroy WE, Misiaszek JE, Staines WR (1997) Sensori-sensory afferent conditioning with leg movement: gain control in spinal reflex and ascending paths. Prog Neurobiol 51:393-421.

Brown TG (1911) The intrinsic factors in the act of progression in the mammal. Proc. R. Soc. London Ser B 84:308-319.

Brown TG (1914) On the nature of the fundamental activity of the nervous centres: together with an analysis of the conditioning of rhythmic activity in progression, and a theory of the evolution of function in the nervous system. J Physiol (Lond) 48:18-46.

Carr PA, Noga BR, Nance DM, Jordan LM (1994) Intracellular labelling of cat spinal neurons using a tetramethylrhodamine-dextran amine conjugate. Brain Res Bulletin 34:447-451.

Cazalets JR, Borde M, Clarac F (1996) The synaptic drive from the spinal locomotor network to motoneurons in the newborn rat. J Neurosci 16:298-306.

Cazalets JR, Borde M, Clarac F (1995) Localization and organization of the central pattern generator for hindlimb locomotion in newborn rat. J Neurosci 15:4943-4951.

Cheng J, Stein RB, Jovanović K, Yoshida K, Bennett DJ, Han Y (1998) Identification, localization, and modulation of neural networks for walking in the mudpuppy (*Necturus*

maculatus) spinal cord. J Neurosci 18:4295-4304.

Cheng J, Stein RB, Jovanović K, Yoshida K (1997) Localization, activation and modulation of networks for walking in mudpuppy spinal cord. Soc Neurosci Abstr 23:207.

Cheng J, Stein RB (1998) Spinal interneurons that generate walking rhythm in the mudpuppy. Soc Neurosci Abstr 24: 1169.

Cheng J, Magnuson DSK (1999) Monosynaptic connections between axons in the ventrolateral funiculus and interneurons in the lumbar spinal cord of the neonatal rat. Soc Neurosci Abstr submitted.

Cohen AH, Wallén P (1980) The neuronal correlate of locomotion in fish. "Fictive swimming" induced in an *in vitro* preparation of the lamprey spinal cord. Exp Brain Res 41:11-18.

Conway BA, Hultborn H, Kiehn O (1987) Proprioceptive input resets central locomotor rhythm in the spinal cat. Exp Brain Res 68:643-656.

Cowley KC, Schmidt BJ (1997) Regional distribution of locomotor pattern-generating network in the neonatal rat spinal cord. J Neurophysiol 77:247-259.

Cowley KC, Schmidt BJ (1994) A comparison of motor patterns induced by *N*-methyl-D-aspartate, acetylcholine and serotonin in the *in vitro* neonatal rat spinal cord. Neurosci Lett 171:147-150.

Delcomyn F (1980) Neural basis of rhythmic behavior in animals. Science 210:492-498.

Deliagina TG, Orlovsky GN, Pavlova GA (1983) The capacity for generation of rhythmic oscillation is distributed in the lumbosacral spinal cord of the cat. Exp Brain Res 53:81-90.
DeLong MR (1978) Possible involvement of central pacemakers in clinical disorders of movement. Federation Proceedings 37:2171-2175.

Edgley SA, Jankowska E, Shefchyk S (1988) Evidence that mid-lumbar neurones in reflex pathways from group II afferents are involved in locomotion in the cat. J Physiol 403:57-71.

Feldman AG, Orlovsky GN (1975) Activity of interneurons mediating reciprocal 1a inhibition during locomotion. Brain Res 84:181-194.

Fritzch B (1993) Fast axonal diffusion of 3000 molecular weight dextrane amines. J Neurosci Methods 50:95-103.

Grillner S (1996) Neural networks for vertebrate locomotion. Sci Amer January 64-69.

Grillner S, Wallén P, Brodin L (1991) Neural network generating locomotor behavior in lamprey: circuitry, transmitters, membrane properties and simulation. Ann Rev Neurosci 14:169-199.

Grillner S, Matsushima T (1991) The neural network underlying locomotion in lamprey-synaptic and cellular mechanisms. Neuron. 7:1-15.

Grillner S (1985) Neurobiological bases of rhythmic motor acts in vertebrates. Science 228:143-149.

Grillner S and Wallen P (1985) The ionic mechanisms underlying N-methyl-D-aspartate receptor-induced, tetrodotoxin-resistant membrane potential oscillations in lamprey neurons active during locomotion. Neurosci Lett 60:289-294.

Grillner S, McClellan A, Sigvardt K, Wallén P, William T (1982) On the neural generation of "fictive locomotion" in a lower vertebrate nervous system *in vitro*. In: Brain stem control of spinal mechanisms (Sjölund B, Björklund A, eds), pp 273-295. Amsterdam: Elsevier Biomedical Press.

Grillner S (1981) Control of locomotion in bipeds, tetrapods, and fish. In: Handbook of Physiology, Sec 2, The nervous system (Brookhardt JM, Mountcastle VB, eds), pp 1179-1236. Bethesda, MD: American Physiological Society.

Guertin PA, Hounsgaard J (1998) Chemical and electrical stimulation induce rhythmic motor activity in an in vitro preparation of the spinal cord from adult turtles. Neurosci Lett 245:5-8.

Hishinuma M, Yamaguchi T (1990) Cervical interneurones oligosynaptically excited from primary afferents and rhythmically active during forelimb fictive locomotion in the cat. Neurosci Lett 111:287-291.

Ho S, O'Donovan MJ (1993) Regionalization and intersegmental coordination of rhythm-generating networks in the spinal cord of the chick embryo. J Neurosci 13: 1354-1371.

Hochman S, Jordan LM, MacDonald JF (1994) *N*-methyl-D-aspartate receptor-mediated voltage oscillations in neurons surrounding the central canal in slices of rat spinal cord. J Neurophysiol 72:565-577.

Hochman S, Jordan LM, Schmidt BJ (1994) TTX-resistant NMDA receptor-mediated voltage oscillations in mammalian lumbar motoneurons. J Neurophysiol 72:2559-2562.

Hochman S, Schmidt BJ (1998) Whole cell recordings of lumbar motoneurons during locomotor-like activity in the in vitro neonatal rat spinal cord. J Neurophysiol 79:743-752.

Hultborn H, Conway BA, Gossard JP, Brownstone R, Fedirchuk B, Schomburg ED,

Enriquez-Denton M, Perreault MC (1998) How do we approach the locomotor network in the mammalian spinal cord? Ann New York Acad Sci 860:70-82.

Iakhnitsa IA, Bulgakova NV, Piliavskii AL (1987) Kinematic analysis of the different types of locomotor movement in rats after deafferentation. Neirofiziologiia 19:520-525.

Iwahara T, Atsuta Y, Garcia-Rill E, Skinner RD (1991) Locomotion induced by spinal cord stimulation in the neonate rat *in vitro*. Somat Mot Res 8:281-287.

Jordan LM (1983) Factors determining motoneuron rhythmicity during fictive locomotion. Symposia of the Society for Experimental Biology. 37:423-444.

Jordan LM (1986) Initiation of locomotion from the mammalian brainstem In: Neurobiology of Vertebrate Locomotion. (Grillner S, Stein PSG, Stuart D, Forssberg H, Herman RM eds), pp 21-37. London: Macmillan.

Jordan LM (1991) Brainstem and spinal cord mechanisms for the initiation of locomotion. In: Neurobiological Basis of Human Locomotion (Shimamura M, Grillner S, Edgerton VR eds), pp3-20. Tokyo: Japan Scientific Societies Press.

Jordan LM (1998) Initiation of locomotion in mammals. Ann New York Acad Sci 860:83-93.

Jovanović K, Petrov T, Greer JJ, Stein RB (1996) Serotonergic modulation of the mudpuppy (*Necturus maculatus*) locomotor pattern *in vitro*. Exp Brain Res 111:57-67.

Jovanović K, Cheng J, Yoshida K, Stein RB (1998) Localization and modulation of rhythmogenic locomotor network in the mudpuppy (Necturus maculatus). Ann New York Acad Sci 860:480-482.

Kiehn O, Johnson BR, Raastad M (1996) Plateau potentials in mammalian spinal interneurons during transmitter-induced locomotor activity. Neuroscience 75:263-273.
Kjaerulff O, Kiehn O (1996) Distribution of networks generating and coordinating locomotor activity in the neonatal rat spinal cord *in vitro*: A lesion study. J Neurosci 16:5777-5794.

Kjaerulff O, Barajon I, Kiehn O (1994) Sulphorhodamine-labelled cells in the neonatal rat spinal cord following chemically induced locomotor activity *in vitro*. J Physiol (Lond) 478:265-273

Kremer E, Lev-Tov A (1997) Localization of spinal network associated with generation of hindlimb locomotion in the neonatal rat and organization of its transverse coupling system. J Neurophysiol 77:1155-1170.

Largo C, Tombaugh GC, Aitken PG, Herreras O, Somjen GG (1997) Heptanol but not

fluoroacetate prevents the propagation of spreading depression in rat hippocampal slices. J Neurophysiol 77:9-16.

Lefurge T, Goodal E, Horch K, Stensaas L, Schoenberg A (1991) Chronically implanted intrafascicular recording electrodes. Ann Biomed Eng 19:197-207.

Li Z. Hatton GI. (1996) Oscillatory bursting of phasically firing rat supraoptic neurones in low-Ca2+ medium: Na+ influx, cytosolic Ca2+ and gap junctions. J Physiol. 496:379-394.

MacLean JN, Hochman S, Magnuson DSK (1995) Lamina VII neurons are rhythmically active during locomotor-like activity in the neonatal rat spinal cord. Neurosci Lett 197:9-12.

MacLean JN, Schmidt BJ, Hochman S (1997) NMDA receptor activation triggers voltage oscillations, plateau potentials and bursting in neonatal rat lumbar motoneurons in vitro. Eur J Neurosci 9:2702-2711.

MacLean JN, Cowley KC, Schmidt BJ (1998) NMDA receptor-mediated oscillatory activity in the neonatal rat spinal cord is serotonin dependent. J Neurophysiol. 79:2804-2808.

McCrea DA, Pratt CA, Jordan LM (1980) Renshaw cell activity and recurrent effects on motoneurons during fictive locomotion. J Neurophysiol 44:475-488.

Magnuson DS, Trinder TC (1997) Locomotor rhythm evoked by ventrolateral funiculus stimulation in the neonatal rat spinal cord in vitro. J Neurophysiol 77:200-206.

Malagodi MS, Horch KW, Schoenberg AA (1989) An intrafascicular electrode for recording of action potentials in peripheral nerves. Ann Biomed Eng, 17:397-410.

Mann-Metzer P, Yarom Y (1999) Electrotonic coupling interacts with intrinsic properties to generate synchronized activity in cerebellar networks of inhibitory interneurons J. Neurosci. 19:3298-3306.

Miller RF, Dacheux R (1976) Dendritic and somatic spikes in mudpuppy amacrine cells: identification and TTX sensitivity. Brain Res 104:157-62.

Noga BR. Fortier PA. Kriellaars DJ. Dai X. Detillieux GR. Jordan LM (1995) Field potential mapping of neurons in the lumbar spinal cord activated following stimulation of the mesencephalic locomotor region. J Neurosci. 15:2203-2217.

O'Donovan M, Sernagor E, Sholomenko G, Ho S, Antal M, Yee W (1992) Development of spinal motor networks in the chick embryo. J Exp Zool 261:261-273.

Orlovsky GN, Feldman AG (1972) Classification of lumbosacral neurons by their

discharge pattern during evoked locomotion . Neurophysiology 4:311-317.
Pearson KG (1995) Proprioceptive regulation of locomotion. Curr Opin Neurobiol 5:786-791.

Pearson KG (1993) Common principles of motor control in vertebrates and invertebrates. Ann Rev Neurosci 16:265-297.

Perrins R (1995) The roles of central cholinergic and electrical synapses made by spinal motoneurones in Xenopus embryos. In: Alpha and Gamma Motor Systems (Taylor A, Gladden MH, Durbaba R eds), pp 48-50, New York: Academic.

Pratt CA, Jordan LM (1987) Ia inhibitory interneurons and Renshaw cells as contributors to the spinal mechanisms of fictive locomotion. J Neurophysiol 57:56-71.

Puskar Z, Antal M (1997) Localization of last-order premotor interneurons in the lumbar spinal cord of rats. J Comp Neurol 389:377-389.

Raastad M, Johnson BR, Kiehn O (1996) The number of postsynaptic currents necessary to produce locomotor-related cyclic information in neurons in the neonatal rat spinal cord. Neuron 17:729-738.

Roberts A, Soffe SR, Dale N (1986) Spinal interneurons and swimming in frog embryos. In: Neurobiology of Vertebrate Locomotion. (Grillner S, Stein PSG, Stuart D. Forssberg H, Herman RM eds), pp 279-306. London: Macmillan.

Roberts A, Tunstall MJ, Wolf E (1995) Properties of networks controlling locomotion and significance of voltage dependency of NMDA channels: simulation study of rhythmic generations sustained by positive feedback. J Neurophysiol. 73:485-495.

Rossignol S (1996) Neural control of stereotypic limb movements. In: Handbook of Physiology. Sec 12, Exercise: Regulation and Integration of Multiple Systems (Rowell LB, Shepherd JT, eds), pp 173-216. New York: Oxford.

Saltiel P, Tresch MC, Bizzi E (1998) Spinal cord modular organization and rhythm generation: an NMDA iontophoretic study in the frog. J Neurophysiol 80:2323-2339.

Schmidt BJ, Hochman S, MacLean JN (1998) NMDA receptor-mediated oscillatory properties: potential role in rhythm generation in the mammalian spinal cord. Ann New York Acad Sci 860:189-202.

Schmued L, Kyriakidis K, and Heimer L (1990) In vivo anterograde and retrograde axonal transport of the fluorescent rhodamine-dextran-amine, Fluoro-Ruby, within the CNS. Brain Res 526:127-134.

Shefchyk S, McCrea D, Kriellaars D, Fortier P, Jordan L (1990) Activity of interneurons

within the L4 spinal segment of the cat during brainstem-evoked fictive locomotion. Exp Brain Res 80:290-295.

Sigvardt KA, Grillner S, Wallen P, Van Dongen PA (1985) Activation of NMDA receptors elicits fictive locomotion and bistable membrane properties in the lamprey spinal cord. Brain Res 336:390-395.

Stein PSG, Victor JC, Field EC, Currie SN (1995) Bilateral control of hindlimb scratching in the spinal turtle: Contralateral spinal circuitry contributes to the normal ipsilateral motor pattern of fictive rostral scratching. J Neurosci 15: 4343-4355.

Stein PSG, McCullough ML, Currie SN (1998) Reconstruction of flexor/extensor alternation during fictive rostral scratching by two-site stimulation in the spinal turtle with a transverse spinal hemisection. J Neurosci 18:467-479.

Székely G (1965) Logical network for controlling limb movements in urodela. Acta Physiol Acad Sci Hung. 27:285-289.

Székely G, Czéh G, Vörös G (1969) The activity pattern of limb muscles in freely moving normal and deafferented newts. Exp Brain Res 9:53-62.

Terakado Y, Yamaguchi T (1990) Last-order interneurones controlling activity of elbow flexor motoneurones during forelimb fictive locomotion in the cat. Neurosci Lett 111:292-296.

Viala D, Viala G, Jordan L (1991) Interneurones of the lumbar cord related to spontaneous locomotor activity in the rabbit. I. Rhythmically active interneurones. Exp Brain Res 84:177-186.

Wallén P, Grillner S (1987) N-methyl-D-aspartate receptor-induced, inherent oscillatory activity in neurons active during fictive locomotion in the lamprey. J Neurosci 7:2745-2755.

Wallén P, Grillner S (1985) The effect of current passage on N-methyl-D-aspartate-induced, tetrodotoxin-resistant membrane potential oscillations in lamprey neurons active during locomotion. Neurosci Lett 56:87-93.

Werblin FS, Dowling JE(1969) Organization of the retina of the mudpuppy, Necturus maculosus. II. Intracellular recording. J Neurophysiol 32:339-355.

Wheatley M, Jovanović K, Stein RB, Lawson V (1994) The activity of interneurons during locomotion in the *in vitro* Necturus spinal cord. J Neurophysiol 71:2025-2032.

Wheatley M, Stein RB (1992) An *in vitro* preparation of the mudpuppy for simultaneous intracellular and electromyographic recording during locomotion. J Neurosci Methods 42:129-137.

Wheatley M, Edamura M, Stein RB (1992) A comparison of intact and *in vitro* locomotion in an adult amphibian. Exp Brain Res 88:609-614.

Witkin JW (1999) Synchronized neuronal networks: the GnRH system. Microscopy Res & Technique. 44:11-18.

Yamaguchi T (1992) Activity of cervical neurons during forelimb fictive locomotion in decerebrate cats. Japanese J Physiol 42:501-514.

Yoshida K, Horch K (1996) Closed-loop control of ankle position using muscle afferent feedback with functional neuromuscular stimulation. IEEE Trans Biomed Eng, 43:167-176.

CHAPTER 6

LOCALIZATION OF RHYTHMOGENIC NETWORK CONTROLLING BIPEDAL LOCOMOTION IN THE MUDPUPPY (*Necturus maculatus*)

INTRODUCTION

Rhythmic repetitive movements, including locomotion, can be generated within the vertebrate spinal cord in the absence of movement-related feedback by virtue of neuronal networks known as central pattern generators (CPGs; Delcomyn, 1980; Grillner, 1981; Rossignol, 1996). Localization and organization of CPG networks were extensively studied in different *in vitro* preparations (Bonnot and Didier 1998; Cazalets et al. 1995; Cheng et al., 1998; Cohen and Wallen 1980; Cowley and Schmidt 1997; Grillner et al. 1991; Ho and O'Donovan 1993; Kahn and Roberts 1982; Kramer and Lev-Tov, 1997). A growing body of evidence suggests that individual CPGs are distributed throughout the spinal cord with rostral segments possessing a greater rhythmogenic capacity then caudal ones (Deliagina et al. 1983; Gelfand et al. 1988; Ho and O'Donovan 1993; Mortin and Stein 1989; Kjaerulff and Kiehn 1996). Distributed organization of locomotor CPGs was first confirmed in experimental preparations isolated from swimming vertebrates like the lamprey (Cohen and Wallen 1980; Grillner et al., 1991), tadpole (Kahn and Roberts 1982) and dogfish (Grillner 1974). Additionally, data obtained from legged vertebrates like the embryonic chick (Ho and O'Donovan 1993), neonatal rat (Cowley and Schmidt 1997; Kjaerulff and Kiehn 1996) and neonatal mouse (Bonnot and Didier 1998; Tao and Droge 1992) provided further support to this notion. In contrast, results obtained in older neonates (Cazalets et al. 1995) suggest that the rhythm generating and pattern organizing locomotor network reside in the first couple of segments of the lumbar spinal cord.

A version of this chapter is in preparation for submission for publication. Jovanović K, Yoshida K, Stein RB (1999).

Although, this discrepancy may reflect the developmental stage or the specific age of the system under investigation, it may also be attributed to methodological and interspecies differences. Moreover, it emphasizes the need for further research in this area.

Wheatley and Stein (1992) developed an *in vitro* preparation isolated from an adult amphibian, mudpuppy (*Necturus maculatus*). Despite being an aquatic amphibian, the mudpuppy walks with an alternating quadrupedal gait characterized by robust and long lasting EMG activity. In many ways, this animal spans the evolutionary gap between primitive lamprey and complex, but more difficult to study mammals. Furthermore, the *in vitro* preparation stays functional for several days when superfused with cooled and oxygenated Ringer's solution. As it comprises the spinal cord and attached forelimb(s), the preparation allows for simultaneous observation of the actual behavior (i.e. rhythmic movement of the forelimbs) and recording of the motor output (EMG). Our previous study (Wheatley et al. 1994) revealed that a single segment of the mudpuppy spinal cord, spanning spinal roots C3 contains sufficient neuronal elements to produce a locomotor rhythm in the attached forelimb. A more recent study (Cheng et al.1998) demonstrated that the CPG for each limb can be further subdivided into distinct flexor and extensor centres exhibiting an inherent rhythmicity. Both studies neglected the transverse coupling system and interlimb coordination typical of locomotion occurring in a natural setting. Therefore, in the present study we examined the location of the rhythmogenic network underlying bipedal locomotion in the mudpuppy. By documenting the effects of acute transverse and midsagittal sectioning of the spinal cord on overall locomotor pattern, an attempt was also made to discern a possible role of descending and segmental mechanisms in interlimb coordination. Preliminary results were published in abstract form (Jovanović et al., 1997).

MATERIALS AND METHODS

In vitro preparation

The experiments were conducted on an *in vitro* brainstem-spinal cord preparations

isolated from adult mudpuppies (n=7; 20-30 cm long) as approved by the Animal Welfare Committee at the University of Alberta. Prior to dissection, the animals were anesthetized by immersion in a solution of 3-aminobenzoic acid ethyl ester (1-g/l; Sigma, St. Louis, MO). The skin and underlying muscles were removed and a dorsal laminectomy was performed from the first to the fifth vertebrae. The first five segments of the spinal cord with the attached forelimbs were then removed from the rest of the body and placed in a Sylgard lined petri dish superfused with cooled (15^0 C) and oxygenated Ringer solution of the following composition (mM): 115 NaCl; 2 $CaCl_2$; 2 KCl; 1.8 $MgCl_2$; 5 Hepes; pH 7.3; glucose, 1g/l. While in the petri dish, the paraspinal muscles were removed and bipolar Teflon insulated silver wires (75µm; Medwire, Leico Inc, New York, NY) were inserted bilaterally into the elbow flexor (*Brachialis*) and extensor (*Extensor ulnae*) muscles in both forelimbs for EMG recording during locomotion (Fig. 6-1 A). After a recovery period (~1h), the preparation was transferred to a Sylgard lined recording chamber and placed dorsal side up. The spinal cord and the forelimbs were then stabilised by pinning the vertebral column and the procoracoid cartilage to the base of the chamber. Throughout the course of experiments the preparation was superfused with a cooled (15-18^0 C) and oxygenated Ringers at a flow rate of 6-10 ml/min.

Locomotion was induced chemically by adding 30-120 µM N–methyl-D-aspartic acid (NMDA; RBI, Oakville, Canada) together with 10 µM D-Serine (D-Ser; Sigma, St. Louis, MO) to the superfusing solution. After well defined locomotion was established and a period of control locomotion was recorded, the spinal cord was bilaterally deafferented by cutting the dorsal roots. Subsequently, the spinal cord was subjected to a series of alternating rostro-caudal transections at different intersegmental levels (Fig. 6-1 B) in order to study localization and organization of the rhythmogenic network underlying bipedal locomotion. With the aid of a surgical dissection microscope (Leica, Germany) lesions were performed gently with a fine microsurgery knife and/or iridectomy scissors (FST, Vancouver, Canada). Following each transection a control period of 10 min. was allowed before recording in order to stabilise the lesion's effect. Usually, locomotion recovered in approximately 60 sec. Prior to midsagittal splitting of the cord special care

was taken to gently remove the *pia mater*, to avoid injuries to the remaining C3 segment, and to ensure that the spinal cord was sectioned along the midline. Changes in the overall locomotor pattern induced by sectioning of the spinal cord were observed as changes in the EMG pattern (rhythm, alternation, cycle duration, coupling) from the control pattern. EMG recordings were preamplified, high-pass filtered (10 Hz), rectified and low-pass filtered (300 Hz) prior to digitization and storage using a commercially available data acquisition system (Digidata 1200B and Axoscope, Axon Instruments). All channels of data were sampled at 50 Hz and later analysed using custom software written by Drs. Richard B. Stein and Ken Yoshida for the Matlab® (the MathWorks, Natick, MA, USA) technical computing environment.

Analysis

The effects of the spinal cord lesions on the locomotor pattern and the rhythm were quantified as changes in the cycle duration, relative phase of muscle activity and the magnitude of coupling between different muscle pairs. The digitized EMG recordings were normalized by their standard deviations, and the cross-covariance functions were calculated for each pairwise combination of the two flexor and two extensor muscles.. These generated a set of four auto correlograms and six cross correlograms for each animal and each treatment of the spinal cord. These auto and cross correlograms transform the data to estimate the statistical correlation coefficient (Pearson's "r") as a function of the relative delay between two continuous functions in time. While correlated rhythmic activity is transformed by this analysis into a periodic function of delay, uncorrelated activity is transformed into a flat function randomly oscillating around 0.

The period of the rhythmic EMG directly corresponds to the period of the correlogram, and was thus quantified by measuring the time between two consecutive minima of the correlogram. The relative phase of EMG activity of the muscles correlated in the correlogram was estimated by measuring the delay to the maximum value of the correlogram divided by the average cycle duration and multiplied by 360°. Finally, the maximum correlation was quantified as a measure of the magnitude of coupling between

Figure 6-1. Mudpuppy *in vitro* preparation

(A) The preparation consisted of first five segments of the mudpuppy spinal cord and both forelimbs attached by their brachial nerves. Rhythmic motor activity was recorded by means of EMG electrodes inserted bilaterally into elbow flexor and extensor muscles. **(B)** Following complete deafferentation, (not shown) the spinal cord was transected at different intersegmental levels indicated by dashed horizontal lines. The labels to the right of the lines are names used for different cuts in the text. Numbers in brackets indicate the order in which spinal cord transections were performed. The extent of the midsagittal cut, performed on an isolated C3 segment, is depicted by boxed dashed line. In the diagram, the C3 segment is represented as an area of the spinal cord between lines marking C3 and C4 cut. BS=brainstem cut.

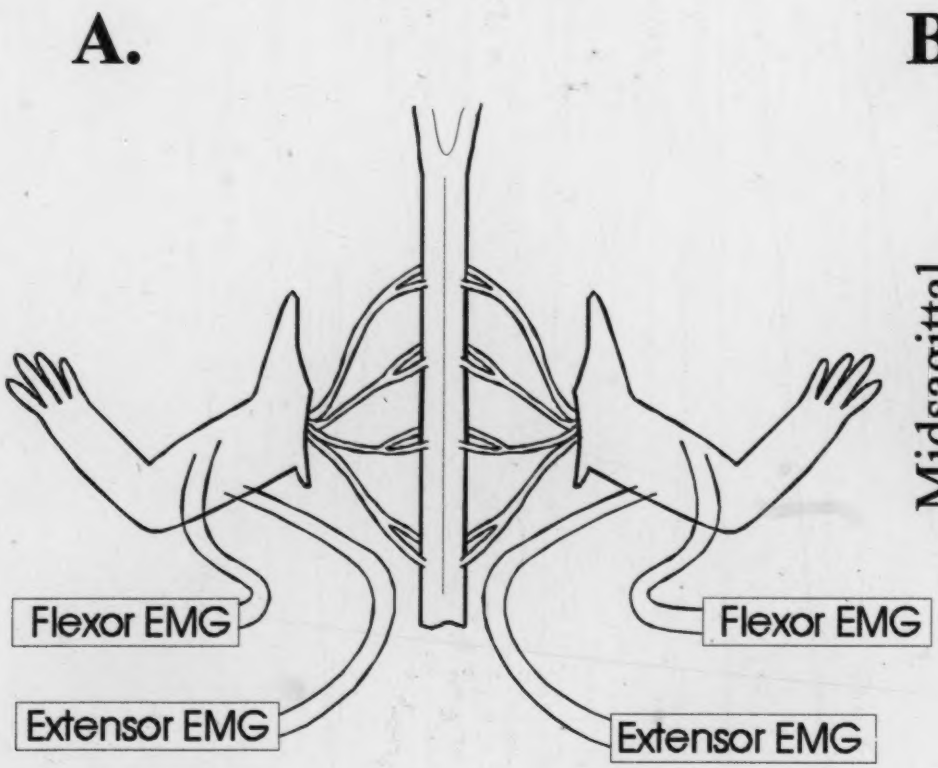
A.
Flexor EMG
Extensor EMG
Flexor EMG
Extensor EMG

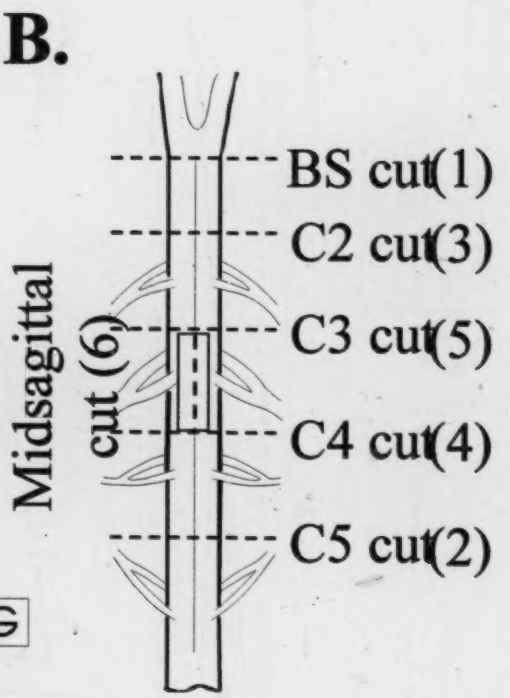
B.
Midsagittal cut (6)
BS cut(1)
C2 cut(3)
C3 cut(5)
C4 cut(4)
C5 cut(2)

different muscle pairs.

The relative phase relations between the activity of different muscles during locomotor sequence was visualized using phase plots (Fig.6-2). The right flexor activity was chosen arbitrarily as the base activity for these phase plots. The phase and amplitude of the peak correlation of the other three muscles were plotted relative to the that of the right flexor to generate points for the following relations: right extensor vs right flexor, left flexor vs right flexor and left extensor vs right flexor. Each phase relationship can be directly measured and derived in two ways as a combination of two other phase relationship. We averaged these three values to obtain a better estimate of the relative phase. For example, the phase of right extensor activity relative to right flexor activity was derived as follows:

$$\triangle RErf = \frac{1}{3} * (\triangle RErf + (\triangle RElf - \triangle RFlf) + (\triangle REle - \triangle RFle))$$

where

$\triangle RErf$ = phase of right extensor vs right flexor

$\triangle RElf$ = phase of right extensor vs left flexor

$\triangle RFlf$ = phase of right flexor vs left flexor

$\triangle REle$ = phase of right extensor vs left extensor

$\triangle RFle$ = phase of right flexor vs left extensor

Prior to this calculation, the phase values had to be adjusted to "flatten" the numerical discontinuity between 0° and 360°. This was done by adjusting the phase values by addition or subtraction of 360° to move this numerical discontinuity out of the range of the values in the average. The expression of the relative phase, as a function of the cycle duration, assumed that the cycle durations found from the set of 10 cross and intramuscle correlograms for each animal/treatment condition are the same. To validate this assumption, statistical analysis using a repeated measures ANOVA was performed for across all sets. This analysis showed that there were no significant differences ($p>0.05$) between any of the cycle durations within these sets.

Figure 6-2. Phase plots of pooled data obtained from seven animals

Phase plots illustrate phase relations between different muscles during recorded locomotor sequences in the mudpuppy. All relative phases were calculated with respect to the right flexor muscle. Each data point, representing one animal, contains information about both relative phase (i.e. phase angle) and coupling strength between different muscles (i.e. radius). With each treatment (e.g.transection of the spinal cord) the distribution of the data points changes. **(A)** The points are scattered in all four quadrants in the control pattern reflecting a great variability in the phase relation and coupling between different muscles. **(B)** Following bilateral deafferentation a major change appears to be an increase in the maximum value of cross-correlation. This is indicated by the increased radius of the data points resulting in an annulus rather than a cluster of points. **(C)** Following the brainstem cut data points still occupy all four quadrants indicating relatively well coordinated pattern and coupling between different muscles. **(D)** After a transection at C5 level data seem to occupy phases between 210 and 90 degrees (external angle). There seems to be little change in the maximum correlation values. Due to a reduction in the spinal cord length, i.e., sectioning at more rostral C2 level **(E)** and caudal C4 level **(F)**, data points are largely clustered in only two quadrants. This in turn indicates further reduction in the relative phase. **(G)** After C3-segment was isolated from rest of the cord all points, except one, are restricted to between 30 and 330 degrees (internal angle), indicating that all EMG activity is nearly synchronous. Stronger coupling among muscles is indicated by increase in radius. **(H)** After a midsagittal cut, the radius decreases indicating that the strength of cross correlation decreases. Activity seems to be synchronous. As two hemicords are completely detached from each other at this point, observed synchronicity is probably due to random occurrence of EMG bursts or/and noise i.e. 60Hz. For intersegmental levels at which the spinal cord was transected please see Figure 6-1.

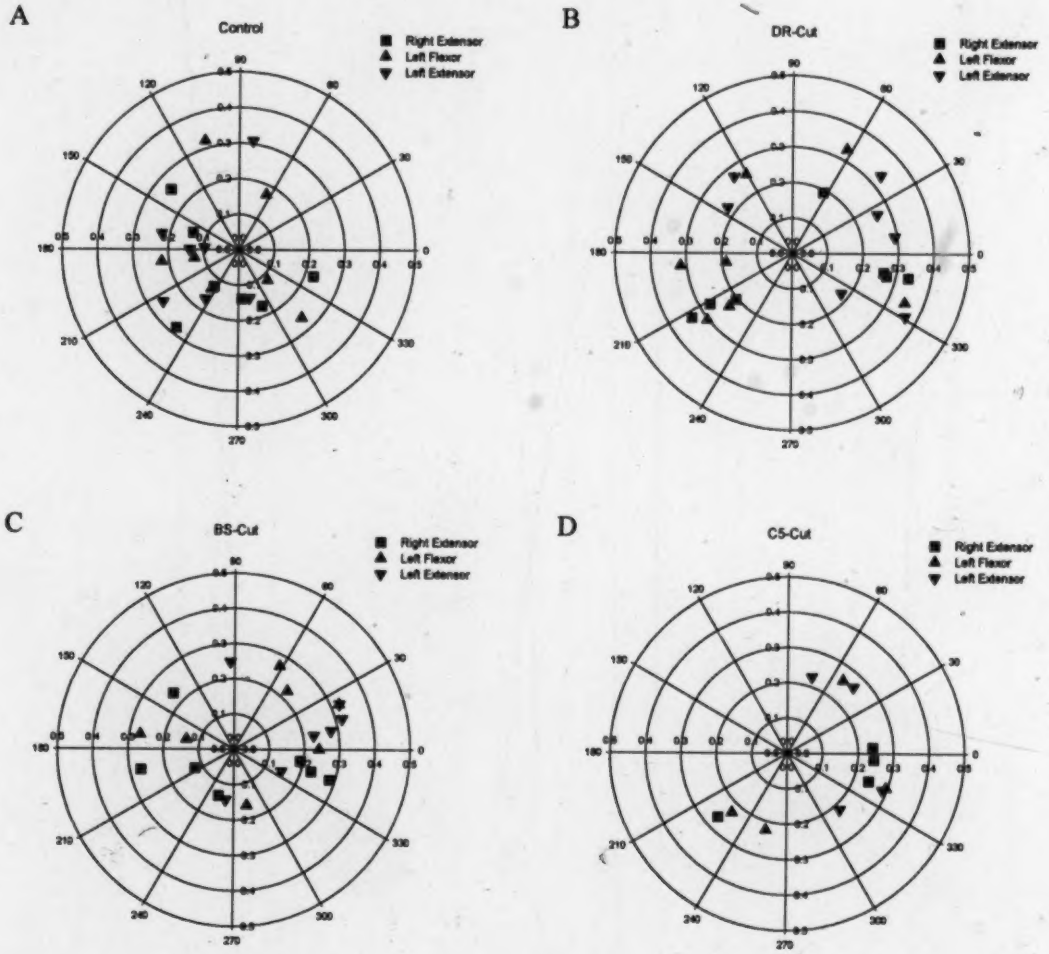
A
Control
Right Extensor
Left Flexor
Left Extensor
B
DR-Cut
Right Extensor
Left Flexor
Left Extensor
C
BS-Cut
Right Extensor
Left Flexor
Left Extensor
D
C5-Cut
Right Extensor
Left Flexor
Left Extensor

E

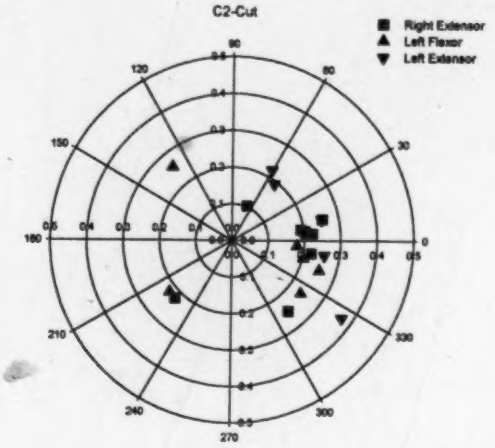
C2-Cut
Right Extensor
Left Flexor
Left Extensor

F

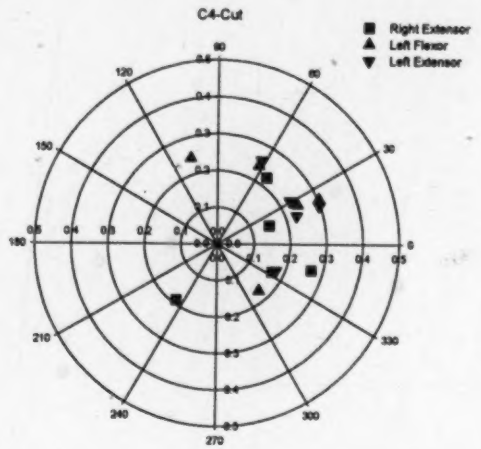
C4-Cut
Right Extensor
Left Flexor
Left Extensor

G

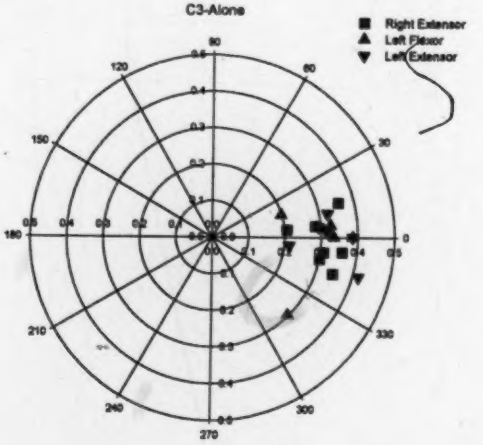
C3-Alone
Right Extensor
Left Flexor
Left Extensor

H

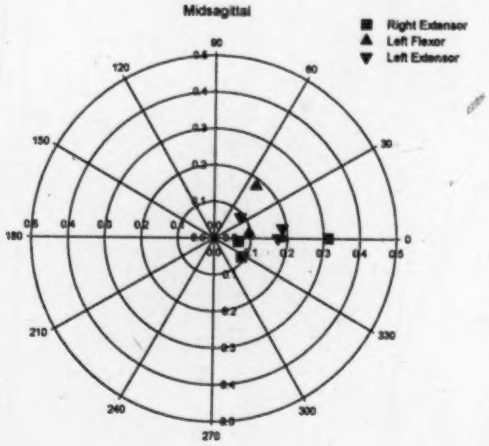
Midsagittal
Right Extensor
Left Flexor
Left Extensor

RESULTS

Similar to a single limb preparation, the 2-limb preparation was also capable of producing rhythmic locomotor activity when superfused with Ringers containing NMDA. However, some differences in the control pattern were observed between the two prior to sectioning the spinal cord. Unlike in the 1-limb preparation, neural correlates of the control pattern in 2-limb preparation exhibited great variability. This is reflected in the phase plots (Fig. 6-2) where the data points are scattered in all four quadrants in the control pattern reflecting a great variability in the phase relation and coupling between different muscles. Unexpectedly, the control pattern in the 2-limb preparation was often characterized by a slower rhythm, a less regular pattern and a weaker coupling between antagonistic muscles within a limb than one observed for the single limb preparation. This weaker coupling was indicated by low maximum values of the peaks in a cross-correlation (Fig. 6-3). In the example shown, the right flexor and right extensor (C) are essentially in phase (positive correlation at t=0), while the left flexor and the left extensor (D) showed the normal alternation (negative correlation at t=0). The opposite sides were weakly coupled with an intermediate phase (306 or 56 degrees). The difference in the magnitude of intralimb coupling (between antagonistic muscles in a single limb) was significantly different between the 1-limb and 2-limb preparations (Student's t-test, $p<0.05$). This perhaps indicates a powerful effect of the sensory input from the contralateral limb on the overall locomotor pattern since all other experimental conditions were similar to those utilized in 1-limb experiments.

Effects of bilateral dorsal rhizotomy

Under natural conditions, centrally generated locomotor programs are constantly modified by afferent signals in order to adjust the ongoing pattern to the changing environment (Pearson 1993; Rossignol 1996). In order to examine to what extent this basic pattern is modified by the sensory input during bipedal locomotion in the mudpuppy, we first bilaterally deafferented the spinal cord by cutting all dorsal roots (C2-C5). Subsequent visual inspection of movements of the limbs showed that they were cyclic and

Figure 6-3. Control locomotor pattern recorded from the forelimbs *in vitro*
During NMDA induced stepping-like forelimb movements EMG recordings were made from the right **(A)** and left **(B)** elbow flexor and extensor muscles. Control walking was characterized by a slow rhythm (i.e.. long cycle durations) and poor EMG alternation. Usually, various levels of co-contractions of antagonistic muscles were observed in one limb. Cross-correlation analysis revealed a weak muscle coupling within **(C, D)** and between **(E)** limbs. Cross-correlation analysis was performed on EMG recordings (300-600 s) obtained from right flexor and right extensor (RF-RE), left flexor and left extensor (LF-LE) and right flexor and left flexor (RF-LF).

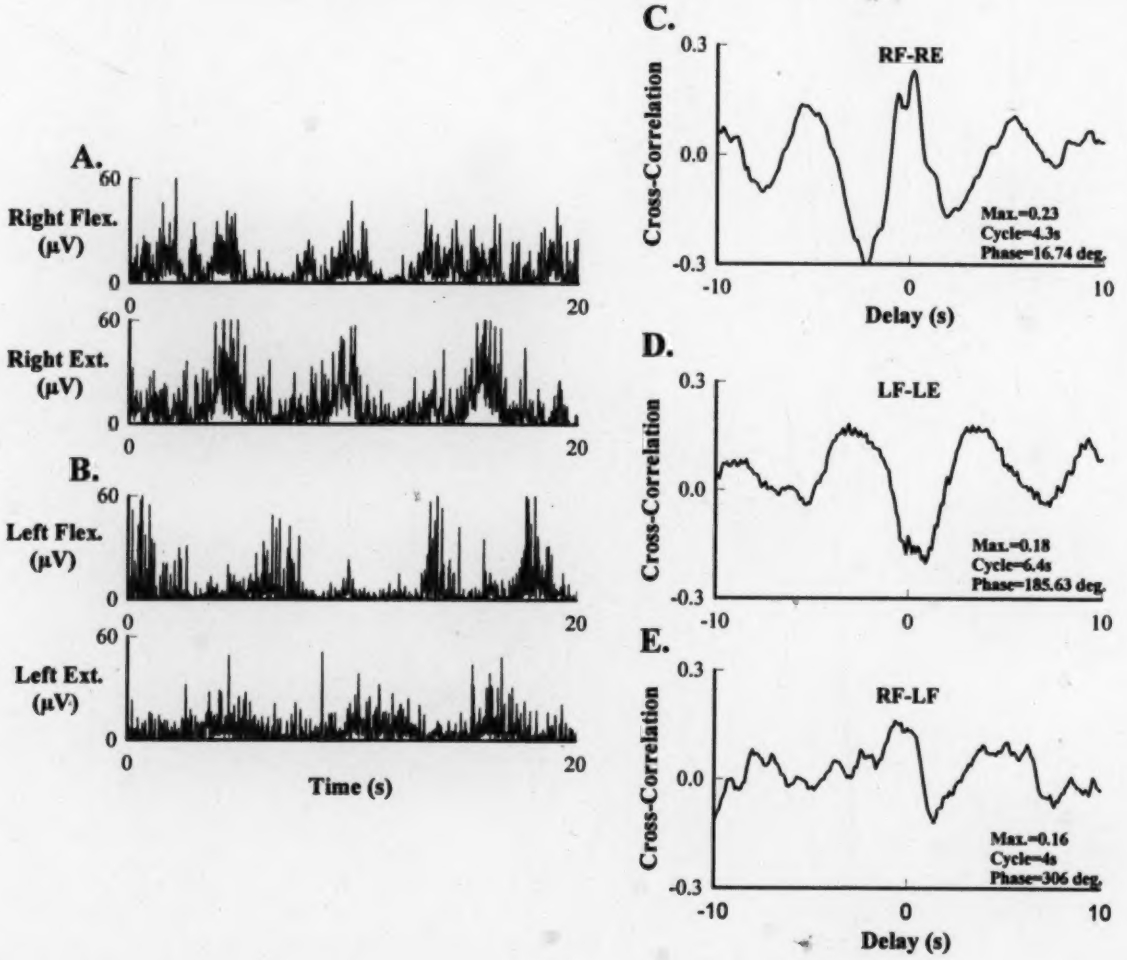
A.
Right Flex. (μV)
Right Ext. (μV)
B.
Left Flex. (μV)
Left Ext. (μV)
60
0
20
Time (s)
C.
RF-RE
Max.=0.23
Cycle=4.3s
Phase=16.74 deg.
D.
LF-LE
Max.=0.18
Cycle=6.4s
Phase=185.63 deg.
E.
RF-LF
Max.=0.16
Cycle=4s
Phase=306 deg.
Cross-Correlation
0.3
0.0
-0.3
-10
10
Delay (s)

Figure 6-4. Locomotor pattern following bilateral dorsal rhizotomy
After removal of sensory input to the spinal cord the overall locomotor pattern was largely improved. This was indicated by the appearance of the antagonistic raw EMG signals and cross-correlation analysis. The resulting locomotor pattern was characterized by improved alternation between antagonistic motoneuronal pools **(A, B)**, reduced cycle duration (i.e.. faster rhythm) and stronger coupling between ipsi- and contralateral muscle pairs. The latter was indicated by an increase in a maximum peak of cross-correlation (compare Max. values in Fig. 3C, D, E and Fig. 4C, D, E). Negative values for all three local minima near zero **(C, D, E)** indicate that the antagonistic motoneuronal pools within a limb and bilaterally, homologous motoneuronal pools were activated relatively out of phase.

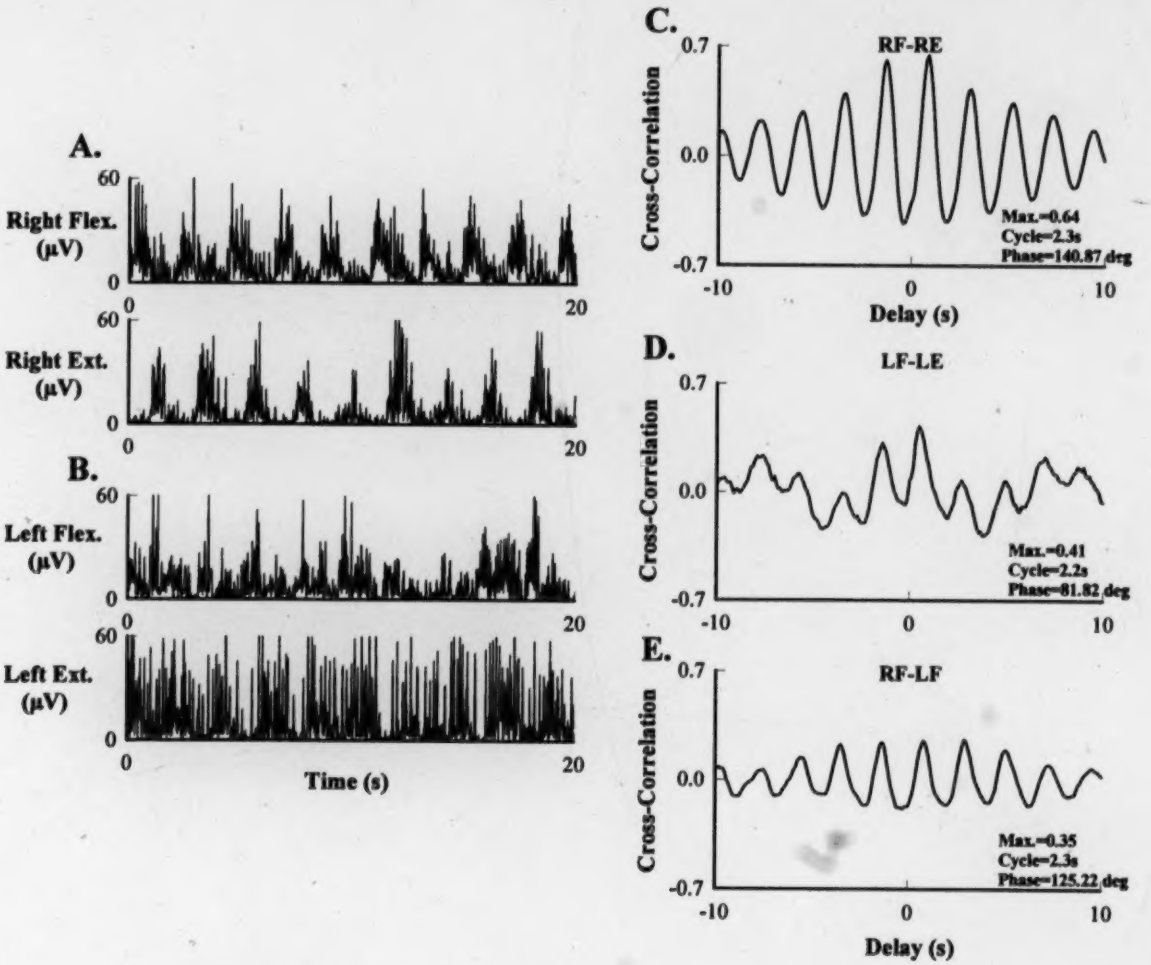
A.
Right Flex. (μV)
Right Ext. (μV)
B.
Left Flex. (μV)
Left Ext. (μV)
60
0
20
Time (s)
C.
RF-RE
Cross-Correlation
0.7
0.0
-0.7
-10
0
10
Max.=0.64
Cycle=2.3s
Phase=140.87 deg
Delay (s)
D.
LF-LE
Max.=0.41
Cycle=2.2s
Phase=81.82 deg
E.
RF-LF
Max.=0.35
Cycle=2.3s
Phase=125.22 deg

locomotor-like; they involved all joints (shoulder to foot) and were not simple flexion-extension of the elbow. As a consequence of deafferentation, the cycle duration decreased (the rhythm became faster; on average 30-40%) compared with the control and alternation between antagonistic muscles in each limb and between limbs was also improved. The latter was indicated by an increase in the relative flexor to extensor angle in each limb and phase angle between contralateral flexor muscles (compare Fig. 6-4 C, D, E with Fig. 6-3 C, D, E). In addition, both intralimb and interlimb coupling were strengthened as indicated by an increase in the positive peak of cross correlation. When data from all seven experiments were pooled together this was also reflected in the increased radius of the data points resulting in an annulus rather than a cluster of points (Fig. 6-2 B). Despite the observed trends, the results were not statistically significant A possible explanation for this could be found in the small number of preparations used in this study (n=7) and a great variability among the preparations.

Effects of rostro-caudal sectioning of the spinal cord

After cutting of dorsal roots the cord was exposed to a series of transections alternating in rostro-caudal position about the critical C3 segment. By sectioning the cord this way we gradually eliminated synaptic input from the brainstem and more rostral neurons to the rhythmogenic network. In addition, by eliminating segments more caudal to the C3 segment all remaining ascending connections originating caudal to the transection were also removed (Green and Soffe, 1998). The most prominent effect observed was a reduction in the flexor to extensor phase which gradually decreased from control (70-205 ^{0}) as the length of the spinal cord was more reduced (0-54 ^{0}) in the C3 segment alone. The phase change first took place between intralimb muscle pairs (some switched following the brainstem cut) while the change between contra lateral muscle pairs occurred only when the C3 was completely isolated. Phase plots show that the distribution of data points changes after each treatment (e.g.transection of the spinal cord; Fig. 6-2). The data points occupied all four quadrants until after a transection at C5 level (6-2 D). At this point, data occupied phases between 210 and 90 degrees (external angle).

Motor pattern produced in isolated C3 spinal segment

Our previous study showed that roughly one segment (C3; 10-15 mm) of the spinal cord is sufficient to generate locomotion in a single forelimb (Wheatley et al. 1994). To test whether this same length of the cord accounts for generating the basic locomotor rhythm as well as providing for interlimb coordination during bipedal locomotion, the segment spanning C3 spinal roots was isolated from both the caudal and the rostral segments. The locomotor rhythm, produced under this condition, was conveyed to the attached forelimbs via only one remaining (C3) pair of ventral roots. As a result, the locomotor rhythm remained intact when isolation was complete, confirming the previous results. However, a lack of alternation (decrease in the flexor to extensor phase angle) was observed between antagonistic muscles within a limb (Fig. 6-5 A, B,C D) as well as between homologous muscles in contralateral limbs (Fig. 6-5E). Figure 6-5 A and B show raw sample data from one experiment. Changes in the locomotor pattern were confirmed by calculating cross-correlation functions (compare Fig. 6-4 C, D, E with Fig. 6-5 C, D, E). While the peak at zero delay was negative following deafferentation, it became positive as the spinal cord was more reduced. In fact, the phase angle between the flexor and extensor EMGs changed gradually from being out of phase (170-70°) after deafferentation to being in-phase (closer to 0°) as the length of the spinal cord decreased. This is also obvious from the phase plot (Fig. 6-2 G) where all points except one are restricted to between 30 and 330 degrees (internal angle) indicating that all activity is nearly synchronous. The rhythmicity of the pattern was also less pronounced then that seen following deafferentation, as can be seen from the shape of the cross-correlation functions at increasing values of delay (Fig. 6-5 C, E). On the other hand, coupling between ipsilateral and contralateral motoneuronal pools increased ($p<0.05$) as the overall EMG pattern became more synchronous (compare Fig. 6-5 C, D, E with Fig. 6-3 C, D, E). Following a washout in Ringer solution, the rhythmic EMG activity could be induced again in the C3 segment. However, the rhythm remained slow and the EMG activity remained largely synchronous (not shown).

Figure 6-5. Locomotor pattern generated in isolated C3 spinal segment
Following removal of the spinal cord segments more rostral and caudal to C3 segment, the rhythm became slower (cycle duration increased) while the EMG pattern became more synchronous **(A, B)**. Although, the rhythm persisted in the isolated segment, cross-correlation analysis confirmed that EMG bursts were occurring largely in phase **(C, D, E)**. The coupling between different motoneuronal pools remained strong as indicated by peaks of the cross-correlation.

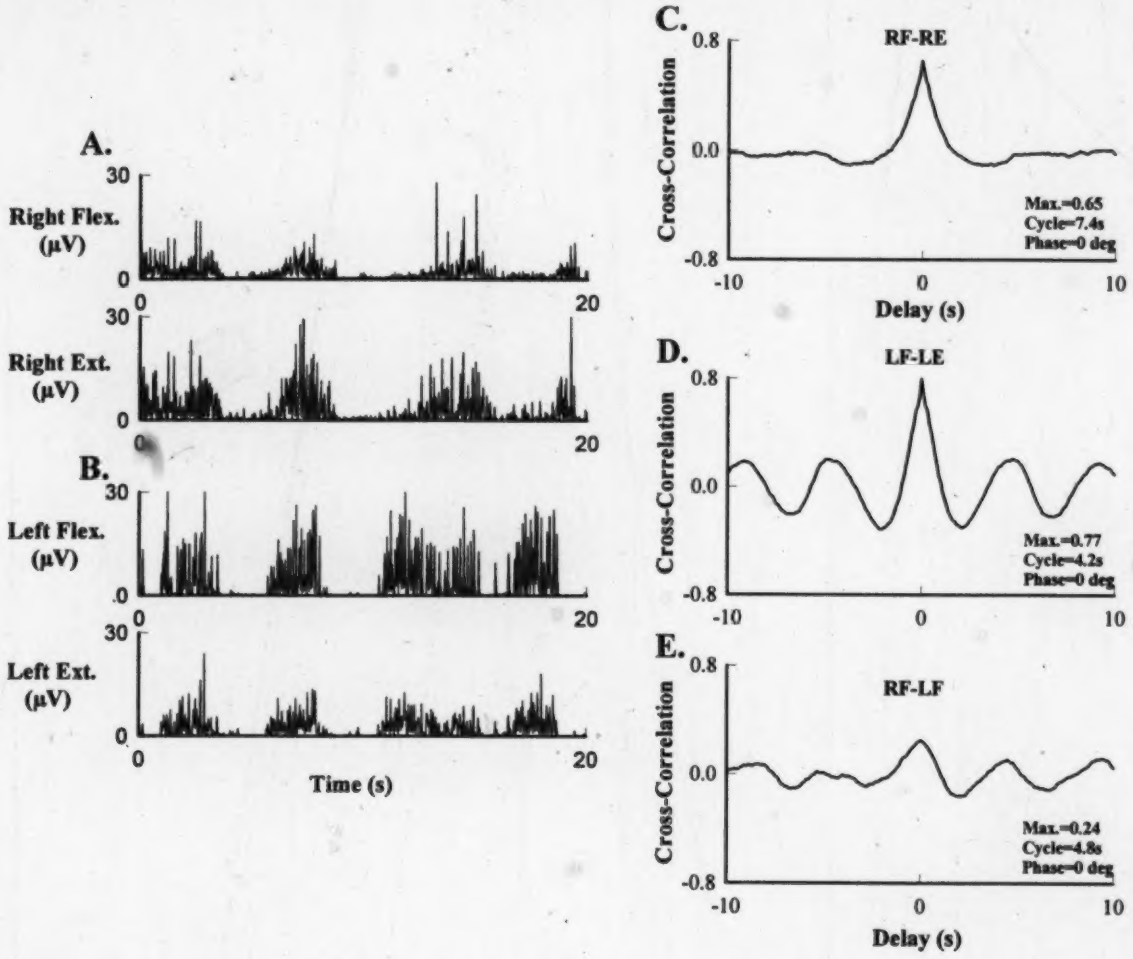
A.
Right Flex. (μV)
Right Ext. (μV)
B.
Left Flex. (μV)
Left Ext. (μV)
30
0
20
Time (s)
C.
RF-RE
D.
LF-LE
E.
RF-LF
Cross-Correlation
0.8
0.0
-0.8
-10
10
Delay (s)
Max.=0.65
Cycle=7.4s
Phase=0 deg
Max.=0.77
Cycle=4.2s
Phase=0 deg
Max.=0.24
Cycle=4.8s
Phase=0 deg

Midsagittal section

After the remaining C3 spinal cord segment was split midsagittally each half-segment was capable of rhythmic bursting (Fig. 6-6). This indicated that each half of a spinal cord segment contained sufficient neuronal substrate for generating motor rhythm. However, it took a much longer time for the rhythm to recover and the overall EMG pattern differed considerably from the control (Fig. 6-6). Generally, EMG bursts occurred in either flexor or extensor muscles in contra lateral limbs but not in both ipsilateral muscles simultaneously (Fig. 6-6 A, B). In addition, the movements of the limbs, generated by isolated spinal cord hemisegments, were observed to be less smooth and displayed limited range of motion. Although rhythmicity persisted in each limb it was weaker than in less reduced preparations, as can be seen from the shape of the cross-correlation functions at increasing values of delay (Fig. 6-6 C, D). Furthermore, cross-correlation analysis revealed that coupling between ipsilateral motoneuronal pools decreased (Fig. 6-6 C, D) while coupling between contralateral motoneuronal pools was completely abolished (Fig. 6-6 E). This is also shown in the phase plot (Fig. 6-2 H) where decrease in cross-correlation is indicated by decrease in the radius.

DISCUSSION

The results have revealed that the network underlying generation and interlimb coordination in forelimb walking resides in the brachial spinal cord of the mudpuppy. Roughly one spinal cord segment (spanning spinal roots C3) is sufficient for generating the basic locomotor rhythm in the attached forelimbs. The results also show that the spinal cord deprived of its supraspinal and peripheral input can produce coordinated rhythmic alternation in both forelimbs, which confirms and extends previous findings from this laboratory (Cheng et al. 1998; Jovanović et al. 1999; Wheatley and Stein 1992; Wheatley et al, 1994).

Figure 6-6. Rhythm in midsagittally hemisected C3 spinal cord segment
After remaining C3 segment was split along the midline, coupling between contralateral motoneuronal pools was abolished **(E)** while a weak rhythmicity remained independently in each limb **(A, B)**. Typically, sequences of rhythmic EMG bursting occurred in either the flexors or extensors but not in both muscles at the same time. This activity coincided with an irregular activity of a much higher frequency in the opposite muscle. Although still present, the rhythmicity was reduced as confirmed by the shape of the cross-correlation function at increasing values of delay **(C, D)**.

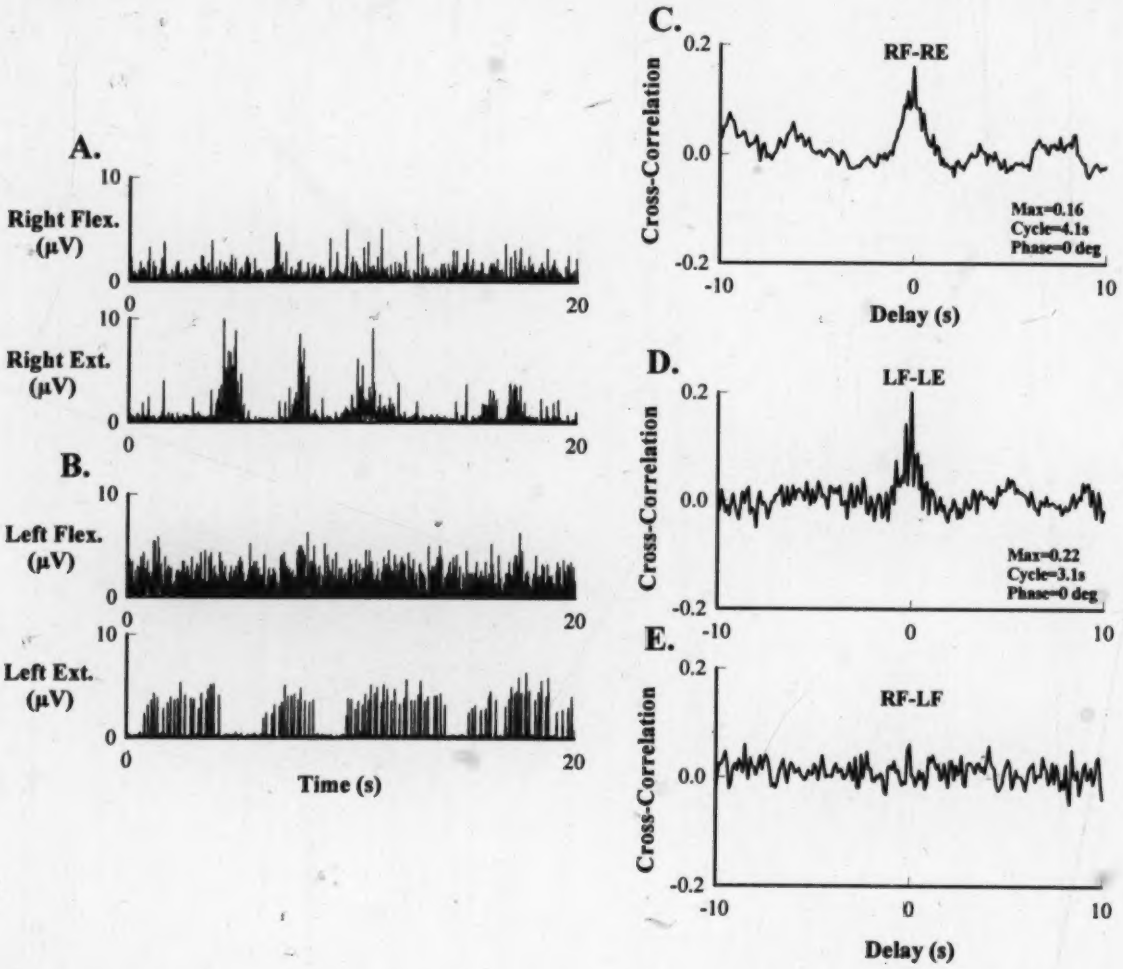
A.
Right Flex. (μV)
Right Ext. (μV)
B.
Left Flex. (μV)
Left Ext. (μV)
10
0
20
Time (s)
C.
RF-RE
Max=0.16
Cycle=4.1s
Phase=0 deg
D.
LF-LE
Max=0.22
Cycle=3.1s
Phase=0 deg
E.
RF-LF
Cross-Correlation
0.2
0.0
-0.2
-10
Delay (s)

Characteristics of control locomotor pattern

Unlike in 1-limb preparations, control patterns recorded in 2-limb preparations were characterized by a large overlap between antagonistic EMGs in one limb, while corresponding contralateral muscles displayed more or less an alternating pattern. Such a pattern of muscle activation proved fairly consistent in different *in vitro* preparations and from one experiment to another. The fact that recordings were made from two closely positioned muscles of small dimensions may suggest that the activity pattern of individual muscles was somewhat influenced by the position of electrodes within the muscle and/or the activity of a neighbouring antagonist. To avoid this possibility EMG wires were repositioned a few times before the actual onset of a recording session. In addition, recordings altered by cross-talk, as confirmed by cross-correlation analysis, were not taken into account during data analysis. Due to the consistency of the observed pattern throughout the sample and the fact that the pattern in the contralateral limb showed the EMG alternation makes us suggest that this is an unlikely explanation. Furthermore, extensive co-contractions of antagonistic muscle pairs were observed during walking in two species *(Triturus cristatus* and *Ambystoma mexicanum)* closely related to the *Necturus.* This was particularly evident in the arm and forearm muscles (Székely and Czéh 1976). Thus, we favour the idea that various degrees of co-contraction of the antagonistic muscle pairs may be normal and regarded as an important factor in the stabilization of the joints and in grading the limb movement during locomotion (Székely and Czéh 1976).

Effects of bilateral deafferentation

It is well established that rhythmic locomotor activity can be generated in the absence of sensory input. However, the extent to which locomotion is affected by sensory deprivation varies among different species. In some, due to its profound effect on locomotor pattern, sensory input was even proposed to be an integral part of the CPG network (Pearson and Wolf 1987; Wolf and Pearson 1987; see also Berkowitz and Laurent, 1996). In contrast, amphibians (e.g. frogs and salamanders) can readily swim,

jump and walk following sensory deprivation of one or more limbs (for review see Székely and Czéh 1976). The present study provides further evidence that well coordinated rhythmic forelimb locomotion can occur after sensory input was removed. The ensuing locomotor pattern appeared to be more rhythmic and the relative phase and coupling between different muscles were improved with respect to the control (compare Fig.6- 4 with Fig. 6-3). These findings are contrary to a prevailing notion that deafferentation renders the locomotor rhythm slower and the pattern more variable (Grillner and Zangger 1979; Gelfand et al, 1988; Stein 1989; for review see Pearson 1993). In conjunction with this study, our recent study (Cheng et al. 1998) demonstrated that cutting dorsal roots C3, C4 and C5 reduced the cycle duration (increased locomotor frequency) in the mudpuppy. Conversely, C2 dorsal root resulted in a longer cycle duration. Finally, after all the dorsal roots were cut the walking-like rhythm became faster in the majority of preparations. Presently, we do not have a simple explanation for these findings. One possible explanation could be that when deprived from realistic sensory cues, CPG(s) subserving forelimb locomotion may oscillate at a frequency higher than in intact animals. An alternative explanation could perhaps be found in different environmental demands imposed on underwater and terrestrial walking, different role of gravitational force being just one of them. Even though, a major role of sensory input is to adjust an ongoing locomotion to a changing environment, underlying strategies may differ between animals fully adjusted to terrestrial walking and the mudpuppy. For instance, a strong stimulus, that would speed up a terrestrial quadruped's locomotion, from walking to running, elicits escape swimming in *Necturus* with the inhibition of the walking CPG as it pulls its legs up tonically close to the body. However, more experiments aimed at elucidating the role of sensory input in mudpuppy locomotion are needed before a final conclusion on its role can be drawn.

Effects of rostro-caudal sectioning of the spinal cord (C3 isolated)

Removal of the spinal cord segments rostral and caudal to the critical segment C3 led to a gradual reduction in relative phase between the antagonistic muscles within a limb and

homologous muscles in contralateral limbs. Finally, when the C3 segment was completely isolated the limbs were moving largely in phase and the pattern was characterized by EMG synchronization between contralateral limbs and within each limb. Numerous pharmacological studies confirm that inhibitory pathways play a key role in mediating alternation between contralateral limbs (Kudo et al. 1991; Cowley and Schmidt 1995; Noga et al.1993) and antiphase coupling between intralimb flexor and extensor muscles (Cowley an Schmidt 1995; Jovanović et al. 1999; Noga et al.1993; Pratt and Jordan 1987). Segmentally distributed commissural interneurons are implicated in mediating reciprocal inhibition at the spinal level (Buchanan 1996; Buchanan and Cohen 1982; Dale et al. 1990; Grillner et al, 1991; Harper and Roberts 1993; Kjaerulff and Kiehn 1997) but direct inhibitory projections originating in the brainstem, are also documented (Wannier et al. 1995; Holstege and Bongers 1991). Thus, removal of either the brainstem and/or different portions of segmental inhibition could have resulted in substantial synchronization between monitored motoneuronal pools in our experiments. Two lines of evidence may lend support to this notion. First, an anatomical study of the smooth newt (*Triturus cristatus*), a species closely related to the *Necturus*, has shown that most inhibitory commissural interneurons reside in rostral parts of the spinal cord (Harper and Roberts 1993). Second, combined anatomical and pharmacological study (Jovanović et al. 1999) confirmed that both GABAergic and glycinergic neurons are distributed throughout the mudpuppy brachial spinal cord. Due to rostro-caudal sectioning of the spinal cord these inhibitory neurons were probably removed, thus eliminating a possible source of coordinated alternation within each limb and between limbs. This, in turn, would increase the magnitude of EMG coupling within each limb and between limbs as observed after the C3 segment was completely isolated. The results also indicate that upon removal of predominant inhibition, excitatory connections existing in parallel, within and between hemicords, became more dominant (Cowley and Schmidt 1995; Hagevik and McClellan 1994; Jovanović et al. 1999; Kremer and Lev-Tov 1997; for review see McClellan 1996).

Rhythmicity in C3 spinal hemisegments

Following midline splitting of the remaining C3 segment, an irregular rhythm was detected in the hemicords. Direct addition of more NMDA to the bath elicited EMG bursts in quiescent muscles and improved the rhythm. Similar experiments involving different species, preparations of different ages, developmental stages and length of the hemisected spinal cord have produced conflicting results. In the spinal cord of *Xenopus* embryos the locomotor rhythm can be observed after complete midline sectioning (Arshavsky et al. 1993; Kahn and Roberts 1982; Soffe 1989). A much slower, NMDA-induced (Kudo and Yamada 1987) or spontaneous rhythm, (Tao and Droge 1992) was observed after hemisecting the hind limb-spinal cord explants in neonatal rats and mice, respectively. In contrast, a regular rhythm in the lamprey was abolished following either midsagittal splitting of the spinal cord or photo ablation of commissural interneurons (Buchanan 1996). Although not shown here, the rhythm was much improved upon increasing bath concentration of NMDA in our experiments after sectioning. Thus, insufficient excitation may be implicated as a possible reason for a lack of maintained activation in participating motoneuronal pools. Additional NMDA following midsagittal sectioning was perhaps able to compensate for the loss of this excitation and thereby re-establish bursting in silent muscles. Disappearance of the rhythm, after the cord was split along the midline, would implicate either contralaterally projecting motoneurones (Székely and Czéh, 1976) or centrally positioned excitatory interneurons (i.e. around central canal Stein et al. 1995) in mediating underlying excitation. Neurons with contralaterally projecting processes were revealed in ventromedial grey matter in the mudpuppy spinal cord by using the intracellular fluorescent dye TMR-dextrane (Jovanović et al. unpublished). However, their role in neuronal circuitry underlying the mudpuppy locomotion remains to be determined.

Statistical significance

We have used cross-correlation analysis to assess functional relationship between antagonistic motoneuronal pools in the forelimbs of the mudpuppy. Although generally

considered to be a more objective analysis method, cross-correlation exhibits an inherent sensitivity to irregularities that may occur in the pattern. For example, pausing of a limb in the middle of the protraction phase or its hyperextension at the end of retraction may result in atypical durations of the step cycle which, in turn may offset the result of the cross-correlation (affecting both cycle duration and phase angle). This may explain the large variability we observed in the control pattern. Furthermore, due to a great variability in the control, changes elicited by different lesions of the cord (and deafferentation) were not statistically significant in spite of observed trends. Great variability about frequently occurring patterns of interlimb coordination (as reflected by a large number of interlimb phase intervals) was previously found in the cat (English 1978; Forssberg 1980). In these studies a single step analysis was used as opposed to the average step analysis that was used in our study. In the former all observed steps were screened to assure that all discontinuous stepping sequences were excluded from subsequent calculations. The resulting patterns were established on the basis of frequency of occurrence. This variability, interpreted as a reflection of the facultative capabilities of the neuronal mechanisms controlling stepping in an intact cat, would allow an animal to shift rapidly between different patterns of interlimb coordination (English 1978). Such capabilities imply a flexibility essential in meeting changing postural demands placed on the locomotor apparatus. Loose coupling between different muscles (supposedly different CPGs) and a great variability in the control walking pattern (lack of preferred pattern) may merely be a reflection of mudpuppy's ability to shift not only between different patterns of interlimb coordination during walking but also to switch between walking and swimming. An occurrence of preferred stepping patterns in the cat might also be a result of adaptation processes that fully terrestrial quadrupeds went through during evolution. Alternatively, lack of statistical significance may be due to the small number of preparations used in this study. Therefore, to further clarify this intriguing issue more experiments are needed.

Concluding remarks

This study provides conclusive evidence for centrally generated interlimb coordination in

the mudpuppy. In addition, it provides evidence that the walking apparatus is capable of generating a variety of locomotor patterns. Switching between different walking patterns and/or walking and swimming appears to be possible due to a loose coupling between different CPG networks. The study also provides information concerning the location of some of the components of the rhythm and pattern generating neuronal network in the mudpuppy. Roughly one segment of the spinal cord appears to be able to control synchronous movement of a pair of forelimbs. The same segment, in the presence of more rostral (descending) inputs, can switch to an alternating (intra- and interlimb) pattern. The cellular mechanisms underlying this interaction are still completely unknown. The advantages offered by the mudpuppy preparation may be helpful in future studies on the linkage between walking and swimming pattern generators.

REFERENCES

Arshavsky YI, Orlovsky GN, Panchin V, Roberts A, Soffe SR (1993) Neuronal control of swimming locomotion: analysis of the pteropod mollusc *Clione* and embryos of the amphibian *Xenopus*. TINS 16 (6): 227-233

Berkowitz A, Laurent G (1996) Central generation of grooming motor pattern and interlimb coordination in locusts. J Neurosci 15:8079-8091

Bonnot A, Didier M (1998) Hemisegmental localization of rhythmic networks in the lumbosacral spinal cord of neonate mouse. Brain Res 793:135-148

Buchanan JT (1996) Lamprey spinal interneurons and their role in swimming activity. Brain Behav Evol 48:287-296

Buchanan JT, Cohen AH (1982) Activities of identified interneurons, motoneurons, and muscle fibers during fictive swimming in the lamprey and effects of reticulospinal and dorsal cell stimulation. J Neurophysiol 47:948-960

Cazalets JR, Borde M Clarac F (1995) Localization and organization of the central pattern generator for hindlimb locomotion in newborn rat. J Neurosci 15:4943-4951

Cheng J, Stein RB, Jovanović K, Yoshida K, Bennett DJ, Han Y (1998) Identification, localization, and modulation of neural networks for walking in the mudpuppy (*Necturus maculatus*) spinal cord. J Neurosci 18:4295-4304

Cohen AH, Wallen P (1980) The neural correlate of locomotion in fish. "Fictive swimming" induced
in an in vitro preparation of the lamprey spinal cord. Exp Brain Res 41:11-18

Cowley KC, Schmidt BJ (1995) Effects of inhibitory amino acids antagonists on reciprocal inhibitory interactions during rhythmic motor activity in the in vitro neonatal rat spinal cord. J Neurophysiol 74:1109-1117

Cowley KC, Schmidt BJ (1997) Regional distribution of locomotor pattern-generating network in the neonatal rat spinal cord. J Neurophysiol 77:247-259

Dale N, Roberts A, Soffe, SR (1990) The anatomy, development and role of glycinergic neurons in the *Xenopus* embryo spinal cord. In: Ottersen OP, Storm-Mathisen J (eds) In: Glycine neurotransmission, John Wiley & Sons, pp. 329-353

Delcomyn F (1980) Neural basis of rhythmic behavior in animals. Science 210:492-498

Deliagina TG, Orlovsky GN, Pavlova Ga (1983) The capacity for generation of rhythmic

oscillation is distributed in the lumbosacral

English AW (1978) Interlimb coordination during stepping in the cat: an electromyographic analysis. J Neurophysiol 42:229-243spinal cord of the cat. Exp Brain Res 53:81-90

Forssberg H, Grillner S, Halbertsma J, Rossignol S (1980) The locomotion of the low spinal cat. II. Interlimb coordination. Acta Physiol Scand 108:283-295

Gelfand IM, Orlovsky GN, Shik M (1988) Locomotion and scratching in tetrapods. In: Cohen AH, Rossignol S, Grillner S (eds) Neural control of rhythmic movements in vertebrates. Wiley & Sons, New York, pp 167-199

Green CS, Soffe SR (1998) Roles of ascending inhibition during two rhythmic motor patterns in Xenopus tadpoles. J Neurophysiol 79:2316-2328

Grillner S (1974) On the generation of locomotion in the spinal dogfish. Exp Brain Res 20:459-470

Grillner S (1981) Control of locomotion in bipeds, tetrapods, and fish. In: Brooks VB (ed) Handbook of physiology. American Physiological Society, Bethesda, MD, pp 1179-1236

Grillner S, Zangger P (1979) On the central generation of locomotion in the low spinal cat Exp Brain Res 34:241-261

Grillner S, Wallen P, Brodin L (1991) Neural network generating locomotor behavior in lamprey: circuitry, transmitters, membrane properties and simulation. Ann Rev Neurosci 14: 169-199

Hagevik A, McClellan A (1994) Coupling of spinal locomotor networks in larval lamprey revealed by receptor blockers for inhibitory amino acids: neurophysiology and computer modeling. J Neurophysiol 4:1810-1829

Harper CE, Roberts A (1993) Spinal cord neuron classes in embryos of the smooth newt Triturus vulgaris: a horseradish peroxidase and immunocytochemical study. Phyl Trans R Soc Lond B 340:141-160

Ho S, O'Donovan MJ (1993) Regionalization and intersegmental coordination of rhythm-generating
networks in the spinal cord of the chick embryo. J Neurosci 13:1354-1371

Holstege JC, Bongers CMH (1991) A glycinergic projection from the ventromedial lower brainstem to spinal motoneurons. An ultrastructural double labeling study in rat. Brain Res 566:308-315

Jovanović K, Yoshida K, Cheng J, Stein RB (1997) Localization of rhythmogenic network controlling bipedal locomotion in mudpuppy (*Necturus maculatus*). Soc Neurosci Abstr 1:206

Jovanović K, Petrov T, Stein RB (1999) Effects of inhibitory neurotransmitters on the mudpuppy (*Necturus maculatus*) locomotor pattern *in vitro*. Exp Brain Res (in press)

Kahn JA, Roberts A (1982) Experiments on the central pattern generator for swimming in amphibian embryos. Phil Trans R Soc Lond B 296:229-243

Kjaerulff O, Kiehn O (1996) Distribution of networks generating and coordinating locomotor activity in the neonatal rat spinal cord in vitro: a lesion study. J Neurosci 16:5777-5794

Kjaerulff O, Kiehn O (1997) Crossed rhythmic synaptic input to motoneurons during selective activation of the contralateral spinal locomotor network. J Neurosci 17:9433-9447

Kremer E, Lev-Tov A (1997) Localization of the spinal network associated with generation of hindlimb locomotion in the neonatal rat and organization of its transverse coupling system. J Neurophysiol. 77:1155-1170

Kudo N. Yamada T (1987) N-methyl-D,L-aspartate-induced locomotor activity in a spinal cord-hindlimb muscle preparation of the newborn rat studied in vitro. Neurosci Letts 75:43-48

Kudo N, Ozaki S, Yamada T (1991) Ontogeny of rhythmic activity in the spinal cord of the rat. In: Shimamura M, Grillner S, Edgerton VR (eds) Neurobiological basis of human locomotion. Tokyo, Japan Scientific Society, pp 127-136

McClellan AD (1996) Organization of spinal locomotor networks: contributions from model systems. Comments Theor Biol 4:63-91

Mortin LI, Stein PSG (1989) Spinal cord segments containing key elements of the central pattern generators for three forms of scratch reflex in the turtle. J Neurosci 9:2285-2296

Noga BR, Cowley KC, Huang A, Jordan LM, Schmidt BJ (1993) Effects of inhibitory amino acid antagonists on locomotor rhythm in the decerebrate cat. Society for Neuroscience Abstracts 19:541

Pearson KG, Wolf H (1987) Comparison of motor patterns in the intact and deafferented flight system of the locust. I. Electromyographic analysis. J Comp Physiol A 160:259-268

Pearson KG (1993) Common principles of motor control in vertebrates and invertebrates. Ann Rev Neurosci 16:265 297

Pratt CA, Jordan LM (1987) Ia inhibitory interneurons and Renshaw cells as a contributors to the spinal mechanisms of fictive locomotion. J Neurophysiol 57:56-71

Rossignol S (1996) Neural control of stereotypic limb movements. In: Brooks VB (ed) Handbook of physiology. American Physiological Society, Bethesda, MD, pp 174-216

Stein PSG (1989) Spinal cord circuits for motor pattern selection in the turtle. Ann NY Acad Sci 563:1-10

Stein PSG, Victor JC, Field EC, Currie SN (1995) Bilateral control of hindlimb scratching in the spinal turtle: contralateral spinal circuitry contributes to the normal ipsilateral motor pattern of fictive rostral scratching. J Neurosci 15:4343-4355

Szekely G (1989) Ontogeny and morphology of neuronal structures controlling tetrapod locomotion. In: Wake DB, Roth G (eds) Complex organismal functions: integration and evolution in vertebrates. Wiley & Sons, pp 117-131

Szekely G, Czeh G (1976) Organization of locomotion. In: Llinas R, Precht W (eds) Frog neurobiology. Springer, Berlin, Heilderberg, New York, pp 765-792

Tao Y, Droge MH (1992) Comparison of spontaneous motor pattern generation in non-hemisected and hemisected mouse spinal cord. Neurosci Letts 144:116-120

Wannier T, Orlovsky G, Grillner S (1995) Reticulospinal neurones provide monosynaptic glycinergic inhibition in lamprey. Neuroreport 6:1579-1600

Wheatley M, Stein RB (1992) An *in vitro* preparation of the mudpuppy for simultaneous intracellular and electromyographic recording during locomotion. J Neurosci Methods 42:129-137

Wheatley M, Jovanović K, Stein RB, Lawson V (1994) The activity of interneurons during locomotion in the *in vitro Necturus* spinal cord. J Neurophysiol 71:2025-2032

Wolf H, Pearson KG (1987) Comparison of motor patterns in the intact and deafferented flight system of the locust. II. Intracellular recording from flight motoneurons. J Comp Physiol A 160:269-279

CHAPTER 7

GENERAL DISCUSSION

To study locomotion in walking vertebrates we used an in vitro preparation isolated from the mudpuppy (*Necturus maculatus*). Originally developed in this lab (Wheatley and Stein1992), the mudpuppy proved to be an excellent model system for many of the reasons outlined throughout the thesis. In this section I will summarize my research and will point out some of the future directions that may lead to a more thorough understanding of central pattern generation in the mudpuppy.

We exploited this system to identify endogenous neurochemical mechanisms involved in locomotor rhythm and pattern generation. Specifically, neurotransmitters such as serotonin, glycine and GABA were of interest since they are implicated in controlling locomotion in all vertebrate species studied to date. Although none of the above neurotransmitters was essential for establishing the locomotor rhythm in the mudpuppy spinal cord they had a profound effect on an ongoing locomotor pattern. Similar findings obtained in lower vertebrates and mammalians are consistent with the hypothesis that there is an evolutionary conservation of neurotransmitters involved in control of locomotion in vertebrates.

Neurons containing the above mentioned neurotransmitters were found to largely coincide with interneurons and motoneurons involved in generating walking-like movements in the brachial spinal cord (Fig. 8-1). However their connections, if any, are presently unknown and future experiments using retrograde tracers should allow one to visualize at least some of these connections. This should be feasible since fluorescently labeled dextrans, such as TMR-D used in this thesis, are relatively resistant to fading and are compatible with other common neurochemical procedures such as immunocytochemistry (Shmued et al. 1990; Carr et al. 1990). Alternatively, pre-labeled motoneurons and intracellularly filled interneurons may also be studied in full mount (Jovanović 1998, unpublished).

Particularly interesting was the finding that the majority of serotonergic cell bodies

Figure 7-1. Schematic illustrating localization of the elbow flexor and extensor centers and rostro-caudal distribution of serotonergic (5-HT), GABAergic and glycinergic cells in the brachial spinal cord of the mudpuppy. The localization of the flexor center in the C2 and part of C3 segment and the extensor center in the C3 and C4 segment is based on data from electrical stimulation and surgical isolation experiments (left half of the spinal cord). Right half of the spinal cord contains patterned columns depicting approximate locations of serotonin-, GABA- and glycine immunopositive neurons. The greatest density of 5-HT immunoreactive profiles was observed between segments C2 and C6. They were observed either at the border between the grey and white matter or close to the midline (m). The majority of glycine-immunopositive neurons were found primarily in the caudal part of segment C3, and throughout segments C4-6 at the border between the grey and white matter. They were also observed in the immediate vicinity of the central canal (m) in segments C1-C3. GABA-immunopositive neurons were present in the caudal part pf the C2 segment, as well as in segmennts C3 and C4. Approximate spacing between two subsequent spinal roots is 5 mm.

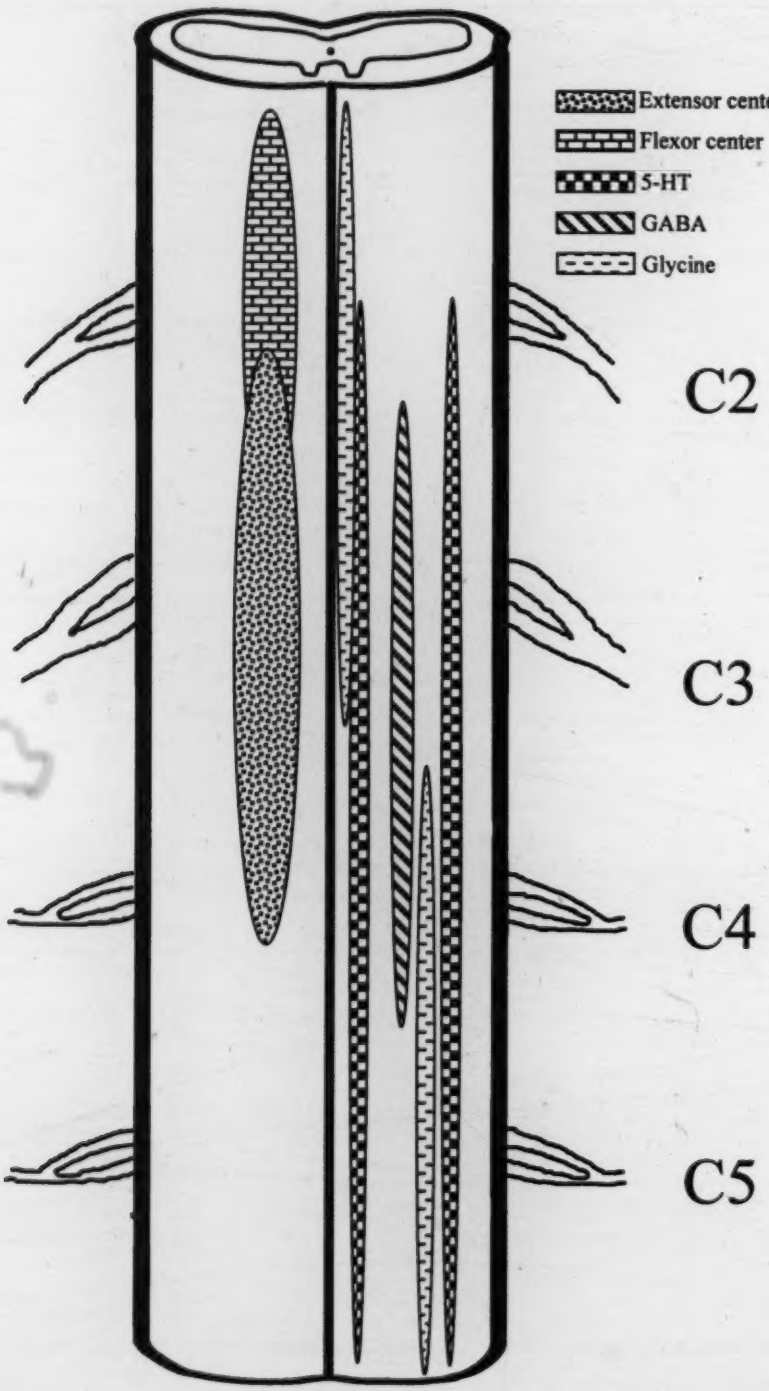
Extensor center
Flexor center
5-HT
GABA
Glycine
C2
C3
C4
C5

were localized within the brachial and lumbar spinal cord which provide innervation of the mudpuppy forelimb and hindlimb, respectively. If this transmitter produces the plateau potential, as expected, then this phenomenon could be studied in detail since there are large serotonergic neurons in the mudpuppy but not in higher vertebrates.

Several lines of evidence indicate that glycine co-exists with GABA in spinal neurons and axon terminals (Todd and Sullivan 1990; Berki et al., 1995) suggesting that the transmitters in the spinal cord could provide fine-tuned mechanisms of inhibitory transmission. Indeed, the comparable effects of $GABA_A$ receptor antagonist bicuculline and glycine receptor antagonist strychnine observed here, may be due to an interaction between GABAergic and glycinergic systems during locomotion. This may also indicate that $GABA_A$ and glycine receptors are co-localized and may interact functionally during locomotion. Future experiments utilising double-immunostaining techniques will help resolve this question.

Combining a number of techniques we identified and localized separate regions of the brachial spinal cord capable of producing flexion and extension of the forelimb. Now that critical evidence has accumulated suggesting that the locomotor CPG can be subdivided into smaller units controlling flexion and extension, further characterization of the physiological and morphological properties of specific interneuronal classes would be useful in understanding the organization of the locomotor CPG. To advance the study of how the *Necturus* CPG controls locomotor behavior, different classes of identified interneurons should be further defined with respect to their synaptic inputs. This could be realistically achieved by stimulating different dorsal roots as well as different regions in the brainstem (Shik 1997). Newly introduced intrafascicular electrodes would be particularly useful as they allow for a quick exchange of stimulation sites without jeopardizing the stability of intracellular recording.

New questions could also be posed as to how the properties of individual neurons may influence the operation of their host circuit. A method for studying the membrane properties of single interneurons is also essential and it may be useful to employ the method of dissociated spinal cord neurons (Dale 1991).

We showed here that some interneurons rhythmically active during mudpuppy locomotion exhibit membrane potential oscillations in the presence of NMDA. However, whether these properties play a significant role in rhythm generation remains to be determined. Even though, they are implicated in locomotor rhythm generation in many vertebrate preparations, no causal link has been established between the presence of transmitter induced intrinsic membrane potential oscillations and rhythm generation itself. In fact, it is somewhat surprising that both the tadpole (Soffe and Roberts 1989) and lamprey (Brodin and Grillner 1986) spinal cord can generate transmitter-induced locomotor activity in the absence of the NMDA-induced membrane oscillations. Although our results indicate that the mudpuppy spinal neurons share this property with many other in vitro preparations, it would be useful to determine whether these TTX-resistant membrane oscillations indeed contribute to cyclical fluctuations during walking.

In light of the accumulating evidence (Roberts and Perrins 1995; Staras 1998) that motoneurons may also play a role in central pattern generation, it would be of interest to investigate whether motoneurons in the mudpuppy share the same oscillatory membrane properties exhibited by the interneurons, whether they make central synapses and whether acetylcholine antagonists affect locomotor rhythm.

As previously confirmed in a single limb preparation, the spinal cord segment spanning dorsal root C3 contains a neural substrate capable of generating walking-like movements involving both forelimbs. However, more rostral sections of the spinal cord and/or crossed spinal connections appeared to be essential for correct phase coupling between the two limbs. These findings raise the possibility that both central mechanisms of behavioral choice and central mechanisms of interlimb coordination can be conveniently studied in this preparation.

The mudpuppy exhibits two forms of locomotion: swimming and walking. They are smoothly integrated in the escape response. An appropriate question for the future is: which interneurons are responsible for switching between the swimming and walking locomotor patterns? Are there separate populations of interneurons controlling swimming and walking, or are different neuromodulatory substances utilized to execute this switch?

As a relatively new model system for locomotion, the in vitro preparation isolated from the mudpuppy needed considerable ground work prior to any complex investigation. I believe that this thesis provides insights into some of the issues related to the operation of the CPG underlying walking in an adult vertebrate. The critical amount of data accumulated over the last several years, regarding the locomotor CPG in the mudpuppy, makes the central control of mudpuppy locomotion a promising system for investigating the cellular basis of vertebrate locomotion.

REFERENCES

Berki ACs, O'Donovan MJ, Antal M (1995) Developmental expression of glycine immunoreactivity and its colocalization with GABA in the embryonic chick lumbosacral spinal cord. J Comp Neurol 362:583-596

Brodin L, Grillner S (1986) Effects of magnesium on fictive locomotion induced by activation of N-methyl-D-aspartate (NMDA) receptors in the lamprey spinal cord in vitro. Brain Res 380:244-252

Carr PA, Noga BR, Nance DM, Jordan LM (1994) Intracellular labeling of cat spinal neurons using a tetramethylrhodamine-dextran amine conjugate. Brain Res Bull 34:447-451

Dale N (1991) The isolation and identification of spinal neurons that control movement in the *Xenopus* embryo. Eur J Neurosci 3:1025-1035

Roberts A, Perrins R (1995) Positive feedback as a general mechanism for sustaining rhythmic and non-rhythmic activity. J Physiol (Paris) 89:241-248

Schmued L, Kyriakidis K, Heimer L (1990) In vivo anterograde and retrograde axonal transport of the fluorescent rhodamine-dextran-amine, Fluoro-Ruby, within the CNS. Brain Res 526:127-134

Shik ML (1997) Locomotor patterns elicited by electrical stimulation of the brain stem in the mudpuppy. Motor Control 1:354-368

Soffe SR Roberts A (1989) The influence of magnesium ions on the NMDA mediated responses of ventral rhythmic neurons in the spinal cord of Xenopus embryos. Eur J Neurosci 1507-515

Todd AJ, Sullivan AC (1990) Light microscope study of the coexistance of GABA-like and glycine-like immunoreactivities in the spinal cord of the rat. J Comp Neurol 296:496-505

Staras K, Kemenes G, Benjamin PR (1998) Pattern-generating role for motoneurons in a rhythmically active neuronal network. J Neurosci 18:3669-3688

Wheatley M, Stein RB (1992) An *in vitro* preparation of the mudpuppy for simultaneous intracellular and electromyographic recording during locomotion. J Neurosci Methods 42:129-137

APPENDIX

APPLICATION OF INTRAFASCICULAR ELECTRODES TO THE *IN VITRO* MUDPUPPY PREPARATION

INTRODUCTION

In vitro preparations provide a useful means to increase our understanding of functionally intact spinal networks for rhythmic movements, such as locomotion. In previous work an *in vitro* spinal cord preparation of the mudpuppy *Necturus maculatus* was developed as a model to determine the spinal circuitry involved in locomotion. The preparation consists of the first five cervical segments of the spinal cord and a single neurologically intact forelimb (Wheatley et al. 1992; Wheatley et al. 1994; Wheatley and Stein 1992). Intracellular recordings from discharging cells during N-methyl D-aspartate (NMDA) induced locomotion were made and correlated with the electromyographic (EMG) patterns of the elbow flexor and extensor muscles in the attached forelimb. Further identification of these cells was made by recording their responses to individual or patterned stimulation of the three pairs of brachial spinal roots (C2-C4) innervating the forelimb. However, the size of the preparation, space limitation and the necessity to keep the spinal roots intact makes the use of multiple sets of suction, needle, or hook electrodes (Djupsjobacka et al. 1994) impractical. Moreover, manipulation of a single spinal root electrode to sequentially test each spinal root is inconvenient and problematic as it increases the time and amount of mechanical movement near the intracellular electrode which increases the risk of losing the cell.

A version of this paper has been submitted for publishing. Yoshida K, Jovanović K, Stein RB (1999) J Neurosci Methods. Contribution to paper: performed all dissections, implanted electrodes and edited manuscript.

We have introduced intrafascicular electrodes to the *in vitro* mudpuppy preparation to resolve these problems. Intrafascicular electrodes are fine wire electrodes that were developed for application in functional neuromuscular stimulation (FNS) in the clinical setting (Lefurge et al. 1991; Malagodi et al. 1989; McNaughton and Horch 1994; Yoshida and Horch 1996; Yoshida and Horch 1993; Yoshida and Horch 1993). The electrodes have been used for stimulation and recording from peripheral nerves and spinal roots, and have greater recording and stimulating topological selectivity as compared to more traditional peripheral nerve based electrodes used for FNS. The wires are fine and flexible enough that each ventral and dorsal root can be individually implanted and maintained without the need for micromanipulators to stabilize the electrodes in the *in vitro* mudpuppy preparation. Furthermore, since the electrodes are able to record as well as stimulate, several other recording/stimulation paradigm options are made available. In the present paper, we describe construction, implantation and implementation of this approach.

MATERIAL AND METHODS

Electrode construction

Detailed description of intrafascicular electrode construction is outlined elsewhere (Malagodi et al. 1989; Lefurge et al. 1991). However, as we have made several major modifications to the initial design, we will report the complete construction of the electrode shown in figure A1-A.

In vitro intrafascicular electrodes are constructed out of a 25 cm length of Teflon® insulated 90% Pt 10% Ir wires (#7750, AM Systems, Carlsborg WA). The diameter of this wire was 25μm bare and between 60-75μm with insulation. A 250 to 500 μm segment of insulation is removed along the length of the wire 3 cm from the end of the wire by edgewise contact to a glowing Pt Ir filament foil. This bared segment becomes the stimulation/recording site and will be referred to as the active site of the electrode. The impedance of the bare active site measured in normal (0.9%) saline at 1 kHz was

between 50 kΩ and 400 kΩ. Greater consistency in this process was achieved by drilling a 450 μm hole into the filament foil using a #78 drill bit and passing the insulated electrode wire through the hole before heating the filament. Heating time and voltage to the filament are controlled using a custom built power supply. This setup can be substituted with a horizontal glass pipette puller with heating time and voltage controls.

The cut end of the wire, 3cm from the active site is insulated by breaking the wire within the insulation at a point about 1/3 the distance between the active site and the end of the wire without breaking the insulation. This is accomplished by repetitively bending the insulated wire sharply with care taken not to break the insulation. Once the conductor is broken, the insulation is stretched apart at the break point so that an 1 mm gap is formed between the two broken ends of the wire within the insulation. The relative positions of these points are shown in the scale drawing of electrode (Fig. A1-B).

The active site is platinized by electro deposition of finely divided platinum black. Anodic deposition (250 mA/cm^2) with respect to a large platinum rod is done at room temperature in Korausch's solution (Geddes 1972) under sonication (FS-3, Fischer Scientific) for 15 minutes. Deposition without sonication results in a heavy deposit of loosely attached platinum black which flakes or rubs off during implant. On the other hand, sonication agitates the wire during deposition to result in a tough and well adhered layer of platinum black. Platinization reduces the interfacial impedance of the electrode down to approximately 1 kΩ (1 kHz in 0.9% saline).

An electrosharpened tungsten needle (15 mm long 50 μm diameter) is constructed and attached to the end of the platinized electrode lead. The profile of the needle is shown in detail in figure 1B which consists of a sharpened point and a notched end. 5 mm of the broken end of the platinized electrode wire is de-insulated by passing the end through a flame. Using a micromanipulator and a stereo microscope the notched end of the needle is aligned with the deinsulated electrode wire. It is soldered together using solder paste (SN62-RA10-BAS86-25g, Multicore) and a flame. Once attached, the junction is further encased in cyanoacrylate glue (Crazy Glue®) so that there is a smooth transition between the needle and electrode wire (Fig A1-B).

Figure A1 - is a drawing of the intrafascicular electrode and it's implant scheme. **(A)** shows the placement of the electrode and the dorsal view of the preparation. These structures are labeled as follows: The dorsal aspect of spinal cord (*SC*), dorsal root (*DR*), ventral root (*VR*), dorsal root ganglion (*DRG*), and spinal nerve (*SN*). An intrafascicular electrode is shown implanted in a dorsal root. Although **(A)** is not a scale drawing, it shows the basic features of the electrode and a successful implant with the active site (a) centered within the spinal root. A scaled drawing of the intrafascicular electrode is shown in **(B)**. Note that the radial axis of the electrode has been enlarged by 15.4 times relative to the longitudinal axis to allow visualization of the parts of the electrode. (a) indicates the active site of the electrode which was between 250 - 500 μm in length. (e) is the 50μm diameter electrosharpened tungsten needle used to penetrate and thread the electrode into the spinal root. It is soldered to the electrode wire at (c) and glued between (c) and (d). A smooth transition between the electrode wire and needle is created by a reduction in the diameter of the needle between (c) and (d) and filling the gap at (d) with a bead of glue. (b) indicates the point where the wire core of the electrode is broken and the Teflon® insulation was stretched out to break electrical contact between the soldered needle and the electrode lead. **(C)** shows the mudpuppy spinal cord-arm preparation showing the relative positions of the various electrodes used in the study. Although up to six spinal roots were implanted with intrafascicular electrodes in the study, **(C)** shows only the C3 spinal roots implanted here for clarity.

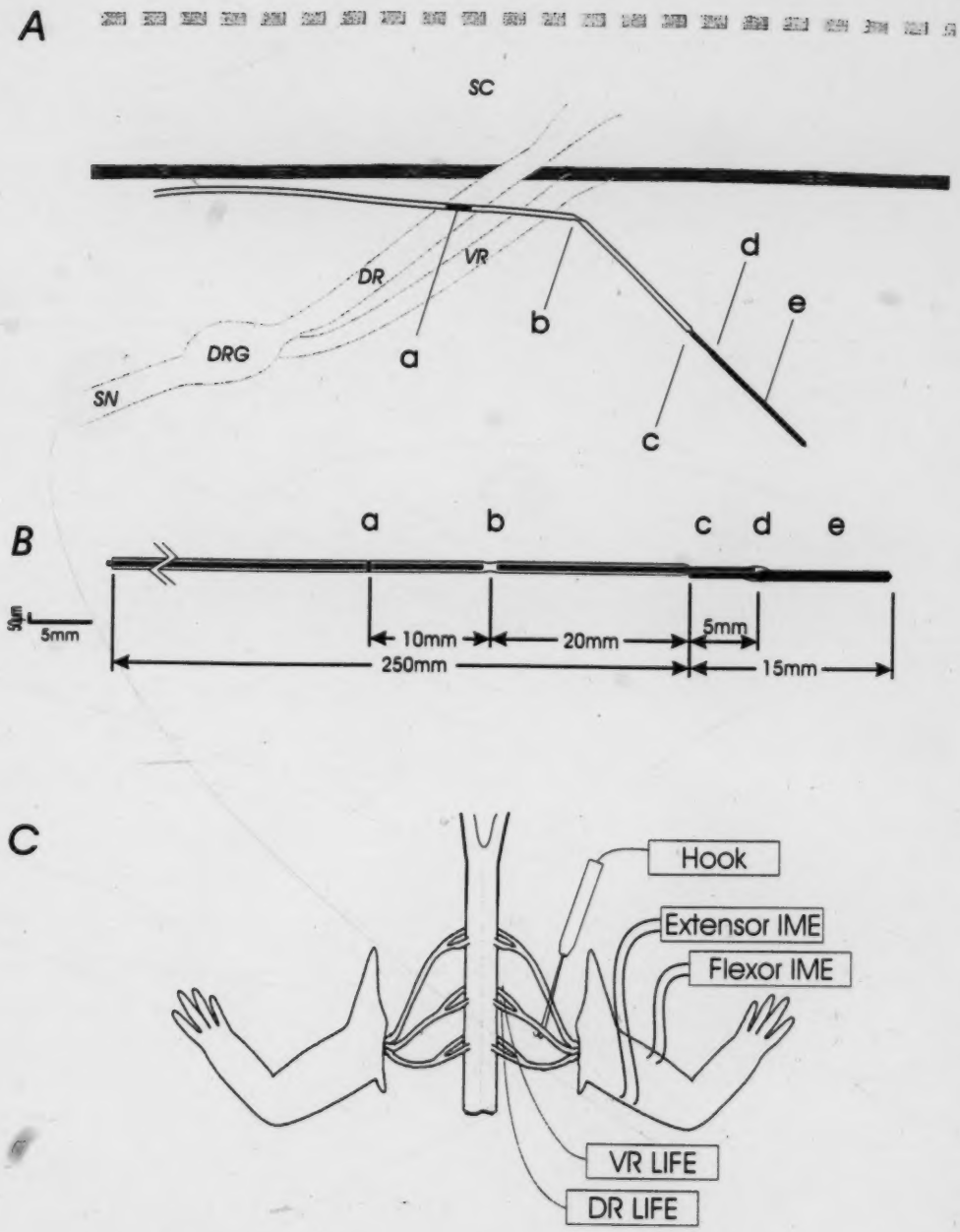
A
SC
DR
VR
DRG
SN
a
b
c
d
e
B
a
b
c
d
e
5mm
10mm
20mm
5mm
250mm
15mm
C
Hook
Extensor IME
Flexor IME
VR LIFE
DR LIFE

Animal preparation

The general details of the animal preparation are described in other papers (Wheatley and Stein 1992) Briefly, experiments (n=9) were conducted on an *in vitro* spinal cord preparation isolated from adult mudpuppies as approved by the Animal Welfare Committee at the University of Alberta. Prior to dissection, the animals were anaesthetized by immersion in a solution of 3-aminobenzoic acid ethyl ester (Sigma, 1 g/l). The skin and underlying muscles were removed and a dorsal laminectomy was performed from the first to the fifth vertebrae. The first five segments of the spinal cord (C1-C5) with the attached forelimb were than removed from the rest of the body and placed in a Sylgard®-lined petri dish superfused with cooled (15°C) and oxygenated Ringer solution of the following composition (mM): 115 NaCl; 2 $CaCl_2$; 2 KCl; 1.8 $MgCl_2$; 5 Hepes; pH 7.3; glucose, 1g/l. While in the petri dish, the brachial plexus was exposed, the paraspinal muscles removed and bipolar Teflon®-coated silver wires (75μM) inserted into the elbow flexor (*Brachialis*) and extensor (*Extensor ulnae*) muscles for EMG recording (Fig. A1-C). After a recovery period of approximately one hour, the preparation was transferred to a Sylgard®-lined recording chamber and placed dorsal side up. The spinal cord and the forelimb were then stabilized by pinning the vertebral column and the procoracoid cartilage to the base of the chamber. Throughout the course of experiments the preparation was superfused with a cooled (15-18° C) and oxygenated Ringers at a flow rate of 5-10 ml/min.

Intrafascicular electrodes were implanted into each of the spinal roots emerging from spinal segments C2, C3 and C4 ipsilateral to the attached arm. The electrodes were implanted nearly perpendicular to the axis of the spinal roots and were parallel to the longitudinal axis of the spinal cord so that they could be routed out without obstructing access to the spinal cord. Care was taken to keep the active sites of the electrodes within the body of the spinal root, to minimize the current shunt out of the root (see Fig. A1-A). An un-implanted, distantly placed intrafascicular electrode was used as an indifferent electrode to the implanted intrafascicular electrodes for recordings. The counter electrode during stimulation was a distantly placed 18 gauge hypodermic needle pushed into the

Sylgard® bottom of the recording chamber.

To enable comparisons between intrafascicular electrodes to a standard electrode, a bipolar hook electrode was constructed using 50μm tungsten wires (#7955, AM Systems, Carlsborg WA) and placed around the C3 spinal nerve (Fig. A1-C). Intrafascicular electrodes were tested in the preparation for ventral root stimulation and recording compound action potentials. Experiments were conducted on 13 implants in 9 preparations.

Ventral root stimulation

We determined whether intrafascicular electrodes implanted in ventral roots were able to activate axons by stimulating through the ventral root electrodes and recording the EMG elicited in the elbow extensor and flexor muscles. These signals were simultaneously recorded using a 12-bit data acquisition system (Axoscope, Axon Instruments). Prior to recording the signals from the bipolar intramuscular electrode pair were differentially amplified 1000x (QT-5, Leaf Electronics) and conditioned (5x gain, band pass filtered 0.1 Hz - 300 Hz).

The stimulus current amplitude was varied from EMG threshold to EMG saturation and back to threshold. Each stimulus intensity was tested with repeated presentation of a 500 μs long rectangular constant current cathodic pulse at the test stimulus current. Stimulus pulses were generated using a channel from a Master 8 (A.M.P.I., Jerusalem, Israel) pulse generator and passed through either a custom built or commercial (Digitmer, Hertfordshire, England) optically isolated stimulus isolation unit. Each stimulus amplitude was repeated 15 times with a stimulus repetition rate of 1 to 2 seconds. The average peak to peak EMG was measured for each stimulus amplitude and plotted to generate an EMG recruitment curve. A similar approach was used to generate recruitment curves with the hook electrode placed around the C3 cervical spinal nerve, as shown in figure A1-C. The constant current stimulation from the opto-isolated stimulation unit was substituted for constant voltage pulses generated by a Grass stimulator (SD-9, Grass Instruments, Cambridge MA) triggered by the Master 8 pulse

generator.

Compound action potential recording

The feasibility of recording neural signals with intrafascicular electrodes in the spinal roots was tested by stimulating nerves peripherally, through intramuscular electrodes implanted in the elbow flexor and extensor muscles, and recording the resulting compound action potential volley proximal to the stimulation site in the spinal nerve (via hook electrode) and spinal roots (via intrafascicular electrodes). A custom built stimulus isolation unit was used to deliver trains of 64 pulses (500 μs long rectangular current controlled pulses) with an inter-stimulus interval of 500 ms to an intramuscular electrode pair in either the elbow extensor or flexor muscle. Signals from intrafascicular electrodes in the C3 spinal roots and the hook electrode around the C3 spinal nerve were collected from 5ms before the stimulus to 20ms after the stimulus for each of the 64 stimulus pulses. These 64 stimulus triggered sweeps were then digitally averaged and the average sweep stored using a 12 bit A/D converter (Digidata 1200B, Axon Instruments) and acquisition software (Axoscope, Axon Instruments) in a 166 MHZ PC. Prior to being digitally sampled, the signals were amplified 10,000x in two steps, 2,000x using a low noise differential preamplifier (QT-5, Leaf Electronics) followed by 5x gain amplifier.

This protocol was repeated at three stimulation amplitudes: Subthreshold, maximal compound action potential amplitude and an intermediate compound action potential amplitude. At the end of the experiment, the spinal nerves were transected or crushed distal to the hook electrode and the protocol was repeated at the amplitude corresponding to maximal compound action potential amplitude.

The conduction velocity of the compound action potentials were determined based on the average of the 64 stimulus triggered sweeps. The spinal nerve was then crushed distal to the hook electrode and the protocol was repeated to determine the post crush averages. These post crush averages were subtracted from the pre crush sweep averages to remove most of the stimulus artifact. Conduction velocities were measured by dividing the distance from stimulating electrode to the recording intrafascicular electrode by the

time from onset of the stimulus artifact to the onset of the compound action potential. Also, the distance between the hook electrode and the recording intrafascicular electrode was divided by the difference in the compound action potential onset times at the two electrodes. These two calculated velocities were averaged to arrive at the estimated conduction velocity of the fastest units.

RESULTS

Ventral root stimulation

We found that increasing stimulus strength delivered to intrafascicular electrodes implanted in the ventral roots increased peak to peak EMG amplitude. Plotting the peak to peak EMG versus stimulus strength results in a EMG recruitment curve. Figure A2 shows one example from a typical experiment. The average threshold stimulus strength for all ventral root implants tested was found to be 30±8.9μA and 17±3.6μA (mean ± SEM., n=13) for the flexor and extensor respectively. The average currents required to reach flexor and extensor EMG saturation were found to be 71±12.0μA and 82±15.7μA (mean ± SEM., n=13) respectively. Recruitment curves using a voltage controlled stimulator instead of a current controlled stimulator were generated for a subset of five of these runs. The threshold voltages were quantified and found to be 330±78 mV (mean ± SEM., n=5).

Stimulus strengths for EMG thresholds and saturation with hook electrodes were found to be 2.8±0.17 V and 4.1±0.30 V respectively. We compared the supra-maximal peak to peak EMG induced via hook electrodes stimulation to those induced via intrafascicular electrodes implanted in the C3 ventral root. Since the absolute amplitudes of EMG varied between preparations, the ratio of the hook electrode to intrafascicular electrode was derived for each preparation's supra-maximal extensor and flexor EMGs. These ratios were then grouped between animals and the result is shown in figure A3. The figure indicates that there is no difference between the supra-maximal EMGs elicited by hook electrodes placed around the spinal nerve and those elicited by intrafascicular electrodes in the ventral root.

Figure A2 - Stimulating through a LIFE implanted in the C3 ventral root results in activation of elbow flexor and extensor muscles. The amount of activation, or recruitment, was estimated by quantifying the peak to peak EMG recorded by intra-muscular electrodes implanted in *Brachialis* and *Extensor ulnae* muscles. Peak to peak EMG was recorded as a function of stimulus strength, which was normalized to the smallest stimulus that resulted in a detectable EMG record. Peak to peak EMG was normalized to the maximum EMG. A typical recruitment curve is shown in the above figure. In this particular case, the thresholds were 31.8μA and 17.6μA for the flexor and extensor curves respectively. Although this curve shows muscle activation, it illustrates that fibers within the spinal root can be recruited by intrafascicular electrodes.

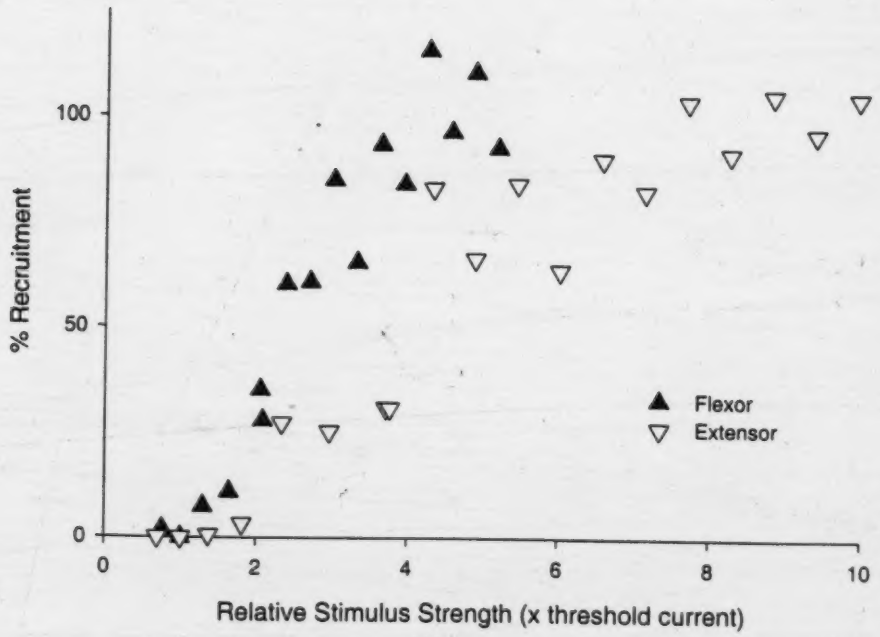
% Recruitment
100
50
0
0
2
4
6
8
10
Relative Stimulus Strength (x threshold current)
Flexor
Extensor

Figure A3 Peak to peak EMG were compared for supra maximal stimulation with intrafascicular electrodes in the C3 ventral root and with hook electrodes around the C3 spinal nerve. The ratio of V_{Hook} to V_{IFE} was calculated separately for the elbow flexor and elbow extensor muscles. The ratios were then averaged between animals. The mean ± SEM are plotted in this figure. 1 represents equivalence of hook and intrafascicular electrode results. The figure shows that there is no difference between the peak to peak EMG evoked with hook electrodes and with intrafascicular electrodes in both muscles.

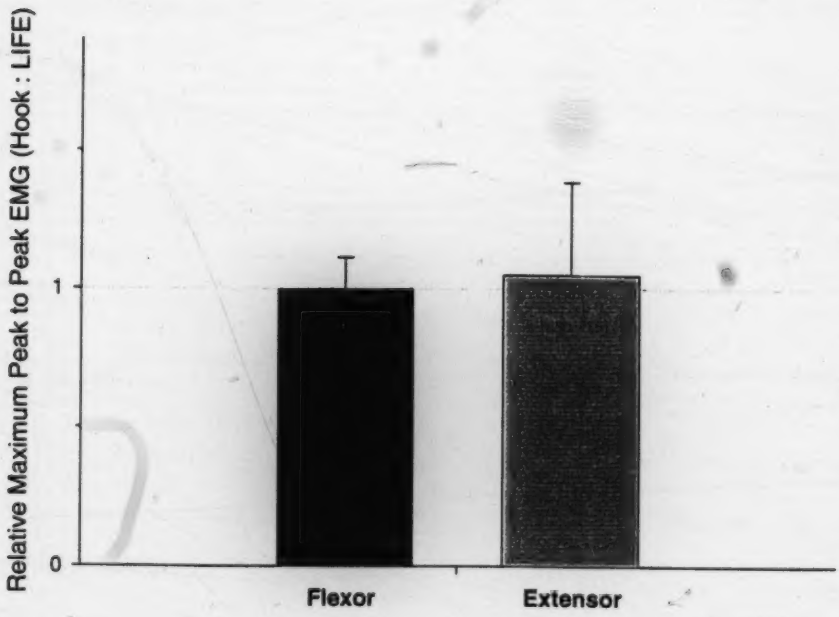
Relative Maximum Peak to Peak EMG (Hook : LIFE)
1
0
Flexor
Extensor

Compound action potential recording

By stimulating through the bipolar EMG electrodes placed in the elbow flexor and extensor muscles, we found that we were able to evoke a response propagating centrally from the periphery. The evoked activity appeared in the spinal nerve hook electrode record before appearing in the spinal root intrafascicular electrode records. Crushing the nerve distal to the hook electrode abolishes the response, with no change in the stimulus artifact and filter RC decay. A typical example of this behavior is shown in figure A4. Since the post crush record gives a good estimate of the stimulus artifact and filter RC decay, these artifacts could be removed from the record by subtracting the post crush record from the pre crush record. This was done to simplify detecting the onset of the evoked activity. The amplitude of the response can be varied by varying the stimulus strength. An example of this is shown in figure A5.

The average peak to peak compound action potentials were quantified for the intrafascicular electrodes implanted in the C3 spinal roots and for the C3 spinal nerve hook electrode during supra-maximal stimulation of the flexor and extensor muscles. They were 44.6 ± 13.7 μV and 28.7 ± 8.51 μV for the C3 dorsal root and ventral root intrafascicular electrodes, while they were 1.1 ± 11.8 μV for the spinal nerve hook. The average relative amplitudes of these compound potentials recorded via intrafascicular electrodes to those recorded via hook electrode were 1.9 and 1.3 ($V_{pp\ IFE} : V_{pp\ hook}$) for the dorsal and ventral roots respectively.

We calculated the conduction velocity and the duration of the compound action potentials for the ventral roots and dorsal roots independently. The fastest components of the compound action potentials for the ventral root and dorsal roots had conduction velocities of 17.5±1.9 and 17.5±1.0 m/s respectively, with no significant difference between them (t-test, $p<0.05$). However, the duration of the compound action potentials were significantly different from one another (t-test, $p<0.05$). They were 2.4±0.3 ms and 1.8±0.1 ms for the compound action potentials recorded in the dorsal root and ventral root respectively. We also observed that the ventral root compound action potentials were typically triphasic, while those of the dorsal root were monophasic as exemplified in

Figure A4 - Supra-maximal stimuli were delivered through the elbow extensor intra-muscular electrode. The resulting maximal compound action potential volley was recorded by the C3 spinal nerve hook electrode and the intrafascicular electrodes implanted in the C3 spinal roots. A typical average record of 64 presentations of stimuli from a particular experiment is shown here. t=0 represents the onset of the stimulus, and the stimulus artifact is seen in all electrodes. The propagating compound action potential results in a deflection which has an onset at t_1 on the spinal nerve hook electrode and at t_2 on both intrafascicular electrodes. This indicates that the fastest components of the compound action potential have similar conduction velocities in both roots. Bars marked as T_{VR} and T_{DR} denote the duration of the compound action potentials. Note that the duration of the dorsal root compound action potential (T_{DR}) is longer than that of the ventral root (T_{VR}). Compound action potentials were eliminated by crushing the spinal nerve distal to the hook electrode.

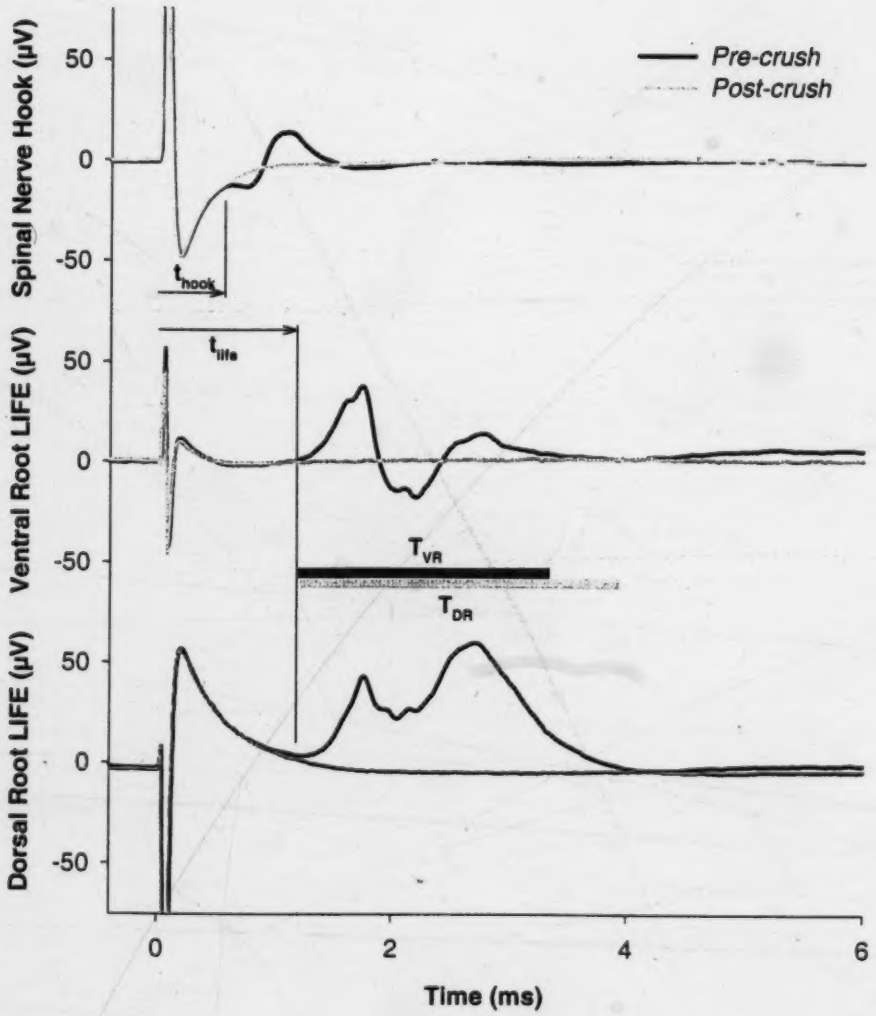
Pre-crush
Post-crush
Spinal Nerve Hook (μV)
Ventral Root LIFE (μV)
Dorsal Root LIFE (μV)
50
0
-50
t_{hook}
t_{life}
T_{VR}
T_{DR}
0
2
4
6
Time (ms)

Figure A5 - shows the three traces recording through intrafascicular electrodes at three levels of stimuli. Stimuli were delivered through the elbow extensor intra-muscular electrode to demonstrate that increasing stimulus strength increases the amplitude of the compound action potential. The evoked response to stimulation through an intramuscular electrode implanted in the elbow extensor muscle at 4.75V, 5.75V and 7V was recorded by an intrafascicular electrode implanted in the C3 ventral root. Although not shown, stimuli greater than 7V did not result in a larger compound action potential indicating that all units had been recruited (saturation). Stimulus artifact and filter responses in the recording were reduced by subtracting the post crush response for each stimulus voltage from the pre-crush response. Note that the magnitude of the compound action potential increases in amplitude and duration with increasing stimulus strength.

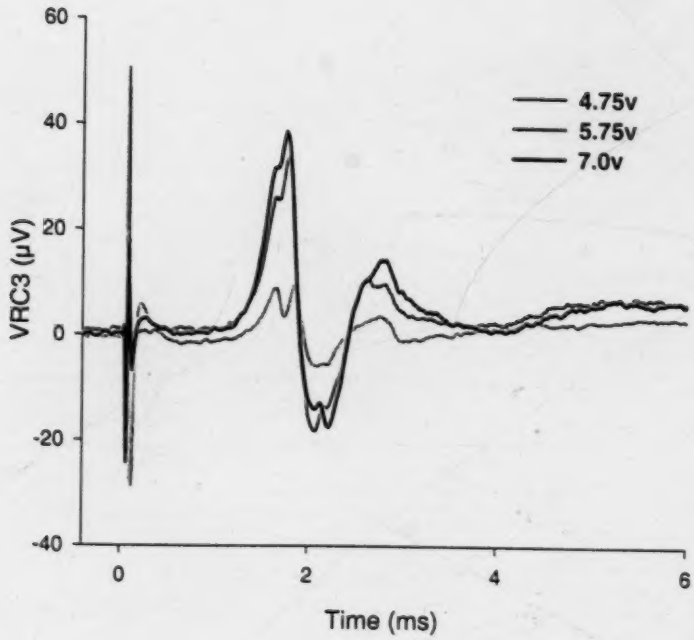
60
40
20
0
-20
-40
VRC3 (µV)
0
2
4
6
Time (ms)
4.75v
5.75v
7.0v

figure A4. The average total conduction distance between the stimulating and the intrafascicular electrodes was 25.5 mm while the distance between the hook electrode and intrafascicular electrode was 11 mm.

DISCUSSION

Intrafascicular electrodes were initially developed for use with FES and are currently being tested for long term safety in animals and efficacy in humans. The present study confirms that intrafascicular electrodes can also be applied under in vitro experimental conditions. Namely, intrafascicular electrodes implanted in ventral roots were able to activate motor axons and elicit EMG in the mudpuppy's elbow extensor and flexor muscles. Induction of graded responses were possible using graded stimuli between threshold and saturation. Furthermore, the maximal EMGs elicited by intrafascicular electrodes, in the ventral root, were found to be equivalent to those evoked with a hook electrode placed around the corresponding spinal nerve. The stimulus strength required to activate fibers in the ventral root was found to be an order of magnitude smaller for intrafascicular electrodes. Intrafascicular electrodes are placed within the body of the nerve and are in direct contact with the tissue they are intended to activate or record. Stimulation through them specifically activates the nerve or spinal root they are implanted in with little or no cross talk. Since their active sites are not exposed to the bath, relatively small stimulus intensities can be used to achieve equivalent levels of activation requiring much higher stimulus intensities with uninsulated hook electrodes.

Intrafascicular electrodes also proved to be useful in recording compound action potentials resulting from stimulation delivered peripherally through intramuscular electrodes. The results show that the compound action potential amplitudes recorded via intrafascicular electrodes in the spinal roots were larger than those recorded via hook electrodes in the corresponding spinal nerve. This was achieved by the intrafascicular electrodes despite recording from a fraction of the fibers in the spinal nerve. This demonstrates an advantage of recording from within the body of the nerve and shows the

attenuating effect of the perineurium when recording neural activity from outside of the nerve. These recordings were made before and after crushing or cutting the spinal nerve just distal to a hook electrode placed between the intrafascicular electrodes in the spinal roots and the stimulation electrodes in the mudpuppy's elbow flexor and extensor muscles. Since the elicited activity disappears from the record, following the nerve crush or cut, with no change to the stimulus artifact we eliminate the possibility that the responses were artifactual.

Although we recorded asynchronous activity from cutaneous mechanoreceptors responding to rubbing or pinching the skin, the activity was found to be small and difficult to distinguish from the random background noise in the recording. Since no effort was made to insulate the root from the surrounding bath, wrapping the roots with an insulator or placing them within a bead of petrolatum jelly may improve these recording characteristics. Nonetheless, we found that compound action potentials can be recorded without the use of petrolatum jelly or mineral oil to limit the current shunt from the root to the bath.

We characterized the conduction velocities for the fastest components of these compound action potentials and found that they were slightly slower than those reported for the large diameter axons in frog sciatic nerve (Erlanger and Gasser 1937; Wijesinghe et al. 1991) which are between 30 and 25 m/s after compensating for the lower temperatures used in our experiments. We compare our results to frog sciatic nerve since, to our knowledge, conduction velocity data for the mudpuppy forelimb nerves do not exist in the literature. The slower conduction velocities in the mudpuppy may reflect interspecies differences or functional differences of the limb and muscles in these two preparations. Several technical issues can also be used to explain the difference. A critical factor in calculating conduction velocities is the measurement of the conduction distance. The relative error for these measurements in the present study is estimated to be between 10-15%. The size of the preparation introduces limits to the lengths of peripheral nerves available. These short distances also increase the effects of localized slowing of conducting action potentials. Delays occur near the stimulating electrode due to virtual

anodic fields produced in the stimulating electric field (Goodall et al. 1995) and due to thinning of afferent fibers just proximal and just distal to the dorsal root ganglion (Erlanger and Gasser 1937). We have not compensated for these effects in the present study since it was not the aim of this study characterize the conduction velocities of the mudpuppy.

An averaging scheme was used for measuring the conduction velocity to reduce the effect of errors in measuring the distances between the various electrodes. While the fastest fibers in the ventral and dorsal roots had the same conduction velocities, the duration and shape of the compound action potentials were different. Dorsal roots, on average, showed a longer lasting compound action potential which may be due to differences in the fibre type distribution in the sensory and motor roots. The dorsal root has a larger distribution of smaller fiber types, which leads to a larger temporal spread in the compound action potential (Erlanger and Gasser 1937). The difference in shapes could also be explained by electrical differences in the extracellular space. Simultaneous extracellular single unit recordings of a particular unit with closely spaced concentric microneurography electrodes have been shown to exhibit a variety of wave shapes (Wu et al. 1998). The differences in shapes of the waveform has been attributed to the electrical anisotropy of the extracellular space, and the position of the recording site relative to the nodes of Ranvier of the active axon. Alternatively, the difference in the shapes between the dorsal root and ventral root compounds can be explained by partial pressure conduction block of the dorsal root fibers by the intrafascicular electrode. The wave shape of action potentials of fibers mechanically blocked by microneurography electrodes were characterized by a biphasic waveform that consisted of a "single positive" deflection followed by a much smaller negative deflection (Wu et al. 1998; Wu et al. 1997; Calancie and Stein 1988; Inglis et al. 1996). Although our recordings were not from single units, the compound action potential is a sum of the resultant synchronized unit volley and should retain some of the characteristics of the single unit waveform.

We were, however, able to elicit withdrawal reflex by pinching the toes. This demonstrates that conduction of action potentials through the implanted dorsal and ventral

roots is maintained. Furthermore, the NMDA induced locomotion was not impaired by the electrodes implanted in the roots. Finally, stimulation through the dorsal root electrodes resulted in a H-reflex response indicating that the ventral root electrodes did not block conduction. Although we cannot directly exclude the possibility that the dorsal root electrode partially blocks nerve conduction, these indirect evidences suggest that blockage of nerve conduction by the electrode is unlikely.

By introducing intrafascicular electrodes to the mudpuppy in vitro preparation we have found that they offer many advantages over traditional hook or suction electrodes. They do not require micromanipulator support and multiple roots can be implanted without sacrificing space for intracellular electrodes or obscuring the view of the preparation. Furthermore, there is no need to use an oil pool or petrolatum jelly to insulate the electrode from the surrounding bath. This eliminates contamination of the bath by oily residues and other components trapped in the oil. These findings have two important implications. Firstly, they demonstrate that intrafascicular electrodes present an elegant solution for nerve stimulation and can functionally replace bulky hook electrodes. Secondly, the small size of intrafascicular electrodes and the convenient method of their implantation in the anesthetized animal make simultaneous stimulation and recording of multiple roots feasible. Intrafascicular electrodes should prove useful in many small in vitro preparations that are increasingly being used in neuroscience.

REFERENCES

Calancie BM, Stein RB. (1988) Microneurography for the recording and selective stimulation of afferents: an assessment. Muscle & Nerve 11: 638-644.

Djupsjobacka M,. Johansson H, Bergenheim M,. and Sandstrom U (1994) A multichannel hook electrode for simultaneous recording of up to 12 nerve filaments. J Neurosci Methods 52: 69-72.

Erlanger J,. Gasser HS (1937) Electrical signs of nervous activity. University of Pennsylvania Press, Philadelphia, PA

Geddes LAL (1972) Electrodes and the measurement of bioelectric events. Wiley-Interscience, New York,

Goodall EV, Kosterman LM., Holsheimer J. Struijk JJ (1995) Modeling study of activation and propagation delays during stimulation of peripheral nerve fibers with a tripolar cuff electrode. IEEE Transactions on Rehabilitation Engineering 3: 272-282.

Inglis JT, Leeper JB, Burke D, Gandevia SC (1996) Morphology of action potentials recorded from human nerves using microneurography. Exp Brain Res 110: 308-314.

Lefurge T, Goodall E, Horch K, Stensaas L, Schoenberg A (1991) Chronically implanted intrafascicular recording electrodes. Annals of Biomedical Engineering 19: 197-207.

Malagodi MS, Horch KW, Schoenberg AA. (1989) An intrafascicular electrode for recording of action potentials in peripheral nerves. Annals of Biomedical Engineering 17: 397-410.

McNaughton,TG, .Horch KW (1994) Action potential classification with dual channel intrafascicular electrodes. IEEE Transactions on Biomedical Engineering 41: 609-616.

Wijesinghe RS, Gielen FL, Wikswo JP (1991) A model for compound action potentials and currents in a nerve bundle. III: A comparison of the conduction velocity distributions calculated from compound action currents and potentials. Annals of Biomedical Engineering 19: 97-121.

Wheatley M, Edamura M, Stein RB (1992) A comparison of intact and *in vitro* locomotion in an adult amphibian. Exp Brain Res 88: 609-614.

Wheatley M,. Jovanović K., Stein RB, Lawson V (1994) The activity of interneurons during locomotion in the *in vitro* Necturus spinal cord. J Neurophysiol 71: 2025-2032.

Wheatley M, Stein RB (1992) An *in vitro* preparation of the mudpuppy for simultaneous intracellular and electromyographic recording during locomotion., J Neurosci Methods 42: 129-137.

Wu G, Ekedahl R,. Hallin RG (1998) Consistency of unitary shapes in dual lead recordings from myelinated fibers in human peripheral nerves: evidence for extracellular single-unit recordings in microneurography, Exp Brain Res 120: 470-478.

Wu G, Hallin RG,. Ekedahl R (1997) Waveform complexity of unit activity recorded with concentric needle electrodes from human peripheral nerves, Exp Brain Res 114: 377-383.

Yoshida K,. Horch K (1996) Closed-loop control of ankle position using muscle afferent feedback with functional neuromuscular stimulation., IEEE Transactions on Biomedical Engineering 43: 167-176.

Yoshida K, Horch K (1993) Reduced fatigue in electrically stimulated muscle using dual channel intrafascicular electrodes with interleaved stimulation., Annals of Biomedical Engineering 21: 709-714.

Yoshida K, Horch K (1993) Selective stimulation of peripheral nerve fibers using dual intrafascicular electrodes., IEEE Transactions on Biomedical Engineering 40: 492-494.